Biosynthesis of biphenyl and dibenzofuran phytoalexins in *Sorbus aucuparia* cell cultures

Von der Fakultät für Lebenswissenschaften

der Technischen Universität Carolo-Wilhelmina

zu Braunschweig

zur Erlangung des Grades eines

Doktors der Naturwissenschaften

(Dr. rer. nat.)

genehmigte

D i s s e r t a t i o n

von Mohammed Nabil Ahmed Khalil
aus Kairo / Ägypten

1. Referent: **Professor Dr. Ludger Beerhues**
2. Referent: **Privatdozent Dr. Wolfgang Brandt**
eingereicht am: **27.05.2013**
mündliche Prüfung (Disputation) am: **14.08.2013**

Druckjahr 2013

„Gedruckt mit Unterstützung des Deutschen Akademischen Austauschdienstes“

Vorveröffentlichungen der Dissertation

Teilergebnisse aus dieser Arbeit wurden mit Genehmigung der Fakultät für Lebenswissenschaften, vertreten durch den Mentor der Arbeit, in folgenden Beiträgen vorab veröffentlicht:

Publikationen

- Chizzali C, Khalil MNA, Beurle T, Schuehly W, Richter K, Flachowsky H, Peil A, Hanke MV, Liu B, Beerhues L: Formation of biphenyl and dibenzofuran phytoalexins in the transition zones of fire blight-infected stems of *Malus domestia* cv. ′Holsteiner Cox′ and *Pyrus communis* cv. ′Conference′. Phytochemistry 77: 179-185 (2012).

- Khalil MNA, Beuerle T, Müller A, Ernst L, Bhavanam VBR, Liu B, Beerhues L : Biosynthesis of the biphenyl phytoalexin aucuparin in *Venturia inaequalis*-treated *Sorbus aucuparia* cell cultures. Submitted (2013).

- Khalil MNA, Brandt W, Beuerle T, Liu B, Beerhues L: Charcterization of two cDNA encoding *O*-methyltransferases participating in biosynthesis of phytoalexins in *Sorbus acuparia* cell cultures. In preparation (2013).

Tagungsbeiträge

- Khalil MNA, Beuerle T, Liu B, Beerhues L: Molecular analysis of biphenyl biosynthesis (Vortrag) Black Forest Retreat 2012 on Molecular Plant Science. Herzogenhorn, Freiburg, Sep 10^{th}-13^{th}.

- Khalil MNA, Beuerle T, Liu B, Beerhues L: Biosynthesis of biphenyl and dibenzofuran phytoalexins in *Sorbus aucuparia* cell suspension cultures (Vortrag) Tagung der Sektion ‘Pflanzliche Naturstoffe’ der Deutschen Botanischen Gesellschaft im Michaeliskloster Hildesheim, 30.09-02.10.2012

Acknowledgment

Thanks to GOD, the source of all knowledge by whose abundant grace this work has come to fruition. He guided us to see his greatness in his creatures.

I would like to express my deep appreciation and gratitude to my supervisor Prof. Dr. *Ludger Beerhues*, for giving me the opportunity to join his workgroup in context of the GERLS scholarship program, for the valuable inspiring scientific discussions and his affectionate, friendly way of guidance and supervision. His trust, support and careful listening and comprehension make it possible to surpass the difficulties of work. Thanks for respecting and discussing my ideas and opinions, even when they appear silly to me or they are not convincing to you. Working with you and in your workgroup taught me many lessons about science and life.

I owe much of the success of this work and most of the knowledge I expanded during the scholarship to Dr. *Till Beuerle*. Thanks a lot for your help and guidance during the chemical synthesis of the substrates and references which were so essential for performing this research and the useful fruitful tips and recommendations throughout the work. Thanks for teaching me that before performing an experiment, it is so important to think about its outcome, asses the alternatives and at the end find a compromise between the resources and goals. For me, you are a great teacher who gives his students all his experience to save their time and efforts and then give them the freedom to research freely. Thanks for your continuous support and respect even when I have done mistakes and your brotherly advices and discussions.

Thanks and appreciation to Dr. *Benye Liu* for his valuable helpful advices in the work, his welcoming approachable personality and kindness. Any time I could ask or discuss anything with him.

Sincere appreciation and gratitude to PD Dr. *Wolfgang Brandt* for performing the modeling work with diligence and enthusiasm and meeting our many questions and requests with patience and comprehension. I am grateful to Prof. Dr. *Ludger Ernst* for measuring and interpreting the NMR data. I am grateful and thankful for Dr. *Helge Scharnhop* and Dr. *Cornelia Chizzali* for establishing the fundamentals of this work, my work was only a continuation for what you started. Your results and the problems you faced helped to save my time and efforts. I appreciate the kind help and the friendly support I get from my colleague Dr. *Cornelia Chizzali*. Great thanks and appreciation to Dr. *Rainer Lindigkeit* for his support during the work in the isotope laboratory. Because of his efforts and care, the work flows smoothly in the institute.

I was lucky to work with a group of kind, helpful and patient colleagues. To enumerate Mrs. *Claudine Theuring* and Mrs. *Kathrin Meier* for their help with the handling of radioactive isotopes, Mrs. *Carolin Rattunde* for her guidance and help by the real time-qPCR and answering my questions, Mrs. *Ines Rahaus* and Mrs. *Doris Glindemann* for help with everyday working. I would like to express my sincere gratitude for Mrs. *Ines Rahaus* for her moral and affectionate support and continuous encouragement throughout the PhD work especially in the first year, when I faced a lot for disappointing results. Listening to your monthly radio program and the discussions ideas about arts, social and cultural issues were a rewarding experience and gave me new perspectives. Thanks for spreading optimism and fun

in the stringent scientific life. Thanks *Doris* for the many presents you gave to me every Christmas and feast, for alerting me, in a friendly way, to my mistakes and asking about my family.

I extend my appreciation to my colleagues, *Islam El-Awaad* , Dr. *Andreas Müller*, Dr. *Iman Abdel-Rahman*, *Malte Büttner*, *Frauke Gumz* for their indispensable help and advise by the molecular and biochemical work. Especial thanks for Islam and Iman for sharing their experiences, success and mistakes with me and the countless scientific discussions. Thanks for your kindness and support.

It was a grace to meet unforgettable sincere friends. The Christmas team: *Maike van Ohlen, Luise Cramer*, *Marion Wiggermann*, *Malte Büttner* and *Frauke Gumz*. I will always remember our happy and joyful conversations and laughter. You were my second family in Germany. Your comprehension, love and respect alleviated my nostalgia. I will be always grateful to the chance meeting and knowing you. I wish you eternal happiness and all the best in your lives. Special Thanks to my friend and colleague *Mina Awadalah* for the happy joyful discussions and work in the laboratory. Great appreciation and gratitude to my colleagues *Nargis Elgahme, Sahar Abdelaziz, Anja Losansky, Ines Bel haj, Ebtesam Ali, Tobias Fiesel, Dennis Reckwell, Maren Lütge, Dibyendu Majumdar* and *Su Zhang* for the friendly working atmosphere and encouragement. Many thanks go to Mrs. *Bettina Böttner* for the interesting conversations and her diligent work.

Thanks a lot for all German language teachers in Egypt and Germany and the workshops held in DAAD-Cairo; they eased the study and life in Germany. I am so grateful to the Egyptian Ministry of Research and High Education and DAAD for co financing and organizing the GERLS program (German Egyptian Research Long- term Scholarship). This program gave me the chance to develop and expand my knowledge, skills and provided me with unforgettable scientific and personal experiences. Many thanks for the German people I met during the language course and in everyday life. I appreciate their hospitality and respect.

Words are not enough to express my hearty gratitude, sincere appreciation and great indebtedness to my *father*, *mother*, *brother* and *sister* for their great care, trust, surveillance, affection, and love. They are the *sun* which enlightens my life and soul, and the *shore* where I find always peace and safe. They play a special role in my life. I owe them my life and success. May GOD make their life full of joy and happiness.

I appreciate this moment, that I had the chance to express these feelings and to make them everlasting.

……***To whom I owe my success and Happiness***,

My Father, Mother
Brother, Sister

Contents

Abbreviations

APS	Ammonium peroxydisulfate
Bam	*Bacillus amyloli*
BIS	Biphenyl Synthase
BLAST	Basic Local Alignment Search Tool
bp	Base pair
BSA	Bovine serum albumin
°C	Degree Celsius
cDNA	Complementary deoxyribonucleic acid
Ci	Curie (unit of radioactivity)
CoA	Coenzyme A
2,4-D	2,4-dichlorophenoxyacetic acid
DAD	Diode array detector
DTT	1,4-dithiothreitol
DNA	Deoxyribonucleic acid
dNTP	Deoxynucleoside triphosphate
EDTA	Ethylenediaminetetraacetic acid
EST	Expessed sequence tag
g	gramme
GC	Gass chromatography
h	hour
Hin	*Haemophilus influenzae*
HPLC	High Performance Liquid Chromatography
IPTG	Isopropyl-β-D-thiogalactopyranoside
K_m	Michaelis-Menten constant
K_{cat}	Turnover number
K_{cat} / K_m	Catalytic efficiency
LB	Luria broth
LS	Linsmaier and Skoog
m	milli
M	Molar
MCS	Multiple cloning site
MS	Mass spectroscopy
min	minute
ml	milliliter
mRNA	Messenger RNA
MSTFA	N-methyl-N-(trimethylsilyl)trifluoroacetamide
NAA	1-Naphthaleneacetic acid
NADPH	Nicotinamide adenine dinucleotide phosphate (reduced form)
NADP	Nicotinamide adenine dincleotide phosphate (oxidized form)
Ni-NTA	nickel-nitrilotriacetic acid
nm	nanometer
OD	Optical density
OMT	*O*-methyltransferase
ORF	Open reading frame
PAGE	Polyacrylamide gel electrophoresis
PCR	Polymerase chain reaction
PKS	Polyketide synthase
PMSF	phenylmethylsulfonyl fluoride

Abbreviations

RNA	Ribonucleic acid
rpm	Revolution per minute
RT	Reverse transcription
RT-PCR	Reverse transcription polymerase chain reaction
s	second
SAM	S-adenosyl-L-methionine
SDS	Sodium dodecyl sulfate
TAE	Tris-acetate-EDTA
Taq	*Thermus aquaticus*
TEMED	N,N,N`,N`-tetramethylethylenediamine
T_m	Melting temperature (primer)
T_a	Annealing temperature
Tris	Tris(hydroxymethyl)aminomethane
UV	Ultraviolet

Amino acids

A	Ala	Alanine
C	Cys	Cysteine
D	Asp	Aspartic
E	Glu	Glutamic
F	Phe	Phenylalanine
G	Gly	Glycine
H	His	Histidine
I	Ile	Isoleucine
K	Lys	Lysine
L	Leu	Leucine
M	Met	Methionine
N	Asn	Asparine
P	Pro	Proline
Q	Gln	Glutamine
R	Arg	Arginine
S	Ser	Serine
T	Thr	Threonine
V	Val	Valine
W	Trp	Tryptophan
Y	Tyr	Tyrosine

Nucleotides

A	Adenine
C	Cytosine
G	Guanine
T	Thymine
U	Uracil

I. Introduction

The subtribe Pyrinae includes many economical fruit trees, e.g. apple and pear. However, these trees are vulnerable to a number of parasitic diseases. Two of the most devastating diseases are scab and fire blight. Members of this subtribe produce biphenyls and dibenzofurans as phytoalexins. However, the biosynthesis of these compounds is poorly investigated. In this study, we try to explore the biosynthesis of these phytoalexins using *Sorbus aucuparia* cell suspension cultures as a model system. Our investigations have encompassed biochemical and molecular biological studies.

1. Subtribe Pyrinae

Pome-bearing plants are grouped in the subtribe Pyrinae. According to a recent classification and phylogenetic studies, these plants along with the closest relatives are grouped in the tribe Pyreae, supertribe Pyrodae, subfamily Spiraeoideae, family Rosaceae (Campbell et al., 2007; Potter et al., 2007). The subtribe Pyrinae contains many important edible fruits, e.g. apple (*Malus*), pear (*Pyrus*), quince (*Cydonia*), loquat (*Eriobotrya*), chokberry (*Aronia*) and serviceberry (*Amelanchier*). Some members are known for their ornamental value, e.g. mountain ash (*Sorbus*), firethorn (*Pyracantha*), hawthorn (*Crataegus*), Japanese quince (*Chaenomeles*), and cotoneaster (*Cotoneaster*). Formerly, pome-bearing plants were classified as subfamily Maloideae. As already mentioned, this subtribe contains some of the most economically important fruit trees. For apples, the world production amounted to 70 million tons, equivalent to US$ 64 milliard (FAO, 2010). The export value is about US$ 6 milliard. The world production of pears is 22 million tons, equivalent to US$ 13 milliard. The export value is around US$ 2 milliard. However, these plants are afflicted by a number of diseases. Two devastating diseases will be discussed because of their serious impact.

2. Parasitic diseases of Pyrinae

2.1 Scab

The disease is caused by the ascomycete fungus *Venturia inaequalis*. It is recorded to infect some genera of the subtribe Pyrinae, for example, *Malus*, *Sorbus, Eriobotrya, Pyracantha and Crataegus* (Jha et al., 2009). Apple scab, the most known scab disease, is the most costly apple disease in terms of control expenditure (Carisse and Bernier, 2002). The control of this disease may require the application of more than 20 fungicides per season (Kollar, 1997). This disease causes appearance of olive-green velvety necrotic or chlorotic lesions on leaves, sepals, pedicels or young leaves of the flower buds. Finally, these lesions acquire metallic black color. Infected mature fruits have small black spots (pin-point scab), but young infected fruits are cracked and have corky lesions. If infection happens at an early time, fruits get deformed and may drop prematurely (Fig. 1-1A) (Agrois, 2005; Jha et al., 2009).

A

B

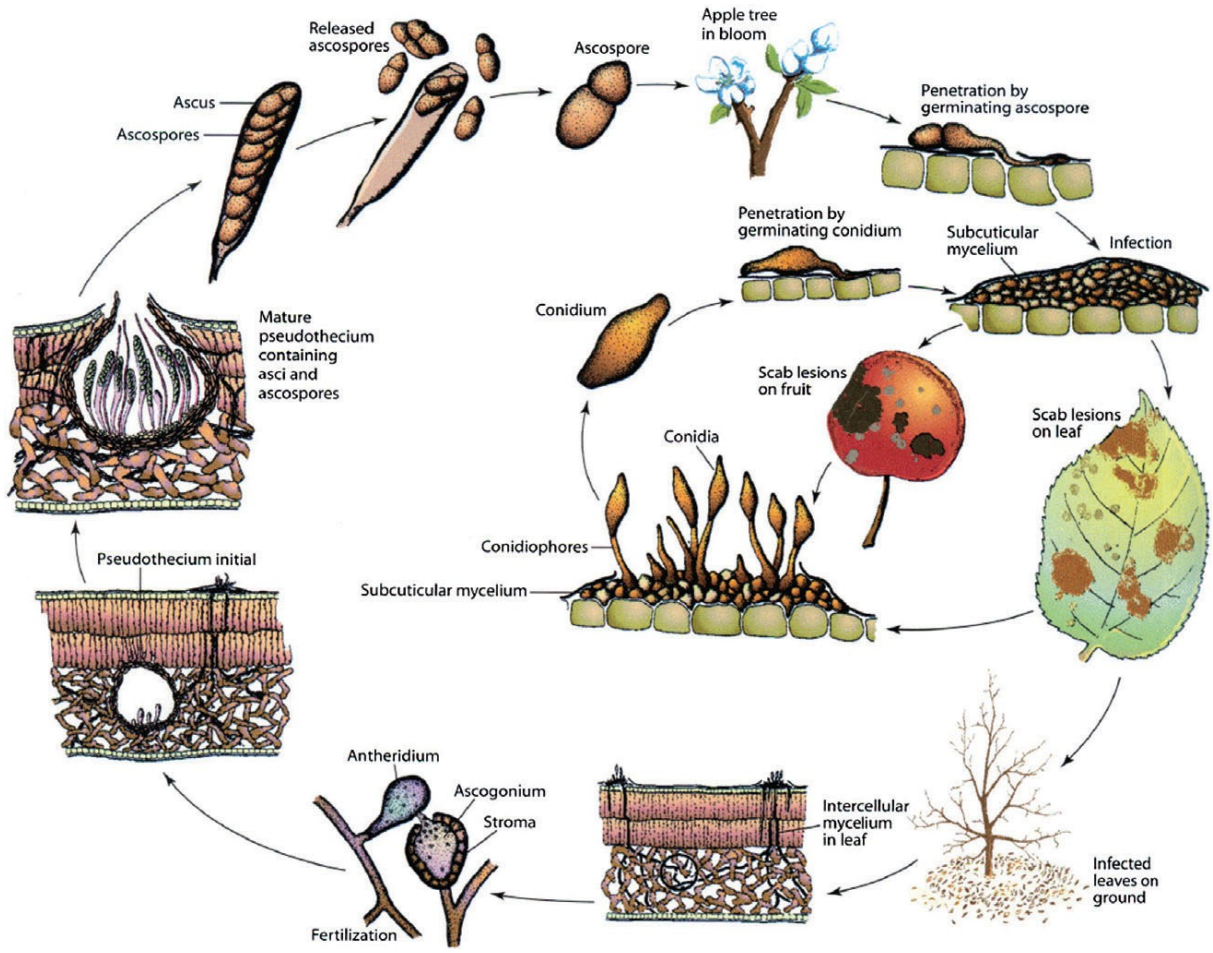

Figure 1-1: Apple scab disease. (A) Symptoms of the disease on infected fruits and leaves. (B) Life cycle of *V. inaequalis*. Subcuticlar mycelium = stroma (Photos and diagram from Agrois 2005, Plant Pathology, 506).

Infection starts when ascospores (sexual spores) fall on leaves or other plant organs. The developed germ tubes penetrate the cuticle layer by producing cutinase enzymes. They do not penetrate deeper and develop into multilayered pesudoparenchymatous structures called stroma (subcuticlar mycelium), which produce conidiophores and conidia (asexual spores) (Fig. 1.1B). These stroma and conidia give the appearance of the lesions characteristic for the disease. Conidia cause secondary infection to other plant parts or are disseminated by wind and rain to infect other trees. By leaves falling in autumn, the fungi switch from the vegetative growth phase into the reproductive phase giving pseudothecium (sexual fruiting bodies). This structure contains asci filled with ascospores. By this way, the fungi overwinter and during this time the ascospores get mature. On the next spring and early summer, the ascospores are released by rain and disseminated to cause infection by the season of bud burst and leaves unfurling, when plants are most susceptible. Then, the cycle is repeated (Agrois, 2005; Bowen et al., 2011; Jha et al., 2009). Comprehensible reviews have been published (Bowen et al., 2011; Jha et al., 2009). They cover the issues of resistant (*R*) genes and avirulence (*avr*) genes involved in apple scab pathosystem and the development of resistant apple sorts.

2.2 Fire blight

This disease is caused by the gram-negative bacterium *Erwinia amylovora* which infects genera of Rosaceae. The majority of species belong to the subtribe Pyrinae, e.g. *Malus*, *Pyrus*, *Sorbus*, *Cotoneaster*, *Crataegus*, *Cydonia* (Bonn and Van der Zwet, 2000). Fire blight is a serious and devastating disease. The economical loss of a severe outbreak in a limited region is so high. For example, a sever outbreak in north-west USA was estimated to be higher than US$ 68 million (Bonn, 1999; Vanneste, 2000). The annual costs of control measurement plus disease-caused loss are valued to US$ 100 million in the USA alone (Norelli et al., 2003). The affected parts of the plant appear brown or dark colored as if they are burnt (Fig. 1-2A).

E. amylovora is spread by wind, rain or pollinating insects. Blossoms, especially the stigma surface, are a major site of infection and multiplication of bacteria (Fig. 1-2B). Bacteria are driven down in the blossom by action of rain or heavy dew. They infect floral nectarines and cause blossom darkening and finally death, i.e, blossom blight. *E. amylovora* bacteria penetrate down more in branches, shoots and leaves causing shoot blight. Finally, the bacteria can proceed further deeper to the root causing rootstock blight. However, the bacteria can infect shoots and other parts by getting access through natural openings, e.g. stomata and wounds. *E. amylovora* overwinters in cankers which are infected, discolored parts of the bark from the previous season. As the weather warms in spring, the bacteria multiply rapidly and emerge in form of ooze; it is a sticky sweet exudate infested with bacteria. Because of its polysaccharide nature, it attracts flies and insects, which in turn help in disseminating and spreading the bacteria. These oozes can also form on twigs, three days after infection (Malnoy et al., 2012; Norelli et al., 2003). Although a lot of studies helped in gaining thorough information about the

bacterium and the disease, the control of the disease seems to be intricate (Vanneste, 2000).

A

B

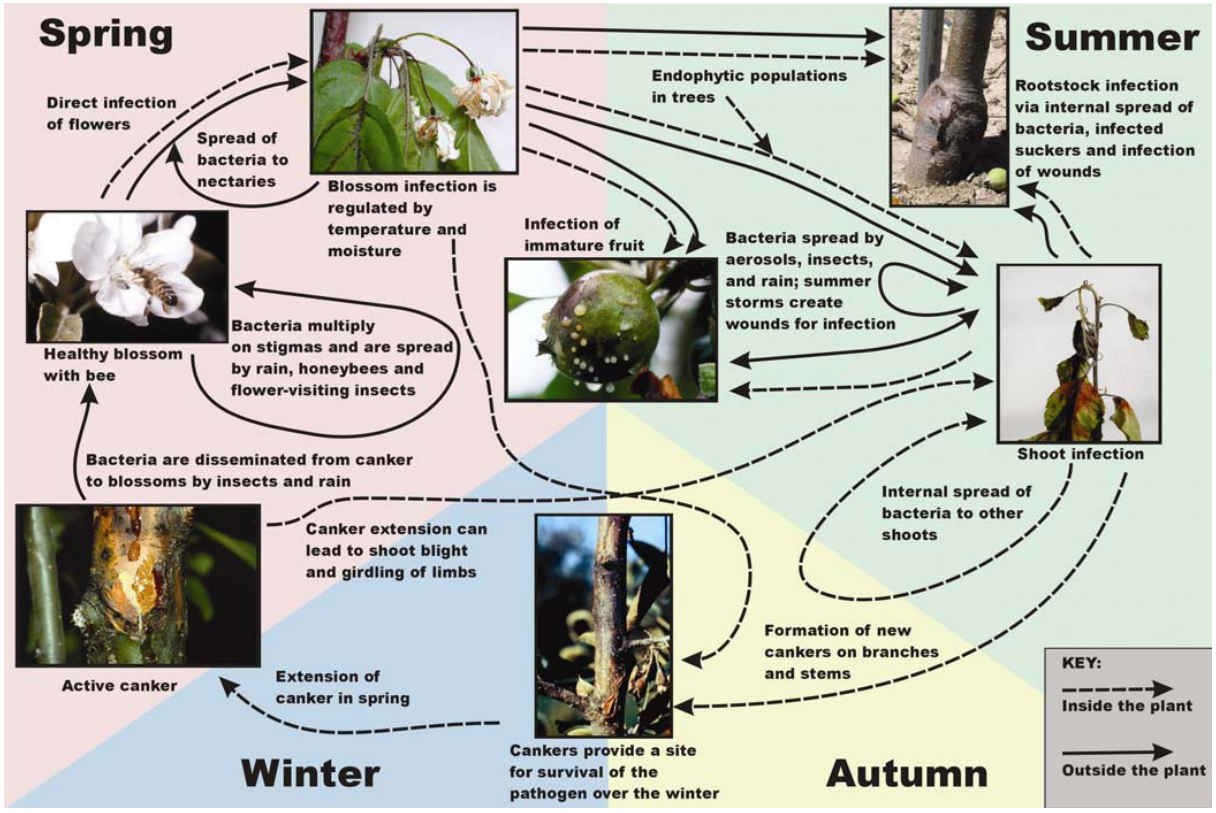

Figure 1-2: Fire blight disease. (A) Symptoms on infected leaves and fruits of pear (from Wikimedia Commons). (B) Life cycle of *E. amylovora* illustrated on apple trees (from Norelli et al. 2003, Plant Disease, 87, 757).

3. Phytoalexins

Plants are not only subjected to a large number of microorganisms, but they are also immobile organisms. This represents a major challenge for plants regarding their adaptation to the surrounding environment. However, plants are resistant to

most of microorganisms, to which they are subjected. They respond to pathogen attack by a variety of actions, for example, reinforcement of cell walls, production of resistance proteins (RP), production of reactive oxygen species (ROS) and the production of antimicrobial compounds. These compounds can be termed as phytoalexins or phytoanticipns depending on their biosynthetic origin. Phytoalexins are defined as "low molecular weight, antimicrobial compounds that are both synthesized by and accumulated in plants after exposure to microorganisms". On the other hand, phytoanticipins are "low molecular weight, antimicrobial compounds that are present in plants before challenge by microorganisms or are produced after infection solely from preexisting constituents". Establishment of these definitions and the distinction between both classes of compounds was introduced by VanEtten (1994). Now, it is accepted that phytoalexins accumulate not only in response to infection but also to stress (Kuć, 1995).

Phytoalexins were first reported by Müller and Borger (1940) during their research on potato (*Solanum tuberosum*) tuber. They had observed that pre-treatment of the tubers with the incompatible (noninfective) race of *Phytophthora inaffestans* induce resistance against a compatible (infective) race of *P. infestans* or the tuber infecting *Fusarium*. It was postulated that the previous exposure of potato to the incompatible fungus race led to production of chemical compounds at the site of inoculation, which in turn protected the tuber from infection by the compatible race. Since then, tremendous investigations studying phytoalexins have been carried out. Over 300 compounds were identified belonging to versatile chemical classes and distributed throughout the plant kingdom (Fig. 1-3). These studies have aimed not only at isolation and structure elucidation of different classes of these compounds, but also at studying their biosynthesis and molecular factors controlling their production.

A controversial issue was elaborated, whether phytoalexins actually play a role in plant resistance to pathogens or they are merely produced because infections disturb plant's metabolism. This issue was addressed in a number of reviews (Hammerschmidt, 1999; Kuć, 1995), which concluded that phytoalexins do play a role in plant resistance to pathogens, but they are not the sole player. This was manifested in (i) knockout *Arabidopsis* lines and (ii) transgenic plants.

Absence or decrease of camalexin levels in mutant *pad* lines of *A. thaliana* has not resulted in complete loss of resistance to the incompatible pathogens when compared to the wild type (Col-0). The mutant lines susceptibility was enhanced to some pathogens but not to others (Glazebrook and Ausubel, 1994; Glazebrook et al., 1997; Thomma et al., 1999). This led to the conclusion that camalexin production is not the only determinant of susceptibility in these mutant lines.

Stilbene synthase (*STS*) encoding genes were successfully transferred to rice (Stark-Lorenzen et al., 1997), tomato (Thomzik et al., 1997), alfalfa (Hipskind and Paiva, 2000), and tobacco (Hain et al., 1993). In these plants, enhanced resistance was observed, but not a complete protection. Both of the aforementioned approaches underline the participation of phytoalexins in plant defense but also highlight the complexity of plant-pathogen interaction and that phytoalexins are not the only key player in this interaction.

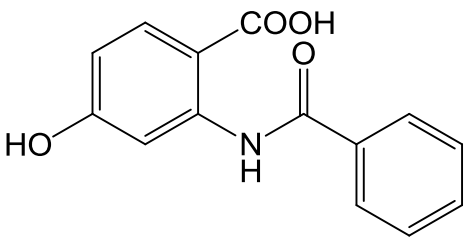

Anthranilamide
Dianthus caryophyllus
Caryophyllaceae

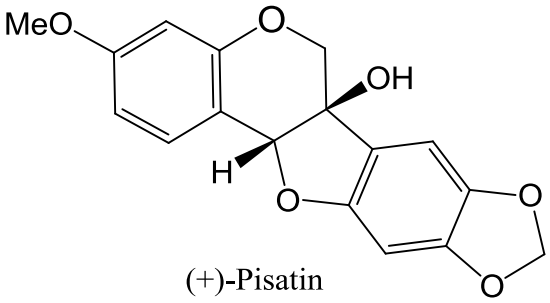

(+)-Pisatin
Pisum sativum
Fabaceae

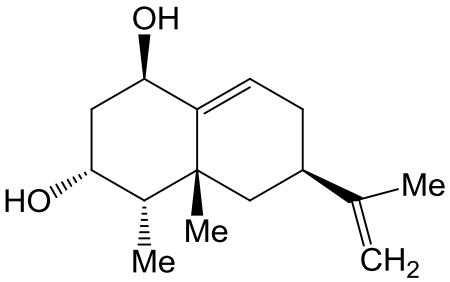

Capsidiol
Capsicum annuum
Solanaceae

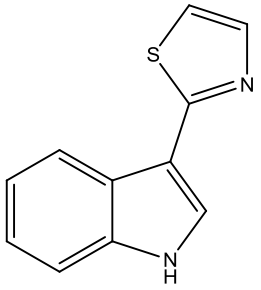

Camalexin
Arabidopsis thaliana
Brassicaceae

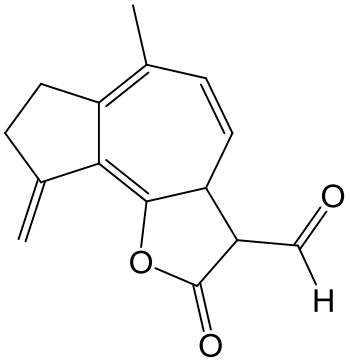

Lettucenin- A
Lactuca sativa
Asteraceae

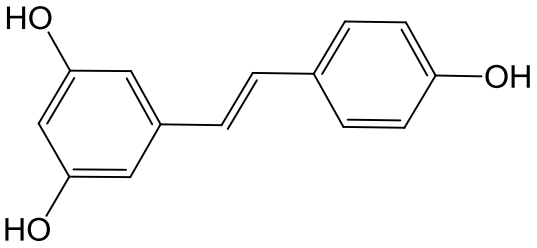

Resveratrol
Vitis vinifera
Vitaceae

Figure 1-3: Selected phytoalexin compounds and their producers.

Elicitors are compounds which are capable of stimulating any type of plant defense (Angelova et al., 2006). They can elicit the production of ROS and phytoalexins and stimulate hypersensitive responses (HR). According to their origin, they can be biotic (derived from the plant or the pathogen) or abiotic, e.g. salts of heavy metals. Biotic elicitors can be further subdivided into exogenous or endogenous. Exogenous elicitors are derived from the pathogen, e.g., components of the fungal cell wall. Endogenous elicitors are released from plants by the action of the pathogen's enzymes, e.g. oligogalacturonides are released from plant cell walls by pectolytic enzymes from pathogens. Biotic elicitors could be of defined chemical composition, e.g., proteins, glycoproteins or oligosaccharides. Elicitors play an important role in production of phytoalexins in plant tissue cultures (Whitehead and Threlfall, 1992). In the course of this study, *S. aucuparia* cell suspension cultures were treated with an extract of *V. inaequalis* as a biotic elicitor.

3.1 Phytoalexins of subtribe Pyrinae

Studies of phytoalexin production in Rosaceae were rather sporadic. However, Harborne and his group have systemically studied phytoalexins production in Rosaceae (Kokubun and Harborne, 1994; Kokubun and Harborne, 1995). They have found that only members of the subfamily Maloideae, now known as subtribe Pyrinae, produce biphenyls and dibenzofurans, upon challenging with heavy metals or after artificial inoculation with fungal spores (Fig. 1-4). Other members of the Rosaceae either have constitutive antimicrobials or produce phytoalexins of other structures. The investigations of the Harborne group encompassed natural infection, inoculation with fungal spores, and treatment of leaves of 130 species with copper ions, followed by investigations of the diseased sapwood of 29 species. Their work led to identification of 5 biphenyls and 14 dibenzofurans. Their work as well as other reports studying phytoalexin production in the Pyrinae has recently been reviewed (Chizzali and Beerhues, 2012). To date, 10 biphenyls and 17 dibenzofurans were isolated from 14 of the 30 Pyrinae genera (Chizzali and Beerhues, 2012). These compounds are accumulated through *de novo* synthesis. Most of the examined plants are able to accumulate these phytoalexins in the sapwood. However, few can accumulate them in leaves. Leaves of *S. aucuparia* accumulate aucuparin after challenge with copper ions (Kokubun and Harborne, 1994). Leaves of *E. japonica* can accumulate aucuparin or eriobofuran upon infection (Morita and Nonaka, 2003; Watanabe et al., 1982). Leaves of *Photinia glabra* accumulated 2`-methoxyaucuparin and 4`-methoxyaucuparin (Widyastuti et al., 1992). Phytoalexins of three genera (*Sorbus, Malus, Pyrus*) will be discussed in details, because of the close relatedness of the structures of their pytoalexins and their importance (Fig. 1-5).

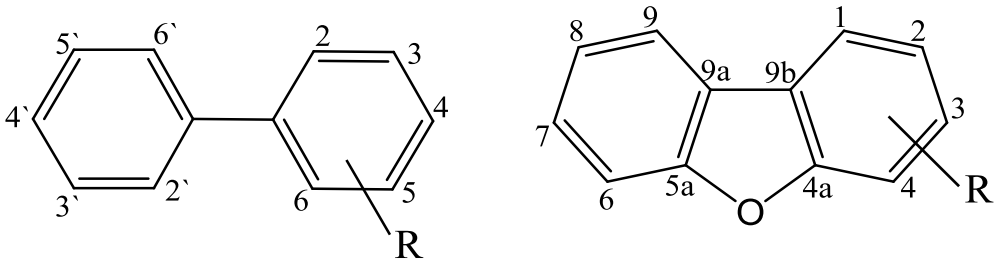

Figure 1-4: Structure and carbon numbering of biphenyl and dibenzofuran nuclei.

Leaves of *S. aucuparia* are reported to accumulate aucuparin upon challenging them with copper ions (Kokubun and Harborne, 1994). In contrast, the sap wood produced five biphenyls upon inoculation with fungal spores of *Nectria cinnabarina* (Kokubun et al., 1995a). The five biphenyls were aucuparin, 4`-methoxyaucuparin, 2`-methoxyaucuparin, 2`-hydroxyaucuparin, isoaucuparin (2'-hydroxy-3,5-dimethoxybiphenyl) (Fig-1-5). Erdtman and his group (1963) had isolated aucuparin and 2`-methoxyaucuparin from the heart wood of *S. aucuparia* as constitutive compounds. However, it should be considered that heart wood originally develops from sap wood upon death or secondary thickening. Moreover, heart wood is constituted of dead cells. So, it is reasonable to suggest that compounds detected in the heart wood could be merely phytoalexins, which had been accumulated in the original sapwood and persisted after its transformation in heart wood. No dibenzofurans were detected in *S. aucuparia* trees. However, elicitor-treated *S. aucuparia* cell cultures accumulated different profiles of biphenyls and dibnezofurans (Hüttner et al., 2010). Three biphenyls were accumulated, namely, aucuparin, noraucuparin and 2`-hydroxyaucuparin, in addition to two dibenzofurans, namely, eriobofuran, and noreriobofuran. This accumulation profile varies depending on the elicitor used. Methyl jasmonate induced accumulation of biphenyls only, while yeast extract, *V. inaequalis* extract, and an autoclaved suspension of *E. amylovora* induced accumulation of both biphenyls and dibenzofurans; with the observation that eriobofuran is the main component in case of treatments using the last two elicitors.

γ-Cotonefuran was isolated from inoculated sap wood of *S. domestica* and *S. chamaemespilus* (Kokubun and Harborne, 1995), but not reported in *S. aucuparia* trees. Aucuparin and 2`-methoxyaucuparin were isolated from wood extract of *S. decora, S. scopulina,* and *S. americana* (Narasimhachari and Von Rudloff, 1962, 1973) as constitutive constituents. However, the authors have located aucuparin and its methyl derivative in heart wood of *S. decora*, but they had not mentioned the location in the other investigated species.

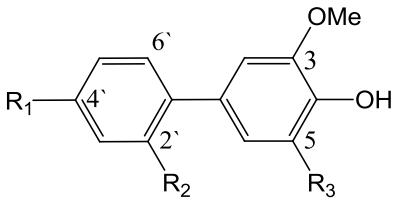

Name	R_1	R_2	R_3
noraucuparin	H	H	OH
aucuparin	H	H	OMe
2`-hydroxyaucuparin	H	OH	OMe
2`-methxoyaucuparin	H	OMe	OMe
2`-*O*-β-D-glucopyranosylaucuparin	H	O-β-Glc	OMe
4`-methoxyaucuparin	OMe	H	OMe

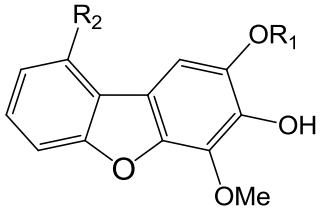

Name	R_1	R_2
noreriobofuran	H	H
eriobofuran	Me	H
9-hydroxy-eriobofuran	Me	OH
malusfuran	Me	*O*-β-Glc

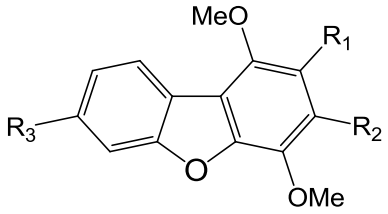

Name	R_1	R_2	R_3
β- pyrufuran	OMe	OH	H
α- pyrufuran	OH	OMe	H
γ- pyrufuran	OH	OMe	OH

Figure 1-5: Biphenyls and dibnezofurans isolated from *Sorbus, Pyrus* and *Malus* species.

P. communis cv 'Hendre Huffcup' produced dibenzofurans when infected with *Chondrostereum purpureum*, the fungus that causes silver leaf disease. Two dibenzofurans (α- and β-pyrufuran) were isolated from the transition interface between the healthy and infected tissues (Kemp et al., 1983). Three dibenzofurans (α-, β-, and γ-pyrufuran) were isolated from the cultivar 'Thorn' (Kemp and Burden, 1984). Kokubun et al., (1995) identified several dibenzofurans from several Pyrus species; β-pyrufuran, γ-pyrufuran from *P. communis*, γ-pyrufuran from *P. nivalis* and *P. ussuriensis,* and 2,8-dihydroxy-3,4,7-trimethoxydibenzofuran in all the aforementioned species. *P. pyraster* contained only the late compound. These compounds were isolated after artificial inoculation of the sap wood with fungal spores. It was concluded that *Pyrus* species are dibenzofurans producers, while *Malus* species are biphenyls producers (Kokubun and Harborne, 1995). However, grafted shoots of *P. communis* cv 'Conference' produced three biphenyls and a single dibenzofuran after inoculation of the shoot tips with *E. amylovora* (Chizzali et al., 2012c). Aucuparin, 2`-hydroxyaucuparin, and 3,4,5-trimethoxybiphenyl were the produced biphenyls, while noreriobofuran was the produced dibenzofuran. These compounds were detected in a dark-pigmented transition zone between the healthy and infected parts of the shoot. These paradoxes, about the production of biphenyls or dibenzofurans, can be attributed to the methodology. Different cultivars were

treated using different procedures (i.e. not the same fungus or bacterium) under different conditions.

Sap wood of *M. domestica* and *M. sieversii* accumulated aucuparin and 2`-methoxyaucuparin. The same compounds, in addition to 4`-methoxyaucuparin, were produced by *M. silvestris* (Kokubun and Harborne, 1995). However, other phenolic compounds not related to biphenyls were also reported in other cases. *M. fusca* and *M. sieboldii* accumulated the flavonoid chrysin. Aucuparin and a triterpene were isolated from a dark-pigmented interface between the healthy and the diseased wood tissues of *M. pumila* (Kemp and Burden, 1986; Kemp et al., 1985). Apart from these results, two other studies have shown a different response. The cell suspension cultures of a scab-resistant cultivar produced biphenyls and a dibenzofuran when treated with yeast extract. Three biphenyls were produced, namely, aucuparin, 2`-hydroxyaucuparin and 2`-*O*-β-D-glucopyranosylaucuparin, in addition to a dibenzofuran, malusfuran (2,4-dimethoxy-3-hydroxy-9-*O*-β-D-glucosyloxydibenzofuran) (Borejsza-Wysocki et al., 1999; Hrazdina et al., 1997). In addition to the last report, grafted shoots of *M. domestica* cv 'Holsteiner Cox' accumulated biphenyls and dibenzofurans when infected with *E. amylovora* (Chizzali et al., 2012c). Phytochemical analysis of a transition zone, which was formed between the dead and healthy parts of the stem, led to identification of four biphenyls and two dibenzofurans. The four biphenyls were 3-hydroxy-5-methoxybiphenyl, noraucuparin, aucuparin and 2`-hydroxyaucuparin. The two dibenzofurans were eriobofuran and noreriobofuran. These compounds were absent from both the dead and healthy parts of the stem.

As far as it was tested, the phytoalexins, biphenyls and dibenzofurans, were isolated only from the sap wood or cortical tissue of the stem. The only two exceptions were *S. aucuparia* and *E. japonica.* As mentioned previously, leaves of *S. aucuparia* accumulated aucuparin upon challenging with mercury ions (Kokubun and Harborne, 1994). An interesting contrast was observed with *Eriobotrya japonica*, which accumulated eriobofuran in leaves (Miyakodo et al., 1985) and aucuparin in the shoots (Watanabe et al., 1982). These events were observed when fungal spores were used for inoculation. Interestingly, a different accumulation pattern took place by inoculation with bacteria (Morita and Nonaka, 2003). Aucuparin accumulated simultaneously with the lesion produced by the leaves. Then, it disappeared when the lesion stopped enlarging; simultaneously with this disappearance, eriobofuran started to accumulate. These events were observed with *P. syringae* pv. eriobotrya, a compatible (pathogenic) variety. However, when *P. syringae* pv. tabaci, an incompatible (nonpathogenic) variety was inoculated, only aucuparin was accumulated. As an explanation for that contrast, it was found that aucuparin strongly inhibit the incompatible variety more than eriobofuran did, but eriobofuran can inhibit the compatible variety more than aucuparin did. So, *Eriobotrya* can control the onset and the type of the phytoalexin produced, depending on the nature of the pathogen. Finallly, only *Sorbus* and *Eriobotrya* produce phytoalexins in leaves. Other species accumulate them in sap wood.

Apart from the family Rosaceae, magnolol (5,5'-diallyl-2,2'-dihydroxybiphenyl) was isolated as a phytolaexin from the twig cortical tissue of *Cercidiphyllum japonicum* (Cercidiphyllaceae) (Takasugi and Katui, 1986).

Beside their role as phytoalexins, biphenyls and dibenzofurans are reported as constitutive constituents in some species of Rosaceae. Aucuparin and eriobofuran were isolated from roots of *Pourthiaea lucida* (Abd El-Razeka et al., 2007). A biphenyl glycoside, 5,5`-dihydroxy-3`-methoxybiphenyl-2-*O*-β-D-glucopyranoside was isolated from the aqueous extract of leaves of *Eriobotrya japonica* (Jiang and Xuan, 2006). Six oxygenated biphenyls, named as fortuneanoside A-F, and six oxygenated dibenzofurans, named fortuneanoside G-L, are present in fruits of *Pyracantha fortuneana* (Dai et al., 2009; Dai et al., 2006, 2008). 2,8-Dihydroxy-3,4,7-trimethoxydibenzofuran was the main component of the methanol extract of the bark (mainly) and wood of *Crataegus pontica* (Kokubun et al., 1995c), while γ- and α-cotonefurans were isolated mainly from the bark and wood tissues of *C. monogyna* (Kokubun et al., 1995b). Lin and his group (2010) have isolated four dibenzofurans, namely, 2-hydroxy-3,4,6-trimethoxydibenzofuran, 2-hydroxy-3,4,9-trimethoxydibenzofuran, 2-hydroxy-3,4,6,9-tetramethoxydibenzofuran, and 1,2-methylenedioxy-3,4,6-trimethoxydibenzofuran, and three biphenyls, namely, 3-hydroxy-2`,5-dimethoxybiphenyl, 2`,3-dihydroxy-5-methoxybiphenyl, and 3-hydroxy-5-methoxybiphenyl from roots of *Rhaphiolepis indica.* Aucuparin and 2`-methoxyaucuparin were isolated from wood extract of *S. decora* (mainly sap wood), *S. scopulina, and S. americana* (no distinction about the nature of the tissue) (Narasimhachari and Von Rudloff, 1962, 1973). Esters of propionic acid and biphenyls were isolated from mature fruits of *S. domestica* (Termentzi et al., 2009).

As a phytochemical class, biphenyls and dibenzofuans are not widely distributed, however, their presence was recorded in some further plants. 3,5-Dimethoxybiphenyl and 3-hydroxy-5-methoxybiphenyl were isolated from roots of *Lindera fruticosa* (Lauraceae) (Song et al., 2006). Prenylated dibenzofurans were found to be the main components of the herb *Achyrocline satureioides* (Asteraceae) (Carney et al., 2002). Oxygenated dibenzofurans are components of the unripe fruits of *Rhodomyrtus macrocarpa* (Myrtaceae) (Igboechi et al., 1984; Trippett, 1957). Oxygenated dibenzofurans substituted with carboxylic groups are reported in *Allium cepa* (Liliaceae) (Carotenuto et al., 1998). Three biphenyls were isolated from *Trifolium repens* (Fabaceae) (Ghosal et al., 1988). Biphenyls and dibenzofurans are present in the trunk of *Berberis koreana* (Berberidaceae) (Kim et al., 2009). Three biphenyls were isolated from *Sassafras randaiense* (Lauraceae) (Fa-Ching et al., 1983) (Takasugi and Katui, 1986). A biphenyl derivative was found in the wood of *Salix caprea* (Salicaceae) (Malterud and Sandanger Dugstad, 1985). An isomer of aucuparin (4`-hydroxy-3,5-dimethoxybiphenyl) was isolated from roots and aerial parts of *Polygala vulgaris* (Polygalaceae) (Dall'Acqua et al., 2002). 3-Hydroxy-1,4,7-trimethoxydibenzofuran was detected in the dichloromethane and hexane extracts of *Hypericum revolutum* ssp. revolutum Vahl and *Hypericum choisianum* Wall. ex. N. Robson (Guttiferae), respectively (Shiu and Gibbons, 2009). A prenylated dibenzofuran was present in the stem bark of *Calophyllum panciflorum* (Guttiferae) (Ito et al., 1996). 3,4,5-Trimethoxy-4`-hydroxybiphenyl was isolated from the aerial part of *H. reflexum.* (Guttiferae) (Cardona et al., 1990). Aucuparin was found in leaves of *Kielmeyera coriacea* (Guttiferae) (Cortez et al., 2002). Prenylated biphenyls were present in *Clusia paralicola* (Guttiferae) (Seo et al., 1999). A series of prenylated biphenyls and a dimeric biphenyl were isolated from *Mourera flaviatilis* (Podostemaceae) (Burkhardt et al., 1992).

4. Biological activities of biphenyls and dibenzofurans

Antimicrobial activities of biphenyls and dibenzofurans against *V. inaequalis* and *E. amylovora* were studied only in two reports. One report studied the antifungal activity of malusfuran and its aglycone on spore germination and germ tube elongation of *V. inaequalis* (Hrazdina et al., 1997). It was shown that both had inhibitory activities, but the aglycone was more active. The second report studied the activity of a series of biphenyls and dibenzofurans on *E. amylovora* (Chizzali et al., 2012c). Thirteen biphenyls and four dibenzofurans were tested. Biphenyls were recorded to have higher antibacterial activity than dibenzofuran analogues, which have the same substitution pattern. 3,5-Dihydroxybiphenyl was recorded to be the most potent compound (MIC = 115 μg/ml). This was one of three studies that compared the activity of biphenyls to dibenzofurans in the same time on the same subject. In a second study, aucuparin and eriobofuran were compared against two varieties of *Pseudomonas syringae* (Morita and Nonaka, 2003). Aucuparin had higher antibacterial activity against *P. syringae* pv. tabaci (incompatible, nonpathogenic), while eriobofuran had higher antibacterial activity against *P. syringae* pv. eriobotrya (compatible, pathogenic). In the third study, the antifungal activity of aucuparin was compared to four dibenzofuan derivatives, namely, eriobofuran, 7-methoxyeriobofuran, 9-hydroxyeriobofuran and α-cotonefuran (Kokubun et al., 1995c). Their activities were found to have no significant differences and had inhibitory action on spore germination and germ tube development. The generalization concluded by Harborne (1997) that the antifungal activity of dibenzofurans is marginally greater than that of biphenyls is arguable because results of independent studies were compared to each others. Antifungal activity of biphenyls and dibenzofurans were assessed in a number of reports against other different fungal spores (Garcia Cortez et al., 1998; Kokubun et al., 1995a; Kokubun et al., 1995b, c, d; Miyakodo et al., 1985; Watanabe et al., 1982; Watanabe et al., 1990; Widyastuti et al., 1991; Widyastuti et al., 1992). They showed inhibitory action on spore germination and germ tube development. Regarding the activity against human pathogens, it was found that penicillin-resistant *Staphylococcus aureus* were more sensitive to aucuparin than penicillin-sensitive *S. aureus* (Cortez et al., 2002). 3-Hydroxy-1,4,7-trimethoxydibenzofuran had weak activity against different strains of *S. aureus*.

In addition to their antimicrobial activity, biphenyls and dibenzofurans have other pharmacological activities. Aucuparin, noreriobofuran and some other biphenyls were reported to have anti-inflammatory activity (Chen et al., 2009; Lin et al., 2010). They suppressed the production of the *N*-formyl-methionyl-leucyl-phenylalanine (fMLP)-induced generation of the superoxide anion, an inflammatory mediator produced by neutrophils. 3-Hydroxy-5-methoxybiphenyl had a moderate low density lipoprotein (LDL) antioxidant activity (Song et al., 2006). Achyrofuran, a prenylated dibenzofuran from *Achyrocline satureioides* (Asteraceae) has an antidiabetic activity (Carney et al., 2002). Biphenyl and dibenzofuran glycosides isolated from the fruit of *Pyracantha fortuneana* had tyrosinase inhibitory activity (Dai et al., 2006, 2008), and hence can be used in cosmetics in skin whitening preparations. Rhodomyrtoxins of the unripe fruits of *Rhodomyrtus macrocarpa* (Myrtaceae) are suspected to have toxic effects and to cause blindness (Igboechi et al., 1984; Trippett, 1957). Biphenyls from *Berberis koreana* have neuroprotective activity, as shown by inhibiting NO production in lipopolysaccharide (LPS)-activated BV-2 cells, a microglial cell line (Kim et al., 2009). A prenylated biphenyl

was found to have DNA strand-scission activity and modest cytotoxic activity (Seo et al., 1999). The above reports show the potential of these compounds and their derivatives to have pharmacological potential and to be useful for the pharmaceutical industry.

5. Biosynthesis of biphenyls and dibenzofurans

Although these constituents were extensively studied on the phytochemical level, their biosynthesis was poorly investigated.

5.1 Biphenyl synthase (BIS), the key enzyme

The scaffold of aucuparin was assumed to develop from the intramolecular cyclization of a polyketide intermediate as benzoic acid derivative (Sultanbawa, 1980). In yeast extract-treated *S. aucuparia* cell cultures, a polyketide synthase catalyzing such an activity was detected (Liu et al., 2004). It catalyzes the iterative condensation of benzoyl-CoA with three malonyl-CoAs to form a tetraketide intermediate, which, in turn, undergoes intramolecular C2 → C7 aldol condensation with loss of a carboxyl group to yield 3,5-dihydroxybiphenyl (Fig. 1-6). The enzyme was called biphenyl synthase (BIS). Its cDNA was isolated and heterologously expressed in *Escherichia coli* (Liu et al., 2007). It is a type-III polyketide synthase (PKS) and shares 53–66% amino acid sequence identity with plant type III PKSs. 3,5-Dihydroxybiphenyl is supposed to be the precursor of the biphenyls and dibenzofurans produced in *S. aucuparia* cell cultures. The rapid induction of *BIS* and its temporal expression profile after elicitation have confirmed its participation in the biosynthesis of the phytoalexins produced by the cultures (Liu et al., 2007, 2010). The preferred aroyl substrate for that enzyme (BIS1) is benzoyl CoA, while *O*-hydroxybenzoyl-CoA (salicoyl-CoA) is less accepted and led to formation of 4-hydroxycoumarin after a single extension reaction (Fig. 1-6). *m*-Hydroxybenzoyl-CoA was also accepted but the reaction yielded m-hydroxybenzoyl diacetic acid lactone. Later, two cDNA encoding additional isozymes were identified (Liu et al., 2010). They have the same properties except that salicoyl-CoA is the preferred substrate. However, no 4-hydroxycoumarin was identified in the cell culture of *S. aucuparia*, probably due to the absence of the starter substrate It could be detected only after feeding of the cultures with salicoyl-*N*-acetylcysteamine.

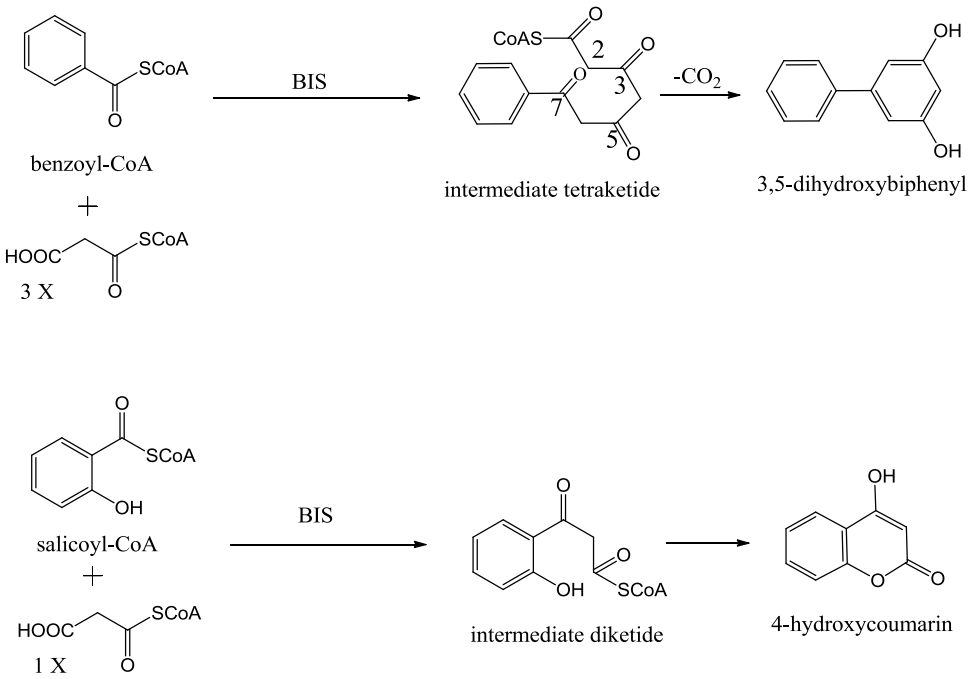

Figure 1-6: Reactions catalyzed by BIS enzymes.

Three cDNAs encoding BIS isoenzymes were cloned from fire-blight-infected shoots of *Malus domestica* cv. 'Holsteiner Cox' (Chizzali et al., 2012b). Only one of them, BIS3 was found to be selectively expressed in the transition zone and absent in the healthy part of the stem. Using immunofluorescence technique, it was found that BIS3 protein was localized in the cortical portion of the transition zone, and specifically at the junctions between neighboring cells. This may indicate the association of the protein with the plasmodesmata (Chizzali et al., 2012a; Chizzali et al., 2012b). Substrate utilization of these three isozymes was similar. They accepted both benzoyl-CoA and salicoyl-CoA to give 3,5-dihydroxybiphenyl and 4-hydroxycoumarin, respectively. They had slight preference to benzoyl-CoA.

cDNAs encoding BIS isoenzymes from *Pyrus communis* were also cloned and functionally characterized (unpublished data).

5.2 Postulated pathway

The detection of BIS activity and its molecular characterization has ended the debate about the origin of the C_6-C_6 skeleton of bipehnyls and dibenzofurans, whether they are derived from radical coupling of simple phenols (Kobayashi et al., 1994) or derived from the shikimate-acetate/malonate pathway via stilbene synthase-like enzymes (Cotterill et al., 1974). Now, it is established that 3,5-dihydroxybiphenyl could be the mother compound from which other known biphenyls are derived e.g. aucuparin, and noraucuparin. It would be a simple cascade of hydroxylation and methylation steps. However, the biosynthsis of dibenzofurans remains open. They are likely to have a derived skeleton, which has similar substitution patterns like biphenyls. However, their simultaneous production in a plant was not detected in the extensive studies led by Harborne, Kokubun and their workgroup (1995), which led the authors to suggest that both biphenyls and dibenzofurans follow parallel biosynthetic pathways, not sequential ones. However,

in the recent years, a few findings contradicting the basis of their suggestion have been accumulated. First, the cell suspension culture of the scab resistant *M. domestica* cv 'Liberty' produced biphenyls and dibezofurans simultaneously (Borejsza-Wysocki et al., 1999; Hrazdina et al., 1997). This finding led Kokubun to question his assumption later in a review article (Grayer and Kokubun, 2001). The authors of the earlier report have postulated a sequential biosynthesis of biphenyls and dibenzofurans in a later publication (Hrazdina and Borejsza-Wysocki, 2003). Hüttner et al. (2010) have reported the simultaneous accumulation of a wide array of biphenyls and dibenzofurans in *S. aucuparia* cell suspension cultures, treated with different elicitors. Morita and Nonaka (2003) have observed that eriobofuran accumulated simultaneously with the disappearance of aucuparin in leaves of *E. japonica,* inoculated with the compatible pathogen *P. syringae* pv. eriobotrya. Although interesting, a simultaneous coexistence has for a long time not been observed in an intact plant. Only recently, a simultaneous accumulation of both classes of compounds was observed in grafted shoots of *M. domestica* cv 'Holsteiner Cox' and *P. communis* cv 'Conference', inoculated with *E. amylovora*. All these findings led the authors to postulate a sequential biosynthetic pathway in a number of publications (Chizzali and Beerhues, 2012; Chizzali et al., 2012a; Hüttner et al., 2010). The postulated biosynthetic transformation is discussed in the following.

The conversion of biphenyls to dibenzofurans is assumed to involve two steps. First, biphenyls will be hydroxylated at the 2`-position to give 2`-hydroxybiphenyl derivatives. Isolation and detection of 2`-hydroxyaucuparin in most of the studied systems is a strong evidence for that postulation and the participation of such intermediates. Intarmolecular cyclization of these 2`-hydroxylated intermediates can proceed by an oxidative phenol coupling mechanism similar to cyclization of benzophenones to xanthones (Peters et al., 1997). Enzymes involved in these conversions could be a 2-oxoglutarate dependent dioxygenase for the hydroxylation step and NADPH-dependent cytochrome P450 monooxygenases for both the hydroxylation and cyclization steps (Fig. 1-7).

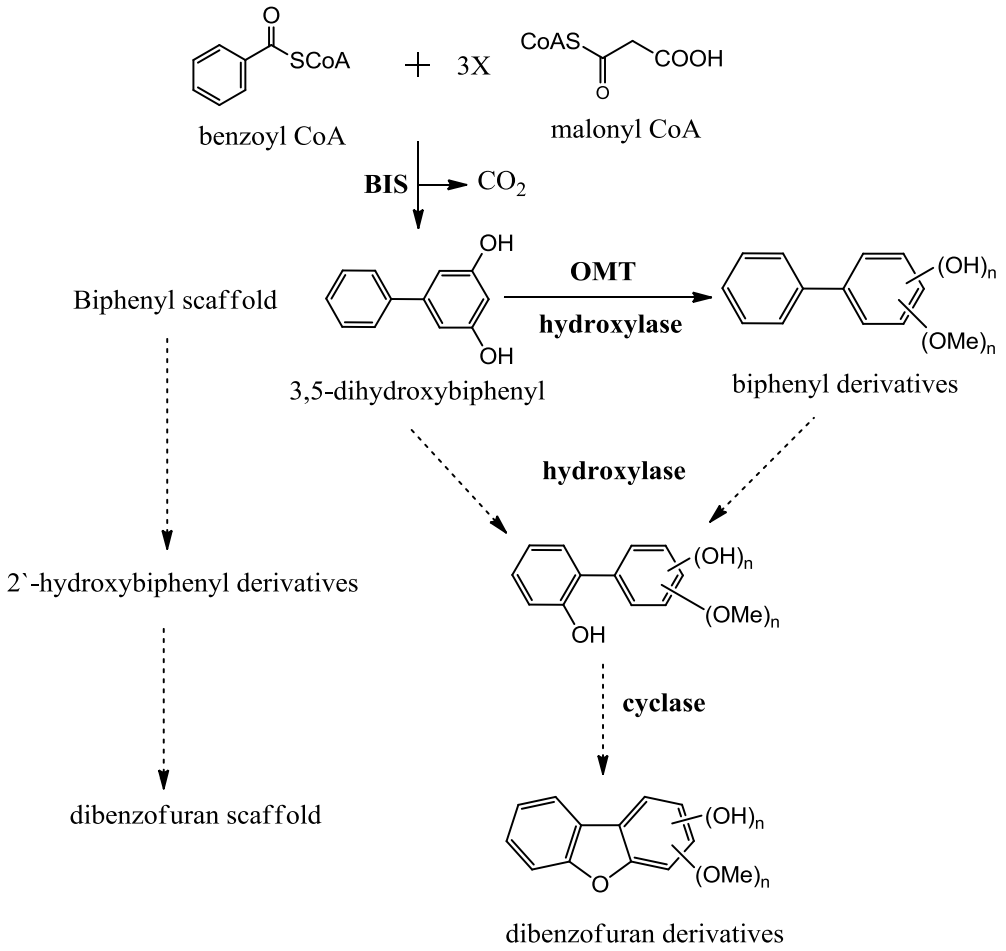

Figure 1-7: Sequential biosynthesis of biphenyls and dibenzofurans starting with the BIS reaction. Names of candidate enzymes are written in bold.

5.2.1 Cytochrome P450 (CYP) enzymes

These enzymes constitute a large group of membrane-bound heme-containing proteins. They have a characteristic absorption peak at 450 nm when they are treated with sodium dithionite and carbon monoxide. This gave rise to the nomenclature of P450 (P designates pigment). It had taken years to link this character to enzymes which are NADPH-dependent. These enzymes catalyze a plethora of different reactions, e.g. hydroxylation, alkylation, oxidation, deamination etc. Most of the enzymes are monoxygenases which catalyze the hydroxylation of the substrate (Chapple, 1998). They need molecular oxygen, which will be activated. One atom of this molecule is incorporated in the substrate and the other one is reduced to water. Some of these enzymes are anchored to the endoplasmic reticulum with their N-terminal anchor sequence, while the catalytic domain is in the cytosol. Electrons are delivered from NADPH via cytochrome P450 reductase (CPR) or from NADH via cytochrome b_5 (cyt b_5) and cytochrome b_5 reductase (Cb_5R). Few cytochrome P450 enzymes are soluble in the chloroplast and utilize electrons delivered by ferrodoxin (Fd) and ferrodoxin reductase (FdR) (Schuler and Rupasinghe, 2011). Classification of cytochrome P450 enzymes is based on their amino acid sequences. Those which share greater than 55% identity are grouped in the same subfamily, while those sharing greater than 40% identity are grouped in the same family. Enzymes are named with CYP, which stands for cytochrome P450,

then a number indicating the family, followed by a letter indicating the subfamily, and finally a number given for the sequence, e.g., CYP73A5, cinnamate-4-hydroxylase from *Arabidopsis thaliana* (Chapple, 1998; Schuler and Rupasinghe, 2011).

5.2.2 2-Oxoglutarate dependent dioxygenase

In contrast to cytochrome P450 enzymes, 2-oxoglutarate-dependent enzymes are soluble and heme-free. They are dependent on molecular oxygen and ferrous ions. The two oxygen atoms are incorporated, where one oxygen atom is incorporated in the substrate, while the other one is incorporated in 2-oxoglutarate, which gives succinate under release of carbon dioxide, as simplified in equations published by De Carolis and De Luca (1994).

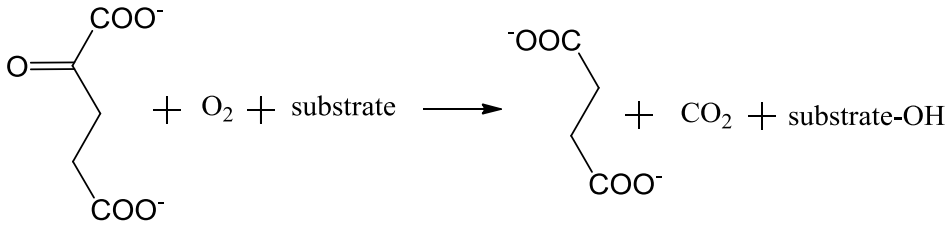

2-oxo-glutarate succinate

A classification of this large family with its diverse members has recently been published. This classification will help in predicting the function of the candidate sequence (Kundu, 2012)

5.2.3 O-methyl transferases (OMT)

Methyltransferases catalyze methylation of oxygen functionalities using S-adenosylmethionine as a co-factor. Plant MTs can be classified either on structural (Noel et al., 2003) or phylogentic bases (Lam et al., 2007). On structural basis, plant MTs are classified into three types. Type 1 MTs are OMTs that methylate hydroxyl groups of phenylpropanoids and their derivatives including chalcones, flavonoids, pterocarpan etc. Type 2 enzymes include CCoA OMTs which methylate caffeoyl and feruloyl CoA derivatives. Type 3 MTs are those which methylate the carboxyl group of benzoic and salicylic acids, and they also include alkaloid N-methyltransferases. On a phylogentic basis, plant OMTs are classified into two major groups A and B. Group A is subdivided into two sister clades. Group A1 encompasses CCoA OMTs, while group A2 encompasses carboxy OMTs. Group B contains the rest of OMTs, its subdivision into two clades B1 and B2 does not offer a sharp distinction in function between the members of the two clades. In both of the aforementioned classifications, it is obvious that the CCoA OMTs and carboxy OMTs are distinct from other OMTs and show a high degree of conservation regarding their structure and function. Other OMTs are COMTs and other phenylpropanoid, alkaloid, flavonoid OMTs. They are believed to have evolved later than CCoA OMTs and to be subjected to repeated evolutionary events which are reflected in the diversity of their substrates (Lam et al., 2007). Members of this group may show either a high degree of substrate specificity (Ibrahim et al., 1987; Willits et al., 2004) or a promiscuous one (Chiron et al., 2000; Frick and Kutchan, 1999; Kota et al., 2004; Maury et al., 1999; Parvathi et al., 2001; Wein et al., 2002)

6. Studied Pyrinae species

S. aucuparia is a deciduous, ornamental tree native to Europe and south of Asia. However, it is widely distributed also in North America. It is known as European mountain ash because of its wide distribution in mountain regions but it is not related to the true ash tree (*Fraxinus* species, family Oleaceae). This mixing was based on the similarity of the leaves of the two species and is reflected in the old German name 'Eberesche' (eber = false, Esche = ash). The tree is 8-10 m tall, rarely reaches 20 m. It has compound pinnate leaves, with 5-7 pairs of leaflets, which are oblong and have serrate margin. The showy creamy white flowers appear in May - June. The fruits are arranged in clusters of yellow to bright red pomes. They are wrongly called berries because of their juicy flesh. These fruits are so attractive and considered as attractant to birds, which is referred to by the German name 'Vogelbeere' and the Latin name aucuparia (avis: bird, captare: catch) (Fig. 1-8A). This fruit has received much attention. It contains an irritant, parasorbic acid, which causes irritation to the mucous membrane of the stomach and intestine. This can lead to salivation, vomiting and, in severe cases, gastritis and diarrhoea (Storm, 1998). However, it transforms in the nontoxic sorbic acid by cooking or drying (Fig. 1-8B). The fruits are classified as weakly toxic. They are used in preparing jams and jellies because of their slightly bitter taste. The fruits are a rich source of vitamin C, provitamin A, chlorogenic and neochlorogenic acids and flavonoids (Gil-Izquierdo and Mellenthin, 2001). The variety 'Edulis' has more sweet taste than the wild one. Now other sweet rowan varieties are available. They are hybrids of *S. aucuparia* with *Malus*, *Pyrus*, *Aronia*, or *Mespilus*. Their phenolic content as well as their antioxidant activities are assessed. The sweet varieties have more anthocyanin content and less caffeoylquinic acids, but they do not differ much in the biological activity from the wild type (Hukkanen et al., 2006; Kylli et al., 2010).

S. aucuparia cell suspension cultures were an asset to study the phytoalexins produced in the subtribe Pyrinae. As already discussed, BIS activity was first detected from this cell culture and its encoding cDNA was first isolated and cloned. The produced biphenyls and dibenzofurans are somewhat representative to those found in apple and pear, the economically important members of the Pyrinae. Simultaneous accumulation of biphenyls and dibenzofurans is a good start for testing the reliability of the postulated pathway. Differential production of these phytoalexins with varying the elicitor could give insights in signal transduction. Several general advantages can be added. The cell cultures are an isolated system that can easily be controlled to avoid the interference with other environmental and nutritional stress factors. Analytical, biochemical and molecular biology approaches can be easily applied. However, one can not get information about the full sequence of events of plant-pathogen interactions.

A

B

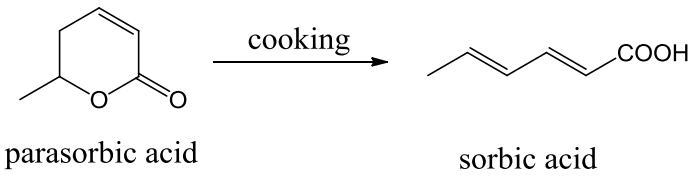

parasorbic acid sorbic acid

Figure 1-8: Leaves, flowers and fruits of *S. aucuparia* (A). Conversion of parasorbic acid upon cooking (B).

7. Scope of the work

Biphenyls and dibenzofurans are the phytoalexins of the economically important rosaceous subtribe Pyrinae. However, little is known about their biosynthesis and, consequently, the molecular factors controlling their production and accumulation. Without the thorough understanding of the biochemical and molecular aspects of this pathway, genetic approaches to manipulate and promote the production of these phytoalexins, and hence this resistance strategy of these plants, will be far from possible. The aim of this thesis is to study the biosynthesis of these phytoalexins at both the enzyme and the gene level. *S. aucuparia* cell cultures will be used for these investigations as a facile system for biochemical and molecular studies. Moreover, the phytoalexins produced are good representatives of those that are formed by apple and pear. The starting point is that 3,5-dihydroxybiphenyl may be the precursor of all the produced phytoalexins. The following different approaches will be applied.

- Feeding experiments using the radioactive tracer 3,5-dihydroxybiphenyl, aimed at testing whether this compound is really the precursor of all biphenyl phytoalexins and, in addition, of dibenzofurans.
- Enzyme assays by incubating possible substrates and intermediates with different protein preparations (microsomal fraction, crude protein extract) in

the presence of different cofactors, aiming to elucidate the detailed biosynthetic steps and the enzymes involved.

- Isolation, cloning, and functional characterization of cDNAs encoding the detected metabolizing enzymes, which is an essential prerequisite for a future manipulation of the expression of these genes.

The ultimate aim is to improve our understanding of the phytoalexin defense response, so that biotechnological approaches can be successfully applied in the future.

II.Material

1. Biological

1.1 Plant Material

Cell suspension cultures of *Sorbus aucuparia* were grown in the dark by 25°C as described before (Liu et al., 2004).

1.2 Fungus

Venturia inaequalis (Cooke) was ordered from DSMZ (Deutsche Sammlung von Mikroorganismen und Zellkulturen). It was designated with the DSM numbers 1002 and D 27, isolated from *Pyrus malus*. It was supplied on malt extract-peptone slant agar.

2. Chemicals

Chemicals, unless otherwise mentioned, were purchased from the following companies: Roth, Sigma-Aldrich, Applichem, Fischer Scientific, Fluka. Deionized water supplied by a Milli-Q water purification system (Sartorius, Germany), was used in preparing all aqueous solutions used in the study. All solutions were autoclaved by 120°C for 20 min. Solutions of thermolabile compounds were sterile-filtered and added to autoclaved solutions under sterile conditions. All salts required for the plant or bacterial culture media were supplied from Roth or Applichem.

Chemical	Supplier
Phytohormones	
2,4-dichlorophenoxyacetic acid (2,4-D)	Fluka
1-naphtylacetic acid (NAA)	Fluka
For fungal culture medium	
Soya peptone	Applichem
Malt extract	Applichem
For bacterial culture Medium	
Yeast	Applichem
Peptone (casein)	Roth
Na Cl	Roth
Agar	Applichem
KH_2PO_4	Roth
K_2HPO_4	Roth
$MgSO_4.7H_2O$	Roth
Glycerol	Roth
Elicitors	
Yeast extract	Applichem
V. inaequalis extract	prepared in our laboratory (Zhang et al., 2000)
Chemicals required for protein extraction and purification from cell culture	
Polyclar®AT	Serva
Seesand	Roth
DTT (dithiothreitol)	Applichem

Stationary phases used in protein desalting and affinity purification	
PD_{10}-cartidge Sepharose G-25 columns	GE Healthcare
Nickel-nitrilotriacetic acid	Qiagen
Chemicals for Enzyme Assays	
NADPH	Applichem
S-adenosymethionine dihydrochloride	Sigma-Aldrich
Benzoyl-CoA, malonyl-CoA	Sigma-Aldrich
Malonyl CoA [2-^{14}C]	ARC American Radiolabeled Chemicals
Benzoic acid [ring-^{14}C]	ARC American Radiolabeled Chemicals
3,5-dihydroxbiphenyl	Lab collection (Chizzali et al., 2012c)
3-hydroxyl-5-methoxybiphenyl	Lab collection (Chizzali et al., 2012c)
Caffeic acid	Roth
5-hydroxyferulic acid	Rare Chemicals GmbH
Pinosylvin	Sigma-Aldrich
Resveratrol	Selleckchem
Reagents for biochemistry and molecular biology	
IPTG	Applichem
dNTPs	Thermo Scientific
Imidazole	Roth
Tris-HCl	Roth
Antibiotics	
Ampicillin	Roth
Chloramphenicol	Applichem
Reagents for GC-MS derivatization	
N-methyl-N-(trimethylsilyl)trifluoroacetamide (MSTFA)	ABCR
Reagents for gel electrophoresis	
peqGold universal agarose	Peqlab
Ethidium bromide	Roth
Acrylamide/Bisacrylamide 30%	Bio-Rad
TEMED	Bio-Rad
Ammonium persulfate	Roth
SDS	Roth
β-mercaptoethanol	Roth
Bromophenol blue	Sigma-Aldrich
Commassie-blue R250 and G250	Merck
Solvents for HPLC	
Methanol, Acetonitrile	Fischer Scientific
Ladder	
Gene Ruler DNA ladder Mix	Thermo Scientific
PageRuler Unstained Protein Ladder	Thermo Scientific

3. Nutrient Media

3.1 Nutrient medium for plant cell culture

LS medium (Linsmaier and Skoog, 1965)

Stock solution composition		**Supplier**
Macro elements (10X)	g/l	
KNO_3	19.0	Roth
NH_4NO_3	16.5	

$CaCl_2.2H_2O$	4.4	
$MgSO_4.7H_2O$	3.7	
KH_2PO_4	1.7	
$Na_2EDTA.2H_2O$	0.41	
$FeSO_4.7H_2O$	0.28	
Micro elemnts (1000X)	**g/l**	Roth
$MnSO_4.H_2O$	16.9	
$ZnSO_4.7H_2O$	10.6	
KI	0.83	
H_3BO_3	6.2	
$Na_2MoO_4.2H_2O$	0.25	
$CuSO_4.5H_2O$	0.025	
$CoCl_2.6H_2O$	0.025	
Vitamins (100X)	**mg/100 ml**	
Thiamine-HCl	4	Serva
Myo-inositol	1000	Roth
Hormones	mg/ml (absolute ethanol)	
2,4-D	1 (220µl/l medium)	Fluka
NAA	1 (186µl/l medium)	Fluka
Sucrose	30 g /l medium	Fluka

The pH is adjusted to 6.0-6.3.

3.2 Bacterial culture media

Medium	**Composition**	
LB medium	Peptone (casein)	10 g/l
	Yeast extract	5 g/l
	NaCl	10 g/l
For solid medium	Agar	1%
SOC Medium	Peptone (casein)	20 g/l
	Yeast extract	5 g/l
	1 M NaCl	10 ml/l
	1M KCl	10 ml/l
	Autoclave and then add the sterile filtered solution of	
	2 M Mg^{2+}	10 ml/l
	2 M glucose	10 ml/l
For induction of protein expression	IPTG (Isopropyl-β-D-thiogalactopydranoside)	0.12 g/ml (0.5 M)
	Final concentration in bacterial culture	0.5 mM
Antibiotic for selection of transformed bacteria	Ampicillin (0.269 M) (100 mg /ml aqueous soln.)	
	Chloramphenicol (0.093 M) (30 mg/ml soln. in ethanol)	
For preservation of bacterial culture	Glycerol:LB (Medium 60:40)	250 µl
	Bacterial culture	750 µl

3.3 Fungal culture media

Malt extract pepton

Medium	**Composition**
Malt extract peptone	Malt extract 30 g/l
	Pepton Soya 3 g/l
For solid medium	Agar 1.5%

4. Buffers and solutions

4.1 Buffers used for gel electrophoresis

DNA- agarose electrophoresis

50X TAE buffer	Tris-HCl	2 M
	EDTA	0.05 M
	Adjust pH to 8 with glacial acetic acid	

To examine DNA products less than 300 bp, 2% agarose gel was prepared; for larger sizes, 1% agarose gel was prepared.

SDS-PAGE electrophoresis

Staking gel (for 2 small gels)	Water	2.72 ml
	1 M Tris-HCl (pH 6.8)	504 µl
	30% Acrylamide/Bis	664 µl
	10% (w/v) SDS	40 µl
	10% (w/v) APS	40 µl
	TEMED	4 µl
Resolving gel (for 2 small gels)	Water	2.3 ml
	1.5 M Tris-HCl (pH 8.8)	1.75 ml
	30% acrylamide/Bis	2.8 ml
	10% (w/v) SDS	70 µl
	10% (w/v) APS	70 µl
	TEMED	2.8 µl
Protein loading buffer (2X)	Water	2.7ml
	0.5 M Tris-HCl (pH 6.8)	1.0 ml
	Glycerol	2.0 ml
	10% (w/v) SDS	3.3 ml
	β-mercaptoethanol	0.5 ml
	0.5% (w/v) bromophenolblue	0.5 ml
SDS-electrode buffer (10X)	Tris base	15 g
	Glycine	72 g
	SDS	5 g
	Water	ad 500 ml
Staining solution	Coomassie blue R-250	1 g
	Mathanol	500 ml
	Acetic acid	75 ml
	Water	ad 1000 ml
Destaining solution	Methanol	200 ml
	Acetic acid	76 ml
	Water	ad 1000 ml

4.2. Buffers and solutions for protein purification

Buffers for extraction and purification of His_6-tagged fusion protein

Lysis buffer	50 mM Na_2HPO_4	3.44 g
	30 mM NaCl	0.87 g
	20 mM Imidazole	0.68 g
	Water	ad 500 ml
Washing buffer	50 mM Na_2HPO_4	3.44 g
	1.5 mM NaCl	0.04 g
	50 mM Imidazole	1.7 g
	Water	ad 500 ml
Elution buffer	50 mM Na_2HPO_4	3.4 g
	300 mM NaCl	8.76 g
	250 mM Imidazole	8.51 g
	Water	ad 500 ml

4.3 Buffers for plasmid isolation (miniprep)

Buffer I (pH 8)	Tris-HCl	50 mM	1.5 g/250 ml
	EDTA	10 mM	0.93 g/250 ml
	RNase A	10µl/ml	
	RNase A was aded freshly benfor use		
Buffer II	NaOH	0.2 M	2 g/250 ml
	SDS	1% (w/v)	2.5 g/250 ml
Buffer III (pH 5.5)	K acetate	2.55 M	62.57 g/250 ml
	Glacial acetic acid to adjust pH		

4.4 Solutions for protein determination

Bradford-dye solution	Coomassie-brilliant blue G-250	100 mg	Dissolve the coomassie blue powder in ethanol and o-phosphoric acid by stirring, and then complete volume with water. Filter and keep protected from light by 4°C.
	Ethanol 96%	50 ml	
	o-phosphoric acid 85% w/v	100 ml	
	Water	ad 1000 ml	

4.5 Solutions for PD_{10} washing and Ni-NTA agarose regeneration

PD_{10} washing solution NaOH (0.15 M)	Wash with 25 ml (5x column volume) then wash with water till getting a neutral eluent.
Ni-NTA agarose washing and regeneration solution. Wash with the following solutions in the same order.	0.2 M acetic acid 30% glycerol Deionized water

5. Materials for molecular biology

5.1 Host cells and cloning vectors

E. coli strain	Genotype
DH5α deliver high yield plasmid preparation for downstream applications chemically competent	*F' φ80δlacZ9M15 end A1hsdR17(rk-mk+)supE44thi-1 λ-gyrA96 relA19(lacZYA-argFV169) deoR*
BL21(DE3)pLysS For protein overexpression (Invitrogen) Chemically comptent	*F-, ompT hsdSB (rB- mB-) gal dcm (DE3) pLysS (CamR)*

5.2 Vector

pRSET-B vector (protein expression)	Invitrogen

5.3 Primers

Label	Sequence
Primers used to amplify the cDNA sequences	
*Sa*OMT1 for BamHI	5`-ATTGGATCCGATGGCTTCTCTAGAGGAACCAAAAGG-3`
*Sa*OMT1 rev HindIII	5`-AGGAAGCTTCTACTTGTAGAATTCCATGAYCCARAGATTAG-3`
*Sa*OMT2 for BamHI	5`-ATTGGATCCGATGGGTTCGACCSBAGAGACTC-3`
*Sa*OMT2 rev HindIII	5`-AGGAAGCTTTCAAATTTTCTTAAGAAAYTCAATGRCATAGRTGTKG-3`
OMTC for BamHI	5`-ATTGGATCCGATGGAAATGCAGGAAGMAMCAGAARTTGAG-3`
OMTC rev HindIII	5´- AGGAAGCTTTTACATAGGGTAGGCCTCAACAATGGAT-3´
Primers used for real-time quantitative RT-PCR and semi-quantitative RT-PCR	
*Sa*OMT1 Q-PCR for	5`-CCAAAAGGCCTTCCTGACATTCCTC-3`
*Sa*OMT1 Q-PCR rev	5`-CTGCATGGAGAAGGACAGCACTG-3`
*Sa*OMT2 Q-PCR for	5`-ATGGGTTCGACCCTAGAGACTCAG-3`
*Sa*OMT2 Q-PCR rev	5`-GAGAATGGAGCCGCTGGCTAG-3`
Actin Q-PCR for	5`-CTCCCTCATGCCATCCTTCGTTTG-3`
Actin Q-PCR rev	5`-CCTCACAATTTCCCGCTCAGCAGT-3`
Tubulin Q-PCR for	5`- CAACCTCAACCGCCTTGTGTCTC-3`
Tubulin Q-PCR rev	5`-GGATTCTGGGGTATGGGACCAAG-3`
BIS1 Q-PCR for	5`- GCGCCTTTGGTTAAGAATCATGGAG-3`
BIS1 Q-PCR rev	5`-GTCTTTTTGGTAGTAGACGTTTGGTGG-3`

for. forward; rev. reverse; restriction sites are underlined.

5.4 Enzymes

Name	Purpose	Supplier
RevertAid H Minus Reverse transcriptase	Reverse transcription	Thermo Scientific
Phusion Hot Start II High fidelity DNA polymerase	High fidelity amplification of DNA	Thermo Scientific
peqGold PureTaq DNA polymerase	Amplification of DNA (used in semiquantitative PCR)	Thermo Scientific
Bam HI, HindIII	Production of sticky ends	Thermo Scientific
T4-DNA ligase	Ligation	Thermo Scientific
RNase A	Digestion of RNA by plasmid isolation	Thermo Scientific
RNase-free DNase I	Digestion of genomic and contaminating DNA by RNA isolation	Qiagen

5.5 Kits

Rneasy® Plant mini Kit	RNA isolation	Qiagen
innuPREP DDOUBLE PURE KIT	purification of PCR product; restriction product or DNA from gel	Analytik Jena biosolutions
Maxima first strand cDNA synthesis Kit for RT-qPCR	Preparation of cDNA for real time qRT-PCR	Thermo Scientific
Maxiam SYBR green qPCR Master Mix	Real-Time Quantitative PCR	Thermo Scientific

6. Equipment

Equipment	Model	Company
Balance LA 230S Sartorius	Germany	Balance LA 230S Sartorius
Autoclave	Vx-120 Systec GmbH	Labor systemtechnik Systec
pH meter	Digital pH meter 325	WTW
Centrifuge	Universal 32R	Hettich
	Biofuge 13 Heraeus Sepatech	Biofuge 13 Heraeus Sepatech
	Sigma 1-15K	Sigma Centrifuges
-80°C freezer	Hera Freeze	Heraeus
Spectrophotometer	Ultrospect 1000	Pharmacia Biotech
Incubator shaker	HT	Infors HT
Thermo block Dri	Block DB-3	Techne
Water purification system	Arium 611 VF	Sartorius, Germany
Clean bench	LaminarAir HLB 2472	Heraeus
	Laminar Air HBB 2460	Heraeus
Heating circulator water bath	MW-4	Julabo

Magnetic rotator	VF2	IKA-Labortechnik (Janke & Kunkel)
Ultrasonic Cell- Disruptor	Sonifier 250	Branson (G. Heinemann)
PCR cycler	T-Proffessional Gradient	Biometra
Real- Time PCR	7500 Fast Real-Time PCR Systems	Applied Biosystems
Gel documentation MultiImage TM	Light Cabient	Alpha In. Corp
Electrophoresis	Mini-Sub Cell	BioRad
	Sub Cell GT	BioRad
	Protein Chamber	Biometra
LSC (Liquid Scintillation counter)	LS 6500	Beckman Coulter, USA
GC-MS	• 6890 gas chromatograph • Jeol Mass spectrometer • ChemStation software	Agilent
	ZB-5 MS (30m, 0.25mm i.d., 0.25 µM ft)	Phenomenex
HPLC	Elite LaChrom series • L-2200 autosampler • quaternary L-2130 Pump equipped with low-pressure gradient • L-2455 diode array detector • EZChrome Elite software	VWR-Hitachi
	HyperClone ODS column (C18, 150 x 4.6 mm, 3µm)	Phenomenex
HPLC for analysis of radiolabeled products	Agilent 1200 series • Agilent HP 1200 binary pump • Agilent HP 1200 autosampler • Agilent 1200 variable wavelength detector. • Gina Star 4.06 software.	Agilent
	Ramona Star radiodetector with soild scintillation analysis cell quartz tube (5.5 mm, 0.37 ml, particle size 45-63 µm)	Raytest GmbH,
	Lichrospher 100 RP 18 E (150 x 4.6 mm, 5 µm)	WICOM

III. Methods

1. Establishment of *V. inequalis* culture and preparation of the elicitor

1.1 Fungal culture

V. inaequalis grew on malt extract peptone agar plates in form of circular to orbicular mycelial colonies. These are cottony yellow-green to olive green and mycelium turns into grey-black to black upon aging. Plates are kept in the dark by 24°C and subdivided every 3-4 weeks by transferring the scrapped mycelia on new media. Sometimes, scrapped mycelia were transferred to 1 ml liquid medium and stored at -80°C, after mixing with 80 % glycerol in a ratio of 625 µl liquid suspension and 375 µl glycerol 80%. Liquid cultures were used to get a large mass of fungal material, enough for the preparation of the elicitor. Freshly scrapped or frozen mycelia were transferred to 50 ml malt extract peptone media in 250 ml flasks. The cultures were kept in the dark by 20 °C and shaken at 95 rpm. They developed in black mycelial pellets.

Figure 2-1: *V. inaequalis* culture. (A) Mycelial colonies on agar plates. (B) Mycelial pellets in liquid medium.

1.2 Preparation of the elicitor (*V. inaequalis* extract)

It is based on extracting the oligosaccharide constituents of the mycelial cell wall, which can elicit the plant defense response. The preparation is based on a method described by Zhang et al. (2000). The liquid cultures were filtered through a Buchner funnel under sterile conditions and washed with autoclaved water. The mycelial pellets were weighed, then ground with acidified water (pH 2) in an autoclaved mortar, then diluted with 50 ml acidified water and boiled for 1 h. After cooling, the extract was filtered through cotton, and then centrifuged. The supernatant was adjusted to pH 5 and then sterile-filtered. The extract is pale yellow in color. The carbohydrate content of the extract is determined colorimetrically by the phenol-sulphuric acid method (Saha and Brewer, 1994). A standard curve was constructed using serial concentrations of glucose. The carbohydrate content of the extract was determined by extrapolation. For elicitation of cell culture, volumes containing 2.7 mg were added to each 50 ml *S. aucuparia* culture (approximately 55 mg/l final concentration).

2. Stabilization of *S. aucuparia* cell suspension cultures

Callus of *S. aucuparia* was initiated from young shoots (Liu et al., 2004). The yellow green callus mass grows on LS medium. Friable masses were transferred to 50 ml LS liquid medium in 250 ml culture. Cell suspension cultures are kept in the dark by 25°C and shaken at 130 rpm. Subdivision was done every 14 days, by transferring 3 g of cells into fresh medium.

3. Elicitation of *in vitro* cultures

Yeast or *V. inaequalis* extracts were used to elicit five-day-old cell cultures (in the linear growth phase). Both extracts were added under sterile conditions. *V. inaequalis* extract was added to a final concentration of 55 mg/l culture, while yeast extract was added to a final concentration of 6 g/l culture. These concentrations were established to give the best response (Hüttner et al., 2010).

4. Time course accumulation of phytoalexins

This experiment was done with 50 ml cell suspension cultures treated with *V. inaequalis* extract. Aliquots (10 ml culture) were taken under sterile conditions at different time points. Preparation of samples for GC-MS analysis and quantification were carried out as described previously (Hüttner et al., 2010). Cells were separated by centrifugation then lyophilized. Dry weight of cells was determined, aliquots of 50 mM 4-phenylphenol (0.02 g) were added as internal standard, then cells were suspended in methanol (7 ml) and extracted by vortexing (1 min) and sonication (3 min). The extraction process was repeated two times more. The methanolic extracts were combined, evaporated to dryness. The residues were extracted with 1 ml ethyl acetate (HPLC grade). Aliquots (300 µl) were transferred to inlets of HPLC vials and left to evaporate. The residue was silylated with 50 µl N-methyl-N-(trimethylsilyl)trifluoroacetamide (MSTFA; ABCR, Karlsruhe, Germany) at 60 °C for 30 min. Silylated samples were analyzed by GC-MS using the following temperature program: 70°C for 3 min, then linear increase of temperature from 70°C-310°C over 24 min (10°C/min) and finally 310°C for 5 min. Helium gas was the carrier gas with a flow rate of 1 ml/min. The injection volume is 1 µl with split ratio 1:10. Quantification of individual compounds was done based on the internal standard 4-phenylphenol. A response factor of 1 was assumed for all compounds, and data are expressed as mg/g DW. Data represent three technical repeats for one biological sample, which in turn is representative for three biological samples.

5. Feeding experiment

5.1 Enzymatic preparation of generally radiolabeled 3,5-dihydroxybiphenyl

Radiolabeld 3,5-dihydroxybiphenyl was prepared by using biphenyl synthase enzyme (BIS). BIS catalyzes the iterative condensation of 3 units of malonyl-CoA and 1 unit of benzoyl-CoA. Radiolabeled malonyl-CoA was commercially available;

so, it was used in the enzyme reactions. Benzoyl-CoA was used in the enzyme reaction at 10 times its K_m value. Equimolar combinations of hot and cold malonyl-CoA at varying concentrations were tested for the maximum incorporation of radioactivity into 3,5-dihydroxybiphenyl. It was found that equimolar amounts of cold and hot malonyl-CoA at two times the K_m value gave the maximum incorporation rate (61.2%). So we have modified the preparation of radiolabeled 3,5-dihydroxybiphenyl described by Liu et al (2004), as will be herein mentioned. Enzyme assays (200 µl) were composed of 7 µl [2-^{14}C] malonyl-CoA (1.27 nmole, 0.07 µCi, 55.2 mCi/mmol), 1.15 nmole malonyl-CoA, 7.4 µM benzoyl-CoA in 0.1 M phosphate buffer (pH 7) and 3 µg BIS. Incubations were left for 30 min by 35°C. The reaction was stopped with 40 µl 10% HCl and the product was extracted twice with 200 µl ethylacetate. Products of 20 incubations were combined to get a satisfactory yield, then evaproted and redissolved in least amount of methanol. Aliquots were taken to measure radioactivity by scintillation. It was inconvenient to purify the product (3,5-dihydroxybiphenyl) further because of the low yield and the moderate stability of the product, however, its identity was confirmed using HPLC. The product was freshly fed to the cell culture.

5.2 Feeding experiment and HPLC analysis

Cells (0.3 g) were inoculated into 5 ml LS medium in 25 ml Erlenmeyer flasks. On the fifth day, the culture was elicited with the extract of *V. inaequalis*. Four and a half hours later, 117 µl methanolic solution of labeled 3,5-dihydroxybiphenyl (0.52 µCi) was fed to the culture under sterile conditions. The later time point was chosen for feeding to avoid possible feedback inhibition of 3,5-dihydroxybiphenyl on *in vivo* BIS. Seventy-two hours later, the cell cultures were centrifuged to separate cells from the culture medium. The supernatants were extracted three times with equal volumes of ethyl acetate. However, no significant labeled products were detected in the medium, so it was not investigated further. Cells were homogenized in methanol (4 ml) and centrifuged. Residue was extracted further by vortexing in methanol and then centrifugation; this was repeated three times. The methanolic extracts were combined and evaporated, and the residues were redissolved in methanol (HPLC grade). Aliquots were taken for HPLC analysis on Agilent 1200 series and radioactivity was measured by scinitillation. The mobile phase consisted of water containing 0.1% formic acid (A) and methanol (B). Gradient elution was used as follows:

Time (min)	Methanol (B) %
0	45
27	45
28	90
33	90
34	45
44	45

5.3 Measuring of radioactivity by scintillation

The principle of liquid scintillation counting depends on mixing the liquid sample with a scintillation cocktail which consists of solvent, emulsifier and a solute (fluor). The energy from β-rays decay is transferred to the fluor which in turn will emit photons of light; the signal is amplified by a photomultiplier tube and converted into an electric pulse which is proportional to the amount of radioactivity.

For measuring the radioactivity, aliquots (2-100 µl) is mixed with 3 ml scintillation cocktail, shaken and then measured.

6. Protein extraction and preparation of microsomal fraction

Cell cultures were harvested 19 h after treatment with elicitors. Cells (30 g) were mixed with seesand (50% w/w), polyclar AT (10% w/w) and homogenized in 0.1 M Tris-HCl buffer (6 ml, pH 7) containing DTT (10 mM) and PMSF (10 µM), in a mortar for 15 min. Cell homogenates were centrifuged at 9.000 × g for 25 min. Supernatant was filtered through PD_{10} column, which was already equilibrated with 25 ml buffer (5 x elution volume of column). This crude protein extracts were used in testing activities of *O*-methyltransferase and hydroxylase activities. To prepare the microsomal fraction, the crude extract was centrifuged at 100.000 × g for 90 min. Microsomal pellets were suspended in 0.1 M Tris-HCl buffer (pH 7) containing sucrose (14% w/v), β-mercaptoethanol (3.5 mM) and PMSF (10 µM). Pellets can be stored in -80°C with no decrease in activity. The additives help to protect the protein integrity. DTT protects free thiol groups from being oxidized. PMSF is an inhibitor of serine protease, which is commonly present in plants. Polyclar AT adsorbs phenolic compounds, which can be polymerized by phenol oxidases from plants to give protein denaturing polymers. Sucrose can replace glycerol as a cryoprotectant; it was used here to avoid increasing the viscosity of the microsomal fraction. Protein concentrations in the crude extract as well as microsomal fraction were determined colorimetrically using Bradford's reagent.

7. Determination of protein content

Colorimetric measurement of protein was carried out using the Bradford protein assay (Bradford, 1976). Coomassie Brilliant Blue G-250 interacts with aromatic and basic amino acids of the protein. The negative charged sulfonate anions of the dye give charges to cationic amino acids which results in exposure of the hydrophobic part of the protein which interacts by the phenyl residues of the dye by van der Waals forces. Upon interaction with protein, the absorption maximum of the dye shifts from 465 nm (red, free form) to 595 nm (blue, bound form). An standard curve is constructed using serial dilutions of bovine serum albumin solution (1 mg/ml). Measured samples consisted of 900 µl Bradford solution completed to 1 ml with the protein solution and the buffer. The blue color reached maximum after two minutes and is stable for 1 h.

8. Enzyme assays

8.1 For O-methyltransferase activity

The incubation mixture (200 µl) consisted of 15 µM possible substrate (3,5-dihydroxybiphenyl; 3-hydroxy-5-methoxybiphenyl; noraucuparin; aucuparin; 2,4-dihydroxydibenzofuran; 2-methoxy-4-hydroxydibenzofuran), S-adenosylmethionine (50 µM) and ascorbic acid (1.5 mM) in 0.1 M Tris-HCl buffer (pH 8.5). The reaction was initiated by addition of cell-free crude protein (40 µg) and the incubation left by 37°C for 20 min. The reaction was stopped by addition of 10% HCl (40 µl). The reaction product was extracted by ethyl acetate (2 × 200 µl), and

then the extract was evaporated to dryness. The residue was dissolved in 60 µl methanol and prepared for HPLC analysis.

In case of SaOMT1

Enzyme assays consisted of 0.65 µg purified protein SaOMT1 incubated in a final volume of 200 µl Tris-HCl buffer (0.1 M, pH 8.5) with 0.24 mM SAM, 0.15 M ascorbic acid and 137.5 µM presumed substrate. Calculations of the kinetic values was carried out using varying concentrations of 3,5-dihydroxybiphenyl (2.5-150 µM) and 2,4-dihydroxydibenzofuran (3.75-150 µM). After 25 min by 35°C, enzyme reactions were stopped by adding 40 µl 10% v/v HCl and the enzyme product was extracted and analyzed as mentioned above.

In case of SaOMT2

Purified SaOMT2 protein (0.6 µg) was incubated in 200 µl Tris-HCl buffer (0.1 M, pH 7) with 0.44 mM SAM, 0.15 M ascorbic acid and 225 µM presumed substrate. Calculation of the kinetic values was carried out with varying concentrations of noraucuparin (5-250 µM), 5-hydroxyferulic acid (15-350 µM) and caffeic acid (15-625 µM). Incubations lasted 25 min by 45°C. Reactions were stopped and the products were analyzed as mentioned before.

8.2 For detection of hydroxylase activity

Presumed activities catalyzed by cytochrome P450 were tested in microsomal fractions while those presumed to be catalyzed by 2-oxoglutarate dependent dioxygenase were tested in crude protein extract.

For hydroxylase activity by cytochrome P450

The incubation mixture (200 µl) consisted of 6 µM presumed substrate (3,5-dihydroxybiphenyl, 3-hydroxy-5-methoxybiphenyl, noraucuparin, aucuparin) and 1 mM NADPH in 0.1 M Tris-HCl buffer (pH 8.5). The reaction was initiated by addition of 80 µg microsomal protein and the incubation left by 22°C for 30 min. The reaction was stopped and the products were analyzed as mentioned before.

For hydroxylase activity by 2-oxoglutarate activity

The incubation mixture (200 µl) consisted of 6 µM - 1,25 mM possible substrate (3,5-dihydroxybiphenyl, 3-hydroxy-5-methoxybiphenyl, noraucuparin, aucuparin), 5 mM 2-oxoglutarate, 0.5 mM ferrous sulphate and 5 mM ascorbic acid in 0.1 M Tris-HCl buffer (pH 7). The reaction was initiated by addition of 100 µg protein and incubation left by 30°C for 30 min. The reaction was stopped and the products were extracted as described above.

8.3 HPLC analysis of enzyme assays

Analysis of enzyme assays including biphenyls or dibenzofurans were carried out on HPLC 1 and the following gradient. The mobile phase consisted of water containing 0.1% phosphoric acid (A) and methanol (B). The following gradients were used

Gradient 1		Compounds analysed	UV (λ max)
Time (min)	Methanol %	3,5-dihydroxybiphenyl; 3-hydroxy-5-methoxybiphenyl; noraucuparin; aucuparin; 2`-hydroxyaucuparin; 2`,3,5-trihydroxybiphenyl.	254 nm, 269 nm, 280 nm
0	50		
18	80		
28	80		
30	100		
32	100		
34	50		
44	50		
Gradient 2			
Time (min)	Methanol %	2,4-dihydroxydibenzofuran; 2-hydroxy-4-methoxydibenzoduran; 4-hydroxy-2-methoxydibenzofuran.	285 nm, 300 nm
0	45		
2	45		
10	65		
20	76		
22	100		
25	100		
27	45		
37	45		
Gradient 3			
Time (min)	Methanol %	Caffeic and ferulic acids	260 nm, 320 nm, 330 nm
0	10		
2	15		
5	15		
10	40		
15	60		
20	90		
21	90		
22	10		
31	10		

Gradient 4		Compounds analysed	UV (λ max)
Time (min)	Acetonitrile %	5-hydroxyferulic acid, sinapic acid	230 nm, 319 nm
0	10		
3	10		
22	61		
24	100		
29	100		
31	10		
41	10		
Gradient 5			
Time (min)	Acetonitrile %	Pinosylvin, pinosylvin monomethyl ether	230 nm, 305 nm
0	40		
5	40		
25	100		
30	100		
32	40		
42	40		

9. Molecular biology methods

9.1 RNA isolation and on-column digestion of genomic DNA

RNA was isolated from cell culture treated with *V. inaequalis* extract. It was isolated using the RNeasy isolation kit (Qiagen). Freshly harvested culture or frozen cells (-80°C) were ground in the presence of liquid nitrogen, which ensures inactivation of RNase enzymes, then 100 mg of the ground cells were vortexed with lysis buffer which contains guanidine thiocyanate. Guanidine thiocyanate denaturates proteins including RNases. Further homogenization of the samples was achieved by centrifugation through QIAshredder™ spin columns. The eluate solution is treated with absolute ethanol and then transferred to RNeasy spin columns where the RNA is selectively bound by the silica-based membrane. After partial washing of the contaminants, genomic DNA is digested on-column by adding buffered solution of DNase I (Qiagen) to the column and left for 15 min at 25°C. DNase I and residual contaminants were then eluted in the following wash steps. Finally, RNA is eluted by nuclease-free water. RNA is stored by -80°C. Integrity and purity of RNA were checked by gel electrophoresis and colorimetrically.

9.2 Determination of RNA concentration

RNA concentration is determined colorimetrically by measuring the absorbance at 260 nm and then using the following equation (Sambrook and Russell, 2001):
Concentration of RNA = absorbance at 260 nm × dilution factor × 40 µg/ml.

10 µl samples were diluted (50×) in water and measured in a 0.5 ml quartz cuvette. To determine purity of RNA, the absorbance at 280 °C was determined. Contaminating proteins increase absorbance at 280 nm. Ratios A_{260}/A_{280} falling in the range of 1.8 - 2 indicate pure samples. Pure RNA samples of ratios A_{260}/A_{280},

which fall in the range of 1.9 - 2 are an important prerequisite for Real-Time Quantitative PCR.

9.3 Reverse transcription

Reverse transcription of total RNA is carried out using M-MuLV (Molony Murine Leukemia Virus) reverse transcriptase. It is genetically engineered to demolish the RNase H activity, so it will not degrade RNA-DNA hybrids, which in turn will yield higher yields of full length cDNA from long templates. The procedure consists of two stages: 1. denaturing the RNA to get rid of the secondary structure. 2. The reverse transcription reaction.

1. Mix 1 µg RNA + 10 pmol 5´CDS primer + water to final volume of 12.5 ml
2. Centrifuge briefly, incubate at 65°C for 5 min. then chill on ice for 5 min, centrifuge
3. Add 4 µl (5×) reaction buffer + 10 u Riboblock^{TM} RNase inhibitor + dNTP (1mM final concentration from each + 200 u Enzyme to total volume 20 µl
4. Incubate at 50°C for 1 h and terminate reaction by heating at 70 °C for 10 min.

cDNA can be stored by -20°C. It is more stable than RNA.

First strand cDNA used as template for Real-Time quantitative PCR is synthesized using the Maxima First Strand cDNA synthesis kit (Thermo Scientific). It offers more robustness and increased cDNA synthesis in shorter time compared to other conventional reverse transcription kits. The reaction mixture composed of 1 µg RNA, 4 µl reaction buffer (5×) (which already contains dNTP, oligo $(dT)_{18}$ and random hexamer primers), 2 µl enzyme mix (which contains the enzyme and Riboblock^{TM} RNase inhibitor) and nuclease free water to a final volume of 20 µl. The reaction mixture was incubated at 25°C for 10 min followed by 30 min at 60°C; longer incubation time and higher temperature were applied to overcome GC-rich RNA templates. Reaction was terminated by heating at 85°C for 5 min. cDNA was divided in aliquots to avoid multiple freeze/thaw cycles.

9.4 Primer design

Good primer design ensures obtaining a specific product at a satisfactory yield. As mentioned elsewhere, certain rules should be taken in consideration by primer design. It is not necessary that the designed primers comply with all the mentioned recommendations.

1. Primer length is between 15-30 nucleotides.
2. GC content is between 40-60%
3. Long stretches of G or C should be avoided.
4. Primers should end with G or C.
5. Difference in T_m between forward and reverse primers should not exceed 1°C.
6. Complementarity between the primer pairs should be avoided to prevent primer dimer formation, and complementarity within the primer should be avoided to prevent hairpin formation.
7. Primers should be checked against their template DNA for undesirable complementarity.
8. For real-time qRT-PCR primers, it is desirable that the last 5 nucleotides at the 3`-end contain no more than two G or C nucleotides. However, from our trials it was found that this rule is not always valid. Important is that the 5`-end has a higher G/C content in order to avoid miss-priming at the 3`-end.

The portion of template DNA to be amplified is selected. Forward as well as reverse primers are designed as mentioned above. The length of primer is adjusted so a high T_m is obtained. Consequently, PCR reaction at high annealing temperature can be carried out. The higher the annealing temperature, the higher the specificity of the reaction. The lower the annealing temperature, the higher the chance for miss-priming and wrong amplification.

In course of this study, primers were designed as follows:

Candidate sequences from the apple genome sequence were aligned; the ones with a high degree of similarity are grouped together. Primer pairs aiming at amplifying the full lengths of these candidates are designed, taking in consideration the factors mentioned above. Then restriction sites are introduced at beginnings of the primers. Between the start codon of the forward primer and the introduced restriction site, one, two, or no nucleotide should be introduced to keep the coding sequence in frame. This depends on the nucleotide sequence of the vector and the restriction site introduced.

9.5 Polymerase chain reaction (PCR)

It is the standard reaction to amplify cDNA starting with trace amounts of DNA. From its name the reaction utilizes a DNA polymerase enzyme and uses a chain or repeated cycles of heating and cooling to amplify the starting amount of DNA. Three cycles are applied: a) denaturation: at 95°C to separate double stranded DNA into single strands. b) Annealing: to allow binding of primers to single DNA strands, this binding is the first starting point for DNA polymerase enzyme. The annealing temperature depends on melting temperature of primers (T_m). It should be neither so high (no binding occurs), nor so low (miss-priming occurs). Usually it is about 5°C less than the T_m. c) extension or elongation: DNA polymerase extends the primer till getting double stranded DNA again. This step is carried out at 72°C, the best temperature for DNA polymerase activity. These sequences of cycles will double the initial amount of DNA template. After 20 cycles, one gets one million double of the initial amount of initial template DNA, so traces of DNA can be detected and amplified to measurable amounts using PCR. A variety of recombinant DNA polymerases are available on the market. Taq-DNA polymerase was used in semi-quantitative RT-PCR study. However, this enzyme has a high error rate (10^{-5}). Therefore, high-fidelity Phusion DNA polymerase was used in amplification of clones which will be downstream used in protein expression. This enzyme possesses 3`-5`-exonuclease activity which allows the proofreading activity with an error rate of 10^{-7}. The composition of each reaction as well as the temperature program is slightly different and by using Phusion DNA polymerase the order of adding the reaction components is important.

Standard PCR using Taq DNA polymerase (25 µl reaction)		Using Phusion DNA polymerase (20 µl reaction)	
Water	Ad 25 µl	Water	Ad to 20 µl
10 × reaction buffer	2.5 µl	5× phusion buffer	4 µl
dNTP (10 mM each)	1 µl	dNTP (10 mM each)	0.4 µl
Forward primer (10 pmol)	1 µl	Forward primer (10 pmol)	1 µl
Reverse primer (10 pmol)	1 µl	Reverse primer (10 pmol)	1 µl
Template DNA (from RT reaction)	1 µl	Template DNA	1 µl
Enzyme (5 U/µl)	1 U	Enzyme (2 U/µl)	0.4 U

PCR program

	Taq DNA polymerase		Phusion DNA polymerase	
Step	Temp. (°C)	Time	Temp. (°C)	Time
initial denaturation	95	3 min	98	30 s
Denatruation	95	30 s	98	10 s
Annealing	50	30 s	50	45 s
Elongation	72	3 min (1min/kb)	72	90 s (30 s/kb)
Final extension	72	10 min	72	10 min

9.6 Agarose gel electrophoresis

It is used for analysis and separation of DNA, RNA based on their size and charge. Small DNA molecules migrate faster than larger molecules through the agarose matrix under effect of electric current. Based on the size range of DNA molecules in the sample, agarose gel is prepared in the range of 0.5-2% agarose in TAE buffer. The higher the proportion of agarose, the smaller the pore size of the matrix and the slower the migration rate. In this study, 2% agarose gel was used to analyze samples shorter than 500 bp length. For larger sizes, 1% agarose gel is used. Ethidium bromide is used for visualization of bands. It intercalates in nucleic acid molecules and its fluorescence increases 20 fold after binding to nucleic acid molecules. According to the number of samples, the corresponding volume of TAE buffer and agarose amount were mixed and boiled in a microwave. After cooling down, ethidium bromide was added and then poured in the gel tray and left to solidify at room temperature. Samples were loaded on gel after mixing with loading dye along with DNA or RNA ladder. Then, samples were run in a gel chamber filled with TAE buffer and under electric current (220 V). The gel was developed till the visible dyes in the loaded sample migrate 2/3 the distance. The gel is visualized under UV-equipped transilluminator.

9.7 DNA purification from agarose gel or after digestion reactions

DNA fragments of the right size were extracted from gel using a kit. First, the gel matrix was solubilized in a buffer by 50°C. The solution was transferred to Nucleospin column where DNA binds to the silica membrane, but other components were washed away using wash buffer. Finally, DNA was eluted by water or elution buffer. In case of purification of DNA fragments after digestion reactions, the reaction product was mixed with wash buffer instead of gel solubilizer buffer. Then the process was continued as mentioned before.

9.8 Digestion of PCR products or vectors

Heterologous expression of the ORF of the amplified cDNA requires inserting the PCR product in an expression vector (plasmid), which can be transferred later to the host bacteria. To achieve this, both the vector and the PCR product are digested with endonuclease(s) to produce either sticky or blunt ends. These complementary ends are then ligated. The used endonuclaease are the ones which have no recognition sites in the target insert sequence but have in the MCS

(multiple cloning site) of the vector. In our case, the overexpression vector was pRSET B (Invitrogen). The ORFs of *Sa*OMT1 and *Sa*OMT2 are amplified with Phusion Hot start II and overexpression primers (III.5.3). The PCR products are digested with BamHI and HindIII and then ligated with digested dephosphorylated vector. Double digestion precautions and recommendation can be determined from the website (http://www.thermoscientificbio.com/webtools/doubledigest/). The restriction reaction used in our case was as follows.

Component	Volume (insert)	Volume (Vector)
DNA content	0.6 µg	10 µg
Bam HI digestion buffer (10×)	1 µl	2 µl
Bam HI	0.5 µl	0.5 µl
Hind III	1 µl	1 µl
Water ad	10 µl	20 µl

Both digestion products were subjected to purification using a kit to exclude residual protein and salts which may inhibit the ligation reaction. The digested vector is subjected to dephosphorylation using shrimp alkaline phosphatase. Dephosphorylation of the 5` group of the vector ends prevent self-ligation of the vector during the ligation reaction. The composition of the dephosphrylation reaction is as follows.

Vector solution	10-40 µl
10× reaction buffer	2 µl
Water ad	49 µl
SAP enzyme 1 U/1 µl	1 µl

The reaction is incubated for 15 min at 37°C, and then the enzyme is inactivated by 65°C for 15 min. The reaction product is purified in order to get rid of residual protein and components which can inhibit the ligation product.

9.9 Ligation of DNA fragments

To promote the ligation reaction, the insert amount should be 2-6 fold more than the vector amount. The vector and insert are mixed together in PCR tubes and kept at 55°C for 5 min, then chilled on ice. This step is done to avoid mispriming of the sticky ends. The tubes are centrifuged and then the buffer and the enzyme are added and the reaction is incubated by 4°C overnight. A negative control reaction which contains all the components except the insert is done in parallel. Ligation reaction (5 µl) is used to transform 50 µl competent cells.

Component	Volume (µl)
Vector	1
DNA insert	6
10× DNA ligase buffer	1
T4 DNA ligase (5 U/µl)	1
Nuclease free water ad	10

9.10 Transformation of DNA products into *E.coli*

Transformations occurred into *E. coli* DH5α and BL21(DE3)pLysS (Ausubel et al., 1994). Chemically competent cells are prepared in our laboratory by calcium chloride method (Cohen et al., 1972; Dagert and Ehrlich, 1979; Mandel and Higa, 1992). This treatment enhances the attachment of plasmid DNA to the bacterial membrane. Ligation product (5 µl) is added to competent cells (50 µl) and left for 25 min on ice, then transferred to a water bath at 40°C for 45 s followed by immediate incubation on ice for 2 min. SOC medium (250 µl) and bacterial suspension is shaken by 37 °C for one and a half hours. The whole bacterial suspension is plated on LB-agar plates containing ampicillin. Transformation of plasmid into BL21(DE3)pLysS follows the same procedure except that the heat shock time is reduced to 20 s, and the selection medium contains chloarmphenicol, in addition to ampicillin. DH5α produces a high yield of plasmid while the BL21 strain is suited for expression of proteins. In case of transformation of plasmids, one µl plasmid solution containing 60-100 ng plasmid is added to 50 µl competent cells.

9.11 Isolation of plasmid DNA by alkaline hydrolysis

It was carried out as described by Birnboim and Doly (1979). A single colony of the transformed DH5α was inoculated into 5 ml LB medium containing 20 µg/ml ampicillin and grown over night at 37°C. On the following day, 4 ml cultures were centrifuged. Bacterial pellets were suspended in ice-cooled buffer I (300 µl) containing RNase A, then buffer II (300 µl) was added and the bacterial suspension was inverted cautiously 6 times and left on ice for 5 min. Lysis of the cell wall took place in addition to denaturation of large chromosomal DNA. RNA is destroyed by RNase I. Precipitation of proteins and denaturation of large chromosomal DNA were done by adding buffer III (300 µl), cautious inversion (6×) and incubation on ice for 20 min. Centrifugation at 13.000 rpm for 10 min was done to exclude the denatured proteins and DNA. The supernatant containing the DNA solution (800 µl) was transferred to a new Eppendorf tube. Residual contaminants and hydrolysed protein were extracted by vortexing with 800 µl chloroform followed by centrifugation at 13.000 rpm for 10 min. The aqueous layer was transferred to a new Eppendorf tube. Isopropanol (0.7 volume) was added, vortexed and followed by centrifugation at 13000 rpm for 30 min to precipitate plasmid DNA. The pellets were washed with 70% ethanol (500 µl) followed by centrifugation at 13.000 rpm for 10 min. The supernatant is discarded and the plasmid pellets are dried by 37°C and then dissolved in 30 µl water. Determination of plasmid concentration is done as mentioned under III.9.2. Restriction analysis to test for the presence of the expected insert is carried out as mentioned under III.9.8.

9.12 Heterologous expression of recombinant proteins

As mentioned before, selection for BL21 bacteria containing the desired clone was carried out by growing the transformed BL21 on agar plates containing ampicillin and chloramphenicol. LB medium [10 ml, containing ampicillin (1.5 mg) and chloramphenicol (450 µg)] was inoculated with one colony and grown overnight (18 h) by 37°C. On the following day, 4 ml from the overnight culture were transferred to 100 ml LB culture containing ampicillin (10 mg). The cultures were grown by 37°C until OD_{600} of 0.6-0.8 was reached. Freshly prepared IPTG was

added at a final concentration of 0.5 mM in order to induce the production of the recombinant protein. The cultures were then incubated at 23°C for 6 h, and then bacterial cells were pelleted by centrifugation at 4°C, each 100 ml into two halves (50 ml). Protein expression was performed by low temperature to slow the metabolic processing of the bacteria and then giving the opportunity for the protein to be rightly folded.

9.13 Extraction of the expressed protein

All procedures were carried out at 4°C. Lysis buffer (5 ml) was added to the bacterial pellets. Cell wall was disrupted by sonication for 5 min at duty cycle 40% and output control of 1.5. Cell debris was separated by centrifugation. The supernatant is mixed with Ni-NTA agarose beads (250 µl) and rotated for 1 h at 4 °C; this time allows binding of the protein to the Ni ions. The slurry is transferred to empty columns and left to drop out the buffer. Unbound protein is eluted using wash buffer (5 ml). The target protein is eluted by using elution buffer which contains a high concentration of imidazole. The eluted protein is desalted by passing through PD_{10} columns.

9.14 SDS-PAGE gel electrophoresis

It is used to separate proteins according to their masses. The protein samples are denaturated in presence of the sample buffer at 95°C for 5 min. During denaturation, the protein is defolded and becomes uniformly coated with negative charges from SDS in the loading buffer. This process will cancel the differences between proteins regarding charge. Glyceol in the sample buffer ensures that samples will sink and settle down in the pockets of the SDS-PAGE, while bromophenol blue dye will help in tracing the development of the gel. Bromophenol blue is a small size dye whose particles migrate faster than any protein. When samples are loaded on the SDS-PAGE gel, proteins will migrate through the two zones; namely, stacking zone gel and resolving zone gel. In the stacking zone, proteins migrate through large pores; no separation takes place, rather all the proteins in a sample will collect as a thin compact band at front of the resolving gel. The resolving gel has a narrower pore size, and proteins will be separated according to their masses. Low molecular weight proteins will run faster than large molecular weight proteins. Bisacrylamide interconnect the polymer chains of acrylamide. The polymerization reaction is initiated by addition of the APS ammonium peroxydisulfate, a radical initiator. TEMED, N,N,N′,N′-tetramethylethylenediamine, is a polymerization catalyst. The degree of polymerization, and hence the pore size of the gel, is dependent on the amount of acrylamide and the pH of polymerization reaction. The stacking gel ingredients are mixed together in a flask, then poured between the glass plates of the instrument and overlaid with water to avoid interaction with air. After gel formation, water is absorbed away with filter paper. The same procedures are carried out for the resolving gel, except that a comb is added to create the sample pockets, no water is used. Protein samples are prepared as mentioned before. Bacterial pellets (from 1 ml bacterial suspension) are suspended in sample buffer (100 µl) and denatured in the same way as protein samples. Samples are loaded on the gel and run at 200 v. The run ends when the dye

bromophenol blue reaches the front of the gel. The gel is taken out for staining. The gel is stained by immersing in coomassie blue solution under gentle shaking for 30 min, then destained by immersing in destaining solution overnight.

9.15 Quantitative Real-Time PCR

In qPCR the progress of the amplification reaction is monitored on time as it occurs. PCR reaction passes three phases. The exponential phase, where the initial amount of DNA is doubled per each cycle because of the presence of a plenty of reagents and nucleotides. Second, linear phase, where the increment of PCR product follows a linear progression and availability of nucleotides and other components becomes more and more consumed. Third, plateau phase, where no further increase in PCR product occurs. During the exponential phase, the PCR product amount is directly proportional to the initial amount. That explains why qPCR results are more accurate and reproducible than conventional end point PCR. All measurements of qPCR are carried out in the exponential phase, so higher accuracy and reproducibility are achieved. Moreover, in conventional PCR further treatments are prone for introducing variability and errors, e.g. gel electrophoresis, staining and blotting. Furthermore, all PCR reactions of reference and target genes in qPCR are carried out at the same cycling conditions on the same instrument. This can not be achieved using conventional PCR if reference and target genes amplifications need different cycling conditions, e.g. number of cycles or temperature.

Two step RT-qPCR protocol was used, where a reverse transcription was first carried out separately. Then qPCR is carried out. This offers more flexibility by work. SYBR green dye chemistry was applied. SYBR green binds to the double-stranded DNA. By each cycle, more PCR product accumulates so higher fluorescent intensity is produced. This approach is easier and cheaper than using fluorescent probe approach, e.g. TaqMan. However, SYBR green can bind nonspecifically to any double stranded product, e.g. primer dimer. So, a melt curve is applied after each amplification reaction along with gel electrophoresis of the product in order to ensure specificity of the reaction. In order to ensure robustness and easiness of the approach a certain precautions should be considered.

Design of the primers

Primers are designed to amplify a 75-250 bp length amplicons from the target sequence. Attention should be paid, not to amplify segments spanning secondary structures. This can be checked using the following softwares. mfold for DNA (http://mfold.bioinfo.rpi.edu/cgi-bin/dna-form1.cgi) or RNA (http://frontend.bioinfo.rpi.edu/applications/mfold/cgi-bin/rna-form1-2.3.cgi). The same precautions taken by designing gene specific primers (III.9.4) apply here also. In addition, long stretches of G or C in the primer should be avoided and to have a G or C at the end of the primer. Primers were designed to have a T_m of 65°C, so the PCR reaction can be carried out by 60°C.

RNA isolation: the same precautions mentioned under (III.9.1) apply here. However, integrity and purity of RNA should be tested. The A_{260}/A_{280} ratio should be in the range of 1.9-2. Agarose gel elctrophoresis should show the presence of the two bands 18S and 28S and absence of smears. Digestion of residual genomic DNA should be performed during RNA extraction. To ensure robustness and high yield by the reverse transcription, a kit was used as mentioned under (III.9.3).

Testing the efficiency of the PCR reactions

A pooled cDNA consisting of equal amounts of the tested samples is used, then a serial dilution (1:5, 1:10, alternately) is done. A standard curve of cDNA input concentration against cycle threshold (Ct) is constructed. The efficiency (E) is calculated from the equation $E = 10^{(-1/slope)}$. The specificity of the PCR product was verified by agarose gel eletrophoresis in addition to checking the melt curve produced by the instrument.

Selection of a reference gene

A reference gene is used for normalization in order to cancel the variations in the starting material (RNA) and variation in the efficiency of the reverse transcription. This reference gene should not be regulated, so its expression level is stable across different samples, i.e., less variation in Ct. Values of Ct from all samples are determined and the coefficient of variation is determined. The gene which has the least CV is selected.

Relative quantification using Pfaffel's method

We wanted to determine the relative expression of a gene, i.e., expression of the gene in a sample (at a time point) relative to a calibrator (zero h). The mathematical model developed by Pfaffel (2001) was used for calculations.

$$\text{Ratio} = (E_{\text{target}})^{\Delta Ct_{\text{target}}(\text{control} - \text{sample})} / (E_{\text{ref}})^{\Delta Ct_{\text{ref}}(\text{control - sample})}$$

The relative expression is reflected in Ct difference and expressed in comparison to a reference gene. This method is simpler than the ΔΔCt approximation method, which necessitates that the efficiency of both target and refence genes to be equal. The increase or decrease in expression is expressed as n-fold relative to the calibrator (zero h)

The qPCR reaction components

Component	Volume	Remarks
Maxima SYBR green qPCR master mix (2x)	10 µl	Contains hot start Taq polymerase, dNTP, $MgCl_2$ (final concentration 2.5 mM), KCl and $(NH_4)_2SO_4$
Forward primer (10 pmole)	0.6 µl	Final concentration 0.3 µM
Reverse primer (10 pmole)	0.6 µl	Final concentration 0.3 µM
ROX solution (10× diluted)	0.04 µl	10 nM, passive reference dye to cancel variation between different wells
Template DNA	7µl	Represent 1 µl from the 20× diluted RT reaction product.
Water, nuclease-free	1.76	To 20µl

To avoid pipetting errors, master mixes were prepared whenever possible.

qPCR Program

Step	Temperature, °C	Time	Remarks
Initial denaturation	95	10 min	Denaturation and activation of the hot start Taq polymerase
denaturation	95	15 s	
Annealing	60	30 s	
extension	72	30 s	Data acquisition is performed at this step
The last three steps are repeated for 40 times before the melt curve step			

Temperature °C	Time	Remarks	
95	15 s	Denaturation of the double stranded product	The gradual increase in temperature from 60°C to 95°C led to decrease in fluorescence. At this stage, data are collected.
60	1 min	Renaturation of the PCR product	
95	15 s	Denaturation	
60	15 s	renaturation	

10. Databases and software

- The Genome Database for Rosaceae (GDR): http://www.rosaceae.org/

It is a curated and integrated web-based relational database, providing centralized access to Rosaceae genomics and genetics data and analysis tools to facilitate cross-species utilization of data. It is used to search apple genome and NCBI *Malus* EST for possible OMTs candidates.

- Basic Local Alignment Search Tool (BLAST): http://blast.ncbi.nlm.nih.gov/Blast.cg

It uses nucleotide or protein query to search nucleotide and protein databases available by website or any set of sequences supplied by the user.

- DNA star lasergene

A software package consists of different programs to manipulate and analyze DNA and protein sequences. From these programs, two were used.

MegAlign generates pairwise and multiple sequence alignments of DNA or protein or a combination of the two quickly and accurately. It was used in alignment of different sequences in addition to calculating the percent identity between different sequences.

EditSeq is a sequence editor and import/export tool. It helped by selecting regions for primer design and locating different nucleotides.

- Mega 5 (Molecular Evolutionary Genetic Analysis) was used to infer the phylogenetic tree (Tamura et al., 2011).

IV. Results

1. Time course of phytoalexin accumulation in *S. aucuparia* cell cultures

It is important to determine the onset and course of phytoalexin accumulation after elicitation. On the basis of this analytical information, the start point to take samples for biochemical and molecular investigations can be accurately determined. It was previously established that *S. aucuparia* cell cultures produce three biphenyls, namely, noraucuparin, aucuparin and 2`-hydroxyaucuparin, and two dibenzofurans, namely, noreriobofuran and eriobofuran (Hüttner et al., 2010). Extraction and analysis were carried out as mentioned under III.4. The results are presented in Figure IV.1. Three biological replicates were used and one to three technical replicates were used per biological replicate. Data are average values of three samples.

The biphenyls aucuparin and noraucuparin can be detected starting from 9 h after elicitation. Three hours later, 2`-hydroxyaucuparin and the dibenzofurans eriobofuran and noreriobofuran can be detected (Fig. IV.1A). Interestingly, accumulation of the intermediates noraucuparin and noreriobofuran followed similar profiles. A sharp increase in the first 24 hours was followed by a sharp decline in the following 12 hours and thereafter a sluggish decline up to the end of day 5. Notably, the noraucuparin content was two to three times higher than the noreriobofuran level. In contrast to that profile, aucuparin, 2'-hydroxyaucuparin, and eriobofuran continued to accumulate in a somewhat linear rate during the 5 days after elicitation. It was surpirising that these compounds accumulated continuously over such a long period of time. Summed up, the accumulation of biphenyls and dibenzofurans were parallel up to 24 hours, then dibnezofurans continue to increase in linear way but biphenyls remain at somewhat constant level (Fig. IV.1B).

A

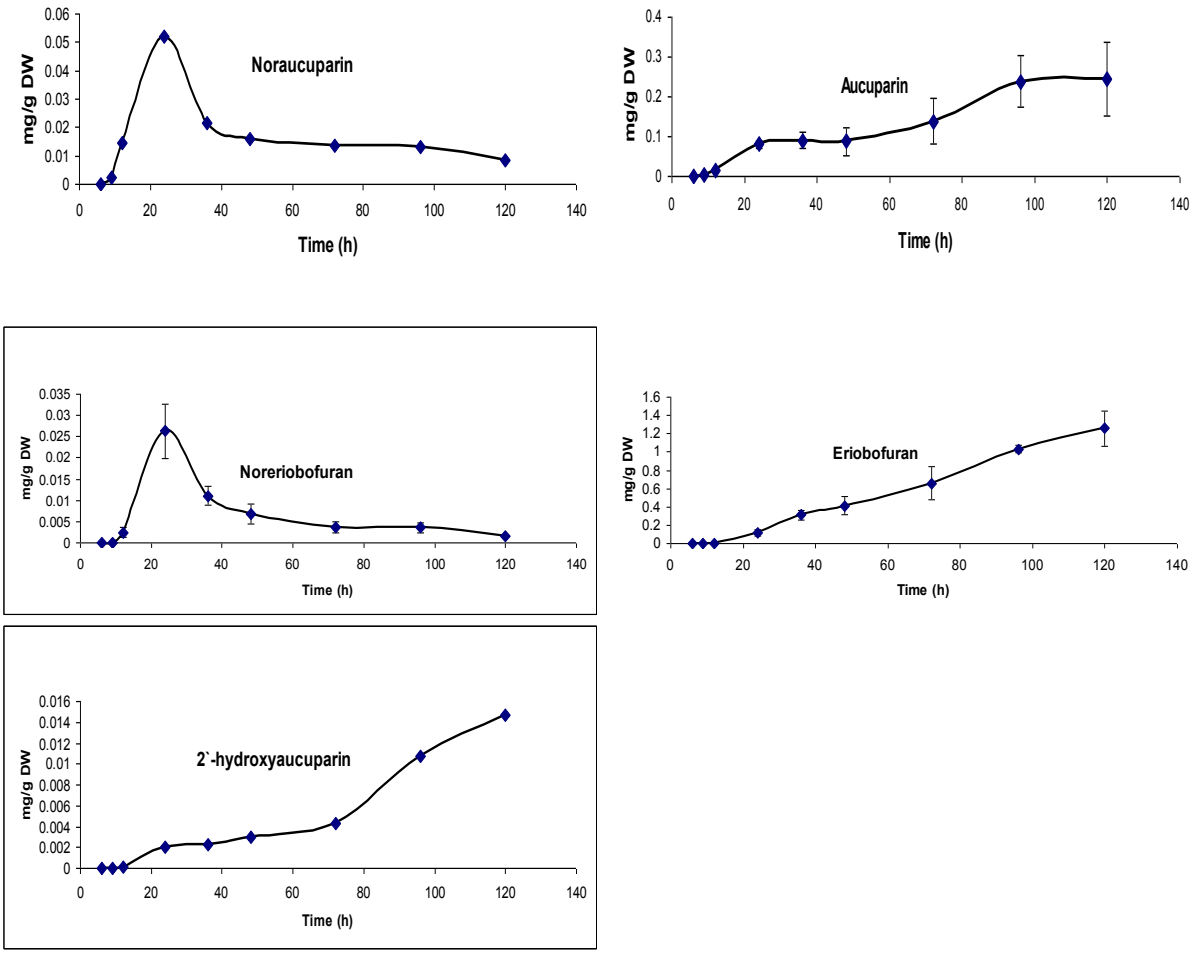

B

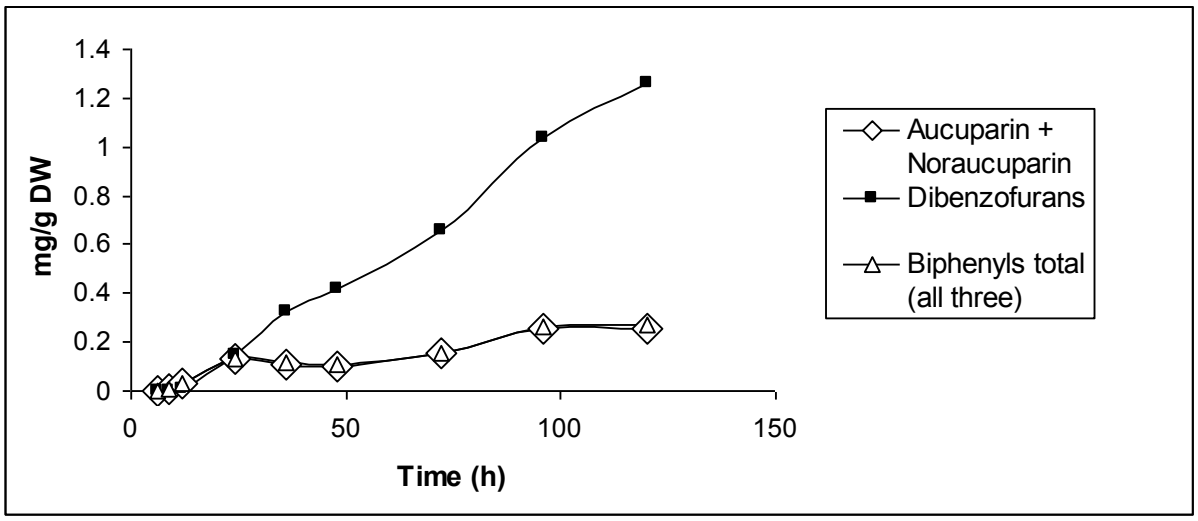

Figure IV.1 Accumulation of phytoalexins in *S. aucuparia* cell cultures.
A. Time courses of accumulation of individual compounds
B. Time courses of accumulation of phytoalexin classes

2. Feeding experiments with radiolabelled precursors

To obtain 3,5-dihydroxybiphenyl as a radioactive tracer, recombinant BIS1 of S. aucuparia (Liu et al., 2007) was incubated with benzoyl-CoA and [2-^{14}C]malonyl-CoA, resulting in the formation of ^{14}C-labeled 3,5-dihydroxybiphenyl. Based on the results obtained from the time course of phytoalexin accumulation, the radioactive tracer was added 3 h after elicitation to avoid any possible feed back inhibition of BIS. Expression of the *BIS* gene is already induced one hour after elicitation (Liu et al., 2007). The tracer 3,5-dihydroxybiphenyl was incorporated efficiently into aucuparin and eriobofuran at rates of 0.6 and 3.37%, respectively, as demonstrated by radiodetector-coupled HPLC analysis (Fig. IV.2). Aucuaprin and eriobofuran are the major biphenyl and dibenzofuran compounds produced by the cell cultures when treated with *V. inaequalis* extract (Hüttner et al., 2010). This time point of harvest, 72 h after elicitation, was chosen to ensure the accumulation of a large amount of dibenzofuran, as shown in Figure IV.1. This late time point also explains the absence of the intermediates noraucuparin and noreriobofuran from the chromatogram. Even later time points were not selected to avoid possible degradation of the products. This is the first solid evidence that 3,5-dihydroxybiphenyl is metabolized downstream not only to produce other biphenyls (aucuparin, noraucuparin) but also to produce dibenzofurans (eriobofuran, noreriobofuran). In a parallel experiment, [U-^{14}C]benzoic acid was fed to the cell cultures, achieving incorporation rates into aucuparin and eriobofuran of 1.1 and 4.6%, respectively.

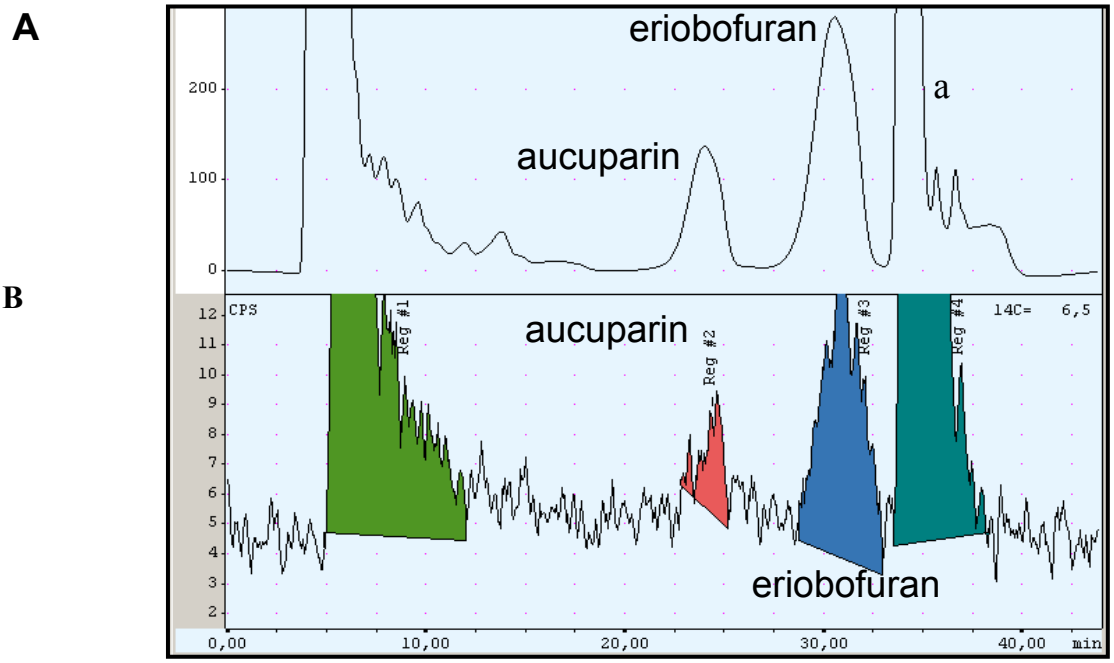

Figure IV.2: Radiodetector-coupled HPLC analysis of extracts from cell cultures fed with radiolabelled 3,5-dihydroxybiphenyl. A, UV-chromatogram; B, radiochromatogram; a, unidentified product.

3. Biochemical investigation of biosynthetic steps metabolizing 3,5-dihydroxybiphenyl

3,5-Dihydroxybiphenyl is the product of BIS. Subsequent steps leading to formation of biphenyls and/or dibenzofurans are not studied. The feeding experiment has shown that 3,5-dihydroxybiphenyl is the precursor of aucuparin and eriobofuran. However, this technique can not show the sequence of intermediate steps involved. Therefore, enzyme assays leading to hydroxylation or methylation of the starter compound were carried out using crude protein extract and microsomal proteins in the presence of different cofactors, depending on the nature of the tested enzyme activity, as mentioned under III.6 and III.8. Once a candidate substrate was accepted by an enzyme, the product in turn is subjected to the same strategy and approach. This procedure was applied to elucidate the sequence of biosynthetic steps leading to formation of aucuparin. Alternative routes are shown in Figure IV.3. The protein preparations were prepared 16 h after elicitation because noreriobofuran reaches its maximum level at 24 hours, as shown by the above accumulation profile. Moreover, BIS activity reaches its maximum 16 h after elicitation (Gaid et al., 2009). So it was assumed that the subsequent enzymes will be active in an approximate time range.

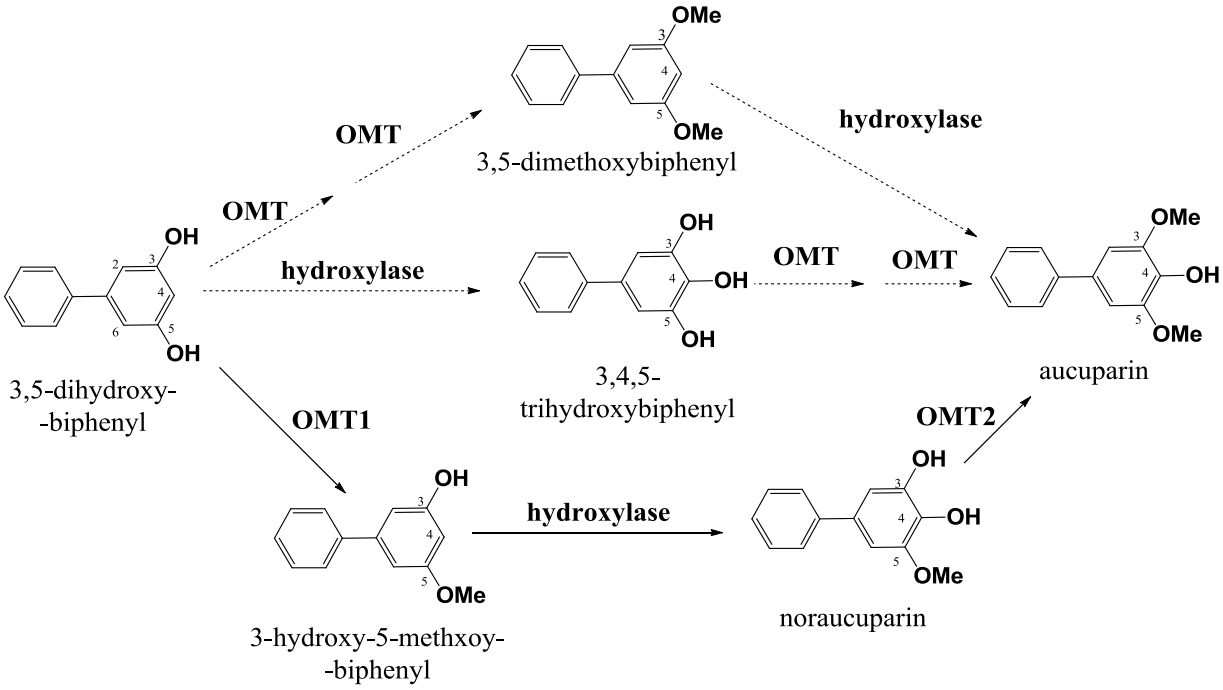

Figure IV.3: Alternative routes of aucuparin biosynthesis in *S. aucuparia* cell cultures. Solid lines indicate steps detected here at the biochemical level. Dashed lines are steps not detected.

It was found that 3,5-dihydroxybiphenyl is converted to aucuparin throught three steps, namely, methylation, hydroxylation, methylation. It first undergoes only one methylation step to yield 3-hydroxy-5-methoxybiphenyl (Fig. IV.3). No further methylation took place even when the time of enzyme incubation was extended or the monomethylated product was used as a substrate against the crude protein extract. Then 3-hydroxy-5-methoxybiphenyl is hydroxylated at the 4-position to give noraucuparin. This enzyme activity was detected in the microsomal fraction. As will be presented later, this enzyme is a cytochrome P450 monoxygenase. 4-

Hydroxylation of 3,5-dimethoxybiphenyl was not detected. Noraucuparin is methylated further to give aucuparin. No further methylation of acuparin at the 4-position took place. Storing the crude protein extract without glycerol caused sharp decrease in the methylation activity of 3,5-dihydroxybiphenyl but no such decrease in the methylation activity of noraucuparin was observed. This finding may indicate that each methylation step is catalyzed by a distinct OMT. In the following sections, the detailed characterization of these three enzymes on the biochemical level is presented.

3.1 Biochemical characterization of *O*-methyltransferase activity in cell-free crude protein extract

3.1.1 Detection of O-methyltransferase activity

Enzyme assays were analyzed using HPLC. Incubating 3,5-dihydroxybiphenyl with the cell-free crude protein extract led to formation of 3-hydroxy-5-methoxybiphenyl. Confirmation of the enzyme activity was carried out doing parallel incubations containing heat denaturated protein. The identity of the product was confirmed by comparing the retention time and the UV spectrum with authentic reference material. Similarly, incubating noraucuparin with the crude cell free extract led to formation of aucuparin (Fig. IV.4). Other possible biphenyl and dibenzofuran substrates were also tested. Only 2,4-dihydroxydibenzofuran was accepted and yielded a single specific product, 2-hydroxy-4-methoxydibenzofuran. In all the above mentioned reactions, only one methylation reaction took place. This was further confirmed by testing the products as potential substrates, which all were not accepted.

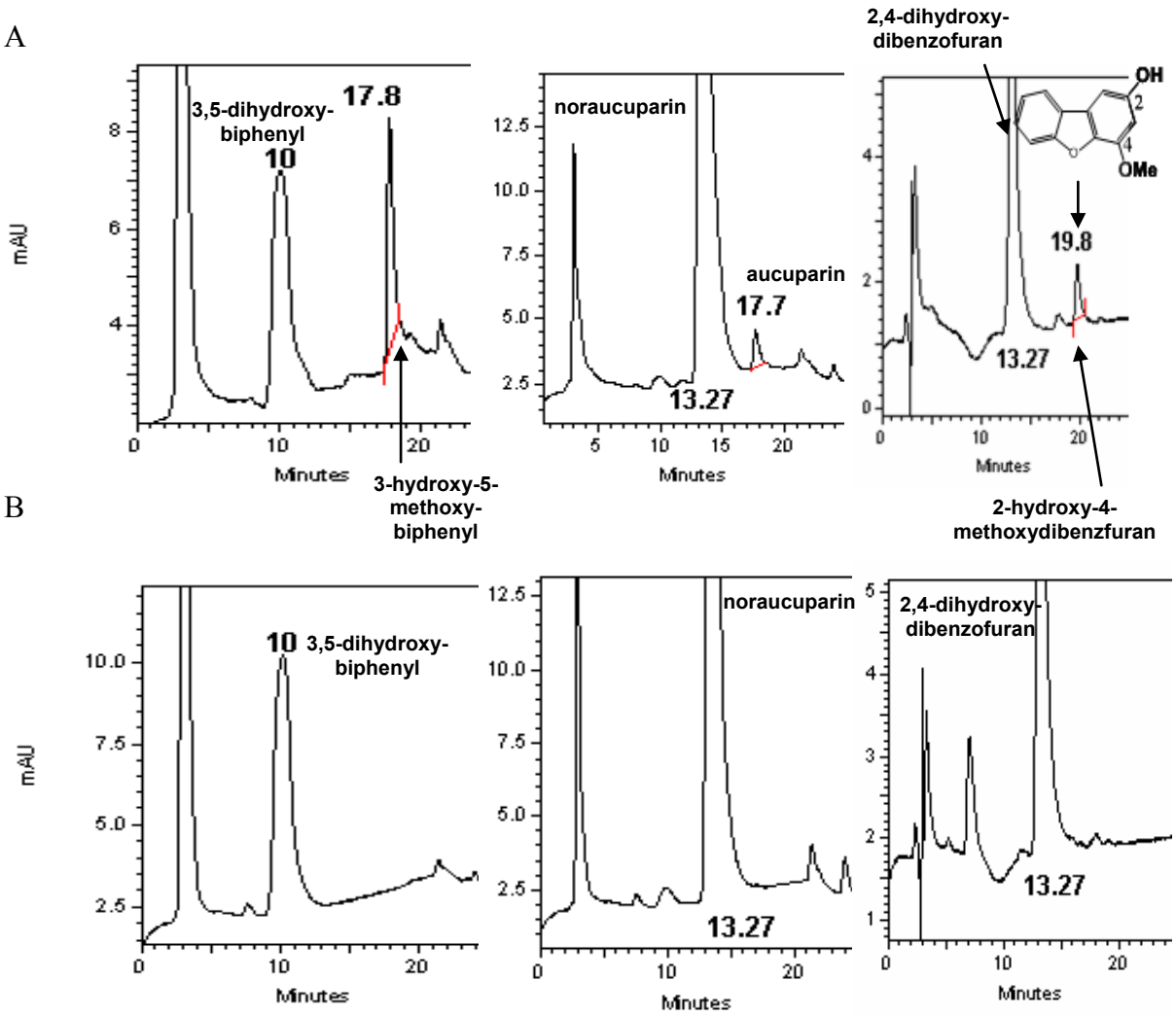

Figure IV.4: HPLC analysis of enzyme assays containing *S. aucuparia* cell-free crude protein extract and various substrates (A). Corresponding control assays containing boiled protein (B).

3.1.2 Determination of the optimum pH and temperature

Proteins are active over a definite range of pH values. The degree of ionization of basic and acidic amino acids of the protein, hence the folding of the protein, depends on the pH of the surrounding solution. At extreme values away from the optimum pH missfolding and denaturation of the enzyme takes place. Regarding the effect of the temperature, the kinetics of the reaction tends to increase with increasing temperature up to a certain limit. At extremely high temperatures, breakage of hydrogen bonds occurs leading to disruption of the tertiary and quaternary protein structure. Determination of the optimum temperature and pH value were carried out at varying temperatures and pH values, respectively, using the same conditions of substrate (3,5-dihydroxybiphenyl) and S-adenosylmethionine concentrations. The optimum pH value fell between 8.5 and 9 with loss of about half the activity at pH 7 and pH 9.5. The optimum temperature was 40°C with loss of 75% activity at 45°C (Fig. IV.5). For subsequent enzyme characterization, a pH of 8.5 and a temperature of 37°C were defined.

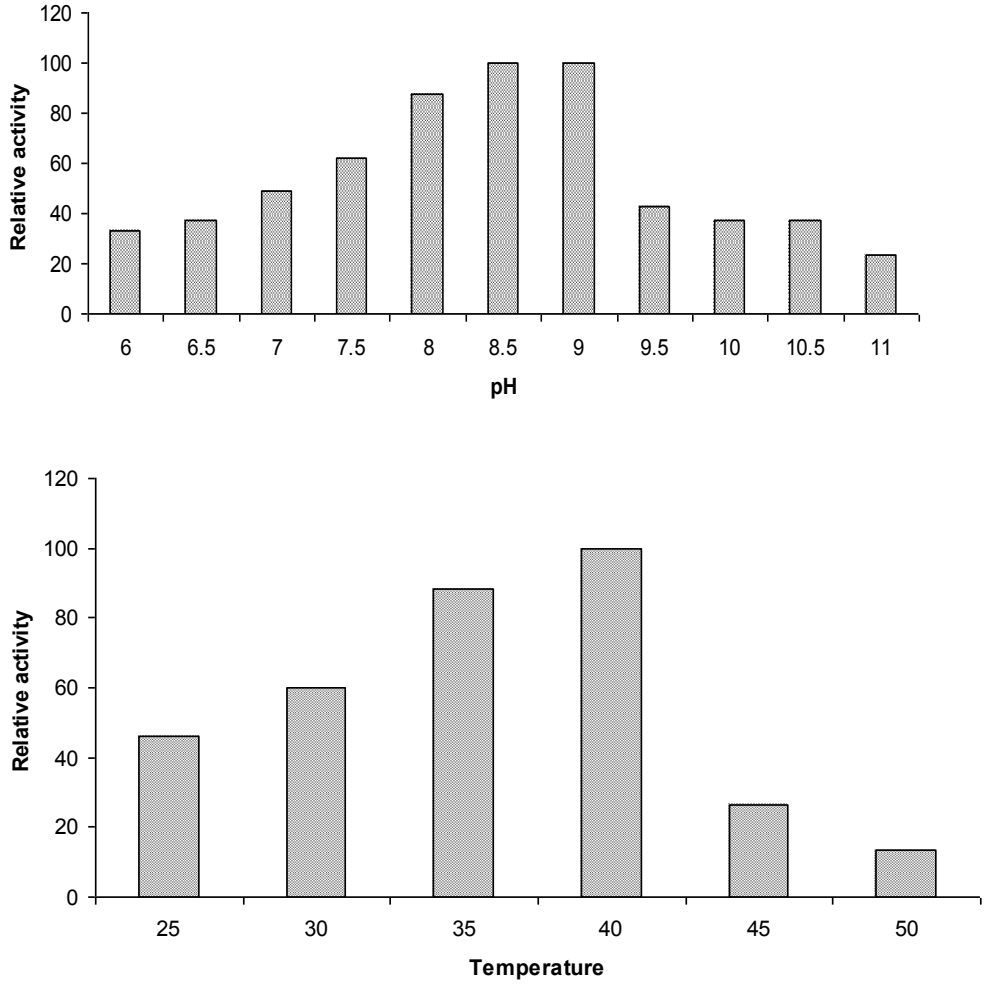

Figure IV.5: Effect of pH and temperature on *O*-methyltransferase activity in *S. aucuparia* cell-free crude protein extract.

3.1.3 Effect of protein concentration and time

Before determining the kinetic parameters of the protein, optimal protein concentration and incubation time should be determined. These data are selected from the linear range of the corresponding curve in order to ensure reproducibility of the results. The accumulation of the product was linear with the incubation time up to 35 min and the crude protein concentration up to 80 µg /assay (Fig. IV.6). Thus, a protein amount of 40 µg/ 200 µl incubation and an incubation time over 20 min were defined for the subsequent characterization of enzyme activity.

A

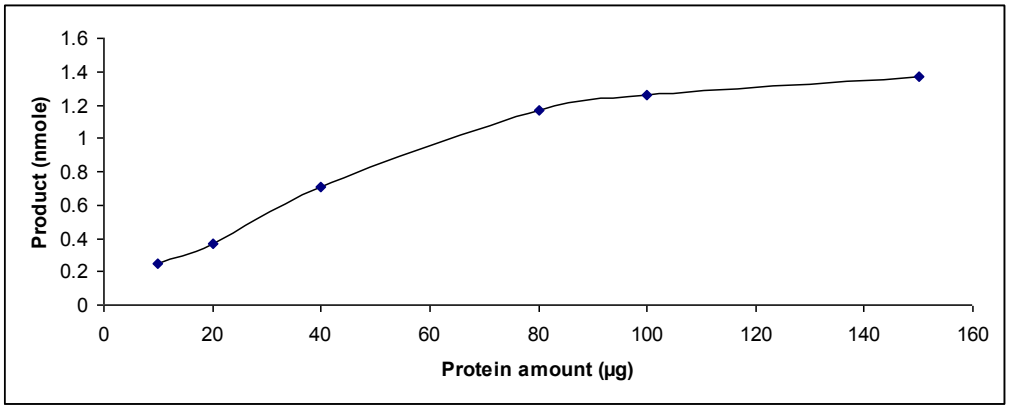

B

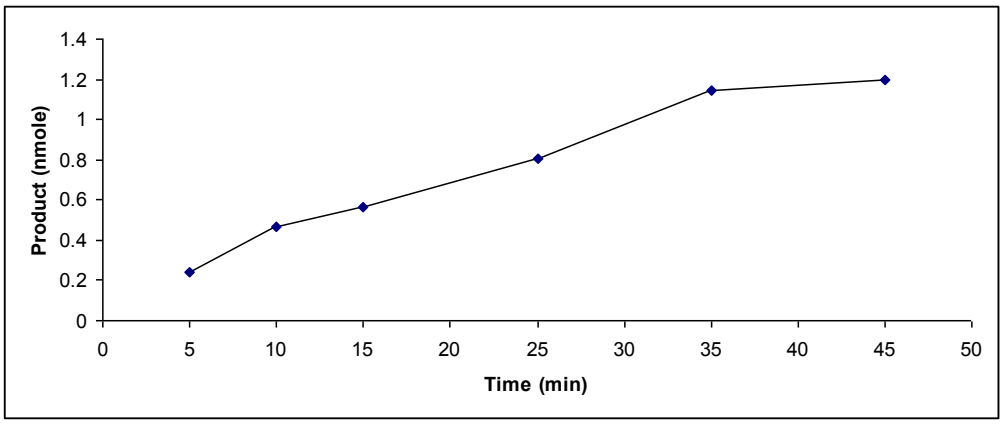

Figure IV.6: Effect of protein concentration and time on *O*-methyltransferase activity in *S. aucuparia* cell-free crude protein extract. The product is 3-hydroxy-5-methoxybiphenyl.

3.1.4 Determination of kinetic parameters

The kinetics of an enzyme reaction is described by the Michaelis-Menten equation. From this equation, certain parameters are derived. The K_m value represents the substrate concentration which results in half-maximal velocity (1/2 V_{max}) for the enzymatic reaction. It is inversely proportional to the substrate affinity, i.e. the lower the K_m value the higher the affinity of the enzyme to the substrate. The kinetic values for the three accepted substrates were calculated from the corresponding Hanes-Woolf plot, whose values agreed with those from hyperbola calculations. These data indicated that 3,5-dihydroxybiphenyl was the best substrate with respect to K_m and V_{max}, followed by 2,4-dihydroxydibenzofuran, the dibenzofuran analogue. The affinity for noraucuparin was least (Table IV.1, Fig. IV.7).

Table IV.1: Kinetic data for substrates accepted by *Sa*OMT activity in cell-free crude protein extract.

Substrate	K_m (µM)	V_{max} (nM/s)
3,5-dihydroxybiphenyl	0.85	0.49
noraucuparin	4.46	0.12
2,4-dihydroxydibenzofuran	1.17	0.10
SAM	3.74	4.25

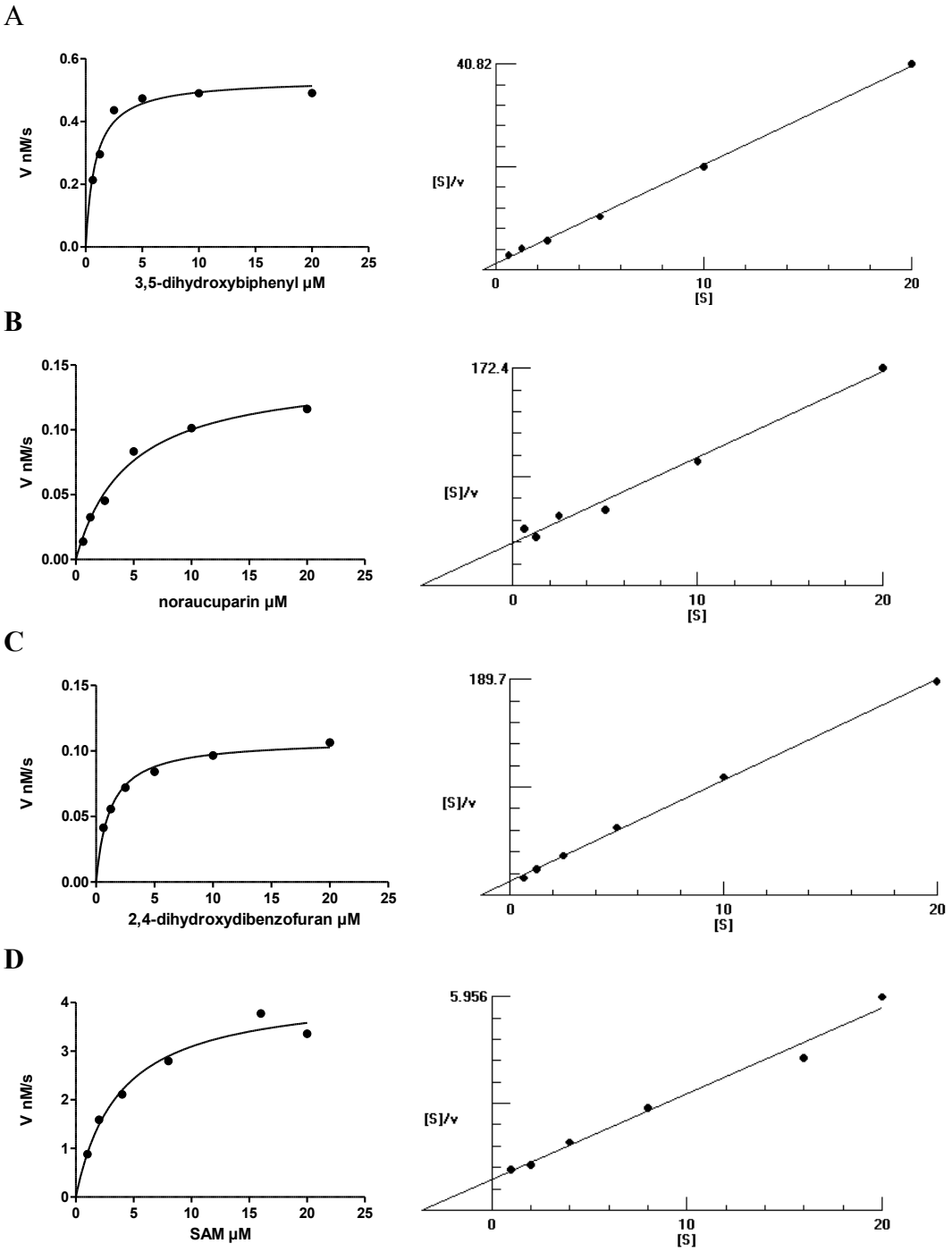

Figure IV.7: Graphical representation of kinetic parameters of *Sa*OMT activity against various substrates through Michaelis-Menten and Hanes-Woolf plots. A, 3,5-dihydroxybiphenyl; B, noraucuparin; C, 2,4-dihydroxydibenzofuran; D, SAM

3.1.5 Enzyme stability upon freezing/thawing

Aliquots of the cell-free protein extract were stored without and with 20% glycerol at -80°C. After 1.5 years their activities were compared to each others. Both the frozen and the glycerol-frozen protein samples catalyzed the methylation of noraucuparin to the same extent. On the contrary, the protein frozen without glycerol catalyzed the methylation of 3,5-dihydroxybiphenyl 75% less compared to the protein frozen with glycerol (Table IV.2). This indicates that both reactions are catalyzed by different OMTs. One catalyzes methylation of 3,5-dihydroxybiphenyl and needs addition of glycerol to preserve its activity upon

freezing/thawing, whereas the other one catalyzes the methylation of noraucuparin and is not affected by freezing.

Table IV.2: Comparing *Sa*OMT activity with 3,5-dihydroxybiphenyl and noraucuparin in cell-free crude protein extracts stored at -80°C.

Protein sample	3,5-dihydroxy-biphenyl	Noraucuparin
Protein frozen without glycerol	32.3 ± 4.4	97.5.3 ± 2.5
Protein frozen with glycerol [a]	100	100

[a] 20% (v/v)

3.2. Biochemical characterization of biphenyl 4-hydroxylase in microsomal fractions from S. aucuparia *cell cultures.*

3.2.1 Detection of biphenyl 4-hydroxylase activity

Microsomal protein fractions were prepared as mentioned under III.6. Enzyme assays were analyzed by HPLC and product identity was confirmed by comparing the retention time and the UV spectrum with authentic reference material. Only 3-hydroxy-5-methoxybiphenyl was accepted as a substrate (Fig. IV.8A). Hydroxylation takes place at the 4 position yielding noraucuparin. Neither 3,5-dihydroxybiphenyl nor 3,5-dimethoxybiphenyl were accepted as substrates. Control assays containing heat-denaturated microsomal protein were carried out in parallel and lacked the enzymatic product (Fig. IV.8B).

A

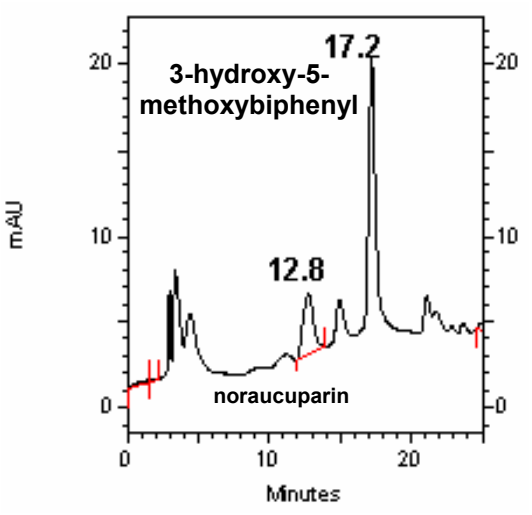

B

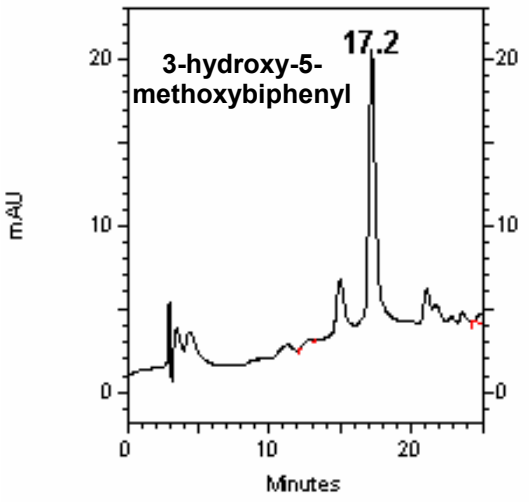

Figure IV.8: HPLC analysis of biphenyl 4-hydroxylase assays.
A. Standard incubation. B. Enzyme assay containing heat-denaturated microsomal protein.

3.2.2 Determination of optimum pH and temperature

The optimum pH was 8.5 with loss of 35 and 20% activity at pH 7 and 9.5, respectively. The optimum temperature is around 20°C with loss of 60% activity each at 7 and 40°C. The temperature and pH optima deviate slightly from those known for most cytochrome P450s, 30°C and pH 7 (Fig. IV.9). For subsequent characterization, enzyme assays were carried out at pH 8.5 and at 20°C.

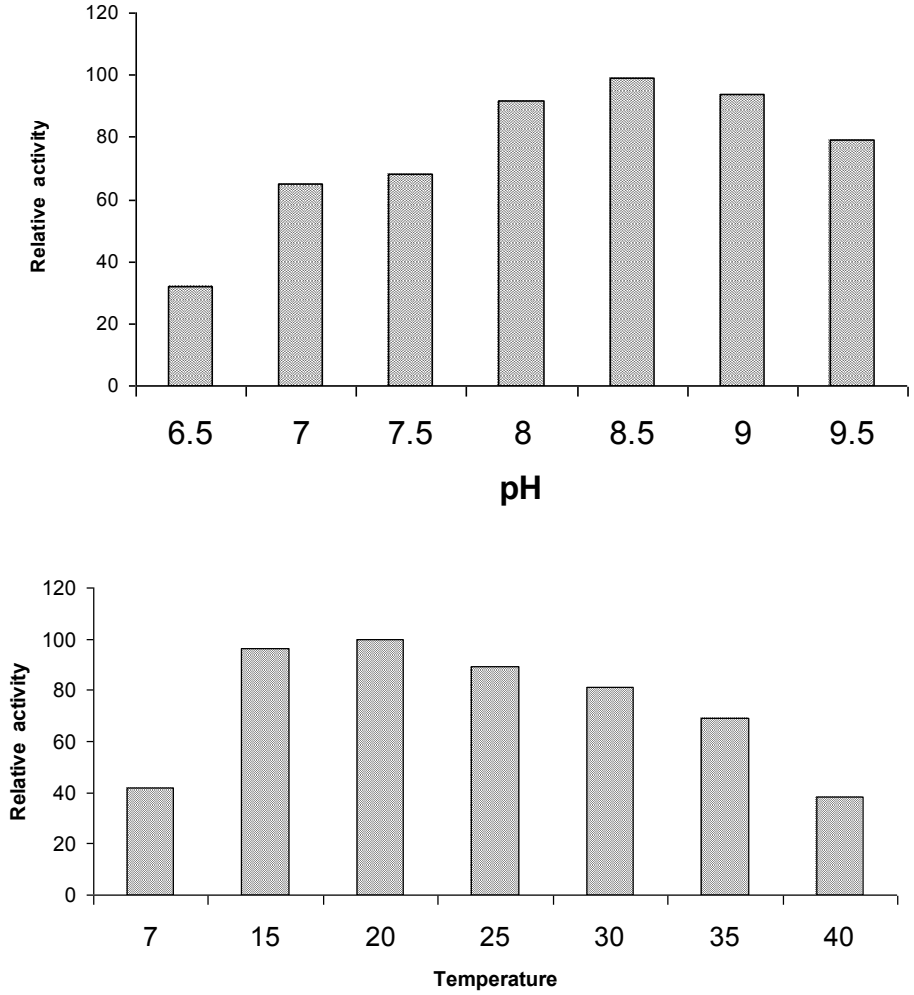

Figure IV.9: Effect of pH and temperature on biphenyl-4-hydroxylase activity.

3.2.3 Effect of incubation time and protein amount

The accumulation of the product was linear even when the incubation time was extended to 90 min or the microsomal protein amount was increased to 300 µg per assay (Fig. IV.10). For the subsequent trials, 80 µg microsomal protein and 30 min were used for the incubation.

A

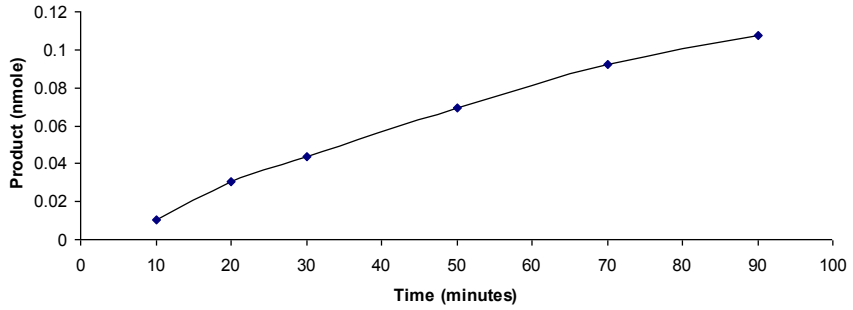

B

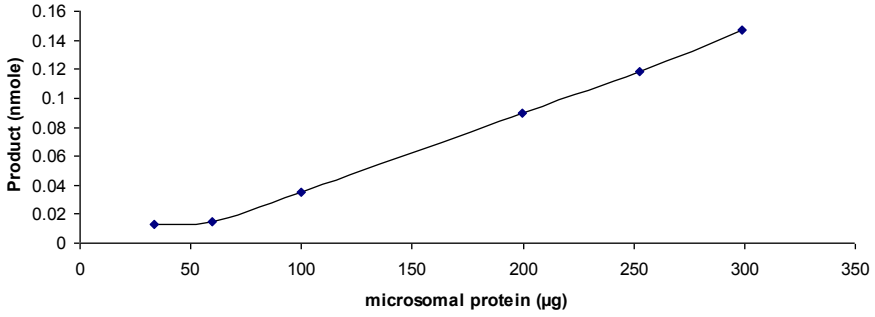

Figure IV.10: Effect of protein amount and time on biphenyl-4-hydroxylase activity. Product is noraucuparin.

3.2.4 Determination of kinetic parameters

The K_m value for 3-hydroxy-5-methoxybiphenyl was estimated to be 0.61 µM, indicating high affinity to the substrate. The V_{max} value was calculated to be 0.38 nM/s, as calculated from Hanes-Woolf plot (Fig. IV.11).

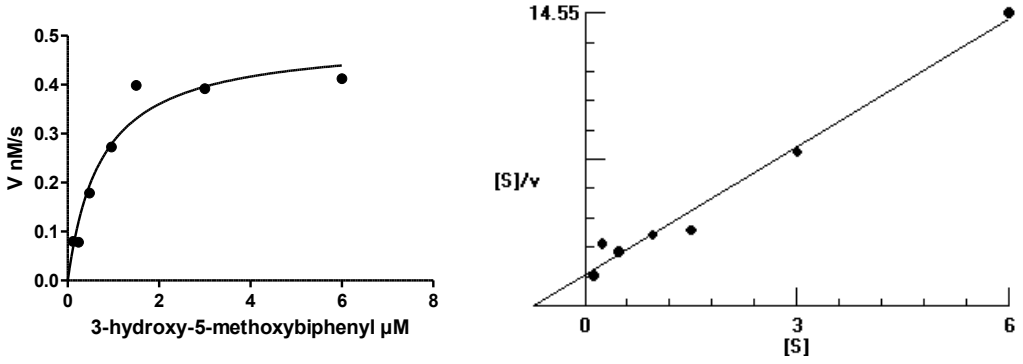

Figure IV.11 Graphical representation of the kinetic parameters of biphenyl 4-hydroxylase through Michaelis-Menten and Hanes-Woolf plots.

3.2.5 Identification of biphenyl 4-hydroxylase as a cytochrome P450 monoxygenase.

Enzyme, whose activities are detected in microsomal fractions, are membrane-bound. Further identification of the nature of these enzymes is necessary.

Cytochrome P450 enzymes are identified through two characters, firstly, their dependence on NADPH and oxygen, secondly, their inhibition by a number of substances, e.g., cytochrome c and imidazole antifungals. Cytochrome c interferes with the flow of electrons from CPR to the cytochrome P450. Miconazole, an imidazole antifungal derivative, was found as an inhibitor of 14α-demethylase enzyme; however, it is known that an inhibitor for one cytochrome P450 can also serve as an inhibitor to other cytochromes (Ortiz de Montellano, 2005). NADH is found to somewhat increase the activity of cytochrome P450 enzymes, as is the case with biphenyl 4-hydroxylase. Dependence on NADPH and inhibition by cytochrome c and miconazole were pronounced and confirmed the identity of biphenyl 4-hydroxylase as NADPH-dependent cytochrome P450 enzyme (Table IV.3).

Table IV.3: NADPH dependence and effect of cytochrome P450 inhibitors on biphenyl 4-hydroxylase activity.

	Relative activity[a]
Standard assay	100
+ NADH	119
- NADPH	1.1
+ 0.5 µM miconazole	43.9
+ 10 µM miconazole	1.4
+ 10 µM cytochrome c	6.9
+ 50 µM cytochrome c	1.3

[a] 0.44 nM/s.

3.3 Biochemical investigations aiming to detect biosynthesis of dibenzofurans

The above feeding experiment (IV.2) has shown that 3,5-dihydroxybiphenyl is the precursor for both biphenyls and dibenzofurans. It is believed that the conversion of biphenyls to dibenzofurans involves two steps. First, hydroxylation at the 2`-position to give 2`-hydroxybiphenyl derivatives, which in turn will be oxidized to give the cyclic product, the dibenzofuran, in a manner similar to the intramolecular cyclization of benzophenones to xanthones (Peters et al., 1998). Our trials focused on detection of either the 2`-hydroxylase or the cyclase activities. The available biphenyls were tested as potential substrates for hydroxylase enzymes in crude extracts (2-oxoglutarate dependent dioxygenases) or in microsomal fractions (cytochrome P450 dependent monooxygenase). 2`,3,5-Trihydroxybiphenyl and 2`-hydroxyaucuparin were tested as substrates for the cyclase enzyme in microsomal fractions. The corresponding cofactors and optimum conditions were applied. The summary of these trials is presented in Figure IV.12. All the enzyme assays failed to detect these catalytic steps. Failure to detect some enzyme activities on the biochemical level can be attributed to either the low titer values (Prescott and Lloyd, 2000) or the poor extractability and stability of enzymes (Schmidlin et al., 2008).

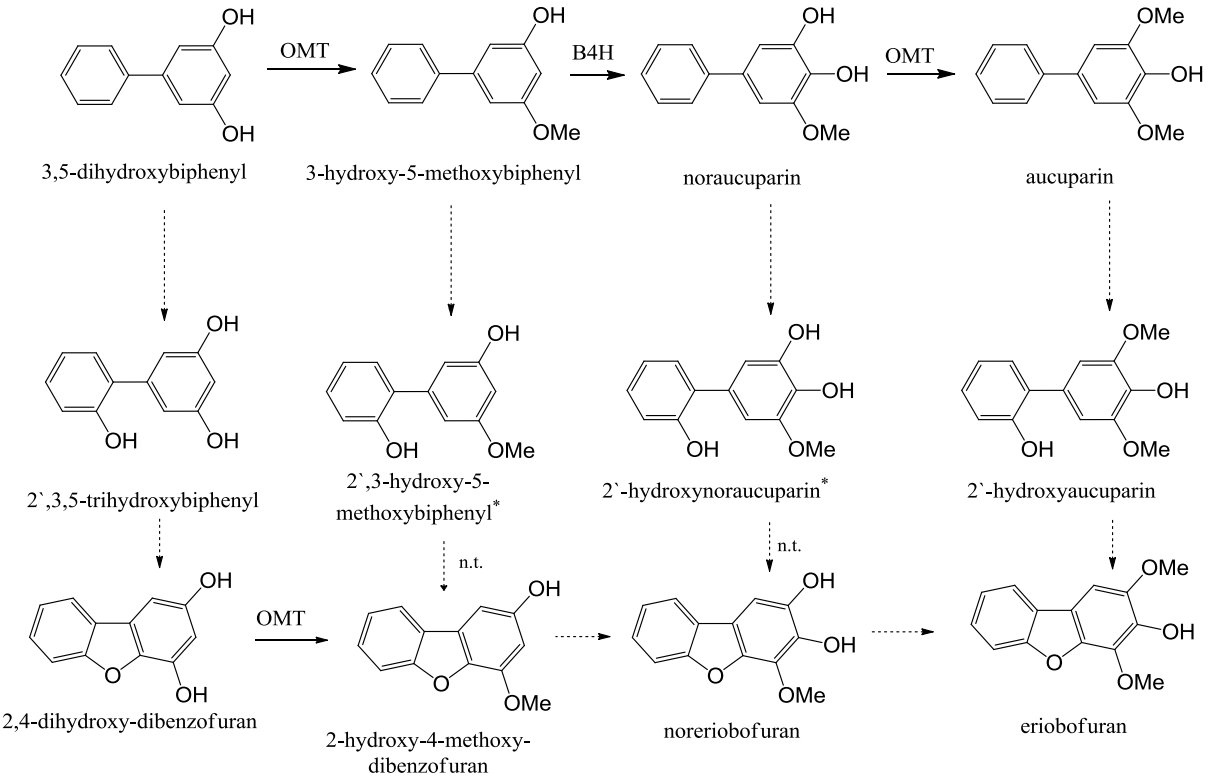

Figure IV.12 Biosynthetic scheme of biphenyls and dibenzofurans produced by *S. aucuparia* cell cultures. Solid lines indicate steps detected on the biochemical level. Dashed lines are postulated steps and were not detectable here. n.t., not tested due to lack of substrates; *unavailable substrate.

4. Isolation and functional characterization of OMT cDNAs involved in aucuparin biosynthesis.

4.1 Candidate gene approach and selection of a probe

Aiming to isolate putative biphenyl OMT cDNAs, a candidate gene approach was applied, which required a selection of a suitable probe encoding an OMT with a definite desired function. Then a genome and/or transcriptome library is searched for similar homologues. The probe should be functionally similar to the anticipated candidate and in case of plant OMTs, it is preferable that the gene product acts on a similar substrate. Stilbenes are structurally close to biphenyls. The major stilbenes found in plants are either resveratrol derivatives, commonly found in *Vitis* sp. (Schmidlin et al., 2008; Xu et al., 2012), or pinosylvin derivatives, commonly found in *Pinus* sp. (Chiron et al., 2000; Jorgensen, 1961). Pinosylvin derivatives are more similar to *Sorbus* biphenyls because ring B in both classes of compounds has no substituents (Table IV.4). From a biosynthetic point of view, their polyketide scaffold is derived from an unsubstituted aromatic CoA ester, cinnamoyl-CoA in case of pinosylvin and benzoyl-CoA in case of biphenyls. Moreover, pinosylvin *O*-methyltransferase (POMT) catalyzes only the methylation of one of the *meta*-dihydroxyl groups of pinosylvin (Chiron et al., 2000), thus exhibiting exactly the same biochemical activity like their peers, biphenyl OMTs. In contrast, resveratrol OMT (ROMT) catalyzes methylation of both meta-positioned hydroxyl groups of resveratrol (Schmidlin et al., 2008). Based on the similarity of the substrate structure and the nature of the catalytic reaction, POMT was selected as a probe to screen the apple genome (Velasco et al., 2010) database and NCBI *Malus* EST collections for

homologs. Both databases are available online on a single website http://www.rosaceae.org/node/1.

Table IV.4 Comparison between activities of pinosylvin OMT (POMT) and resveratrol OMT (ROMT)

Name	POMT	ROMT
Source organism	*Pinus sylvestris*	*Vitis vinifera, V. pseudoreticulata*
Reaction catalyzed	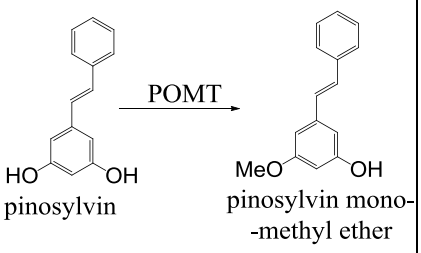 pinosylvin → pinosylvin mono--methyl ether Catalyzes only one methylation step, no further methylation occurs even when the monomethylated product is used as asubstrate.	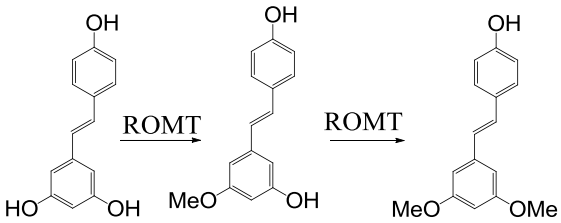 resveratrol → resveratrol mono--methyl ether → pterostilbene Catlyzes two sequential methylation steps, the monomethylated product can be detected upon short incubation time.
Substrate specificity	Accepts a broad range of compounds, with greater activity toward catechol, esculetin, astringenin (3,5,4`,5`-tetrahydroxystilbene), caffeic acid, 5-hydroxyferulic acid, quercetin, caffeoyl-CoA, and smaller activity toward resveratrol, luteolin.	Accepts to a lesser degree: orcinol, caffeic acid, eugenol, pterostilbene
Phylogenetic analysis (Schmidlin et al., 2008)	More related to COMT from different species	More related to orcinol OMTs from *Rosa*, eugenol OMT and chavicol OMT from *Ocimum basilicum*
Our target is one methylation step	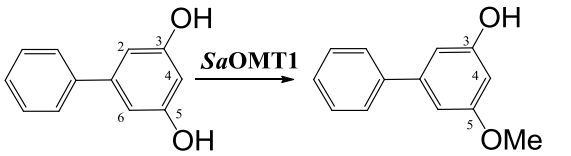 3,5-dihydroxy--biphenyl → 3-hydroxy-5-methxoy--biphenyl 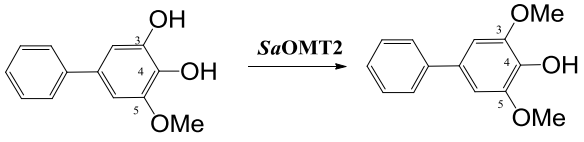 noraucuparin → aucuparin	

4.2 Candidate sequences in apple genome and EST databases

Malus and *Sorbus* are taxonomically and phylogenetically related (Campbell et al., 2007; Potter et al., 2007). Additionally, *BIS* homologs from *Malus* and *Sorbus* had more than 90% identity on the nucleotide level (Chizzali et al., 2012b). So, candidates from *Malus* will be closely related to putative candidates in *Sorbus*, therefore the aforementioned genome databases were screened and the results are presented in Table IV.5. Candidates were subdivided in three groups based on the degree of identity to the probe POMT and to each others, when compared on the amino acid sequence level. Group one shares 57-55% identity, while the second group has 50-48% identity. Each group represents one candidate and can be amplified with the same primer set because the 5`- and 3`- ends are nearly identical except for two or three nucleotides. At these positions degeneracy was integrated in the primer sequences. The corresponding primer sets are mentioned under II.5.3. In all the identified candidate sequences, restriction sites of *Bam*HI and *Hind*III were absent. Consequently, the restriction site of *Bam*HI was integrated in the forward primers, while the restriction site of *Hind*III was integrated in the reverse primers. By using these primers, we could amplify the full ORF of the candidates supplied with additional restriction sites on both ends, which in turn facilitates the further cloning work.

Table IV.5: Candidates from the apple genome and the NCBI *Malus* EST library upon screening with POMT.

Group[a]	Candidates in *Malus* EST	Percent identity to template POMT	Candidates among predicted CDS in the apple genome	Percent identity to template POMT	Function later determined.
One	ABEEAA00393 (Royal Gala seedling leaves infected with *V. inaequalis*)	57	MDP 0000208322 MDP 0000396450 MDP 0000135207 MDP 0000271124 MDP 0000656929	57-55	*Sa*OMT2
Two	ABPBB00532 (M9 root tips)	48	MDP 0000552625 MDP 0000456277 MDP 0000466546	50-48	*Sa*OMT1
Three	ABDAA00260 (Royal Gala fruit stored for 24 h under low oxygen/high CO_2)	41	MDP0000703981 MDP0000642867 MDP0000328025	43	No product after RNA digestion with DNaseI

[a] Candidates are grouped on the basis of amino acid sequence identity to each other and to POMT . Members of each group can be amplified with only one set of primers because 5`- and 3`- ends of the open reading frames are identical.

4.3 Amplification of cDNAs encoding SaOMTs

A cDNA pool was prepared by reverse transcription of RNA isolated 9 h after elicitation and used as a template for PCR reaction (III.9.3). The primer sets used for amplification of the candidates are mentioned under II.5.3. The cDNAs were amplified using proof-reading Phusion DNA polymerase Hot start II and the PCR program under III.9.5. The primer set *Sa*OMT2 was used to amplify members of group one (Table IV.5) and gave a product of 1098 bp in length, which had 58.7% identity on the protein level with POMT and was designated as *Sa*OMT2. The primer set *Sa*OMT1 was used to amplify members of group two and gave a product of 1113 bp in length, which had 47.4% identity on the protein level with POMT and was designated as *Sa*OMT1 (Fig. IV.13) The primer set OMTC gave no product when RNA was digested during preparation with DNase I, indicating that this gene is not transcribed.

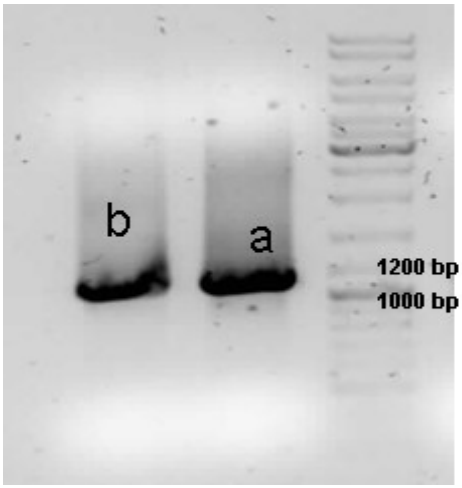

Figure IV.13: Gel electrophoresis of PCR products for *Sa*OMTs.
a. *Sa*OMT1 cDNA. b. *Sa*OMT2 cDNA.

4.4 Heterologous expression of *Sa*OMT cDNAs

The PCR products of the aforementioned reactions were purified, digested and ligated to pRSET B expression vector between *Bam*HI and *Hind*III restriction sites (III.9.7-III.9.9) (Fig. IV.14). The ligation product was introduced in *E. coli* DH5α (III.9.10.) to obtain a large amount of this plasmid, followed by plasmid isolation (III.9.11). Confirmation of successful ligation was carried out by restriction analysis (Fig. IV.14). Sequencing of the insert starting from T7 promoter was performed to ensure the correct orientation of the insert and its presence in the right frame. Plasmids were transferred in BL21(DE3)pLysS for carrying out heteologuos expression (III.9.12, III.9.13). Successful expression of proteins and confirmation of their production as soluble proteins were carried out by SDS-PAGE. Band sizes of ~ 42-44 kDa were expected (39-41 kDa + 3 kDa N-terminal tag). Indeed, these bands were induced upon addition of IPTG and constituted major bands in the crude soluble protein. Finally, they were eluted from the Ni-NTA gel bed (Fig. IV.15)

A

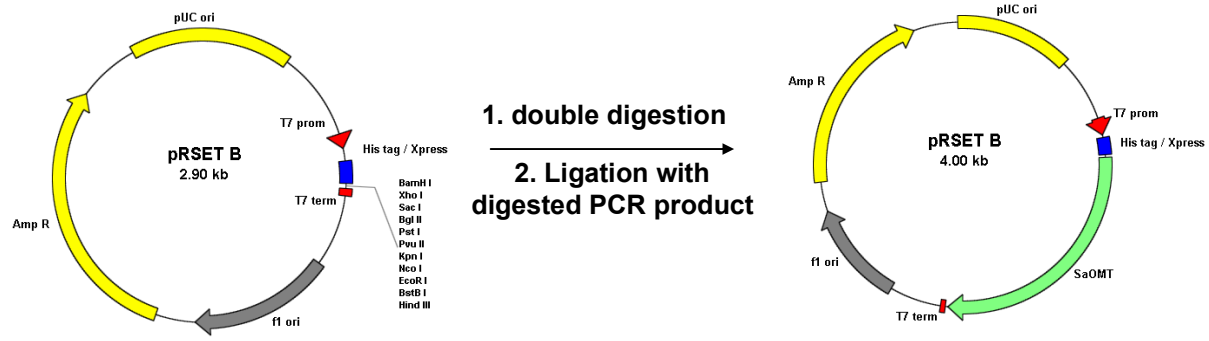

B

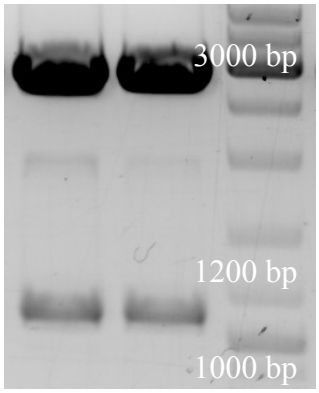

Figure IV.14: Construction of the expression vector for *Sa*OMT cDNAs. A. vector maps, B. confirmation of successful ligation and presence of the inserts.

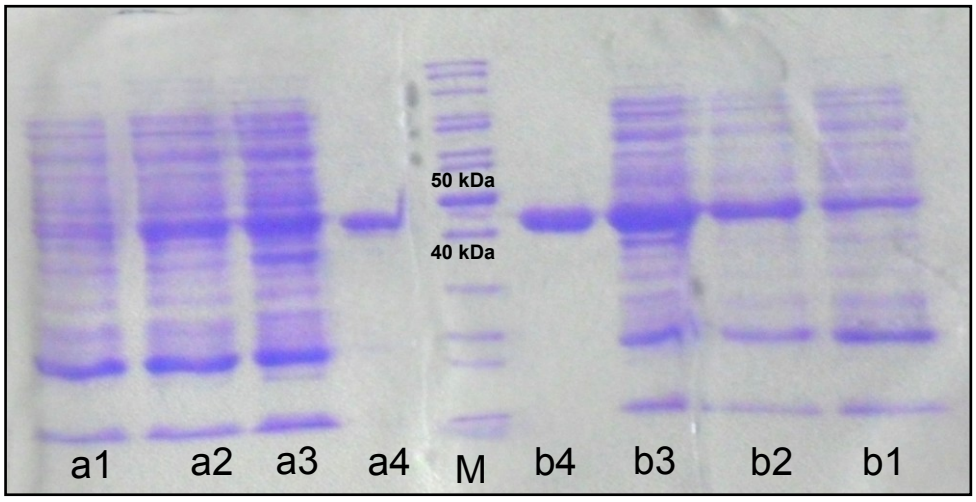

Figure IV.15: SDS-PAGE of the over-expressed proteins *Sa*OMT1 and *Sa*OMT2.
a: *Sa*OMT1 (3,5-dihydroxybiphenyl OMT)
b: *Sa*OMT2 (noraucuparin OMT)
1: crude protein extract before addition of IPTG
2: crude protein extract after addition of IPTG
3: crude soluble protein after addition of IPTG (a: 21.7 µg, b: 18.75 µg)
4: purified protein eluted from a Ni-NTA agarose matrix (a: 3.8 µg, b: 5.7 µg)

4.5 Biochemical characterization of recombinant *Sa*OMTs

In all the following sections, characters were determined using 3,5-dihydroxybiphenyl as a substrate for *Sa*OMT1 and noraucuparin for *Sa*OMT2, unless otherwise mentioned. Ascorbic acid is added to the incubation in order to protect substrates and products from oxidation. Enzyme assays were carried out using the affinity-purified enzymes without cleaving the His-tag.

4.5.1 Determination of temperature and pH optima

*Sa*OMT1 and *Sa*OMT2 had distinct properties when compared to each other. The maximum catalytic activity and stability of *Sa*OMT1 was at pH 8-9 and 35°C. Subsequent enzyme assays were carried out at pH 8.5 and 35°C (Fig. IV.16)

For *Sa*OMT2, the best conditions were pH 7 and 40-50°C. Such a high temperature was recorded also for an alkaloid OMT (Frick and Kutchan, 1999). Subsequent enzyme assays were carried out at pH 7 and 45°C (Fig. IV.17).

A

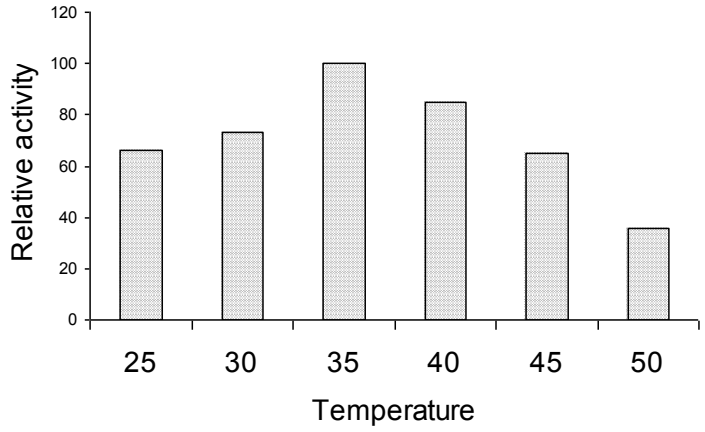

B

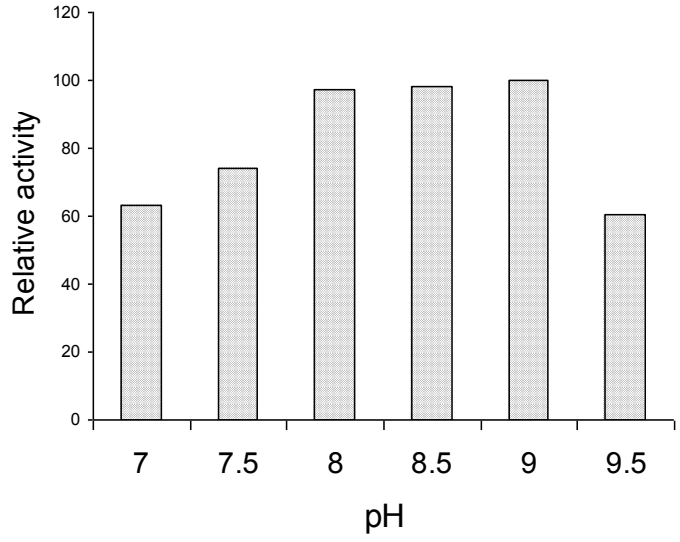

Figure IV.16: Effect of pH and temperature on *Sa*OMT1 activity. Data are mean values of three independent experiments.

A

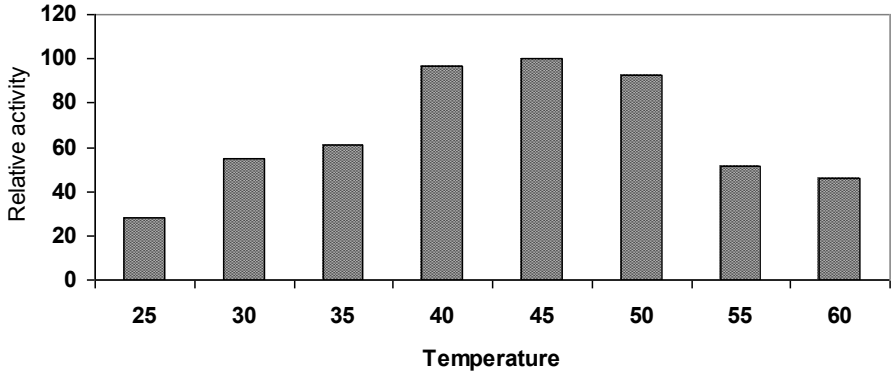

B

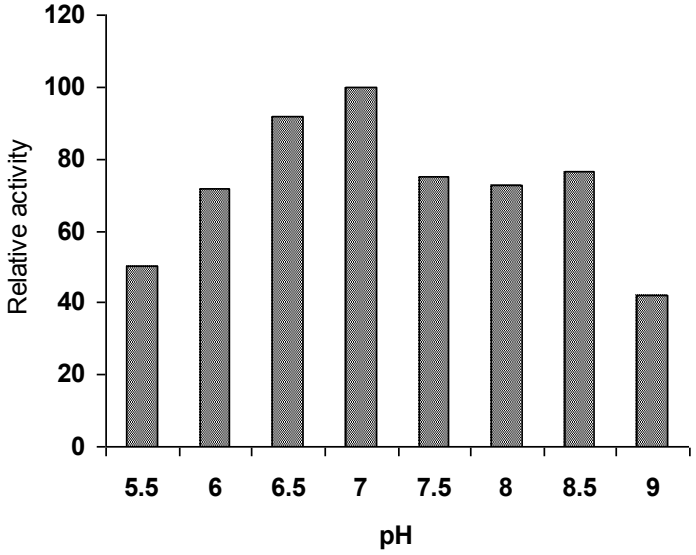

Figure IV.17: Effect of pH and temperature on *Sa*OMT2 activity. Data are mean values of three independent experiments.

4.5.2 Effect of incubation time and protein amount

The accumulation of the product 3-hydroxy-5-methoxybiphenyl was linear up to 50 min incubation time and up to 1.5 µg of pure *Sa*OMT1 protein per assay (Fig. IV.18)

For *Sa*OMT2, accumulation of noraucuparin was linear up to 35 min incubation time and up to 0.65 µg of pure protein per assay (Fig. IV.19).

For subsequent assays, 0.65 µg *Sa*OMT1 and ~0.6 µg *Sa*OMT2 were used. The incubation time was 25 min for both enzymes.

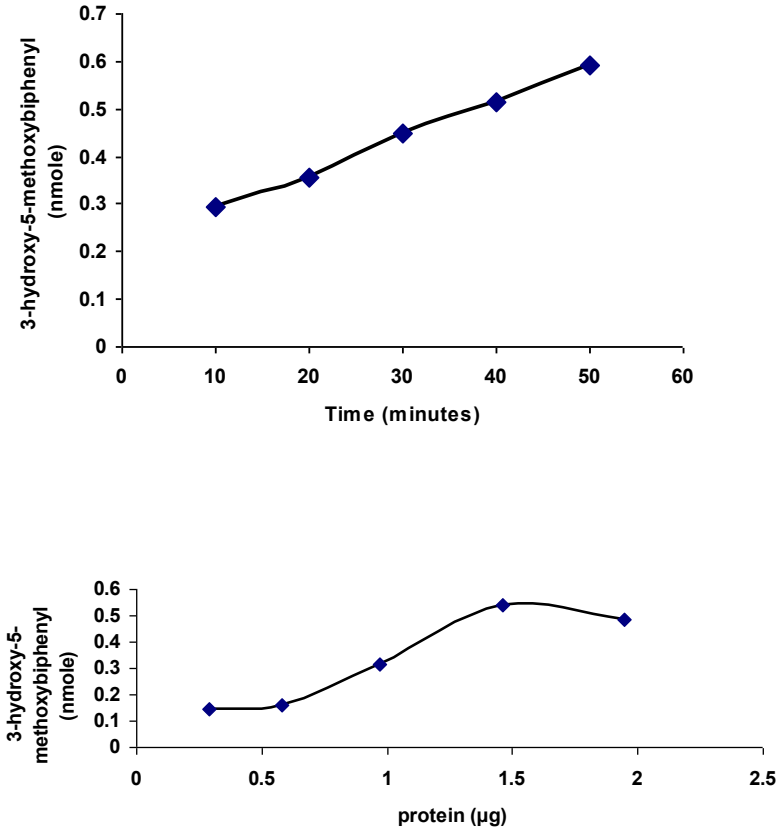

Figure IV.18: Effect of time and protein amount on *Sa*OMT1 activity. Data are means of three independent experiments.

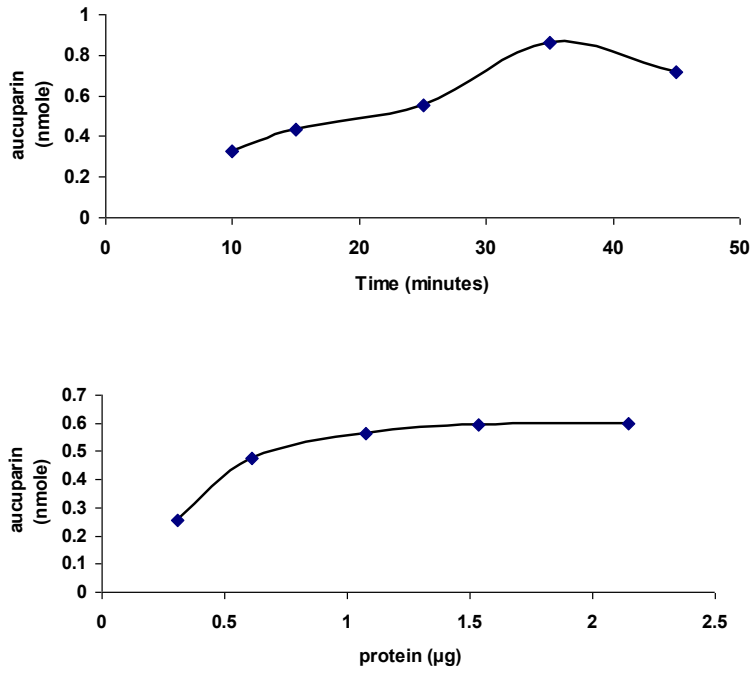

Figure IV.19: Effect of time and protein amount on *Sa*OMT2 activity. Data are means of three independent experiments.

4.5.3 Determination of substrate specificities

Both *Sa*OMT1 and *Sa*OMT2 were tested under the respective optimum assay conditions with a number of potential substrates (Fig. IV.20).

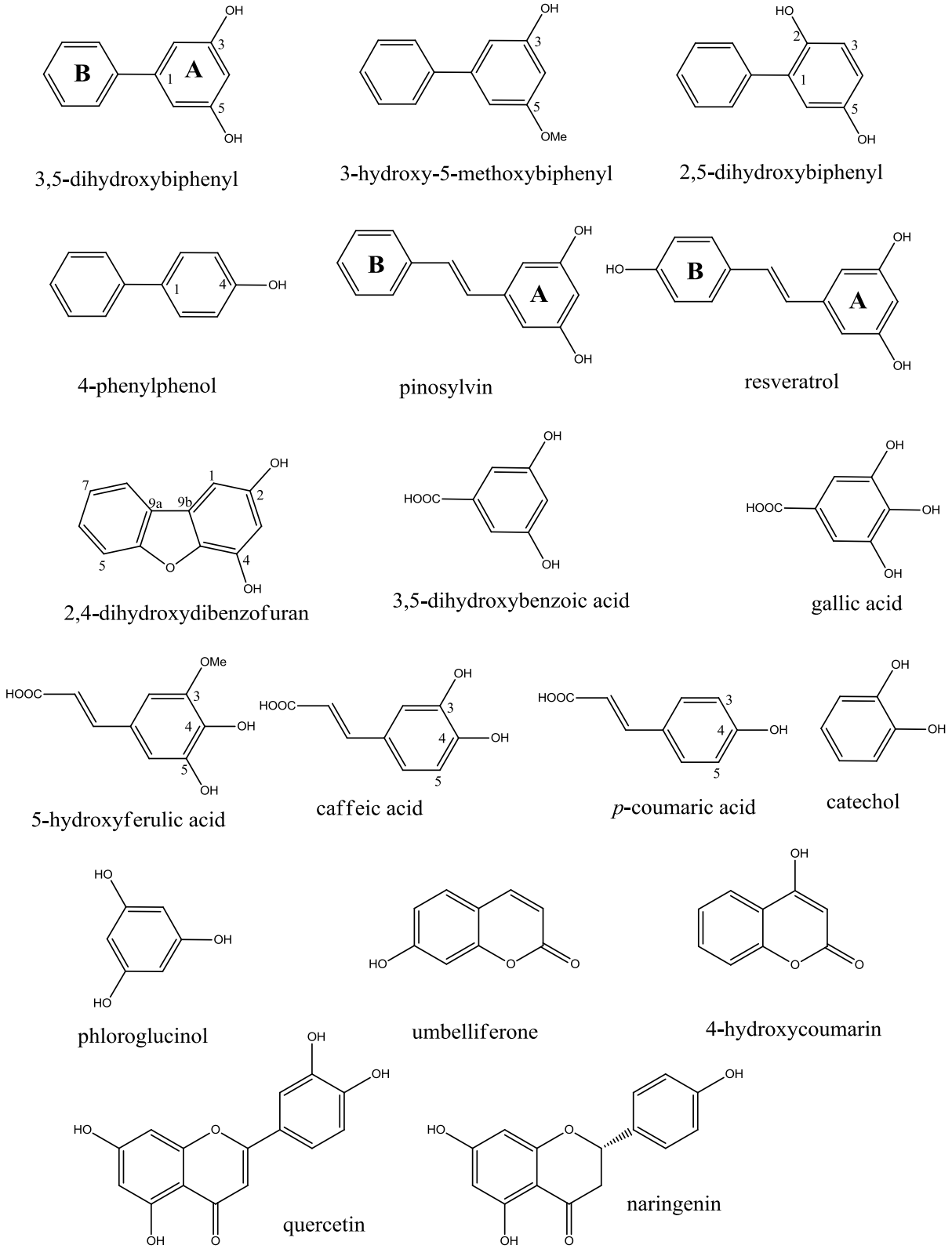

Figure IV.20: Compounds tested as potential substrates for *Sa*OMT1 and *Sa*OMT2 .

*Sa*OMT1 shows a high degree of substrate specificity regarding the substitution pattern and the molecular size of the substrate. *Sa*OMT1 methylates only the *meta*-dihydroxylated substrates, namely, 3,5-dihydroxybipheny, 2,4-dihydroxydibenzofuran, and pinosylvin. Similar substrates with different substitution patterns were not accepted, e.g. 2,5-dihydroxybiphenyl, 3-hydroxy-5-methoxybiphenyl and 4-phenylpenol (Fig. IV.20). Interestingly, no small molecules with the same substitution pattern were accepted, e.g. 3,5-dihydroxybenzoic acid, phloroglucinol and gallic acid. Nor was resveratrol, which is larger than pinosylvin, accepted. Substrates belonging to phenylpropanoic acids, flavonoids or coumarins were not accepted either. *Sa*OMT1 catalyzes only methylation of 3,5-dihydroxybiphenyl, 2,4-dihydroxydibenzofuran and pinosylvin (Table III). For all three reactions catalyzed by *Sa*OMT1, only one methylation step takes place and the methylated product is not accepted for a further methylation step (Fig. IV.21).

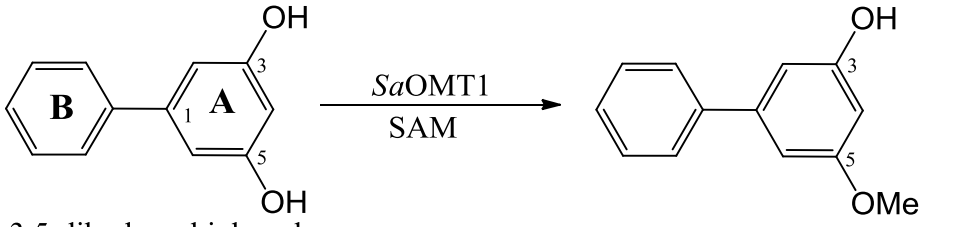

3,5-dihydroxybiphenyl

3-hydroxy-5-methoxybiphenyl

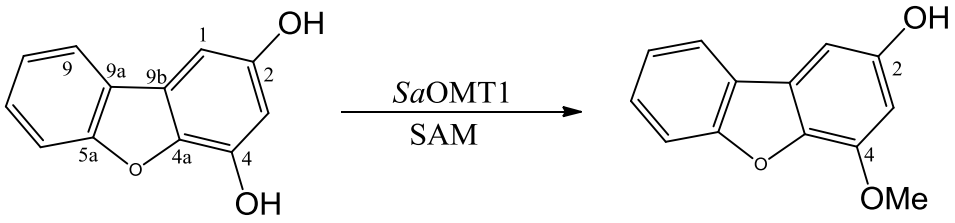

2,4-dihydroxydibenzofuran

2-hydroxy-4-methoxydibenzofuran

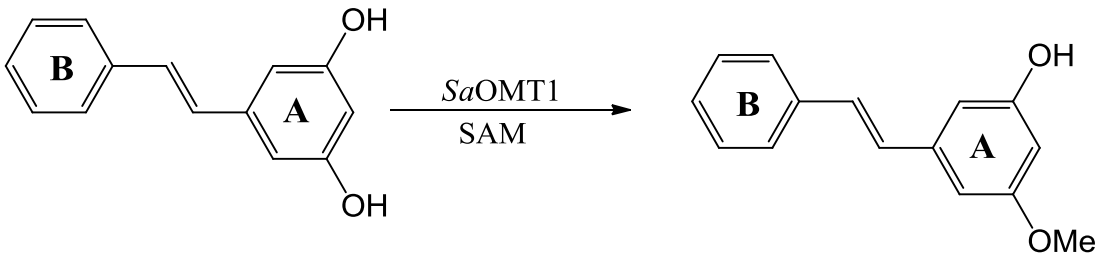

pinosylvin

pinosylvin monomethylether

Figure IV.21: Substrates methylated by *Sa*OMT1.

Conversely, *Sa*OMT2 shows more relaxed substrate specificity. Noraucuparin, 5-hydroxyferulic acid and caffeic acid are the most preferable substrates (Fig. IV.21, IV.22). Additionally, *Sa*OMT2 accepts substrates of *Sa*OMT1 with low catalytic activity (Table IV.6). Importantly, substrates belonging to other classes, e.g. small phenolics, are not accepted, which is similar to *Sa*OMT1. For all the accepted substrates, only one methylation step for a *meta*-hydroxyl group is catalyzed. Interestingly, both *Sa*OMT1 and *Sa*OMT2 are quite different from their

probe, POMT, in that they do not accept resveratrol as a substrate. Moreover, although *Sa*OMT2 had a relatively relaxed substrate specificity, it was more specific than POMT, which catalyzes methylation of flavonoids, coumarins, and small phenolic molecules, e.g. catechol, even at higher velocities than its physiological substrate pinosylvin (Chiron et al., 2000). This underlines the high specificity of the recombinant proteins from *S. aucuparia*. Identities of all the reaction products were verified by HPLC analysis in comparison with reference compounds except for pinosylvin monomethyl ether, whose identity was confirmed by GC-MS because of the lack of authentic reference material (Fig. IV.23, IV.24).

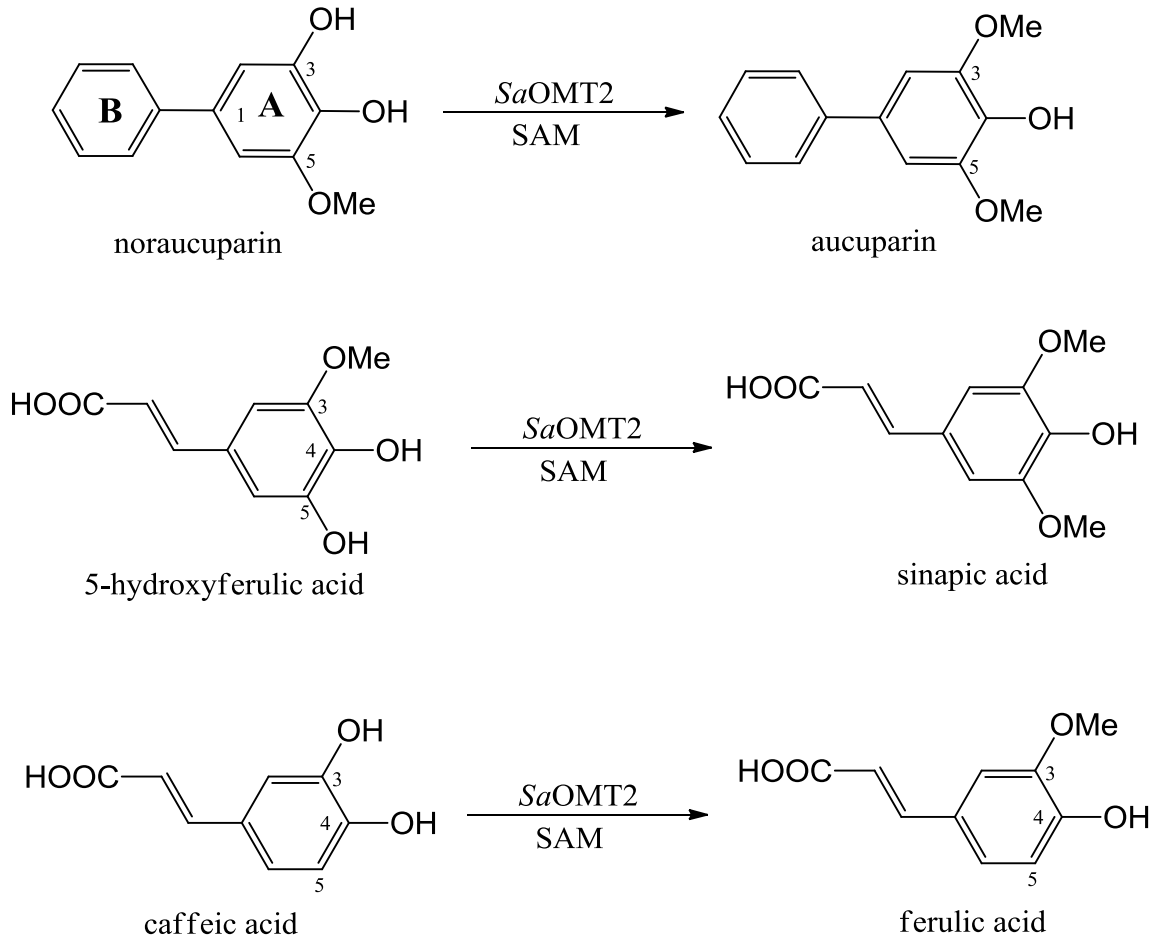

Figure IV.22: Substrates methylated by *Sa*OMT2.

Table IV.6: Relative activity of *Sa*OMT1 and *Sa*OMT2 with different substrates.

*Sa*OMT1		*Sa*OMT2	
Substrate	Relative activity (%)	Substrate	Relative activity (%)
3,5-dihydroxybiphenyl	100[a]	noraucuparin	100[b]
		5-hydroxyferulic acid	190.5
2,4-dihydroxy-dibenzofuran	64.4	caffeic acid	68.5
		2,4-dihydroxy-dibenzofuran	10
pinosylvin	52	pinosylvin	9.3
		3,5-dihydroxybiphenyl	1.5
[a] 10.4 nkat/µg protein		[b] 53 nkat/µg protein	

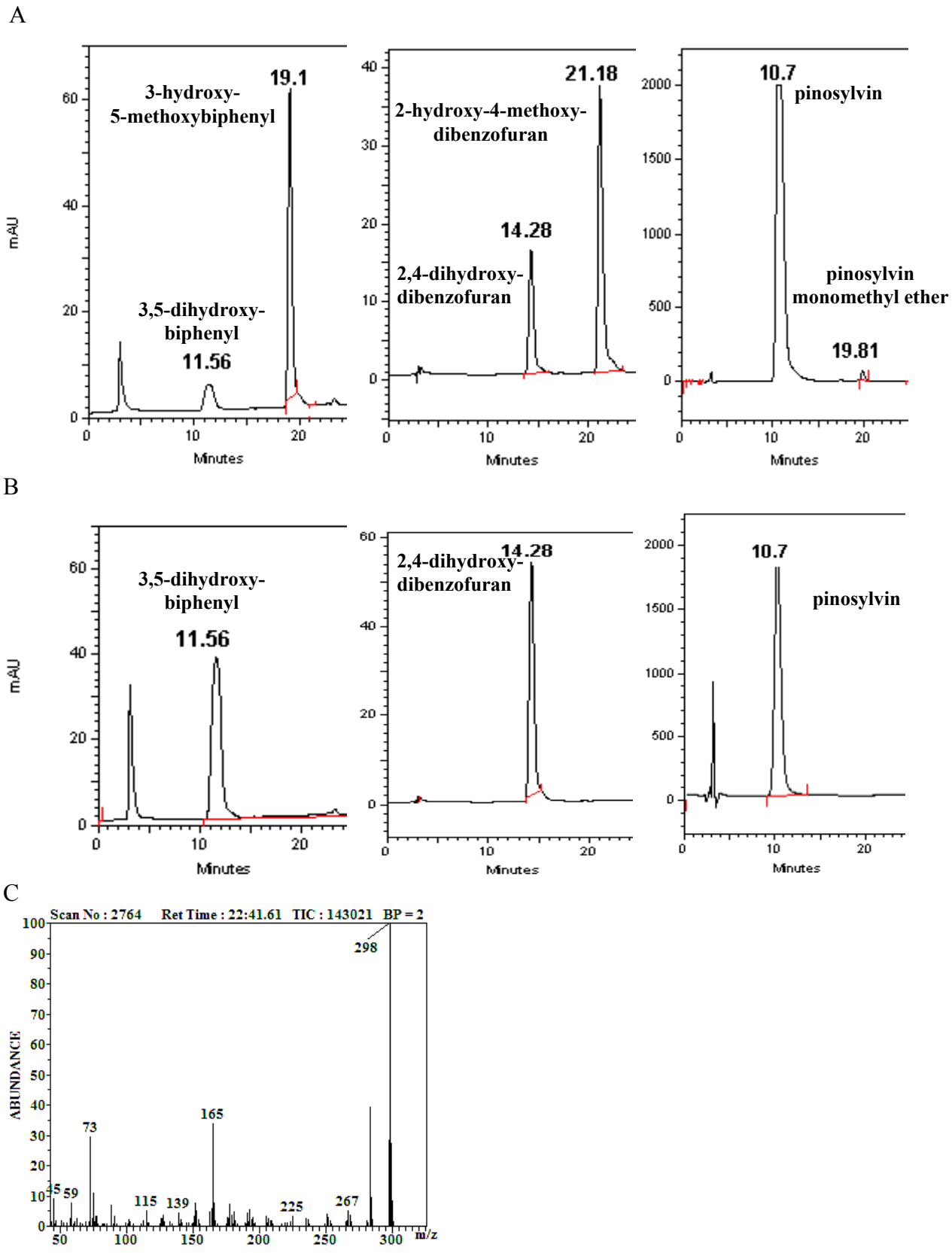

Figure IV.23: HPLC analysis of *Sa*OMT1 assays.
A. assays with active protein. B. assays with boiled protein C. Mass spectrum of silylated pinosylvin monomethylether.

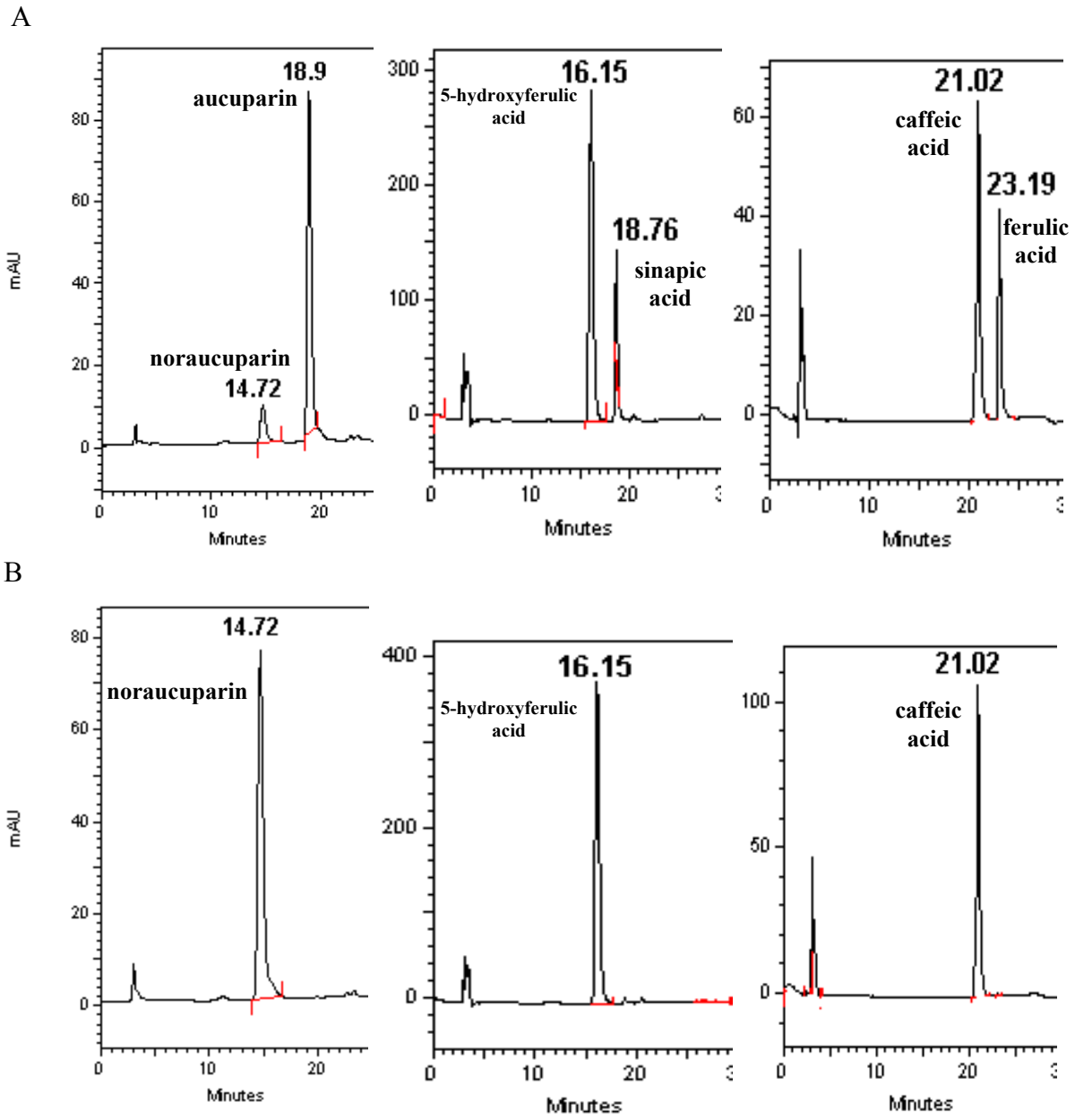

Figure IV.24: HPLC analysis of *Sa*OMT2 assays.
A. assays with active protein. B. assays with boiled protein

4.5.4 Determination of kinetic parameters

This characterization helps in determining the preferred substrate for each enzyme. K_m values reflect the enzyme affinity to different substrates. K_{cat} is the turnover number, which reflects how efficiently an enzyme transforms a substrate. K_{cat}/K_m is called the catalytic efficiency. It can be used to compare between utilization of different substrates by one enzyme and to compare the catalytic efficiency between different enzymes. Moreover, it is a good measure of substrate specificity because it assesses the interaction between the enzyme and the substrate in the ground state as well as in the transition state (Copeland, 2002). Based on this information, we can determine the best substrate for each enzyme. The summaries of the kinetic data for the two enzymes are presented below (Table IV.7) (Fig. IV.25, IV.26).

Table IV.7: Kinetic parameters of *Sa*OMT1 and *Sa*OMT2. Data are average values of three determinations.

Enzyme	Calculated subunit mass (Da)	Protein concentration in enzyme assay	Substrate	K_m (μM)	V_{max} ($nM.s^{-1}$)	K_{cat} (s^{-1})	K_{cat}/K_m ($s^{-1}.M^{-1}$)
*Sa*OMT1[a]	41027	73.1 nM	3,5-dihydroxy-biphenyl	28.38	18.4	0.15	5285.4
			2,4-dihydroxy-dibenzofuran	28.45	6.31	0.052	1827.8
*Sa*OMT2[b]	39820	78.7 nM	noraucuparin	38.05	35.97	0.29	7964.6
			5-hydroxy-ferulic acid	55.96	66.64	0.53	9471.0
			Caffeic acid	83.4	36.13	0.29	3649.8

[a] K_m for SAM is 39.58 μM. [b]K_m for SAM is 83.01 μM

*Sa*OMT1 had equal affinity to 3,5-dihydroxybiphenyl and 2,4-dihydroxydibenzofuran (the same K_m value); however, conversion of the biphenyl substrate was catalyzed 3 times more efficiently than that of the dibenzofuran (K_{cat}, V_{max}) (Table IV.7). So, 3,5-dihydroxbiphenyl is the best substrate, as reflected by the K_{cat}/K_m value. It is straightforward to assign *Sa*OMT1 as 3,5-dihydroxybiophenyl OMT. Notably, 2,4-dihydroxydibenzofuran and its methylation product, 2-hydroxy-4-methoxydibenzofuran, were not detected before in any Pyrinae species.

*Sa*OMT2 has the highest affinity towards noraucuparin. The K_m value for 5-hydroxyferulic acid was 1.5-fold and that for caffeic acid 2-fold higher.(Table IV.7). However, 5-hydroxyferulic acid is 2-fold more efficiently converted than noraucuparin, with a 1.2-fold higher K_{cat}/K_m ratio. Judging these two parameters against each other, *Sa*OMT2 may be assigned as a multifunctional enzyme with greater affinity for noraucuparin but greater catalytic efficiency with 5-hydroxyferulic acid.

A

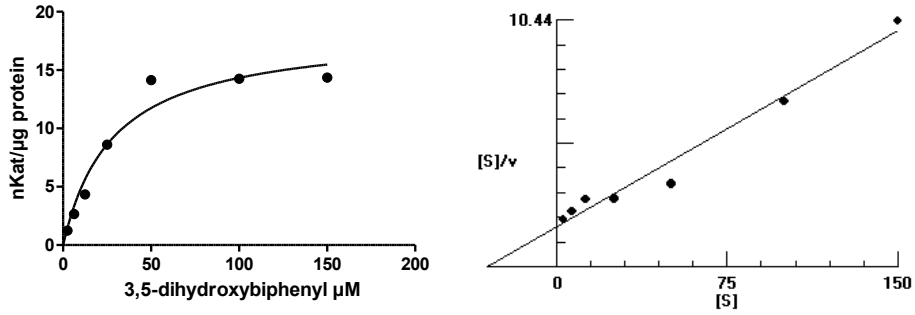

B

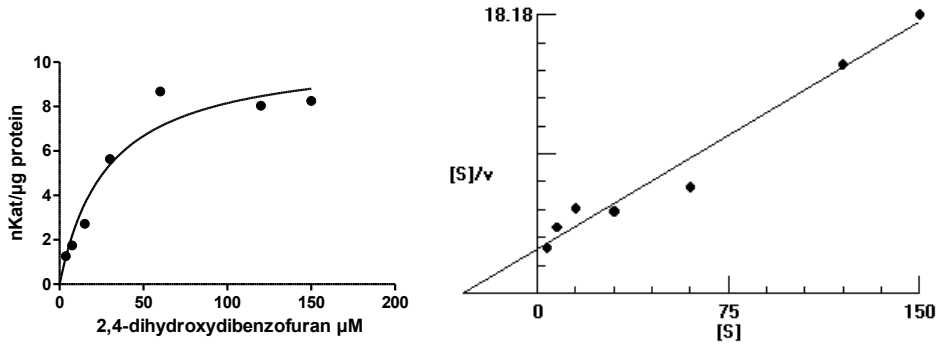

C

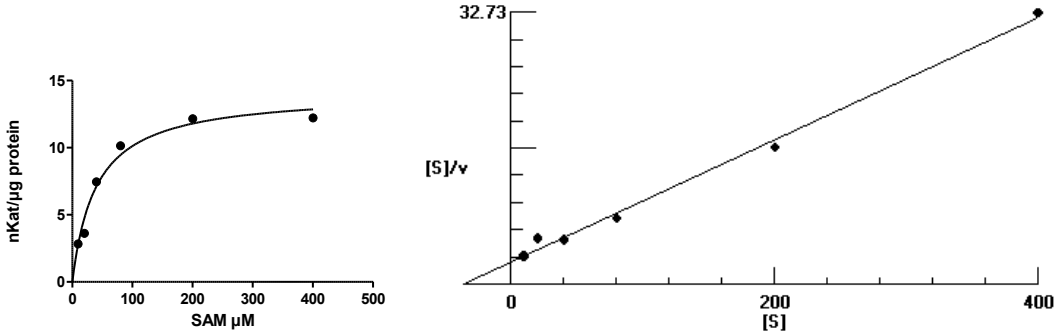

Figure IV.25 Graphical representation of enzyme kinetics of *Sa*OMT1 through Michaelis-Menten and Hanes-Woolf plots. A. 3,5-diydroxybiphenyl as substrate, B. 2,4-dihydroxydibenzofuran as substrate, C. SAM as cofactor

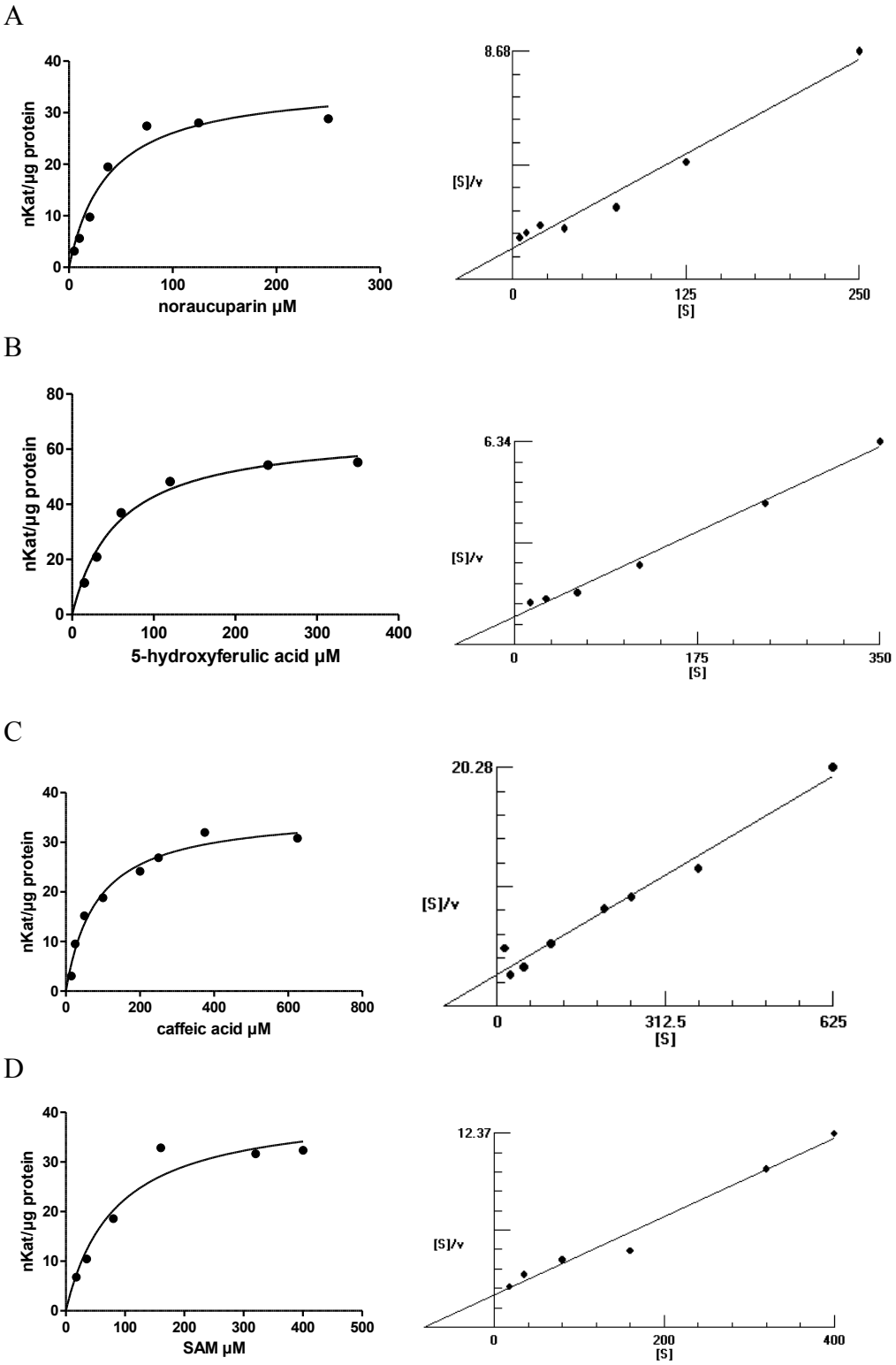

Figure IV.26: Graphical representation of enzyme kinetics of *Sa*OMT2 through Michaelis-Menten and Hanes-Woolf plots. A. noraucuparin as substrate, B. 5-hydroxyferulic acid as substrate, C. caffeic acid as substrate, D. SAM as cofactor

4.5.5 Utilization of noreriobofuran by *Sa*OMT2

The chemical synthesis of noreriobofuran was not successful and classical isolation from elicitor-treated cell cultures yielded only trace amounts. This prompted us to incubate the purified recombinant protein *Sa*OMT2 with a methanol

extract from the cell cultures, which contained both noraucuparin and noreriobofuran. HPLC analysis demonstrated that both substrates were utilized by the enzyme, which led to disappearance of both peaks in the incubation chromatograms (Fig. IV.27). Noreriobofuran is structurally similar to noracuparin, in analogy to the relation between 3,5-dihydroxybiphenyl and 2,4-dihydroxydibenzofuran.

A

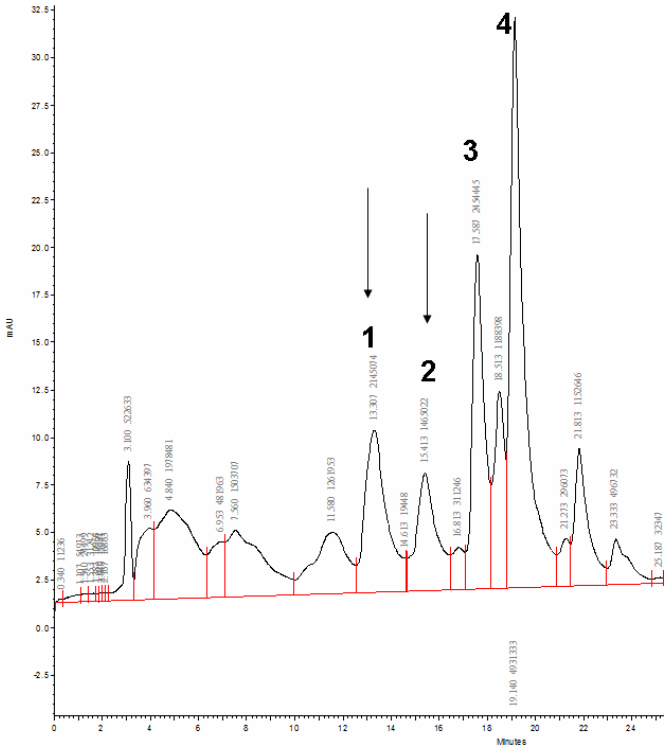

B

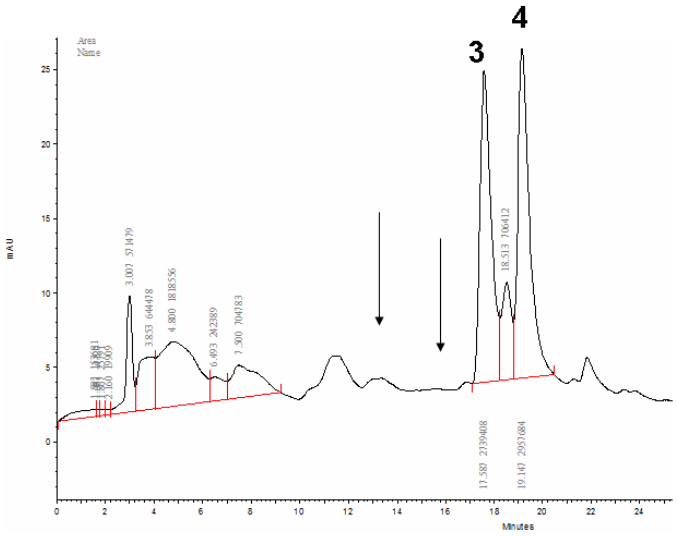

Figure IV.27: HPLC analysis of incubations containing *Sa*OMT2 and methanolic *S. aucuparia* extract. A, assay with heat-denaturated protein. B, assay with active protein, indicated by disappearance of the peaks of noraucuparin (1) and noreriobofuran (2). Peak 3, aucuparin; peak 4, eriobofuran.

4.6 Gene expression analyses

4.6.1 Semiquantitative RT-PCR

Expression of the *SaOMT1* and *SaOMT2* genes was analyzed in addition to *Actin* and *BIS1* (Fig. IV.28). *Actin* served as a control to ensure equality of RNA levels used. BIS1 synthesizes 3,5-dihydroxybiphenyl, which then serves as a substrate for *Sa*OMT1. The accumulation of *BIS1* transcripts after elicitation with *V. inaequalis* extract agrees with that reported after elicitation with yeast extract (Liu et al., 2007). The expression is strongly induced after induction, reaches a maximum after 3-6 h and rapidly decreases, resulting in poor transcript levels after 24 h and later. *SaOMT1* expression parallels that of its predecessor enzyme BIS. Its transcription is strongly and rapidly upregulated after induction reaches a maximum after 3-6 h and then declines gradually over 72 h post-treatment (Fig. IV.28). In contrast to the previous two, *SaOMT2* expression shows an increase within the first hours and thereafter a relatively stable level over the tested 72 h post-treatment.

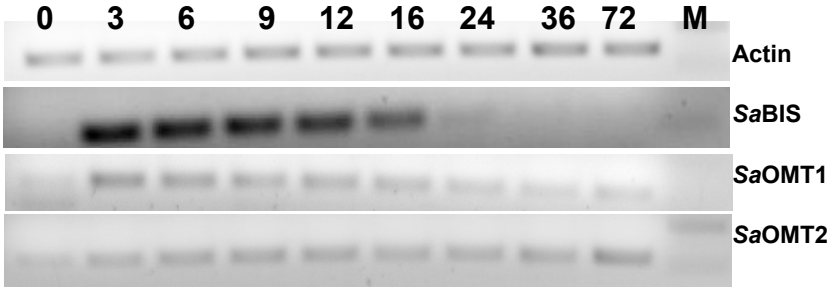

Figure IV.28: Semiquantitative RT-PCR analysis of *SaOMTs*, *BIS* and *Actin* expression. Numbers indicate hours after elicitation.

4.6.2 Quantitative Real-Time PCR

The accuracy and reliability of the results obtained here depends to a large extent on the purity and integrity of the prepared RNA samples. The purity was checked through the A_{260}/A_{280} ratio. These values were greater than 1.9. The integrity was checked by agarose gel electrophoresis (2%). Appearance of two distinct bands of ribosomal 18S and 28S RNA was confirmed (Fig. IV.29).

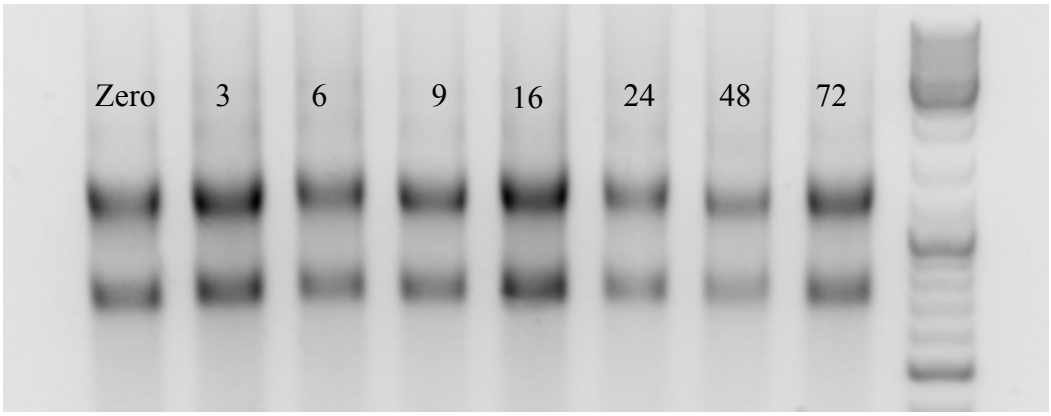

Figure IV.29: Agarose gel with separated RNA samples prepared for real-time qRT-PCR. Numbers indicate hours post-elicitation.

Before carrying out the experiment, the efficiency of the PCR reaction using the designed primers should be checked, which was performed by plotting the quantity of the input cDNA against Ct values and calculating the efficiency from the equation $E=10^{(-1/slope)}$. Ideally, the efficiency should fall in the range 90-110%; however, values as low as 81% are also working (Pfaffl et al., 2001). On the other hand, the specificity of the PCR reactions is checked by the melt curve and agarose gel electrophoresis of the product. The calculated efficiency values and the experimentally determined Ct values were used in the calculation of relative expression as described under III.9.15. The data obtained are presented in Fig. IV.30.

Table IV.8: Efficiency of the qPCR reactions.

Name of the reaction	Slope of the standard curve	R^2	Efficiency[a] (%)
BIS1	-3.46	0.994	93.06 ± 2.5
SaOMT1	-3.56	0.994	94.55 ± 0.05
SaOMT2	-3.73	0.997	87.36 ± 2.3
Tubulin	-3.84	0.999	86.73 ± 3

[a] average of three experiments ± SD

The expression profiles of the three investigated genes were interesting. *BIS* expression was rapidly and strongly upregulated after induction by *V. inaequalis*, reaching a maximum at 6 h, whereafter the transcript level continuously declined (Fig. IV.30). Similarly, *SaOMT1* expression was rapidly and strongly upregulated, reaching the maximum at 3-6 h. Then, like *BIS*, it started to decrease and reached low level after 48 h. In contrast to the previous two, *SaOMT2* expression was not strongly upregulated and increased more slowly. It reached a maximum at 6 h and remained at this level up to 16 h. Thereafter, the transcript level started to decline. The mRNA levels of all three genes remained constant between 48 and 72 h. The decrease in the transcript level of *SaOMT2* in relation to its maximum was not so dramatic as for *BIS and SaOMT1*. The relatively constant level over a long period was consistent with the observation that aucuparin tended to accumulate at a sluggish but progressive rate.

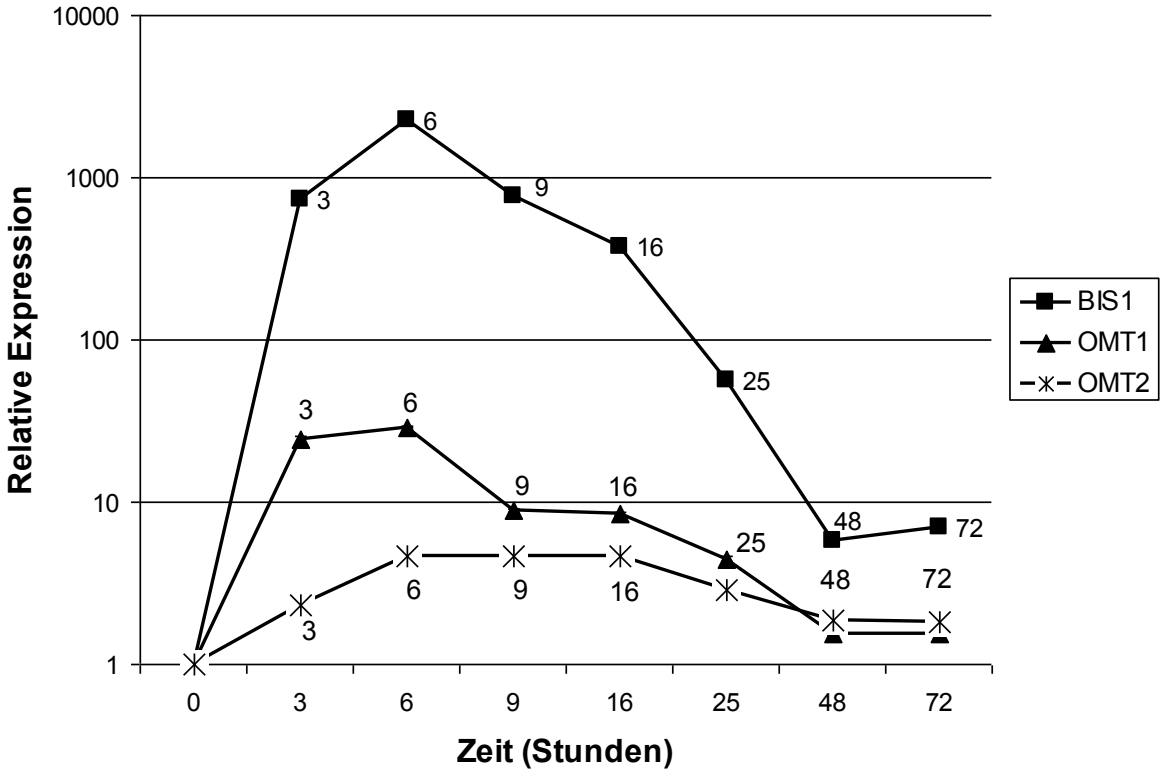

Figure IV.30: Relative transcript levels of *BIS1, SaOMT1* and *SaOMT2,* determined by real-time qRT-PCR. SD do not exceed 2%

5. Homology modeling of *S. aucuparia* OMTs

Quite a number of plant OMTs were crystallized previously (Liu et al., 2006; Louie et al., 2010; Zubieta et al., 2001; Zubieta et al., 2002). Of these enzymes, alfalfa COMT served as a base for modeling of SaOMT1 and SaOMT2 because of high similarities on the amino acid level, namely 50.1% and 83.6%, respectively. The models as well as the alignment showed the high degree of conservation of motifs responsible for SAM binding and slight modifications related to substrate binding.

In *Sa*OMT2, two amino acids are involved in catalysis, namely His-269 and Glu-329 (Fig. IV.30). The mechanism of transmethylation is quite established to take place as SN^2 substitution reaction (Louie et al., 2010; Zubieta et al., 2001). His-269 abstracts the proton of the hydroxyl group to form a phenolate anion which simultaneously attacks the labile methyl group of SAM. Glu-329 acts as a hydrogen bond acceptor for the His-269 ND1 nitrogen and this will position the other His-269 NE1 nitrogen in the right conformation to deprotonate the hydroxyl group of the substrate. The carboxylate group of Asp-270 stabilizes the 4-hydroxyl group of noraucuparin by formation of a H-bond, which helps to sequester the substrate and to orient the 3-hydroxy group in close proximity to SAM (Fig. IV.30A). Such interaction will be absent in case of 3-hydroxy-5-methoxybiphenyl and 3,5-dihydroxybiphenyl, which lack the 4-hydroxyl moiety, explaining the inactivity towards these substrates. The methoxy group of noraucuparin or 5-hydroxyferulic acid is stabilized by hydrophobic interaction with Phe-176 and Ile-316 (Fig. IV.30A, IV.30B). The presence of a hydrophobic pocket that accommodates the meta-methoxy group explains the high affinity for noraucuparin and 5-hydroxyferulic acid over caffeic acid. So far, the docking model explains the high affinity towards noraucuparin and 5-hydroxyferulic acid. Nevertheless, it explains further the differences in kinetic data between these two substrates. Ring B of noraucuparin is stabilized by hydrophobic interaction with the amino acids Met-180, Ile-316, Ile-319 and Leu-127, which explains the higher affinity towards noraucuparin (1.5 fold lower K_m) (Fig. IV.30A), while the polar carboxylate group of 5-hydroxyferulic acid is merely stabilized by H-bonding with Asn-131 (Fig. IV.30B). By catalysis, however, 5-hydroxyferulic acid is stabilized further by a salt bridge between the carboxylate ion and the protonated histidine side chain. These interactions can explain why 5-hydroxyferulic acid is slightly more efficiently utilized than noraucuparin; this is reflected in the higher Vmax and K_{cat}/K_m ratio (Table IV.7). The observation that *Sa*OMT2 can convert noreriobofuran to eriobofuran is further evidenced by the modeling studies. The active site of *Sa*OMT2 is well suited to accommodate noreriobofuran (Fig. IV.30C). Here, the 3-hydroxyl group of noreriobofuran, equivalent to the 4-hydroxyl group of noraucuparin, interacts with Asp-270. The methoxy group occupies the same hydrophobic pocket occupied by the methoxy group of noraucuparin. The phenyl ring of noreriobofuran will display the same hydrophobic interaction displayed by ring B of noraucuparin. Even more stabilization will be achieved by hydrogen bonding between the furan oxygen and the side chain of Asn-131. In this aspect, *Sa*OMT2 acts similar to hydroxyisoflavanone 4`-O-methyltransferase (HI4`OMT) from alfalfa, which catalyzes the methylation of 2,7,4`-trihydroxyisoflavanone as well as the 3-O-methylation of 6a-hydroxymaackiain. Both substrates were found to have the same three dimensional conformations upon interaction with the enzyme (Liu et al., 2006). Conversion of substrates with similar three-dimensional structures can be

catalyzed either by the same enzyme or by homologues (Liu et al., 2006; Rimando et al., 2012).

Figure. IV.30: Docking models of different substrates in the *Sa*OMT2 active site.

A. Docking arrangement of noraucuparin. B. Docking arrangement of 5-hydroxyferulic acid. C. Docking arrangement of norerioboforan. The substrates are represented in green carbon atoms, SAM in pink carbon atoms, and the amino acids of the active sites are highlighted in light grey color. Oxygen atoms are represented in red color, nitrogen atoms in blue, and sulphur atoms in gold. Hydrogen bonds are represented as black dashed lines, while the interaction between the methyl moiety of SAM and the phenolic hydroxyl group of the substrate is marked as red dashed line.

A

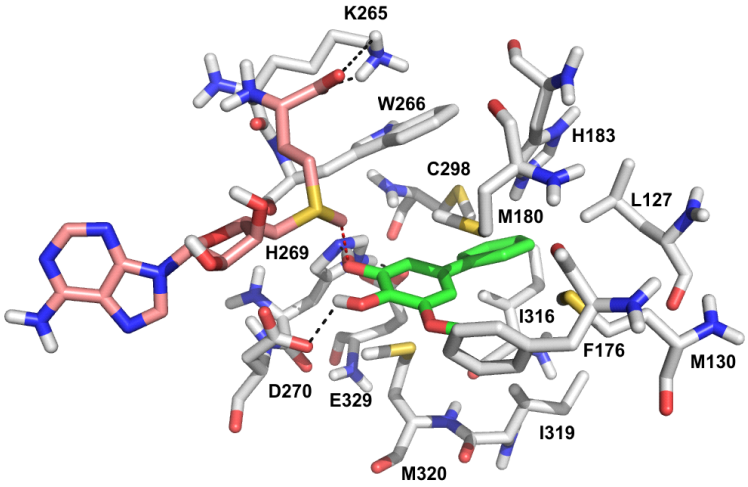
K265
W266
H183
C298
M180
L127
H269
I316
F176
M130
D270
E329
I319
M320

B

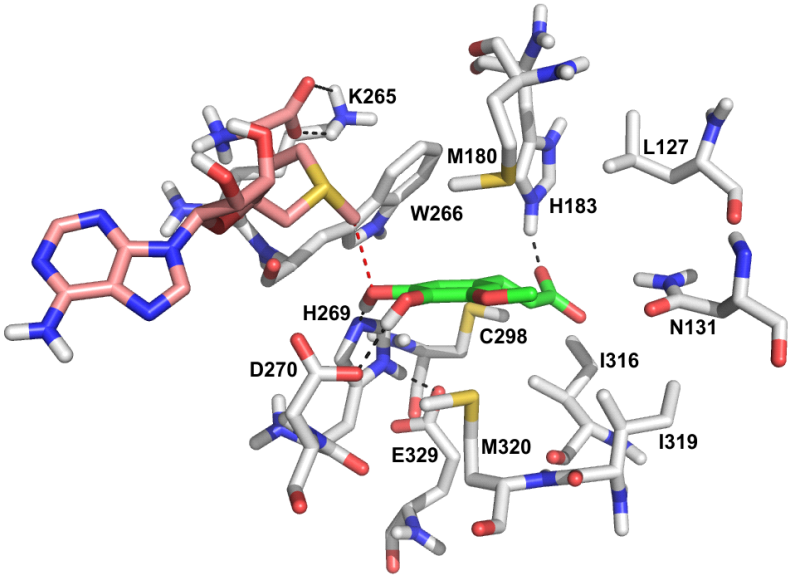
K265
M180
L127
W266
H183
H269
C298
N131
D270
I316
E329
M320
I319

C

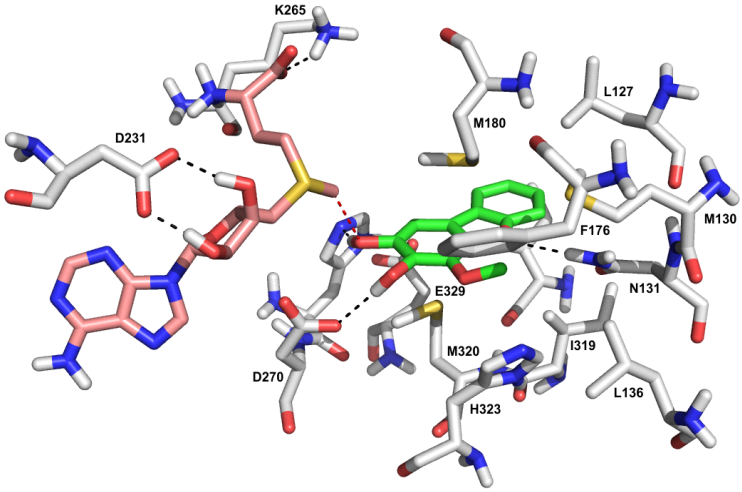
K265
L127
M180
D231
M130
F176
E329
N131
M320
I319
D270
L136
H323

In *Sa*OMT1, His-276 and Glu-336 are responsible for catalysis in the same manner explained before for *Sa*OMT2 (Fig. IV.31). Deprotonation and methylation of one of the meta-dihydroxy groups of the substrate will follow the same manner as explained in case of *Sa*OMT2. Interestingly, the other meta-hydroxyl group forms hydrogen bonds with the carboxylate group of the methionine residue of SAM. Similar interaction will not be present in case of 3-hydroxy-5-methoxybiphenyl, which explains why this compound is not accepted as a substrate and methylation of 3,5-dihydroxybiphenyl occurs only in one hydroxyl group (Fig. IV.31A). Also, this explains the inactivity towards noraucuparin, 5-hydroxyferulic acid and caffeic acids, which have no meta hydroxyl group. It is worth mentioning that interaction of the substrate with SAM directly at a position other than the sulphur group was not found previously; in our case, as in other plant OMTs, the amino group of the conserved Lys-272 interacts with the carboxylate group of the methionine residue of SAM (Fig. IV.31A) (Liu et al., 2006; Louie et al., 2010; Zubieta et al., 2001; Zubieta et al., 2002). Ring B of 3,5-dihydroxybiphenyl is positioned in a hydrophobic pocket formed by Leu-323, Val-134, Val-138, Met-187 and Phe-273. Similar interactions can be found with 2,4-dihdroxydibenzofuran (Fig. IV.31A, IV.31B); here is appreciable that 3,5-dihydroybiphenyl and 2,4-dihydroxydibenzofuran have equal K_m values. The 4-hydroxyl group of 2,4-dihydroxydibenzofuran will be the one that will be methylated while the other 2-hydroxyl group will interact with SAM similarly to the meta-hydroxyl group of 3,5-dihydroxybiphenyl. The unsubstituted phenyl ring of the dibenzofuran will be stabilized further by the hydrophobic interaction with Leu-323, Met-137, Val-134, Met-187 and Phe-273 (Fig. IV.31B). The docking models show that 2,4-dihydroxydibenzofuran is not flexibly rotating like the biphenyl, which can explain the lower catalytic efficiency. This lack of free rotation may hinder the conformational changes carried out by the enzyme. Interestingly, the opposite conformation of the dibenzofuran substrate, which will cause the methylation to take place on the 2-hydroxyl group, is not favorable. In that case the furan oxygen and its lone pair of electrons would not favorably interact with the imidazole side chain of His-190. Therefore, methylation takes place always on the 4-hydroxyl group. Again, this shows the potential that OMTs can catalyze methylation of structurally similar biphenyls and dibezofurans.
In both *Sa*OMT2 and *Sa*OMT1, ring B occupies a hydrophobic cavity. This explains why both enzymes can catalyze the mehylation of pinosylvin but not resveratrol, in which a hydroxyl group is present in ring B, and this hydrophilic substituent will not reside efficiently in the active site. The docking model of pinosylvin in the active site of *Sa*OMT1 is illustrated in Figure IV.31C).

Figure IV.31: Docking models of different substrates in the *Sa*OMT1 active site.
A. Docking arrangement of 3,5-dihydroxybiphenyl. B. Docking arrangement of 2,4-dihydroxydibenzofuran. C. Docking arrangement of pinosylvin. The substrates are represented in green carbon atoms, SAM in pink carbon atoms, and the amino acids of the active sites in light grey color. Oxygen atoms are represented in red color, nitrogen atoms in blue. Hydrogen bonds are represented as black dashed lines, while the interaction between the methyl of SAM and the phenolic hydroxyl group of the substrate is highlighted as red dashed line. The distance between the sulphur atom of SAM and the oxygen atom of the substrate amounts to 2.8 Å.

A

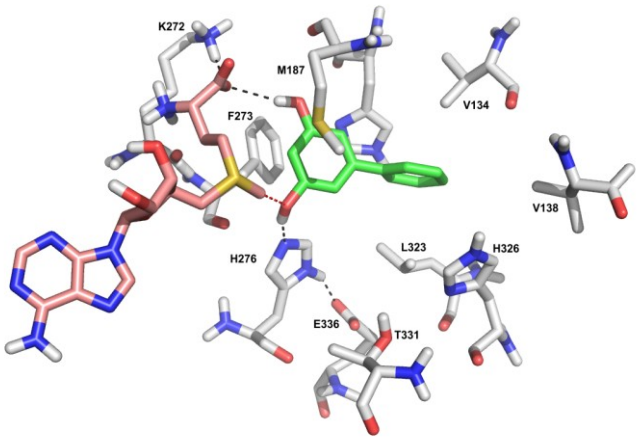
K272
M187
F273
V134
V138
H276
L323
H326
E336
T331

B

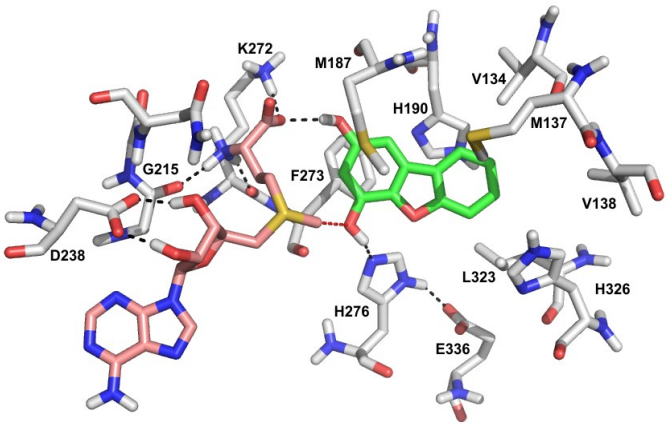
K272
M187
V134
H190
M137
G215
F273
V138
D238
L323
H326
H276
E336

C

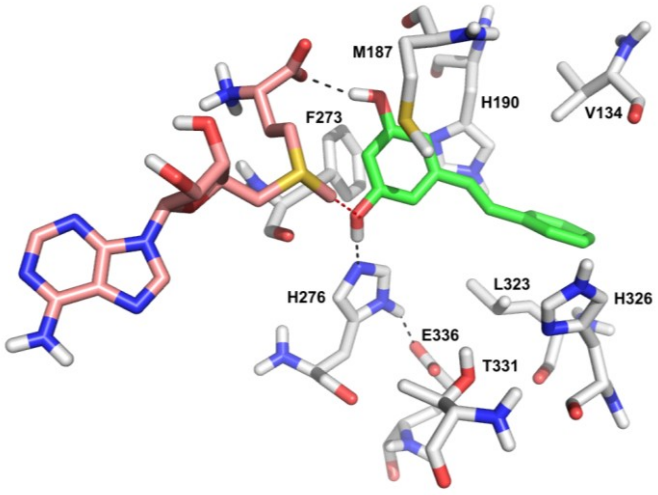
M187
H190
V134
F273
H276
L323
H326
E336
T331

Table IV.9: Summary of features of *Sa*OMT1 and *Sa*OMT2

	*Sa*OMT1	*Sa*OMT2
Optimum pH	8.5	7
Optimum Temperature	35	45
Best substrate (s)	3,5-dihydroxybiphenyl (highly specific)	Noraucuparin, 5-hydroxyferulic acid, (noreriobofuran) (promiscuous specificity)
Control of substrate specificity through	Hydrophobic interactions	Hydrophobic interaction in addition to hydrogen bonds
Induction and accumulation of the transcript	Rapidly and strongly after elicitation, then gradual decline	Slowly and moderately, then persisting over a longer time
% identity to POMT	47,4	58.7
% identity to each other	49.3	49.3
cDNA length (bp)	1113	1098
Molecular mass (Da)	41027	39820

V. Discussion

1. Downstream utilization of 3,5-dihydroxybiphenyl

As described in the Introduction, 3,5-dihydroxybiphenyl is postulated to be the precursor of biphenyls and dibenzofurans produced by *S. aucuparia* cell cultures. This compound was not isolated from or detected in any plant species so far, indicating that this compound is further metabolized downstream. Therefore, feeding of labeled precursors is an asset to answer questions about involvement of certain intermediates in the biosynthesis of natural products (Abd El-Mawla et al., 2001; Boyer and Zeevaart, 1986; Kudakasseril et al., 1987; Stadler et al., 1987; Zook, 1998). The results obtained here have shown that feeding of the radioactive tracer 3,5-dihydroxybiphenyl resulted in getting not only radioactively labeled aucuparin but also eriobofuran, the dibenzofuran analogue. This is the first concrete evidence that biphenyls are the precursors of dibenzofurans. Moreover, it substantiates that the biosynthesis of both classes of compounds is sequential, which can explain why the incorporation rate in eriobofuran is higher than that in aucuparin (3.4% versus 0.6%). Eriobofuran appears to be the ultimate product of the flow of the metabolites. So, the major portion of radioactivity incorporated in the intermediates formed from 3,5-dihydroxybiphenyl streams in eriobofuran.

Interestingly, the time course of eriobofuran accumulation shows that this product increases progressively over 5 days after elicitation, similar to the profile that aucuparin has. This observation also suggests a biosynthetic relationship between these two compounds. A similar event of continuous accumulation over a long period of time was observed with the accumulation of malusfuran, which extended over 4 days in apple cell cultures (Harzdina et al., 1997). 3,5-Dihydroxybiphenyl can be taken up by the cell cultures to produce the intermediates noraucuparin, noreriobofuran and other intermediates, which will ultimately be transformed to aucuparin and eriobofuran. Detailed information about the intermediate steps should be collected, which prompted us to carry out enzyme assays using protein from the phytoalexin-producing cell cultures.

The enzyme assays enabled us to elucidate the biosynthetic pathway leading to aucuparin (Fig. V.1). Surprisingly, 3,5-dihydroxybiphenyl was methylated in only one position to give the intermediate 3-hydroxy-5-methoxybiphenyl and even more astonishingly this compound was the only one accepted by biphenyl-4-hydroxylase to yield noraucuparin. 3,5-Dimethoxybiphenyl is not accepted as a substrate by that enzyme. Noraucuparin is further methylated to yield aucuparin. Molecular biology experiments detailed below have shown that these methylation steps are catalyzed by two different OMTs, indicating a highly coordinated pathway where every enzyme delivers the right substrate for the next step.

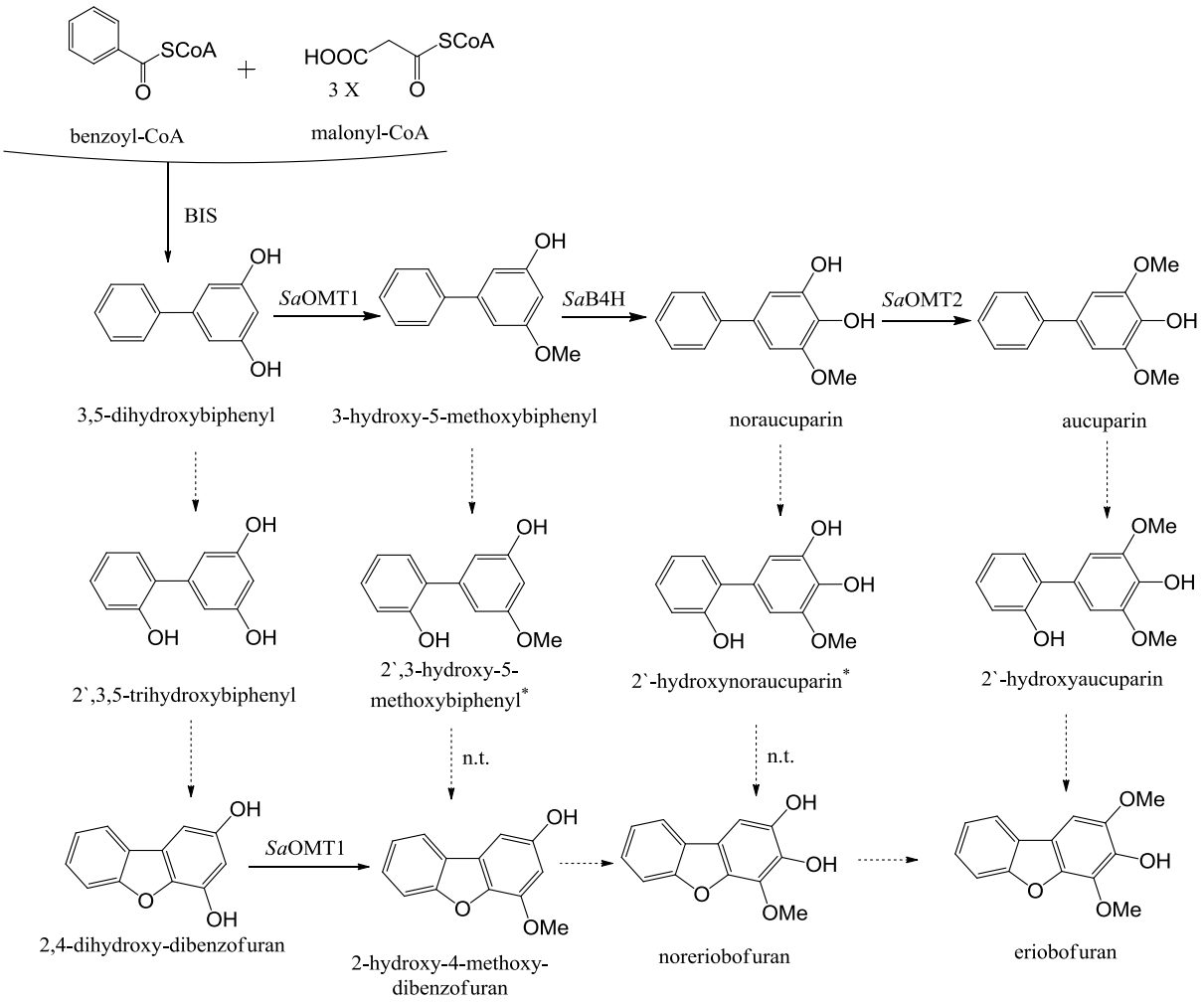

Figure V.1 Biosynthesis of biphenyls and dibenzofurans in elicitor-treated *S. aucuparia* cell cultures. Solid lines mark confirmed steps, dashed lines so far undetectable steps. n.t., not tested due to lack of substrates; * unavailable substrate.

The conversion of biphenyls to dibenzofurans is supposed to involve two steps, first, hydroxylation at 2`-position to give 2`-hydroxybiphenyl derivatives, e.g. 2`-hydroxyaucuaprin. Then, these intermediates will be oxidized to give the cyclic products, the dibenzofurans. Two enzyme classes are known to be responsible for aromatic hydroxylation, namely 2-oxoglutrate dependent dioxygenases or cytochrome P450 monoxygenases. These counterparts can replace each other in different plants (Frey et al., 2003; Lukacin et al., 2001). Enzyme assays carried out using crude protein extracts with 2-oxoglutarate and Fe^{+2} as well as microsomal proteins in the presence of NADPH both failed to detect this activity. This failure to detect some enzyme activities on the biochemical level can be attributed to either the low titer values (Prescott and Lloyd, 2000) or the poor extractability of enzymes (Schmidlin et al., 2008). We evaluated the usefulness of using an inhibitor to determine the nature of the enzyme involved.

The biosynthetic flow can be inhibited by feeding the cells with an inhibitor. Consequences of such an inhibition will be reflected in the metabolites profile. There are a number of inhibitors for each class of the presumed enzymes. Prohexadione-Ca is commonly used as an inhibitor of 2-oxoglutarate dependent dioxygenase (Frey et al., 2003; Roemmelt et al., 2003). It resembles the structure of the cofactor 2-oxoglutarate and can therefore inhibit all members of the family to an effective degree. On the other hand, inhibitors of cytochrome

P450 enzymes are not general inhibitors. Their inhibitory action is specific rather than selective (Rademacher, 2000). As an example, ancymidol inhibits microsomal enzymes involved in gibberellin biosynthesis in *Marah macrocarpus* but can not inhibit cinnamate-4-hydroxylase in *Sorghum bicolor* (Coolbaugh et al., 1978). This can be partially attributed to the fact that the inhibition effect of these enzymes depends to a certain degree on the structural similarity between the inhibitor and the substrate. So, it is not so accurate to use an inhibitor for a cytochrome P450 enzyme, for which the preferred substrate is not yet known.

It was incentive to us to test the effect of prohexadione-Ca on accumulation of dibenzofurans to see whether or not 2-oxoglutarate dependent dioxygenase activity plays a role in this biosynthesis. Our trial led to no conclusive results (data not shown). An explanation can be fathomed from previous work. Application of prohexadione-Ca was a successful approach when it is applied to intact plants, e.g., *Malus x domestica* (Roemmelt et al., 2003) and *Rosa* x *hybrida* (Schlangen et al., 2003) or to maize seedlings (Frey et al., 2003). In all the aforementioned cases, complete absence of flavonoids (*Malus* and *Rosa*) or benzoxazinoid compounds (maize) was found in addition to formation of new profiles of metabolites. So, the inhibitory effect was pronounced. However, when the same approach was applied to carrot cell suspension cultures (Ilan and Dougall, 1992), only 11% decrease in anthocyanins was observed, far away from complete inhibition. However, in the last example, prohexadione-Ca was used as an inhibitor for gibberellin biosynthesis, which in turn should increase the anthocyanin production because gibberellins suppress the production of anthocyanins (Ilan and Dougall, 1992). So it was not clear if the concentration used in this report affected gibberellin biosynthesis only or also anthocyanin biosynthsis. In intact plants, *Malus* and *Rosa*, disappearance of metabolites was attributed to a direct inhibitory effect of prohexadione-Ca on 2-oxoglutrate dependent dioxygenases not to a secondary effect to inhibition of gibberellin biosynthesis. In seedlings of maize, cloning of a cDNA encoding 2-oxoglutarate dependent dioxygenase, which is involved in the biosynthesis of benzoxazine, substantiated the results of the inhibition studies. So it is clear that the inhibition studies can not stand alone as evidence for the involvement of an enzyme in a certain biosynthetic pathway. Substantial information is required, which in case of dibenzofuran formation is missing. So, it is still open how the nature of the enzymes catalyzing these steps and the intermediates involved look like. A promising approach may be the construction of a subtracted cDNA library between methyl jasmonate-tretaed and *V. inaequalis*-treated *S. aucuparia* cell cultures. Methyl jasmonate induces biphenyls only, whereas the fungus causes mainly eriobofuran formation. The subtracted library would thus be enriched in the transcripts involved in dibenzofuran biosynthesis.

2. Functional characterization of recombinant *Sa*OMTs

Sequencing projects and advances in the field of bioinformatics provide scientists with a plethora of information which can help in discovering, characterizing and annotation of new genes. The candidate gene approach makes use of these resources. A well studied gene is used as a probe to discover homologs or other related genes. The right choice of a probe is critical, careful selection helps to a large degree in getting the expected result. This approach was successful in isolating a cDNA for resveratrol OMT (ROMT) from *Vitis vinifera* (Schmidlin et al., 2008). *Orcinol OMT* was used as a probe because of the similarity in structure between the substrates resveratrol and orcinol on one side and the products pterostilbene and 3,5-dimethoxytoluene on the other side. Based on these observations, we postulated that the candidate biphenyl OMTs involved in the biosynthesis of aucuparin are related to stilbene OMTs because of structure similarity. As discussed before, *pinosylvin OMT* (*POMT*) was

selected as a probe to search the apple genome as well as the NCBI *Malus* EST collection. Two clones were found in the NCBI *Malus* EST collection. One clone was detected in leaves of Royal Gala seedlings infected with *V. inaequalis*. The other clone encodes OMT in the root tip, a metabolically active tissue. These results served as signs for promising clones. The approach led to detection of *SaOMT1* and *SaOMT2*. On the protein level, *Sa*OMT2 and *Sa*OMT1 share 58.7% and 47,4% identity with POMT, 30.7% and 31.5% identity with ROMT, respectively. Both enzymes catalyze only a one step methylation reaction as their probe POMT, which agrees with the biochemical characterization of the enzyme activities in cell-free crude protein extract from *S. aucuparia* cell cultures.

The properties of *Sa*OMT1 and *Sa*OMT2 are divergent from each other; however, their properties embody the multitudinousness of the plant OMTs family. Regarding substrate utilization, *Sa*OMT1 shows a high degree of substrate specificity similar to some flavonoid OMTs, which are specific to a limited number of substrates and catalyze methylation at specific sites (Ibrahim et al., 1987; Willits et al., 2004). *Sa*OMT1 catalyzed only methylation of *meta*-dihydroxylated biphenyl, dibenzofuran, and stilbene. The two best substrates are 3,5-dihydroxybiphenyl and 2,4-dihydroxydibenzofuran (K_m = 28 µM each). However, assignment of function of that protein as 3,5-dihydroxybiphenyl OMT was based on the turn over rate (V_{max}), which was three times higher with 3,5-dihydroxybiphenyl. Consequently, the catalytic efficiency of *Sa*OMT1 with 3,5-dihydroxybiphenyl (K_{cat}/K_m = 5285.4 $s^{-1}M^{-1}$) was three times that with 2,4-dihydroxydibenzofuran (K_{cat}/K_m = 1827.8 $s^{-1}M^{-1}$). Moreover, conversion of 3,5-dihydroxybiphenyl to 3-hydroxy-5-methoxybiphenyl seems to be the physiological reaction. The substrate 3,5-dihydroxybiphenyl is the product of BIS (Liu et al., 2007). The OMT product 3-hydroxy-5-methoxybiphenyl was detected in apple (Chizzali et al., 2012c). On the contrary, presence of 2,4-dihydroxydibenzofuran and its OMT product 2-hydroxy-4-methoxydibenzofuran were not reported before. This activity can thus be an *in vitro* activity due to structure and conformation similarities between the two substrates.

*Sa*OMT2 shows broader substrate specificity. In addition to biphenyl and dibnzofuran, it also accepts the phenylpropanoids 5-hydroxyferulic acid and caffeic acid. In this aspect, *Sa*OMT2 is similar to a number of plant OMTs which have promiscuous substrate specificity (Chiron et al., 2000; Frick and Kutchan, 1999; Gauthier et al., 1998; Li et al., 1997; Liu et al., 2006; Maury et al., 1999; Parvathi et al., 2001; Wein et al., 2002). However, on the contrary to all the aforementioned examples, *Sa*OMT2 has the highest affinity to noraucuparin, i.e. the lowest K_m (38 µM), although the catalytic efficiency (K_{cat}/K_m = 7964 $s^{-1}M^{-1}$) is somewhat lower than that with the second best substrate, 5-hydroxyferulic acid (K_{cat}/K_m = 9471 $s^{-1}M^{-1}$). *Sa*OMT2 is not like OMTs from *Pinus sylvestris* and *Thalictrum tuberosum* which accept a broad spectrum of substrates belonging to different classes (Chiron et al., 2000; Frick and Kutchan, 1999). Additionally, *Sa*OMT2 is not like OMT from strawberry which has low affinity and catalytic efficiency to one of its presumed physiological substrates, 2,5-dimethyl-4-hydroxy-3(2H)-furanone (DMHF). The K_m values are 440 and 146 µM for DMHF and caffeic acid, respectively, and the K_{cat}/K_m values are $2.95x10^{-5}$ and $3.06x10^{-3}$ $\mu M^{-1}min^{-1}$ for DMHF and caffeic acid, respectively (Wein et al., 2002). So, based on the kinetic data here determined, assignment of function of *Sa*OMT2 as noraucuparin OMT is highly confirmed. Function assignment of these promiscuous OMTs is also dependent on the onset and the profile of expression of their encoding genes. The onset of upregulation of *Sa*OMT2 after elicitation and the stable transcript level over three days is further evidence that fortifies the assignment of the *Sa*OMT2 function, as discussed below in more detail. The structural similarity between noraucuparin and noreriobofuran prompted us to postulate that *Sa*OMT2 can accept noreriobofuran in an event similar to *Sa*OMT1. Moreover, the perfect fitting of 2,4-dihydroxydibenzofuran into the active site of *Sa*OMT1 has fortified this assumption.

Therefore, we carried out incubations of the purified *Sa*OMT2 with an *S. aucuparia* cell cultures extract rich in both noraucuparin and noreriobofuran. Interestingly, both compounds were utilized by the enzyme, as indicated by disappearance of the substrate peaks in HPLC chromatograms. Control incubatins containing boiled protein or lacking SAM were carried out in parallel. Noreriobofuran and eriobofuran were previously isolated from the cell cultures of *S. aucuparia* (Hüttner et al., 2010) and are reported to be present in other species of the Pyrinae (Chizzali and Beerhues, 2012). The time courses of aucuparin and eriobofuran accumulation are quite superimposable. This observation may allude that the biosyntheses of both compounds are synchronized and that the methylation steps leading to their accumulations can be catalyzed by a single protein. Based on the aforementioned arguments, we can postulate that *Sa*OMT2 is also participating in biosynthesis of noreriobfuran.

Although *BIS1*, *SaOMT1* and *SaOMT2* participate in the same pathway, their expression profiles were different from each other. It was remarkable that the transcript levels of *BIS* and *SaOMT1* followed similar accumulation patterns, however, *BIS* was the most strongly upregulated gene. The nearly superimposable induction profiles of *BIS1* and *SaOMT1* can explain why the intermediate 3,5-dihydroxybiphenyl cannot be detected. As it is formed by BIS, it is rapidly metabolized by OMT1 and has no chance to be accumulated. In contrast, expression of *SaOMT2* was not as strongly induced as that of the other two genes, however, the transcript amount remained at maximum level from 6 to 16 h and its decrease was not as dramatic as for the other ones. These findings can explain why accumulation of aucuparin starts after 6 hours and then continues to increase in a linear matter over 5 days after elicitation. The transcript level of *SaOMT2* is more or less stable over this time period. A last observation should be considered; eriobofuran has the same accumulation pattern like aucuparin, which can serve as evidence that *Sa*OMT2 is also involved in methylation of noreriobofuran, not only noraucuparin. However, such a conclusion requires further investigation, such as knocking-out these OMTs in an *in vivo* system and subsequent examining the nature of the accumulated compounds (Pinçon et al., 2001; Tu et al., 2010). Finally, this perfect consistency of metabolite and transcript levels suggests that the involved proteins behave similarly. These results further confirm the annotation of the studied genes.

Structural biology and modeling studies explain the relationship between structure and function of biological macromolecules. Protein and substrate structures determine substrate specificity and reactivity. Much information can not be inferred from the primary structure of proteins. The primary structures of plant OMTs show a high degree of conservation, especially for the motifs which bind SAM (Fig. V.2) (Ibrahim, 1997; Joshi and Chiang, 1998; Liu et al., 2006; Louie et al., 2010; Zubieta et al., 2001). Despite of that, plant OMTs can discriminate between different substrates by two means: (i) shape selectivity determined by the van der Waals interactions of the aliphatic and aromatic amino acids lining the active site and (ii) specific hydrogen bonding patterns (Gang et al., 2002; Zubieta et al., 2001). Contribution of both of these interactions to the substrate specificity in *Sa*OMT1 and *Sa*OMT2 are evident. Hydrophobic interactions play a major role in substrate specificity of *Sa*OMT1, no hydrogen bonds are involved in stabilizing the substrate in the active site, except the one with SAM. The richness of the *Sa*OMT1 active site with aliphatic and aromatic amino acids, e.g. Leu, Val, Met, Phe, and His, allows *Sa*OMT1 to accept only 3,5-dihydroxybiphenyl as a substrate and its dibenzofuran analogue. Surprisingly, these interactions also determined that methylation of 2,4-dihydroxydibenzofuran takes place only in the 4-hydroxy moiety. The conformer in which the other hydroxyl group of 2,4-dihydroxydibenzofuran is not feasible to reside in the active site. Moreover, these hydrophobic interactions explain why resveratrol is not accepted as substrate but pinosylvin is accepted. Similar hydrophobic interactions are evident in *Sa*OMT2, however, additional

hydrogen bonding (the second mean) contributes to the substrate specificity of this enzyme. Hydrogen bonds of Asp-270 to the 4-hydroxyl group of noraucuparin and to the 3-hydroxyl group of noreriobofuran help in recognition and stabilization of the substrate in the active site. Moreover, a hydrogen bond between Asn-131 and the furan oxygen of noreriobofuran is an explanation for the activity of that enzyme towards the physiological substrate noreriobofuran. The presented docking models of both OMTs studied explain that plant OMTs can catalyze methylation reactions in two pathways as long as the substrates have similar structures and conformations (Liu et al., 2006).

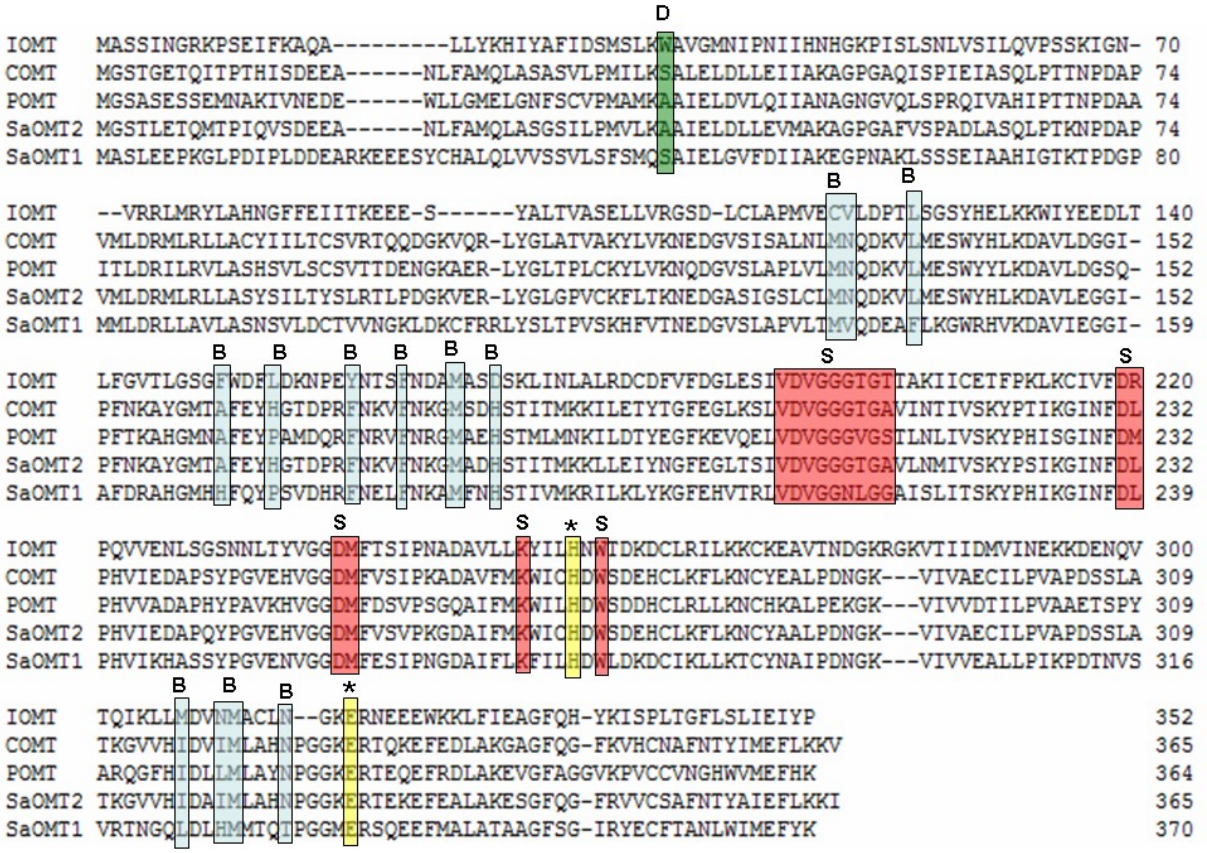

Figure V.2. Alignment of the amino acid sequences of the *Sa*OMTs and selected OMTs from other species, namely caffeic acid OMT (COMT) and isoflavone OMT (IOMT) from *Medicago sativa* (alfalfa COMT, AAB46623.1; alfalfa IOMT, O22309.1) as well as pinosylvin OMT (POMT) from *P. sylvestris*. Boxes labeled with **S** are residues which bind SAM; boxes marked with ***** are the catalytic residues; boxes marked with **B** are residues which bind the substrate; the box labeled with **D** is responsible for dimer formation.

3. Phylogenetic characterization of *Sa*OMTs

To examine the relatedness between the two new cloned genes and *POMT* and *ROMT* on one side and the relatedness to other plant *OMTs* on the other side, a Maximum Likelihood phylogenetic tree was constructed using homologs of *SaOMTs* in addition to *ROMT* and *POMT* homologs, similar to the tree constructed by Schmidlin et al. (2008). As studied before, *POMT* and *ROMT* had evolved independently from different *OMT* ancestors (Schmidlin et al., 2008). As expected the new *SaOMTs* are related to their probe, *POMT*, and all the three occupy a clade distinct from that occupied by *ROMT*. Both *SaOMT1* and *SaOMT2* are related to the *COMT* family as well as their probe *POMT*. It was obvious that

SaOMT1 and *SaOMT2* are quite distant from each other (Fig. V.3). They occupy distant branches, which complies with the observation that *SaOMT1* shows higher substrate selectivity and has thus undergone more independent evolutionary events. Cloning of other *OMTs* from *Sorbus* and the related species *Malus* and *Pyrus* is a perquisite to trace back the ancestor and the exact pylogenetic relationships between both genes. The hypothesis that a gene duplication event occurred, followed by divergent evolution which led to emergence of the highly specific *SaOMT1* and the promiscuous *SaOMT2*, needs more detailed studies of *OMTs* in *S. aucuparia* and related genes in closely related species such as *Malus* and *Pyrus*.

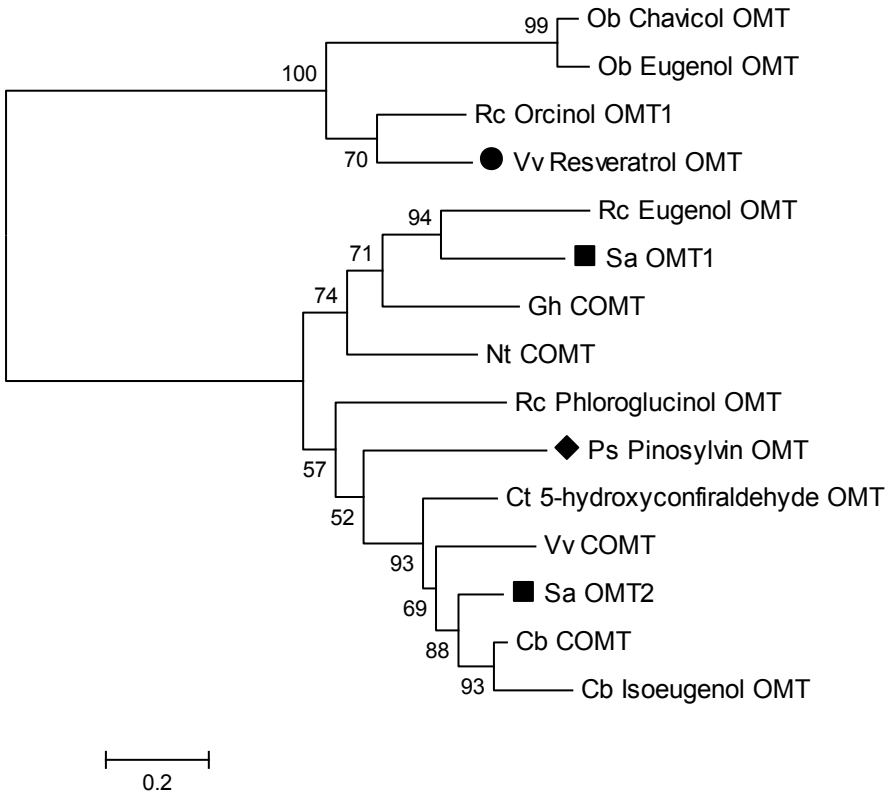

Figure V.3. Phylogenetic tree of selected OMT amino acid sequences. *Sa*OMTs and the template POMT from *P. sylvestris* are marked by quadrangles, while the other template ROMT from *V. vinifera* is marked by a circle. (Vv Resveratrol OMT, accession no. FM178870, *Vitis vinifera,* grapevine; Vv COMT, AF239740, *V. Vinifera,* grapevine caffeic acid OMT; Rc Orcinol OMT1, AJ439741, *Rosa chinensis,* Chinese rose; Ob Chavicol OMT, AF435007, *Ocimum basilicum*, basil; Ob Eugenol OMT, AF435008, *O. basilicum,* basil; Cb Isoeugenol OMT,U86760, *Clarkia breweri;* Cb COMT, AF006009, *C. breweri* caffeic acid OMT; Nt COMT, AF484252, *Nicotiana tabacum* caffeic acid OMT; Ps Pinosylvin OMT, (Chiron et al., 2000) *Pinus sylvestris*, Scots pine pinosylvin OMT; Rc Eugenol OMT, BAC78826.1, *R. chinensis*; Rc phloroglucinol OMT, BAC78826.1, *R. chinensis*; Ct 5-hydroxyconiferaldehyde OMT, BAG71895.1, *Carthamus tinctorius;* SaOMT1 *S. aucuparia*. 3,5-dihydroxybiphenyl OMT; SaOMT2 *S. aucuparia* noraucuparin OMT; Gh COMT, ACZ06242.1, *Gossypium hirsutum*, caffeic acid OMT.

*Sa*OMT2 has promiscuous substrate specificity like some other plant OMTs (Frick and Kutchan, 1999; Kota et al., 2004; Maury et al., 1999; Parvathi et al., 2001; Wein et al., 2002).

Such enzymes are regarded as potential source for evolution of either new specificities or new reactions (O'Brien and Herschlag, 1999; Ober, 2005). They can also serve as an economical alternative for plants to adapt to a new environment or new selection pressure (Liu et al., 2006). For example, OMT in *T. tuberosum* participates in production of toxic alkaloids and phenylpropanoids as well as in reinforcing the plant cell wall upon elicitation (Frick and Kutchan, 1999). A similar scenario can be applied to *Sa*OMT2. Such activity not only requires the development and/or recruitment of the right enzyme but also its expression in the right tissue at the right time, i.e. temporal and spatial expression control (Ober, 2005; Pichersky and Gang, 2000). Furthermore, the substrate availability determines the formation of the methylated product (Schwab, 2003). These multifunctional enzymes (in terms of substrate) can evolve rapidly into specific enzymes (O'Brien and Herschlag, 1999). However, it is economical to plants when one enzyme participates in synthesizing toxic phytoalexins in addition to reinforcing the cell wall (Frick and Kutchan, 1999). This may explain why such enzymes are kept by plant cells instead of evolving these promiscuous proteins into more specific ones, so as to benefit from the plurality of functions of these enzymes (Liu et al., 2006). Although it was not investigated before, suppression of expression of genes encoding these enzymes can reveal their involvement in different pathways and the real role they play. Similar studies were applied to COMT and CCoAOMT and contributed to our understanding of the roles of these enzymes in lignin biosynthesis (Pinçon et al., 2001; Tu et al., 2010; Zhang et al., 2012).

4. Perspectives

3,5-Dihydroxybiphenyl, among the other phytoalexins, was found to have the highest antibacterial activity against the fire-blight pathogen *E. amylovora* (Chizzali et al., 2012c). Thus, this compound can offer plants an advantage against that pathogen; however, it was not detected at the site of infection. On the one hand, it may be that the presence of variable mixtures of biphenyls and dibenzofurans has a synergistic activity and hence their inhibitory effect is stronger than a single active compound. A study about a possible synergistic activity is not performed yet. On the other hand, the presence of an array of phytoalexins may allow plants to have a broad resistance against more than one pathogen. Transgenic approaches aiming at introduction of one new phytoalexin into a susceptible plant resulted in neutralizing the severe symptoms associated with the infection but did not endow plant resistance (He and Dixon, 2000; Hipskind and Paiva, 2000). It was concluded that more that one phytoalexin substance or class are essential to provide resistance to plants (Dixon, 2001).

Phytolaexins can qualitatively be found in both resistant and susceptible plants. The difference is in the onst of accumulation and extent. It was manifested that these two factors play an important role in conferring resistance to plants. Soybean varieties resistant to *Phytophthora megasperma* were found to accumulate 6a-hydroxyphaseollin 10-100 times faster than the susceptible varieties. Moreover, the accumulated amount was 100-400 times the ED_{50} concentration for inhibition of mycelial growth, while susceptible varieties accumulated amounts that were only 1-4 times the ED_{50} (Keen, 1971). In another example, other resistant soybean cultivars accumulated much higher concentrations of glyceollin than susceptible ones did (Yoshikawa et al., 1978). Coniferyl alcohol and coniferyl aldehyde accumulated more rapidly in resistant flax genotypes than in susceptible ones, which was manifested in restricting the fungal growth and reducing the lesion sizes, i.e., ameliorating the symptoms (Keen and Littlefield, 1979). Accumulation of these reports led many authors to conclude and affirm that the onset and the extent of phytoalexin production play a critical role in conferring resistance to plants (Dixon, 2001; Hammerschmidt, 1999; Kuć, 1991, 1995). Interestingly, overexpression of isoflavone *O*-methyltransferase (IOMT) in *Medicago sativa*

enhanced the resistance against the fungus *Phoma medicaginis* as a result of earlier and increased production of the isoflavone medicarpin (He and Dixon, 2000).

Grafted shoots of apple and pear produce biphenyls and dibenzofurans at a late time point after inoculation with *E. amylovora* (Chizzali et al., 2012c). The phytoalexins can be detected in the transition zone on the 28th day. Of course, the migration of *Erwinia* bacteria from the shoot tip downward the stem took time, but still the response was late and weak. During that time, ooze emerged from the dead parts of the plant and helped in disseminating the bacteria and hence the disease. The production of biphenyls and dibenzofurans seems to be confined to sap wood tissues of apple and pear. Even when the cell cultures of the resistant *M. domestica* cultivar 'Liberty' produced biphenyls and dibenzofurans (Borejsza-Wysocki et al., 1999; Hrazdina et al., 1997), the micropropagated plants and the fruits failed to form them (Hrazdina and Borejsza-Wysocki, 2003). In conclusion, if one aims to enhance resistance of Pyrinae species through production of phytoalexins, one should aim at two targets: (1) production of large amounts in short time after exposure to pathogen, (2) conferring this trait to other tissues and organs, e.g., blossoms and leaves, which come first in contact with *Erwinia* or *Venturia*. Phytoalexin production in these organs will serve as a barrier against infection. Leaves of *Eriobotrya japonica* produce aucuparin and eriobofuran as phytoalexins (Morita and Nonaka, 2003), which indicates the possibility of achieving this aim. As a relatively fast approach in apple and pear, *BIS* may be expressed under the control of a strong and constitutive promoter, e.g. the 35S promoter. Nevertheless, it will need carrying out analysis of the genuine promoters controlling the expression of the involved genes, to know what switches them on and what makes them tissue-specific. However, this may not be sufficient because leaves of *M. domestica* cv. 'Holsteiner Cox' accumulated MdBIS2 transcripts but failed to produce biphenyls. So, it will also be necessary to study the translational level and to elucidate the signal transduction chain controlling the expression. In short, studying the molecular factors regulating the expression of the genes involved can decipher the problem of late expression and restricted localization. These strategies may boost the resistance of the vulnerable Pyrinae trees.

VI. Summary

- The subtribe Pyrinae of the Rosaceae involves a number of economically important fruit trees, e.g., apple and pear. However, these plants are afflicted by numerous devastating infectious diseases, such as fire blight and scab. In this study, *S. aucuparia* cell cultures, treated with an extract of the scab-causing fungus, were used as a model system. As a defense response, biphenyls and dibenzofurans are produced as phytoalexins. Their scaffolds are derived from the precursor 3,5-dihydroxybiphenyl, which is synthesized by biphenyl synthase (BIS). The aim of this study was to elucidate the downstream steps converting this precursor to other biphenyls and dibenzofurans.

- The radioactive tracer 3,5-dihydroxybiphenyl, which was enzymatically synthesized, was incorporated into aucuparin and eriobofuran by rates of 0.6 and 3.37 %, respectively. This indicates that biphenyls are the precursors of dibenzofurans and the biosynthetic routes of the two classes of compounds are sequential rather than parallel.

- Conversion of 3,5-dihydroxybiphenyl to aucuparin involves three steps, which have the following sequence: methylation, 4-hydroxylation, methylation. The biochemical investigations revealed that the two methylation steps are catalyzed by distinct *O*-methyltransferases (OMTs), which differ in stability and properties. The hydroxylation is catalyzed by a NADPH-dependent cytochrome P450 monoxygenase, as demonstrated by use of common CYP inhibitors. This membrane-bound enzyme has an absolute specificity for 3-hydroxy-5-methoxybiphenyl. The pH and temperature optima were 8.5 and 22°C.

- Using a candidate gene approach, pinosylvin OMT (POMT) was used as a probe to search the apple genome sequence for possible candidates participating in aucuparin formation. cDNAs encoding the two OMTs involved were successfully cloned, heterologously expressed, and functionally characterized.

- *Sa*OMT1 catalyzed the methylation of 3,5-dihydroxybiphenyl to 3-hydroxy-5-methoxybiphenyl. The cDNA has an ORF of 1113 bp, which encodes 371 amino acids. It shares 47.4 % identity with POMT on the amino acid level. The enzyme has a narrow substrate specificity. Based on the catalytic efficiency (K_{cat}/K_m), 3,5-dihydroxybiphenyl is the best substrate. The pH and temperature optima are 8.5 and 35°C.

- *Sa*OMT2 catalyzed the methylation of noracuparin to aucuparin. The ORF of the cDNA is 1098 bp long and encodes 366 amino acids. It shares 58.7 % identity with POMT on the amino acid level. The enzyme has a more relaxed substrate specificity. Based on the catalytic efficiency (K_{cat}/K_m), 5-hydroxyferulic acid and noraucuparin are the best substrates. The pH and temperature optima are 7.0 and 45°C. The enzyme also catalyzes conversion of noreriobofuran to eriobofuran.

- The onset and the time course of the accumulation of transcripts for the *Sa*OMTs confirmed the assignment of functions and agreed with the differences in the accumulation profiles of the metabolites.

- Homology modeling studies showed that *Sa*OMT1 controls the substrate specificity via shape selectivity, which is determined by van der Waals interactions of the aliphatic and aromatic amino acids lining the active site. *Sa*OMT2 uses the same type of interaction in addition to hydrogen bonding. The modeling studies explained the kinetic properties of both enzymes and their ability to catalyze methylation of the dibenzofuran analogues.

- Phylogentic analysis showed that both *Sa*OMTs as well as POMT are related to plant caffeic acid OMTs (COMTs).

- Steps involved in converting biphenyls to dibenzofurans are still open. Biochemical investigations led to detection of neither 2`-hydroxylase nor cyclase activities. In the future, molecular genetic approaches may be applied.

VII. References

Abd El-Mawla, A.M., Schmidt, W., and Beerhues, L. (2001). Cinnamic acid is a precursor of benzoic acids in cell cultures of *Hypericum androsaemum* L. but not in cell cultures of *Centaurium erythraea* RAFN. Planta *212*, 288-293.

Abd El-Razeka, M.H., Chang, H.-S., Lee, S.-J., Tsai, I.-L., and Chen, I.-S. (2007). Biphenyls from *Pourthiaea lucida*. Biochemical Systematics and Ecology *35*, 248-250.

Agrois, G.N. (2005). Plant Pathology, 5 th edn (San Diego, California, USA: Academic Press Ltd,).

Angelova, Z., Georgiev, S., and Roos, W. (2006). Elicitation of plants. Biotechnology & Biotechnological Equipment *20*, 72-83.

Ausubel, F.M., Brent, R., Kingston, R.E., Moore, D.D., Seidman, J.G., Smith, J.A., and Struhl, K. (1994). Current protocols in molecular biology (Greene Publishing Associates and John Wiley & Sons, Inc. NY).

Birnboim, H.C., and Doly, J. (1979). A rapid alkaline extraction procedure for screening recombinant plasmid DNA. Nucleic acids research *7*, 1513-1523.

Bonn, W.G. (1999). Opening address. Acta Horticulturae *489*, 171-176.

Bonn, W.G., and Van der Zwet, T. (2000). Distribution and economic importance of fire blight . In Fire blight: the disease and its causative agent, *Erwinia amylovora*, J.L. Vanneste, ed. (Wallingford, UK: CABI Publishing), pp. 37-53.

Borejsza-Wysocki, W., Lester, C., Attygalle, A.B., and Hrazdina, G. (1999). Elicited cell suspension cultures of apple (*Malus*×*domestica*) cv. Liberty produce biphenyl phytoalexins. Phytochemistry *50*, 231-235.

Bowen, J.K., Mesarich, C.H., Bus, V.G., Beresford, R.M., Plummer, K.M., and Templeton, M.D. (2011). *Venturia inaequalis*: the causal agent of apple scab. Molecular Plant Pathology *12*, 105-122.

Boyer, G.L., and Zeevaart, J.A.D. (1986). 7′-hydroxy (-)-R-abscisic acid: A metabolite of feeding (-)-R-abscisic acid to *Xanthium strumarium*. Phytochemistry *25*, 1103-1105.

Bradford, M.M. (1976). A rapid and sensitive method for the quantitation of microgram quantities of protein utilizing the principle of protein-dye binding. Analytical Biochemistry *72*, 248-254.

Burkhardt, G., Schild, W., Becker, H., and Grubert, M. (1992). Biphenyls and xanthones from the podostemaceae. Phytochemistry *31*, 543-548.

Campbell, C.S., Evans, R.C., Morgan, D.R., Dickinson, T.A., and Arsenault, M.P. (2007). Phylogeny of subtribe Pyrinae (formerly the Maloideae, Rosaceae): Limited resolution of a complex evolutionary history. Plant Systematic Evolution *266*, 119-145.

Cardona, M.L., Fernández, I., Pedro, J.R., and Serrano, A. (1990). Xanthones from *Hypericum reflexum*. Phytochemistry *29*, 3003-3006.

Carisse, O., and Bernier, J. (2002). Effect of environmental factors on growth, pycnidial production and spore germination of *Microsphaeropsis* isolates with biocontrol potential against apple scab. Mycological Research *106*, 1455-1462.

Carney, J.R., Krenisky, J.M., Williamson, R.T., and Luo, J. (2002). Achyrofuran, a new antihyperglycemic dibenzofuran from the South American medicinal plant *Achyrocline satureioides*. Journal of Natural Products *65*, 203-205.

Carotenuto, A., Fattorusso, E., Lanzotti, V., and Magno, S. (1998). Porric Acids A−C new antifungal dibenzofurans from the bulbs of *Allium Porrum* L. European Journal of Organic Chemistry *1998*, 661-663.

Chapple, C. (1998). Molecular genetic analysis of plant cytochrome P450-dependent monoxygenases. Annual Review of Plant Physiology and Plant Molecular Biology *49*, 311-343.

Chen, J.J., Luo, Y.T., Liao, C.-H., Chen, I.S., and Liaw, C.C. (2009). A new dibenzofuran and further constituents from the stems of *Pourthiaea lucida* with inhibitory activity on superoxide generation by neutrophils. Chemistry & Biodiversity *6*, 774-778.

Chiron, H., Drouet, A., Claudot, A.C., Eckerskorn, C., Trost, M., Heller, W., Ernst, D., and Sandermann, H., Jr. (2000). Molecular cloning and functional expression of a stress-induced multifunctional *O*-methyltransferase with pinosylvin methyltransferase activity from Scots pine *(Pinus sylvestris* L.). Plant Molecular Biology *44*, 733-745.

Chizzali, C., and Beerhues, L. (2012). Phytoalexins of the Pyrinae: Biphenyls and dibenzofurans. Beilstein Journal of Organic Chemistry *8*, 613-620.

Chizzali, C., Gaid, M., Belkheir, A., Beuerle, T., Hänsch, R., Richter, K., Flachowsky, H., Peil, A., Hanke, M.-V., Liu, B.*, et al.* (2012a). Phytoalexin formation in fire blight-infected apple. Trees *27*, 477-484.

Chizzali, C., Gaid, M.M., Belkheir, A.K., Hansch, R., Richter, K., Flachowsky, H., Peil, A., Hanke, M.V., Liu, B., and Beerhues, L. (2012b). Differential expression of biphenyl synthase gene family members in fire-blight-infected apple 'Holsteiner Cox'. Plant Physiology *158*, 864-875.

Chizzali, C., Khalil, M.N.A., Beuerle, T., Schuehly, W., Richter, K., Flachowsky, H., Peil, A., Hanke, M.-V., Liu, B., and Beerhues, L. (2012c). Formation of biphenyl and dibenzofuran phytoalexins in the transition zones of fire blight-infected stems of *Malus domestica* cv. 'Holsteiner Cox' and *Pyrus communis* cv. 'Conference'. Phytochemistry *77*, 179-185.

Cohen, S.N., Chang, A.C., and Hsu, L. (1972). Nonchromosomal antibiotic resistance in bacteria: genetic transformation of Escherichia coli by R-factor DNA. Proceedings of the National Academy of Sciences of the United States of America *69*, 2110-2114.

Coolbaugh, R.C., Hirano, S.S., and West, C.A. (1978). Studies on the specificity and site of action of alpha-cyclopropyl-alpha-[p-methoxyphenyl]-5-pyrimidine methyl alcohol (ancymidol), a plant growth regulator. Plant Physiology *62*, 571-576.

Copeland, R.A. (2002). Kinetics of Single-Substrate Enzyme Reactions. In Enzymes (John Wiley & Sons, Inc.), pp. 109-145.

Cortez, D.A.G., Filho, B.A.A., Nakamura, C.V., Filho, B.P.D., Marston, A., and Hostettmann, K. (2002). Antibacterial activity of a biphenyl and xanthones from *Kielmeyera coriacea*. Pharmaceutical Biology (Formerly International Journal of Pharmacognosy) *40*, 485-489.

Cotterill, P.J., Owen, P.J., and Scheinmann, F. (1974). Extractives from Guttiferae. Part XXVIII. Structure and synthesis of new biphenyls from *Pentaphalangium solomonse* Warb. Journal of the Chemical Society Perkin Transactions *1*, 2423-2429.

Dagert, M., and Ehrlich, S.D. (1979). Prolonged incubation in calcium chloride improves the competence of *Escherichia coli* cells. Gene *6*, 23-28.

Dai, Y., Zhou, G.-X., Kurihara, H., Ye, W.C., and Yao, X.S. (2009). A biphenyl glycoside from *Pyracantha fortuneana*. Natural Product Research *23*, 1163-1167.

Dai, Y., Zhou, G.X., Kurihara, H., Ye, W.C., and Yao, X.S. (2006). Biphenyl glycosides from the fruit of *Pyracantha fortuneana*. Journal Natural Products *69*, 1022-1024.

Dai, Y., Zhou, G.X., Kurihara, H., Ye, W.C., and Yao, X.S. (2008). Fortuneanosides G-L, dibenzofuran glycosides from the fruit of *Pyracantha fortuneana*. Chemical & Pharmaceutical Bulletin *56*, 439-442.

Dall'Acqua, S., Innocenti, G., Viola, G., Piovan, A., Caniato, R., and Cappelletti, E.M. (2002). Cytotoxic compounds from *Polygala vulgaris*. Chemical & Pharmaceutical Bulletin *50*, 1499-1501.

De Carolis, E., and De Luca, V. (1994). 2-Oxoglutarate-dependent dioxygenase and related enzymes: biochemical characterization. Phytochemistry *36*, 1093-1107.

Dixon, R.A. (2001). Natural products and plant disease resistance. Nature *411*, 843-847.

Erdtman, H., Eriksson, G., and Norin, T. (1963). Aucuparin and methoxyaucuparin, two phenolic biphenyl derivatives from the heartwood of *Sorbus aucuparia* L. Acta Chemica Scandinavica *17*, 1151-1156.

Fa-Ching, C., Juh-Shyong, L., and Yuh-Meei, L. (1983). Biphenyls from the heartwood of taiwan sassafras. Phytochemistry *22*, 616-617.

FAO (Food and Agriculture Organization of the United Nations), 2010. FAOSTAT home page, http://faostat.fao.org/site/613/default.aspx#ancor.

Frey, M., Huber, K., Park, W.J., Sicker, D., Lindberg, P., Meeley, R.B., Simmons, C.R., Yalpani, N., and Gierl, A. (2003). A 2-oxoglutarate-dependent dioxygenase is integrated in DIMBOA-biosynthesis. Phytochemistry *62*, 371-376.

Frick, S., and Kutchan, T.M. (1999). Molecular cloning and functional expression of *O*-methyltransferases common to isoquinoline alkaloid and phenylpropanoid biosynthesis. The Plant Journal *17*, 329-339.

Gaid, M.M., Sircar, D., Beuerle, T., Mitra, A., and Beerhues L. (2009). Benzaldehyde dehydrogenase from chitosan-treated *Sorbus aucuparia* cell cultures. Journal of Plant Physiology *166*,1343-1349.

Gang, D.R., Lavid, N., Zubieta, C., Chen, F., Beuerle, T., Lewinsohn, E., Noel, J.P., and Pichersky, E. (2002). Characterization of phenylpropene *O*-methyltransferases from sweet basil: facile change of substrate specificity and convergent evolution within a plant *O*-methyltransferase family. The Plant Cell *14*, 505-519.

Garcia Cortez, D.A., Young, M.C.M., Marston, A., Wolfender, J.L., and Hostettmann, K. (1998). Xanthones, triterpenes and a biphenyl from *Kielmeyera coriacea*. Phytochemistry *47*, 1367-1374.

Gauthier, A., Gulick, P.J., and Ibrahim, R.K. (1998). Characterization of two cDNA clones which encode *O*-methyltransferases for the methylation of both flavonoid and phenylpropanoid compounds. Archives of Biochemistry and Biophysics *351*, 243-249.

Ghosal, S., Singh, S.K., and Srivastava, R.S. (1988). Shilajit part 2. Biphenyl metabolites from *Trifolium repens*. Journal of Chemical Research *196*, 165-166.

Gil-Izquierdo, A., and Mellenthin, A. (2001). Identification and quantitation of flavonols in rowanberry (*Sorbus aucuparia* L.) juice. European Food Research and Technology *213*, 12-17.

Glazebrook, J., and Ausubel, F.M. (1994). Isolation of phytoalexin-deficient mutants of *Arabidopsis thaliana* and characterization of their interactions with bacterial pathogens. Proceedings of the National Academy of Sciences of the United States of America *91*, 8955-8959.

Glazebrook, J., Zook, M., Mert, F., Kagan, I., Rogers, E.E., Crute, I.R., Holub, E.B., Hammerschmidt, R., and Ausubel, F.M. (1997). Phytoalexin-deficient mutants of *Arabidopsis* reveal that *PAD4* encodes a regulatory factor and that four *PAD* genes contribute to downy mildew resistance. Genetics *146*, 381-392.

Grayer, R.J., and Kokubun, T. (2001). Plant-fungal interactions: the search for phytoalexins and other antifungal compounds from higher plants. Phytochemistry *56*, 253-263.

Hain, R., Reif, H.J., Krause, E., Langebartels, R., Kindl, H., Vornam, B., Wiese, W., Schmelzer, E., Schreier, P.H., Stocker, R.H.*, et al.* (1993). Disease resistance results from foreign phytoalexin expression in a novel plant. Nature *361*, 153-156.

Hammerschmidt, R. (1999). PHYTOALEXINS: What have we learned after 60 years? Annual review of phytopathology *37*, 285-306.

Harborne, J.B. (1997). Recent advances in chemical ecology. Natural Product Reports *14*, 83-98.

He, X.-Z., and Dixon, R.A. (2000). Genetic manipulation of isoflavone 7-*O*-methyltransferase enhances biosynthesis of 4′-*O*-methylated isoflavonoid phytoalexins and disease resistance in alfalfa. The Plant Cell *12*, 1689-1702.

Hipskind, J.D., and Paiva, N.L. (2000). Constitutive accumulation of a resveratrol-glucoside in transgenic alfalfa increases resistance to *Phoma medicaginis*. Molecular Plant-Microbe Interactions *13*, 551-562.

Hrazdina, G., and Borejsza-Wysocki, W. (2003). Response of scab-susceptible (McIntosh) and scab-resistant (Liberty) apple tissues to treatment with yeast extract and *Venturia inaequalis*. Phytochemistry *64*, 485-492.

Hrazdina, G., Borejsza-Wysocki, W., and Lester, C. (1997). Phytoalexin production in an apple cultivar resistant to *Venturia inaequalis*. Phytopathology *87*, 868-876.

Hukkanen, A.T., Polonen, S.S., Karenlampi, S.O., and Kokko, H.I. (2006). Antioxidant capacity and phenolic content of sweet rowanberries. Journal of Agricultural and Food Chemistry *54*, 112-119.

Hüttner, C., Beuerle, T., Scharnhop, H., Ernst, L., and Beerhues, L. (2010). Differential effect of elicitors on biphenyl and dibenzofuran formation in *Sorbus aucuparia* cell cultures. Journal of Agricultural and Food Chemistry *58*, 11977-11984.

Ibrahim, R.K. (1997). Plant O-methyl-transferase signatures. Trends in Plant Science *2*, 249-250.

Ibrahim, R.K., De Luca, V., Khouri, H., Latchinian, L., Brisson, L., and Charest, P.M. (1987). Enzymology and compartmentation of polymethylated flavonol glucosides in *chrysosplenium americanum*. Phytochemistry *26*, 1237-1245.

Igboechi, C.A., Parfitt, R.T., and Rowan, M.G. (1984). Two dibenzofuran derivatives from fruits of *Rhodomyrtus macrocarpa*. Phytochemistry *23*, 1139-1141.

Ilan, A., and Dougall, D. (1992). The effect of growth retardants on anthocyanin production in carrot cell suspension cultures. Plant Cell Reports *11*, 304-309.

Ito, C., Miyamoto, Y., Rao, K.S., and Furukawa, H. (1996). A novel dibenzofuran and two new xanthones form *Calophyllum panciflorum*. Chemical & Pharmaceutical Bulletin *44*, 441-443.

Jha, G., Thakur, K., and Thakur, P. (2009). The *Venturia* apple pathosystem: pathogenicity mechanisms and plant defense responses. Journal of Biomedicine & Biotechnology *2009*, 680160.

Jiang, L.L., and Xuan, L.J. (2006). A new biphenyl glycoside from the leaves of *Eriobotrya japonica*. Chinese Chemical Letters *17*, 35-37.

Jorgensen, E. (1961). The formation of pinosylvin and its monomethyl ether in the sapwood of *Pinus resinosa* AIT. Canadian Journal of Botany *39*, 1765-1772.

Joshi, C., and Chiang, V. (1998). Conserved sequence motifs in plant S-adenosyl-L-methionine-dependent methyltransferases. Plant Molecular Biology *37*, 663-674.

Keen, N.T. (1971). Hydroxyphaseollin production by soybeans resistant and susceptible to *Phytophthora megasperma* var. sojae. Physiological Plant Pathology *1*, 265-275.

Keen, N.T., and Littlefield, L.J. (1979). The possible association of phytoalexins with resistance gene expression in flax to *Melampsora lini*. Physiological Plant Pathology *14*, 265-280.

Kemp, M.S., and Burden, R.S. (1984). Isolation and structure determination of [gamma]-pyrufuran, a third induced antifungal dibenzofuran from the wood of *Pyrus communis* L. infected with *Chondrostereum purpureum* (Pers. ex Fr.) Pouzar. Journal of the Chemical Society, Perkin Transactions 1 *0*, 1441-1443.

Kemp, M.S., and Burden, R.S. (1986). Phytoalexins and stress metabolites in the sapwood of trees. Phytochemistry *25*, 1261-1269.

Kemp, M.S., Burden, R.S., and Loeffler, R.S.T. (1983). Isolation, structure determination, and total synthesis of the dibenzofurans α- and β-pyrufuran, new phytoalexins from the wood of *Pyrus communis* L. Journal of the Chemical Society, Perkin Transactions 1 *0*, 2267-2272.

Kemp, M.S., Holloway, P.J., and Burden, R.S. (1985). 3β,19α-Dihydroxy-2-oxours-12-en-28-oic acid: a pentacyclic triterpene induced in the wood of *Malus pumila* Mill. infected with *Chondrostereum purpureum* (Pers. ex Fr.) Pouzar., and a constituent of the cuticular wax of apple fruits. Journal of Chemical Research, Synopses *5*, 154-155.

Kim, K.H., Choi, S.U., Ha, S.K., Kim, S.Y., and Lee, K.R. (2009). Biphenyls from *Berberis koreana*. Journal of Natural Products *72*, 2061-2064.

Kobayashi, A., Koguchi, Y., Kanzaki, H., Kajiyama, S., and Kawazu, K. (1994). A new type of antimicrobial phenolics produced by plant peroxidase and its possible role in the chemical defense system against plant pathogens. Zeitschrift für Naturforschung C *49*.

Kokubun, T., and Harborne, J.B. (1994). A survey of phytoalexin induction in leaves of the Rosaceae by copper ions. Zeitschrift für Naturforsch, C *49*, 628-634.

Kokubun, T., and Harborne, J.B. (1995). Phytoalexin induction in the sapwood of plants of the Maloideae (Rosaceae): Biphenyls or dibenzofurans. Phytochemistry *40*, 1649-1654.

Kokubun, T., Harborne, J.B., Eagles, J., and Waterman, P.G. (1995a). Antifungal biphenyl compounds are the phytoalexins of the sapwood of *Sorbus aucuparia*. Phytochemistry *40*, 57-59.

Kokubun, T., Harborne, J.B., Eagles, J., and Waterman, P.G. (1995b). Dibenzofuran phytoalexins from the sapwood of *Cotoneaster acutifolius* and five related species. Phytochemistry *38*, 57-60.

Kokubun, T., Harborne, J.B., Eagles, J., and Waterman, P.G. (1995c). Dibenzofuran phytoalexins from the sapwood tissue of *Photinia, Pyracantha* and *Crataegus* species. Phytochemistry *39*, 1033-1037.

Kokubun, T., Harborne, J.B., Eagles, J., and Waterman, P.G. (1995d). Four dibenzofuran phytoalexins from the sapwood of *Mespilus germanica*. Phytochemistry *39*, 1039-1042.

Kollar, A. (1997). Aktuelle Forschung an dem bedeutendsten Erreger im Apfelbau, dem Apfelschorfpilz *Venturia inaequalis*. Nachrichtenblatt Deutscher Pflanzenschutzdienst *49*, 131-136.

Kota, P., Guo, D., Zubieta, C., Noel, J., and Dixon, R.A. (2004). *O*-Methylation of benzaldehyde derivatives by “lignin specific” caffeic acid 3-*O*-methyltransferase. Phytochemistry *65*, 837-846.

Kuć, J. (1991). Phytoalexins: Perspectives and prospects. In Mycotoxins and Phytoalexins, R.P. Sharma, and D.K. Salunkhe, eds. (Boca Raton: CRC Press), pp. 595-603.

Kuć, J. (1995). Phytoalexins, stress Metabolism, and disease resistance in plants. Annual Review of Phytopathology *33*, 275-297.

Kudakasseril, G.J., Lam, L., and Staba, E.J. (1987). Effect of sterol inhibitors on the incorporation of ^{14}C-isopentenyl pyrophosphate into artemisinin by a cell-free system from *Artemisia annua* tissue cultures and plants. Planta Medica *53*, 280-284.

Kundu, S. (2012). Distribution and prediction of catalytic domains in 2-oxoglutarate dependent dioxygenases. BMC Research Notes *5*, 410.

Kylli, P., Nohynek, L., Puupponen-Pimia, R., Westerlund-Wikstrom, B., McDougall, G., Stewart, D., and Heinonen, M. (2010). Rowanberry phenolics: compositional analysis and bioactivities. Journal of Agricultural and Food Chemistry *58*, 11985-11992.

Lam, K.C., Ibrahim, R.K., Behdad, B., and Dayanandan, S. (2007). Structure, function, and evolution of plant *O*-methyltransferases. Genome *50*, 1001-1013.

Li, L., Popko, J.L., Zhang, X.H., Osakabe, K., Tsai, C.J., Joshi, C.P., and Chiang, V.L. (1997). A novel multifunctional *O*-methyltransferase implicated in a dual methylation pathway associated with lignin biosynthesis in loblolly pine. Proceedings of the National Academy of Sciences of the United States of America *94*, 5461-5466.

Lin, C.-H., Chang, H.-S., Liao, C.-H., Ou, T.-H., Chen, I.-S., and Tsai, I.-L. (2010). Anti-inflammatory biphenyls and dibenzofurans from *Rhaphiolepis indica*. Journal of Natural Products *73*, 1628-1631.

Linsmaier, E.M., and Skoog, F. (1965). Organic growth factor requirements of tobacco tissue culture. Physiologica Plantarum *18*, 100-127.

Liu, B., Beuerle, T., Klundt, T., and Beerhues, L. (2004). Biphenyl synthase from yeast-extract-treated cell cultures of *Sorbus aucuparia*. Planta *218*, 492-496.

Liu, B., Raeth, T., Beuerle, T., and Beerhues, L. (2007). Biphenyl synthase, a novel type III polyketide synthase. Planta *225*, 1495-1503.

Liu, B., Raeth, T., Beuerle, T., and Beerhues, L. (2010). A novel 4-hydroxycoumarin biosynthetic pathway. Plant Molecular Biology *72*, 17-25.

Liu, C.J., Deavours, B.E., Richard, S.B., Ferrer, J.L., Blount, J.W., Huhman, D., Dixon, R.A., and Noel, J.P. (2006). Structural basis for dual functionality of isoflavonoid *O*-methyltransferases in the evolution of plant defense responses. The Plant Cell *18*, 3656-3669.

Louie, G.V., Bowman, M.E., Tu, Y., Mouradov, A., Spangenberg, G., and Noel, J.P. (2010). Structure-function analyses of a caffeic acid *O*-methyltransferase from perennial ryegrass reveal the molecular basis for substrate preference. The Plant Cell *22*, 4114-4127.

Lukacin, R., Matern, U., Junghanns, K.T., Heskamp, M.L., Britsch, L., Forkmann, G., and Martens, S. (2001). Purification and antigenicity of flavone synthase I from irradiated parsley cells. Archives of Biochemistry Biophysics *393*, 177-183.

Malnoy, M., Martens, S., Norelli, J.L., Barny, M.A., Sundin, G.W., Smits, T.H., and Duffy, B. (2012). Fire blight: applied genomic insights of the pathogen and host. Annual Review of Phytopathology *50*, 475-494.

Malterud, K.E., and Sandanger Dugstad, E.K. (1985). 4,2`-dihydroxy-3,5-dimethoxybiphenyl, a new phenol from the wood of *Salix caprea* L. Zeitschrift für Naturforsch B: J Biosci *40*, 853-854.

Mandel, M., and Higa, A. (1992). Calcium-dependent bacteriophage DNA infection. 1970. Biotechnology (Reading, Mass.) *24*, 198-201.

Maury, S., Geoffroy, P., and Legrand, M. (1999). Tobacco *O*-methyltransferases involved in phenylpropanoid metabolism. The different caffeoyl-coenzyme A/5-hydroxyferuloyl-coenzyme A 3/5-O-methyltransferase and caffeic acid/5-hydroxyferulic acid 3/5-*O*-methyltransferase classes have distinct substrate specificities and expression patterns. Plant Physiology *121*, 215-224.

Miyakodo, M., Watanabe, K., Ohno, N., Nonaka, F., and Morita, A. (1985). Isolation and Structural Determination of Eriobofuran, A New Dibenzofuran Phytoalexin from Leaves of Loquat, *Eriobotrya japonica* L. Journal of Pesticide Science *10*, 101-106.

Morita, A., and Nonaka, F. (2003). Two phytoalexins extracted from leaf lesions of loquat canker and their inhibition of plant bacteria. Kyushu Plant Protection Research *49*, 45-49.

Müller, K.O., and Borger, H. (1940). Experimentelle Untersuchungen über die Phytophthorainfestans-Resistenz der Kartoffel. Arbeiten der Biologischen Reichsanstalt für Land Forstwirtschaft *23*, 189-231.

Narasimhachari, N., and Von Rudloff, E. (1962). The chemical composition of the wood extractives of *Sorbus decora* (Sarg.) Schneid. Canadian Journal of Chemistry *40*, 1118-1122.

Narasimhachari, N., and Von Rudloff, E. (1973). Lyoniside and aucuparins from wood of North American *Sorbus* species. Phytochemistry *12*, 2551-2552.

Noel, J.P., Dixon, R.A., Pichersky, E., Zubieta, C., and Ferrer, J.L. (2003). Chapter two Structural, functional, and evolutionary basis for methylation of plant small molecules. In Recent Advances in Phytochemistry, T.R. John, ed. (Elsevier), pp. 37-58.

Norelli, J.L., Jones, A.L., and Aldwinckle, H.S. (2003). Fire blight management in the Twenty-first Century: Using new technologies that enhance host resistance in apple. Plant Disease *87*, 756-765.

O'Brien, P.J., and Herschlag, D. (1999). Catalytic promiscuity and the evolution of new enzymatic activities. Chemistry & Biology *6*, R91-R105.

Ober, D. (2005). Seeing double: gene duplication and diversification in plant secondary metabolism. Trends in Plant Science *10*, 444-449.

Ortiz de Montellano, P.R. (2005). Inhibition of cytochrome P450 enzymes. In Cytochrome P450: Structure, mechanism and biochemistry O.d.M. PR, ed. (Kluwar Academic/Plenum Publishers, New York), pp. 247-323.

Parvathi, K., Chen, F., Guo, D., Blount, J.W., and Dixon, R.A. (2001). Substrate preferences of *O*-methyltransferases in alfalfa suggest new pathways for 3-*O*-methylation of monolignols. The Plant Journal *25*, 193-202.

Peters, S., Schmidt, W., and Beerhues, L. (1998). Regioselective oxidative phenol couplings of 2,3′,4,6-tetrahydroxybenzophenone in cell cultures of *Centaurium erythraea* RAFN and *Hypericum androsaemum* L. Planta *204*, 64-69.

Pfaffl, M.W., (2001) A new mathematical model for relative quantification in real-time RT-PCR. Nucleic Acids Research 29, 2002-2007.

Pfaffl, M.W., Lange, I.G., Daxenberger, A., and Meyer, H.H.D. (2001). Tissue-specific expression pattern of estrogen receptors (ER): Quantification of ERα and ERβ mRNA with real-time RT-PCRNote. APMIS *109*, 345-355.

Pichersky, E., and Gang, D.R. (2000). Genetics and biochemistry of secondary metabolites in plants: an evolutionary perspective. Trends in Plant Science *5*, 439-445.

Pinçon, G., Maury, S., Hoffmann, L., Geoffroy, P., Lapierre, C., Pollet, B., and Legrand, M. (2001). Repression of *O*-methyltransferase genes in transgenic tobacco affects lignin synthesis and plant growth. Phytochemistry *57*, 1167-1176.

Potter, D., Eriksson, T., Evans, R.C., Oh, S., Smedmark, J.E.E., Morgan, D.R., Kerr, M., Robertson, K.R., Arsenault, M., Dickinson, T.A.*, et al.* (2007). Phylogeny and classification of Rosaceae. Plant Systematics and Evolution *266*, 5-43.

Prescott, A.G., and Lloyd, M.D. (2000). The iron(II) and 2-oxoacid-dependent dioxygenases and their role in metabolism. Natural Product Reports *17*, 367-383.

Rademacher, W. (2000). GROWTH RETARDANTS: Effects on gibberellin biosynthesis and other metabolic pathways. Annual Review of Plant Physiology and Plant Molecular Biology *51*, 501-531.

Rimando, A.M., Pan, Z., Polashock, J.J., Dayan, F.E., Mizuno, C.S., Snook, M.E., Liu, C.J., and Baerson, S.R. (2012). In planta production of the highly potent resveratrol analogue pterostilbene via stilbene synthase and *O*-methyltransferase co-expression. Plant Biotechnology Journal *10*, 269-283.

Roemmelt, S., Zimmermann, N., Rademacher, W., and Treutter, D. (2003). Formation of novel flavonoids in apple (*Malus x domestica*) treated with the 2-oxoglutarate-dependent dioxygenase inhibitor prohexadione-Ca. Phytochemistry *64*, 709-716.

Saha, A.K., and Brewer, C.F. (1994). Determination of the concentrations of oligosaccharides, complex type carbohydrates, and glycoproteins using the phenol-sulfuric acid method. Carbohydrate Research *254*, 157-167.

Sambrook, J., and Russell, D.W. (2001). Molecular cloning: a laboratory manual, 3rd edn (NewYork:Cold Spring Harbor Laboratory Press).

Schlangen, K., Gosch, C., Roemmelt, S., Knott, J., Fischer, T., Treutter, D., Forkmann, G., Stich, K., and Halbwirth, H. (2003). Can prohexadione-Ca induce antimicrobial flavonoids in Rose? European Journal of Horticultural Science *68*, 137-143.

Schmidlin, L., Poutaraud, A., Claudel, P., Mestre, P., Prado, E., Santos-Rosa, M., Wiedemann-Merdinoglu, S., Karst, F., Merdinoglu, D., and Hugueney, P. (2008). A stress-inducible resveratrol *O*-methyltransferase involved in the biosynthesis of pterostilbene in grapevine. Plant Physiology *148*, 1630-1639.

Schuler, M.A., and Rupasinghe, S.G. (2011). Chapter 5 - Molecular and Structural Perspectives on Cytochrome P450s in Plants. In Advances in Botanical Research, K. Jean-Claude, and D. Michel, eds. (Academic Press), pp. 263-307.

Schwab, W. (2003). Metabolome diversity: too few genes, too many metabolites? Phytochemistry *62*, 837-849.

Seo, E.-K., Huang, L., Wall, M.E., Wani, M.C., Navarro, H., Mukherjee, R., Farnsworth, N.R., and Kinghorn, A.D. (1999). New biphenyl compounds with DNA strand-scission activity from *Clusia paralicola*. Journal of Natural Products *62*, 1484-1487.

Shiu, W.K.P., and Gibbons, S. (2009). Dibenzofuran and pyranone metabolites from *Hypericum revolutum* ssp. revolutum and *Hypericum choisianum*. Phytochemistry *70*, 403-406.

Song, M.-C., Nigussie, F., Jeong, T.-S., Lee, C.-Y., Regassa, F., Markos, T., and Baek, N.-I. (2006). Phenolic Compounds from the Roots of *Lindera fruticosa*. Journal of Natural Products *69*, 853-855.

Stadler, R., Kutchan, T.M., Loeffler, S., Nagakura, N., Cassels, B., and Zenk, M.H. (1987). Revision of the early steps of reticuline biosynthesis. Tetrahedron Letters *28*, 1251-1254.

Stark-Lorenzen, P., Nelke, B., Hänßler, G., Mühlbach, H.P., and Thomzik, J.E. (1997). Transfer of a grapevine stilbene synthase gene to rice (*Oryza sativa* L.). Plant Cell Reports *16*, 668-673.

Storm, K. (1998). Beiträge zur Vogelbeere. In Berichte aus der Bayerischen Landesanstalt für Wald und Forstwirtschaft (Freising, Deutschland: Bayerischen Landesanstalt für Wald und Forstwirtschaft (LWF), pp. 81-85.

Sultanbawa, M.U.S. (1980). Xanthonoids of tropical plants. Tetrahedron *36*, 1465-1506.

Takasugi, M., and Katui, N. (1986). A biphenyl phytoalexin from *Cercidiphyllum japonicum*. Phytochemistry *25*, 2751-2752.

Tamura K., Peterson D., Peterson N., Stecher G., Nei M. and Kumar S. (2011). MEGA5: Molecular evolutionary genetics analysis using maximum likelihood, evolutionary distance, and maximum parsimony methods. Molecular Biology and Evolution *28*, 2731-2739.

Termentzi, A., Zervou, M., and Kokkalou, E. (2009). Isolation and structure elucidation of novel phenolic constituents from *Sorbus domestica* fruits. Food Chemistry *116*, 371-381.

Thomma, B.P., Nelissen, I., Eggermont, K., and Broekaert, W.F. (1999). Deficiency in phytoalexin production causes enhanced susceptibility of *Arabidopsis thaliana* to the fungus *Alternaria brassicicola*. The Plant Journal *19*, 163-171.

Thomzik, J.E., Stenzel, K., Stöcker, R., Schreier, P.H., Hain, R., and Stahl, D.J. (1997). Synthesis of a grapevine phytoalexin in transgenic tomatoes (*Lycopersicon esculentum* Mill.) conditions resistance against *Phytophthora infestans*. Physiological and Molecular Plant Pathology *51*, 265-278.

Trippett, S. (1957). 76. Toxic constituents of the Australian finger cherry, *Rhodomyrtus macrocarpa* benth. Journal of the Chemical Society (Resumed) *0*, 414-419.

Tu, Y., Rochfort, S., Liu, Z., Ran, Y., Griffith, M., Badenhorst, P., Louie, G.V., Bowman, M.E., Smith, K.F., Noel, J.P.*, et al.* (2010). Functional analyses of caffeic acid *O*-methyltransferase and cinnamoyl-CoA-reductase genes from perennial ryegrass (*Lolium perenne*). The Plant Cell *22*, 3357-3373.

VanEtten, H.D., Mansfield, J.W., Bailey, J.A., and Farmer, E.E. (1994). Two classes of plant antibiotics: Phytoalexins versus "Phytoanticipins". The Plant Cell *6*, 1191-1192.

Vanneste, J.L. (2000). What is Fire Blight? Who is *Erwinia amylovora*? How to control it? In Fire blight: the disease and its causative agent, *Erwinia amyolovora*, J.L. Vanneste, ed. (Wallingford, UK: CABI Publishing), pp. 1-6.

Velasco, R., Zharkikh, A., Affourtit, J., Dhingra, A., Cestaro, A., Kalyanaraman, A., Fontana, P., Bhatnagar, S.K., Troggio, M., Pruss, D.*, et al.* (2010). The genome of the domesticated apple (*Malus x domestica* Borkh.). Nature Genetics *42*, 833-839.

Watanabe, K., Ishiguri, Y., Nonaka, F., and Morita, A. (1982). Isolation and Identification of Aucuparin as a Phytoalexin from *Eriobotrya japonica* L. Agricultural and Biological Chemistry *46*, 567-568.

Watanabe, K., Widyastuti, S.M., and Nonaka, F. (1990). Two Biphenyl Compounds from *Rhaphiolepsis umbellata* as Its Phytoalexin. Agricultural and Biological Chemistry *54*, 1861-1862.

Wein, M., Lavid, N., Lunkenbein, S., Lewinsohn, E., Schwab, W., and Kaldenhoff, R. (2002). Isolation, cloning and expression of a multifunctional *O*-methyltransferase capable of forming 2,5-dimethyl-4-methoxy-3(2H)-furanone, one of the key aroma compounds in strawberry fruits. The Plant Journal *31*, 755-765.

Whitehead, I.M., and Threlfall, D.R. (1992). Production of phytoalexins by plant tissue cultures. Journal of Biotechnology *26*, 63-81.

Widyastuti, S.M., Nonaka, F., Watanabe, K., Maruyama, E., and Sako, N. (1991). Accumulation and antifungal Spectrum of 4'-methoxyaucuparin as a new phytoalexin in *Rhaphiolepis umbellata* Makino. Japanese Journal of Phytopathology *57*, 232-238.

Widyastuti, S.M., Nonaka, F., Watanabe, K., Sako, N., and Tanaka, K. (1992). Isolation and characterization of two aucuparin-related phytoalexins from *Photinia glabra* Maxim. Japanese Journal of Phytopathology *58*, 228-233.

Willits, M.G., Giovanni, M.t., Prata, R.T.N., Kramer, C.M., De Luca, V., Steffens, J.C., and Graser, G. (2004). Bio-fermentation of modified flavonoids: an example of in vivo diversification of secondary metabolites. Phytochemistry *65*, 31-41.

Xu, Y., Xu, T.F., Zhao, X.C., Zou, Y., Li, Z.Q., Xiang, J., Li, F.J., and Wang, Y.J. (2012). Co-expression of VpROMT gene from Chinese wild *Vitis pseudoreticulata* with VpSTS in tobacco plants and its effects on the accumulation of pterostilbene. Protoplasma *249*, 819-833.

Yoshikawa, M., Yamauchi, K., and Masago, H. (1978). Glyceollin: its role in restricting fungal growth in resistant soybean hypocotyls infected with *Phytophthora megasperma* var. sojae. Physiological Plant Pathology *12*, 73-82.

Zhang, C.H., Mei, X.G., Liu, L., and Yu, L.J. (2000). Enhanced paclitaxel production induced by the combination of elicitors in cell suspension cultures of *Taxus chinensis*. Biotechnology Letters *22*, 1561-1564.

Zhang, K., Bhuiya, M.-W., Pazo, J.R., Miao, Y., Kim, H., Ralph, J., and Liu, C.-J. (2012). An engineered monolignol 4-*O*-methyltransferase depresses lignin biosynthesis and confers novel metabolic capability in *Arabidopsis*. The Plant Cell *24*, 3135-3152.

Zook, M. (1998). Biosynthesis of camalexin from tryptophan pathway intermediates in cell-suspension cultures of *Arabidopsis*. Plant Physiology *118*, 1389-1393.

Zubieta, C., He, X.Z., Dixon, R.A., and Noel, J.P. (2001). Structures of two natural product methyltransferases reveal the basis for substrate specificity in plant *O*-methyltransferases. Nature Structural Biology *8*, 271-279.

Zubieta, C., Kota, P., Ferrer, J.L., Dixon, R.A., and Noel, J.P. (2002). Structural basis for the modulation of lignin monomer methylation by caffeic acid/5-hydroxyferulic acid 3/5-O-methyltransferase. The Plant Cell *14*, 1265-1277.

VIII. Appendix

A. Sequences

>ORF of *Sa*OMT1
ATGGCTTCTCTAGAGGAACCAAAAGGCCTTCCTGACATTCCTCTTGATGATGAAG
CAAGGAAAGAAGAAGAGAGCTACTGCCATGCACTGCAGCTGGTGGTTTCTTCAGT
GCTGTCCTTCTCCATGCAGTCAGCAATTGAGCTTGGCGTTTTTGACATCATAGCCA
AAGAGGGTCCAAATGCCAAGCTCTCTTCATCTGAGATCGCAGCTCACATCGGAAC
CAAGACCCCTGACGGACCCATGATGCTAGATCGCCTTCTAGCTGTCCTGGCCAGC
AACTCCGTGCTCGACTGCACAGTTGTTAACGGCAAACTTGACAAGTGTTTCCGGA
GGCTATACAGCCTTACCCCTGTGTCCAAGCACTTTGTGACTAATGAAGATGGTGT
TTCCTTAGCCCCTGTGTTGACTATGGTTCAAGACGAGGCCTTCTTAAAGGGCTGGC
GTCACGTGAAAGATGCAGTTATTGAAGGAGGAATTGCATTTGACAGAGCTCATGG
GATGCACCACTTTCAGTATCCAAGTGTCGACCATAGGTTTAATGAATTATTCAAC
AAGGCAATGTTCAACCATAGCACCATAGTTATGAAGAGAATTCTCAAGCTCTACA
AAGGTTTTGAGCACGTTACGCGGCTTGTTGATGTTGGTGGTAATTTGGGAGGGGC
AATTAGTCTAATCACTTCTAAGTATCCACATATTAAGGGCATCAATTTTGACTTAC
CTCATGTTATAAAACATGCCTCCTCTTATCCTGGTGTTGAAAATGTAGGAGGAGA
CATGTTTGAAAGTATTCCAAATGGGGATGCCATTTTTTTGAAGTTCATACTTCATG
ACTGGTTGGATAAAGACTGCATAAAGTTATTGAAAACTTGTTACAACGCAATTCC
AGACAATGGAAAAGTGATCGTGGTGGAGGCACTTCTCCCAATTAAGCCAGATACT
AACGTATCTGTGAGGACCAACGGCCAACTTGATCTGCATATGATGACTCAAACCC
CGGGAGGGATGGAGAGGAGCCAAGAAGAATTCATGGCCTTAGCAACTGCTGCTG
GATTTAGTGGCATCAGATATGAATGTTTCACTGCTAATCTTTGGATCATGGAATTC
TACAAGTAG

>ORF of *Sa*OMT2
ATGGGTTCGACCGTAGAGACTCAGATGACTCCAATCCAAGTCTCCGACGAAGAA
GCCAACCTCTTCGCCATGCAGCTAGCCAGCGGCTCCATTCTCCCCATGGTGCTCA
AGGCAGCCATCGAGCTCGACCTCCTCGAGGTCATGGCAAAAGCCGGGCCTG
GCGCTTTTGTTTCTCCGGCTGACTTAGCTTCGCAGCTGCCGACTAAGAACCCCGAC
GCCCCCGTCATGCTGGACCGCATGCTGCGCCTCCTGGCCAGCTACTCCATCCTCAC
TTACTCCCTCCGCACACTTCCCGACGGCAAAGTCGAGCGGCTGTACGGCCTCGGC
CCCGTCTGCAAGTTTTTGACAAAGAACGAGGATGGTGCTTCCATTGGTTCTCTCTG
CCTCATGAATCAGGACAAGGTCCTTATGGAGAGCTGGTACCACTTGAAAGATGCA
GTCCTTGAAGGAGGTATCCCTTTCAACAAGGCCTATGGAATGACTGCTTTTGAGT
ACCATGGCACTGACCCCAGATTCAACAAGGTCTTCAACAAGGGAATGGCTGACC
ACTCTACCATTACCATGAAGAAACTTCTTGAGATCTACAATGGCTTTGAGGGCCT
CACATCCATCGTTGATGTTGGTGGTGGCACCGGCGCTGTTCTTAATATGATCGTCT
CTAAATACCCTTCGATTAAGGGCATTAACTTCGACTTGCCTCATGTCATTGAAGAT
GCTCCCCAATATCCTGGTGTGGAGCACGTTGGAGGAGACATGTTTGTTAGTGTTC
CAAAGGGAGATGCAATTTTCATGAAGTGGATATGCCACGACTGGAGTGACGAGC
ATTGCTTGAAATTTTTGAAGAACTGCTATGCTGCGCTCCCAGACAATGGGAAGGT
AATTGTTGCTGAGTGCATTCTTCCGGTAGCTCCGGACAGTAGCCTTGCCACCAAG
GGAGTTGTCCATATCGACGCGATCATGTTAGCTCACAACCCCGGCGGAAAAGAG
AGGACGGAGAAGGAGTTCGAGGCCTTGGCTAAGGAATCTGGATTCCAAGGCTT
TCGAGTTGTGTGCTCTGCTTTCAACATCTATGCCATTGAGTTTCTTAAGAAAATTT
GA

B. Chemical synthesis of biphenyls and dibenzofurnas

In course of this study, a number of biphenyls and dibenzofurans were synthesized. They served as substrates and/or analytical reference compounds. Here we present the methods applied and a short comment.

B.1 Synthesis of dibenzofurans

Synthesis of dibenzofurans was carried out as described by Oliveira et al. (2003). The synthesis consisted of two steps:

1) Formation of diaryl ether using Ullmann synthesis, where an arylhalide is coupled to a phenol in presence of copper (I) oxide.
2) Cyclization of the diaryl ether to the corresponding dibenzofuran by oxidative coupling, using palladium acetate in presence of acetic acid. Using pivalic acid did not result in better yield (Scheme 1).

Demethylation was carried out using MgI_2 as described by Bao et al. (2009). Although, in that report, MgI_2 acted as a selective demethylating agent for biphenyl derivatives, the opposite was true in case of dibenzofurans. Using three equivalents of MgI_2 yielded a mixture of various demethylated dibenzofurans.

The outlined procedures led to the successful synthesis of eriobofuran, 2,4-dihydroxydibenzofuran, 2-hydroxy-4-methoxydibenzofuran and 4-hydroxy-2-methoxydibenzofuran. However, preparation of noreriobofuran was not successful. The demethylation reaction resulted in a mixture of isomers, which could not be separated and purified. Trials to use BBr_3 instead of MgI_2 were not successful, as well, although BBr_3 was used in preparation of α- and β-pyrufurans (Carvalho et al., 1985). Hence, for this compound another demethylating reagent or alternative synthesis routes should be considered.

The yield of the synthesized dibenzofurans was 30-50% lower than reported by Oliveira et al. (2003). This can be attributed to the presence of more oxygenated functional groups. However, extending the reaction time and repeated addition of phenol improved the yields, but still not to the reported yields. Recently, a new method for synthesis of dibenzofurans from 2`-hydroxybiphenyls (2-arylphenols) has been published (Xiao et al., 2011).

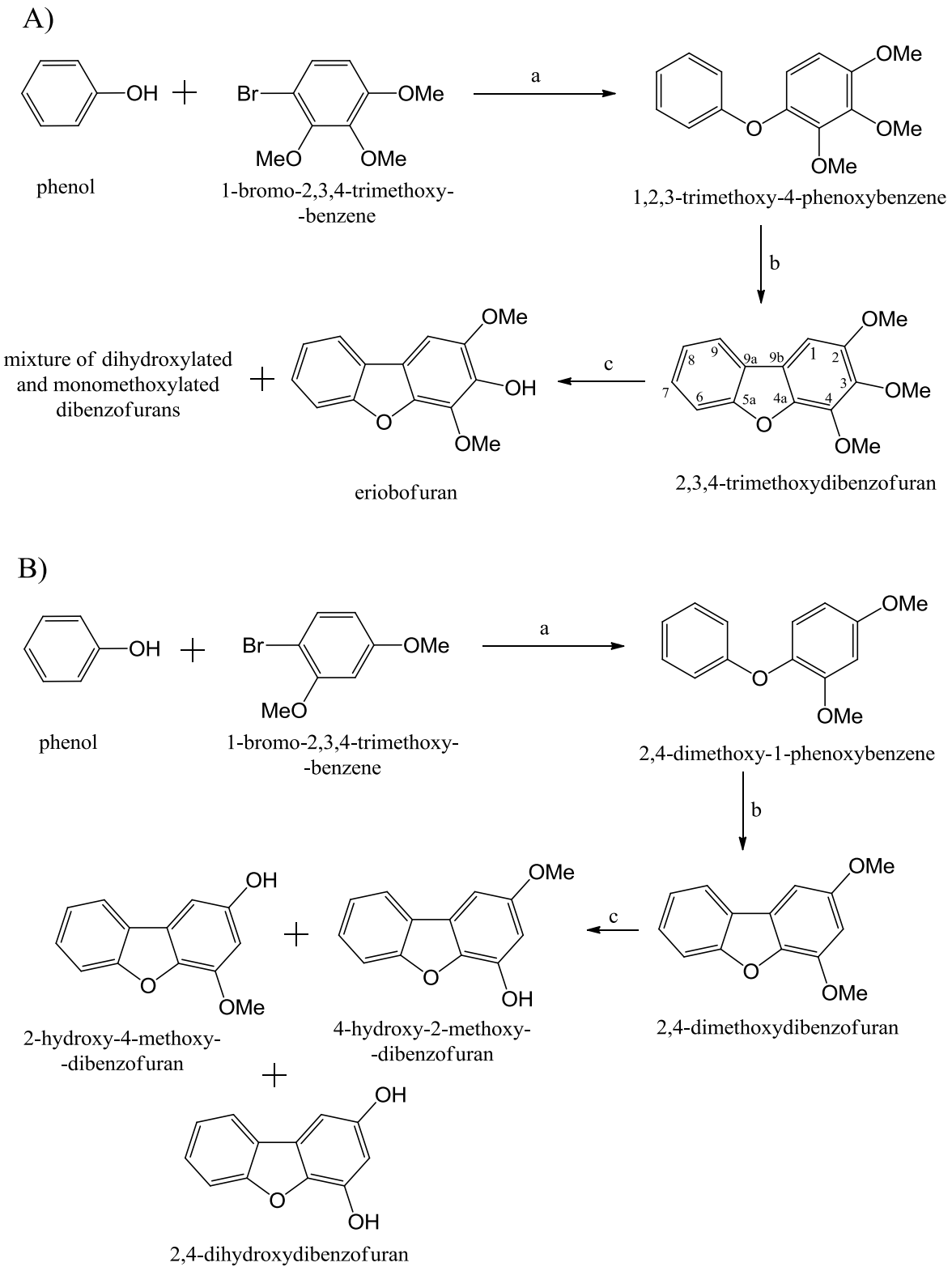

Scheme 1. Synthesis of dibenzofurans.
A) eriobofuran B) dioxygenated dibenzofuran derivatives.
a) Cu_2O, K_2CO_3, reflux. b) palladium acetate /acetic acid, reflux. c) MgI_2, 80°C, solvent-free conditions.

B.2 Synthesis of biphenyls

Since its introduction (Miyaura et al., 1981), Suzuki coupling reaction plays an important role in the synthesis of biaryl derivatives. As recognition of his work, Akira Suzuki has been awarded the Nobel Prize in Chemistry in 2010. Reviews about its scope and applications have been recently published (Kotha et al., 2002; Suzuki, 2004). The formation of C-C bonds is achieved by cross coupling of a haloarene with arylboronic acid in presence of tetrakis(triphenylphosphine) palladium (0) and a base.

Synthesis of 3,4,5-trimethoxybiphenyl was carried out as described by Hüttner et al. (2010). Selective demethylation of the methoxy group at position 4 was carried out by using MgI_2 (Bao et al., 2009), which led to the formation of aucuparin. Using large excess of MgI_2 did not affect the selectivity of the reaction but resulted in higher yields. A second single demethylation reaction was carried out using BBr_3 to yield noraucuparin (Scheme 2A).

Synthesis of 2`-hydroxyaucuparin followed a similar reaction sequence (Scheme 2B). However, some modifications were done to get a better yield as recommended by Watanabe et al., (1992). Pinacol ester of aryl boronic acid was used in presence of strong base (K_3PO_4) and in absence of water to avoid hydrolytic deboronation. Such reaction conditions led to satisfactory yields even with sterically demanding compounds, e.g. as in our case *ortho* benzyloxy groups. Using large excess of MgI_2 led to a debenzylation of the 2`-benzyloxy group and the demethylation at position 4 in a single step, which led to formation of 2`-hydroxyaucuparin.

Lewis acids are widely applied in demethylation of methoxy groups in *ortho* relationship to a carbonyl group or to other methoxy groups. A lot of boron halides and magnesium halides have been examined and studied. It is supposed that the metal will coordinate to the *ortho* dioxygenated functions and the methyl group will be removed by nucleophilic attack of the halogen anion (Anioł et al., 2008; Yamaguchi et al., 1999). A similar reaction mechanism can be postulated here (scheme 3). In our case, demethylation using MgI_2 was successfully applied to synthesize aucuparin and 2`-hydroxyaucuparin in a feasible convenient way.

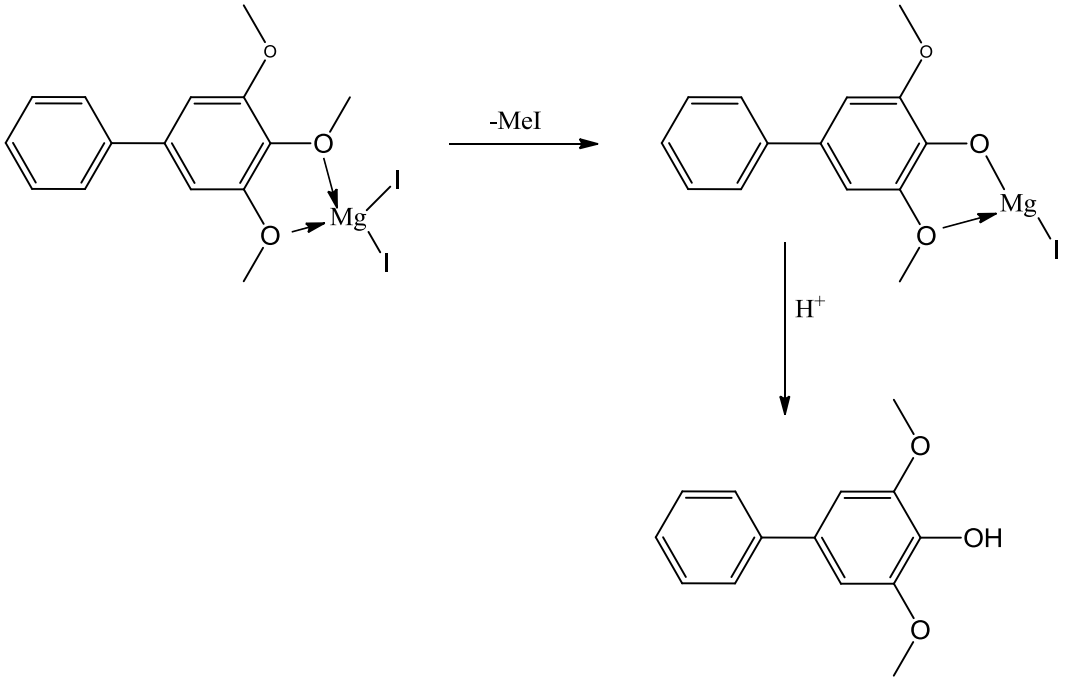

Scheme 3. Demethylation of 3,4,5-trimethoxydibenzofuran with MgI_2 to yield aucuparin.

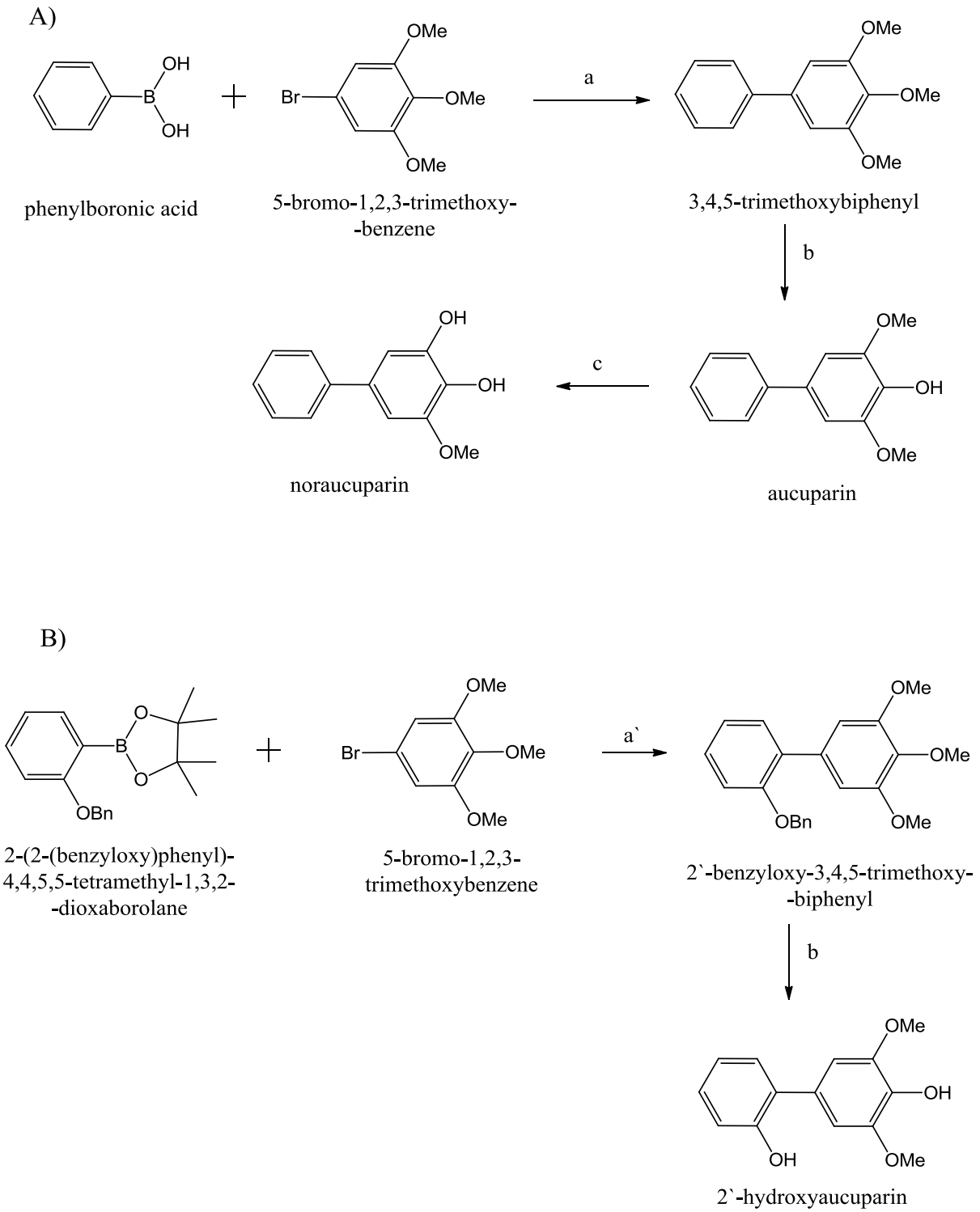

Scheme 2. Synthesis of biphenyls.
A) aucupain and noraucuparin. B) 2`-hydroxyaucuparin.
a) Na_2CO_3, $Pd(PPh_3)_4$; a`) K_3PO_4, $Pd(PPh_3)_4$, reflux; b) MgI_2, 80°C; c) BBr_3, RT.

B.3 References

Anioł, M., Szymańska, K., and Żołnierczyk, A. (2008). An efficient synthesis of the phytoestrogen 8-prenylnaringenin from isoxanthohumol with magnesium iodide etherate. Tetrahedron *64*, 9544-9547.

Bao, K., Fan, A., Dai, Y., Zhang, L., Zhang, W., Cheng, M., and Yao, X. (2009). Selective demethylation and debenzylation of aryl ethers by magnesium iodide under solvent-free conditions and its application to the total synthesis of natural products. Organic & Biomolecular Chemistry *7*, 5084-5090.

Carvalho, C., Russo, A., and Sargent, M. (1985). Boron trichloride as a selective demethylating agent for hindered ethers: a synthesis of the phytoalexins α- and β-Pyrufuran, a synthesis of tri-O-methylleprolomin and its demethylation. Australian Journal of Chemistry *38*, 777-792.

Hüttner, C., Beuerle, T., Scharnhop, H., Ernst, L., and Beerhues, L. (2010). Differential effect of elicitors on biphenyl and dibenzofuran formation in *Sorbus aucuparia* cell cultures. Journal of Agricultural and Food Chemistry *58*, 11977-11984.

Kotha, S., Lahiri, K., and Kashinath, D. (2002). Recent applications of the Suzuki–Miyaura cross-coupling reaction in organic synthesis. Tetrahedron *58*, 9633-9695.

Miyaura, N., Yanagi, T., and Suzuki, A. (1981). The Palladium-Catalyzed Cross-Coupling Reaction of Phenylboronic Acid with Haloarenes in the Presence of Bases. Synthetic Communications *11*, 513-519.

Oliveira, A.M.A.G., Raposo, M.M.M., Oliveira-Campos, A.M.F., Griffiths, J., and Machado, A.E.H. (2003). Synthesis of psoralen analogues based on dibenzofuran. Helvetica Chimica Acta *86*, 2900-2907.

Suzuki, A. (2004). Organoborane coupling reactions (Suzuki coupling). Proceedings of the Japan Academy, Series B *80*, 359-371.

Watanabe, T., Miyaura, N., and Suzuki, A. (1992). Synthesis of Sterically Hindered Biaryls via the Palladium-Catalyzed Cross-Coupling Reaction of Arylboronic Acids or their Esters with Haloarenes. Synlett *1992*, 207-210.

Xiao, B., Gong, T.-J., Liu, Z.-J., Liu, J.-H., Luo, D.-F., Xu, J., and Liu, L. (2011). Synthesis of Dibenzofurans via Palladium-Catalyzed Phenol-Directed C–H Activation/C–O Cyclization. Journal of the American Chemical Society *133*, 9250-9253.

Yamaguchi, S., Nedachi, M., Yokoyama, H., and Hirai, Y. (1999). Regioselective demethylation of 2,6-dimethoxybenzaldehydes with magnesium iodide etherate. Tetrahedron Letters *40*, 7363-7365.

C. **Experimental**

C.1 Synthesis of eriobofuran

C.1.1 Synthesis of 1,2,3-trimethoxy-4-phenoxybenzene

1-bromo-2,3,4-trimethoxybenzene (5 g, 20.24 mmol), phenol (2.35 g, 24.6 mmol), K_2CO_3 (1.4 g, 10.12 mmol) and Cu_2O (4.44 g, 31 mmol) were mixed and refluxed in oil bath (120°C). Phenol (317 mg, 3.36 mmol) was added after one hour. Then additional phenol (317 mg) was added three times every one and half hour. After 7 hours, the reaction mixture was cooled to RT, extracted with CH_2Cl_2 (50 ml). The organic phase was filtered, washed with 1M NaOH (3×50 ml) and dried over anhydrous Na_2SO_4. The crude product was purified using silica gel column chromatograpy (CC) and CH_2Cl_2 as eluent to yield 1,2,3-trimethoxy-4-phenoxybenzene (1.2 g, 4.6 mmol, yield: 22.8%). Experimental data for 1,2,3-trimethoxy-4-phenoxybenzene: Figures A.1-A.6.

MS (70 eV), *m/z* (% rel abundance) 260 (100, $[M]^+$), 245 (33, $[M]^+$-15), 214 (9), 202 (9), 185 (9), 159 (9), 131 (12), 105 (11), 91 (17), 77 (40, $[Ph]^+$); RI (ZB5-MS) 1924, RI (VF5-MS) 1935.

^{1}H-NMR (600 MHz, $CDCl_3$, TMS) 7.29 (m, 2H, H- 3`, 5`), 7.02 (m, 1H, H-4`), 6.92 (m, 2H, H-2`,6`), 6.74 (d, 1H, *J* = 9.1 Hz, H-5), 6.62 (d, 1H, *J* = 9.1 Hz, H-6), 3.916 (s, 3H, 2-OMe), 3.866 (s, 3H, 3-OMe), 3.8349 (s, 3H, 1-OMe).

^{13}C-NMR (150 MHz, $CDCl_3$, TMS) 158.62 (C-1`), 150.44 (C-1), 146.29 (C-3), 143.29 (C-2), 142.65 (C-4), 129.5 (C-3`, C-5`), 122.16 (C-4`), 116.37 (C-2`, C-6`), 116.12 (C-5), 106.56 (C-6), 61.24 (2,3- OMe), 56.21 (1-OMe).

C.1.2 Synthesis of 2,3,4- trimethoxydibenzofuran

1,2,3-trimethoxy-4-phenoxybenzene (1.2 g, 4.6 mmol) and $Pd(OAc)_2$ (1 g, 4.1 mmol) were suspended in 99.4% AcOH (10 ml) and refluxed for 7 hours. After cooling to RT, CH_2Cl_2 (50 ml) was added. The organic solution was filtered and then washed with water several times till free from acidity. The crude product was chromatographed using silica gel CC and $CHCl_3$ as eluent. The product-containing fractions were then purified using RP-18 and MeOH : H_2O (90:10) as eluent. The yield was 36.6% (434 mg, 1.68 mmol). Experimental data for 2,3,4-trimethoxydibenzofuran: Figures A.7-A.14.

MS (70 eV), *m/z* (% rel abundance) 258 (100, $[M]^+$), 243 (99, $[M]^+$-15), 228 (9, $[M]^+$-30), 215 (12), 200 (42), 185 (47), 155 (12), 139 (12), 129 (30), 113 (12), 101 (35); RI (ZB5-MS) 2153, 258 m/z.

^{1}H-NMR (600 MHz, $CDCl_3$, TMS) 7.86 (ddd, 1H, *J* = 0.7, 1.3, 7.7 Hz, H-9), 7.57 (dt, 1H, *J* = 1, 8.3 Hz, H-6), 7.41 (ddd, 1H, *J* = 1.3, 7.2, 8.3 Hz, H-7), 7.32 (ddd, 1H, *J* = 1, 7.2, 7.7 Hz, H-8), 7.13 (s, 1H, H-1), 4.26 (s, 3H, 4-OMe), 3.98 (s, 3H, 2-OMe), 3.96 (s, 3H, 3-OMe).

^{13}C-NMR (150 MHz, $CDCl_3$, TMS) 156.44 (C-5a), 150.53 (C-2), 142.65 (C-4a), 141.01 (C-3), 139.29 (C-4), 126.39 (C-7), 124.49 (C-9a), 122.62 (C-8), 120.1 (C-9), 119.85 (C-9b), 111.73 (C-6), 96.65 (C-1), 61.64 (3-OMe), 61.19 (4-OMe), 56.57 (2-OMe).

C.1.3 Preparation of eriobofuran

Preparation of magnesium iodide etherate solution

Magnesium iodide etherate (4.35 mmol) was prepared by mixing I_2 crystals (1.1 g, 4.35 mmol) with magnesium powder (0.21 g, 8.69 mmol) in dry diethyl ether. The mixture was protected from light and left in ultrasonic bath for approximately 20 min under stream of argon gas until the solution was colorless. The magnesium

iodide etherate solution was filtered to get rid of the non-reacted magnesium. The whole prepared solution was utilized in the reaction.

2,3,4-trimethoxydibenzofuran (374 mg, 1.45 mmol) was dissolved in dry ether. Both reactant solutions were mixed and evaporated under vacuum. The residue was heated in oil bath at 80°C under continuous stream of argon gas for 90 min. The reaction was stopped by addition of water (50 ml), $Na_2S_2O_3$, 5% HCl (20 ml). The aqueous phase was extracted with CH_2Cl_2 (3×50 ml). The organic layer was then washed with saturated solution of $NaHCO_3$ then with brine and dried over anhydrous Na_2SO_4. Fractionation of the crude product over silica gel CC (using 2% MeOH in CH_2Cl_2) yielded two fractions A, B.

Fraction A was further purified on silica gel column using CH_2Cl_2 as eluent to yield eriobofuran (130 mg, 0.5 mmol, 36% yield). The spectroscopic properties were identical to published data (Hüttner et al., 2010). Experimental data for eriobofuran: Figures A.15-A.16.

MS of mono-TMS derivative (70 eV), *m/z* (% rel abundance) 316 (50, $[M]^+$), 286 (100), 271 (11), 243 (16), 226 (3), 187 (5), 161 (3), 143 (5), 101 (4), 73 (15); RI (VF5-MS) 2232.

^{1}H-NMR (600 MHz, $CDCl_3$, TMS) 7.82 (ddd, 1H, *J* = 0.7, 1.3, 7.6, H-9), 7.55 (ddd, 1H, *J* = 0.7, 0.9, 8.2, H-6), 7.37 (ddd, 1H, *J* = 1.3, 7.3, 8.2, H-7), 7.29 (ddd, 1H, 0.9, 7.3, 7.6, H-8), 7.11 (s, 1H, H-1), 5.83 (s, 1H, OH), 4.26 (s, 3H, 4-OMe), 4.01 (s, 3H, 2-OMe).

Faction B was purified on a silica gel column using petr. ether/EtOAc (6:4) as eluent to yield a mixture of dihydroxylated monomethylated dibenzofurans (23 mg, 0.1 mmol) which could not be purified to yield pure compounds.

C.2 Synthesis of monomethoxylated and dihydroxydibenzofuran

C.2.1 Synthesis of 2,4-dimetoxy-1-phenoxybenzene

1-bromo-2,4-dimethoxybenzene (16.1 g, 74.2 mmol), phenol (8.6 g, 91.52 mmol), K_2CO_3 (5.12g, 37.1 mmol) and Cu_2O (16.3g, 113.6 mmol) were mixed and refluxed. After one hour, phenol (1.16 g, 12.36 mmol) was added. The same amount of phenol was then added every 1.5 h for three times. After 7 h, the reaction mixture was cooled to RT and diluted with chloroform 100 mL and filtered through cotton. The filtrate was washed with NaOH (1M) to remove excess phenol, and then dried over Na_2SO_4. The product was separated by silica gel CC using CH_2Cl_2/ pet. ether (40:60) as eluent. The yield was 31% (5.36 g, 23.3 mmol). Experimental data for 2,4-dimetoxy-1-phenoxybenzene: Figures (A.17-A.22).

MS (70 eV), *m/z* (% rel abundance) 230 (100, $[M]^+$), 215 (15, $[M]^+$-15), 200 (2, $[M]^+$-30), 187 (6), 171 (4), 153 (11), 125 (10), 110 (4), 91 (4), 77 (14, $[Ph]^+$); RI (VF5-MS) 1866.

^{1}H-NMR (400 MHz, $CDCl_3$, TMS) 7.26 (m, 2H, H-3`, 5`), 6.99 (m, 1H, H-4`), 6.95 (d, 1H, *J* = 8.7 Hz, H-6), 6.89 (m, 2H, H-2`, 6`), 6.58 (d, 1H, *J* = 2.8 Hz, H-3), 6.45 (dd, 1H, *J* = 2.8, 8.7 Hz, H-5), 3.81 (s, 3H, 4-OMe), 3.78 (s, 3H, 2-OMe).

^{13}C-NMR (100 MHz, $CDCl_3$, TMS) 158.83 (C-1`), 157.28 (C-4), 152.54 (C-2), 138.18 (C-1), 129.38 (C-3`, 5`), 122.32 (C-6), 121.81 (C-4`), 116.09 (C-2`, 6`), 104.19 (C-5), 100.66 (C-3), 55.94 (2-OMe), 55.62 (4-OMe).

C.2.2 Synthesis of 2,4-dimethoxydibenzofuran

2,4-dimetoxy-1-phenoxybenzene (6.75 g, 29.4 mmol) and $Pd(OAc)_2$ (5.85 g, 25.8 mmol) were suspended in 99.4% AcOH (59 ml) and refluxed for 7 hours. After cooling to RT, the reaction was extracted with CH_2Cl_2 (200 ml). The organic phase

was separated and washed with water (100 ml each) several times until the water phase was free acid (neutral pH). The crude product was chromatographed using silica gel CC and CH_2Cl_2/pet. ether (25:75). The yield was 12% (810 mg, 3.55 mmol). Experimental data for 2,4-dimethoxydibenzofuran: Figures A.23-A.28.

MS (70 eV), *m/z* (% rel abundance) 228 (100, $[M]^+$), 213 (26, $[M]^+$-15), 199 (7, $[M]^+$-29), 185 (40), 170 (26), 155 (4), 142 (11), 126 (10), 114 (16); (RI (VF5-MS) 2079.

^{1}H-NMR (600 MHz, $CDCl_3$, TMS) 7.89 (ddd, 1H, *J* = 0.7, 1.3, 7.7 Hz, H-9), 7.59 (dt, 1H, *J* = 1.6, 8.3 Hz, H-6), 7.44 (ddd, 1H, *J* = 1.3, 7.3, 8.3 Hz, H-7), 7.32 (ddd, 1H, *J* = 1, 7.3, 7.7 Hz, H-8), 6.98 (d, 1H, *J* = 2.3 Hz , H-1), 6.62 (d, 1H, *J* = 2.3 Hz, H-3), 4.03 (s, 3H, 4-OMe), 3.91 (s, 3H, 2-OMe).

^{13}C-NMR (150 MHz, $CDCl_3$, TMS) 156.71 (C-2), 156.54 (C-5a), 145.83 (C-4), 140.22 (C-4a), 127.04 (C-7), 125.17 (C-9b), 124.59 (C-9a), 122.51 (C-8), 120.58 (C-9), 112.02 (C-6), 99.36 (C-3), 94.31 (C-1), 56.17 (4-OMe), 55.99 (2-OMe).

C.2.3 Preparation of monomethoxylated and dihydroxydibenzofuran

MgI_2 etherate solution (7.17 mmol) was prepared from I_2 crystals (1.8 g, 7.17 mmol I_2) and magnesium powder (0.35 g, 14.34 mmol), as described before (synthesis of eriobofuran). This solution was mixed with a solution of 2,4-dimethoxydibenzofuran (545 mg, 2.39 mmol) in dry ether (10 ml) and evaporated under reduced pressure. The residue was heated at 80°C for 10 hours under continuous stream of argon gas. The reaction was stopped by addition of saturated solution of NH_4Cl (50 ml) (an alternative to $Na_2S_2O_3$ and washing with $NaHCO_3$, (Anioł et al., 2008)) and the resulting solution was made acidic using aqueous HCl (5%). The aqueous phase was extracted with CH_2Cl_2 (3×50ml) and dried over anhydrous Na_2SO_4. The reaction product was fractionated on silica gel CC using pet. ether/ EtOAc (65:35) to yield two fractions A, B with R_f values of 0.8 and 0.24, respectively.

Fraction A (323 mg) was further purified using silica gel CC and pet. ether/ EtOAc (8:2) to yield 4-hydroxy-2-methoxydibenzofuran (267 mg, 1.24 mmol, 52.2% yield, R_f = 0.64) and compound 2-hydroxy-4-methoxydibenzofuran (12 mg, 0.056 mmol, 2.3% yield, R_f = 0.4).

Experimental data for 4-hydroxy-2-methoxydibenzofuran: Figures A.29-A.33.

MS of mono-TMS derivative (70 eV), *m/z* (% rel abundance) 286 (100, $[M]^+$), 271 (53, $[M]^+$-15), 256 (62, $[M]^+$-30), 240 (9), 228 (9), 213 (7), 197 (7), 185 (10), 126 (10), 114 (5), 73 (18); RI (ZB5-MS) 2086.

^{1}H-NMR (400 MHz, $CDCl_3$, TMS) 7.89 (ddd, 1H, *J* = 0.6, 1.3, 7.7 Hz, H-9), 7.54 (ddd, 1H, *J* = 0.7, 0.7, 8.7 Hz, H-6), 7.44 (ddd, 1H, *J* = 1.3, 7.2, 8.4 Hz, H-7), 7.32 (td, 1H, *J* = 1, 7.5 Hz, H-8), 7 (d, 1H, *J* = 2.4 Hz, H-1), 6.66 (d, 1H, *J* = 2.4 Hz, H-3), 5.5 (br. s, OH), 3.88 (s, 3H, 2-OMe).

^{13}C-NMR (100 MHz, $CDCl_3$, TMS) 156.76 (C-2), 156.54 (C-5a), 141.31 (C-4), 139.14 (C-4a), 127.23 (C-7), 125.49 (C-9b), 124.79 (C-9a), 122.7 (C-8), 120.88 (C-9), 111.84 (C-6), 102.26 (C-3), 95.89 (C-1), 56.07 (2-OMe).

Experimental data for 2-hydroxy-4-methoxydibenzofuran: Figures A.34-A.39

MS of mono-TMS derivative (70 eV), *m/z* (% rel abundance) 286 (100, $[M]^+$), 271 (64, $[M]^+$-15), 256 (4, $[M]^+$-30), 243 (7), 211 (7), 185 (6), 139 (7), 126 (12), 114 (7), 73 (20); RI (ZB5-MS) 2133.

^{1}H-NMR (400 MHz, $CDCl_3$, TMS) 7.86 (ddd, 1H, *J* = 0.7, 1.3, 7.7 Hz, H-9), 7.59 (dt, 1H, *J* = 0.8, 8.3 Hz, H-6), 7.45 (ddd, 1H, *J* = 1.3, 7.3, 8.2 Hz, H-7), 7.32

(td, 1H, *J* = 1, 8 Hz, H-8), 6.95 (d, 1H, *J* = 2.3 Hz, H-1), 6.58 (d, 1H, *J* = 2.3 Hz, H-3), 4.03 (s, 3H, 4-OMe).

^{13}C-NMR (100 MHz, $CDCl_3$, TMS) 156.66 (C-5a), 152.21 (C-2), 145.87 (C-4), 140.16 (C-4a), 127.26 (C-7), 125.6 (C-9b), 124.29 (C-9a), 122.55 (C-8), 120.74 (C-9), 112.03 (C-6), 99.16 (C-1), 97.63 (C-3), 56.27 (4-OMe).

Fraction B (120 mg) was purified using silica gel CC and CH_2Cl_2/MeOH/ HCOOH, (5: 0.15: 0.05) to yield 2,4-dihydroxydibenzofuran (70 mg, 0.35 mmol, 13.68% yield). Experimental data for 2,4-dihydroxydibenzofuran: Figures A.40-A.44.

MS of di-TMS derivative (70 eV), *m/z* (% rel abundance) 344 (100, $[M]^+$), 329 (40, $[M]^+$-15), 271 (5), 255 (5), 211 (4), 181 (4), 157 (5), 126 (6), 73 (75); RI (ZB5-MS) 2136.

^{1}H-NMR (400 MHz, $CDCl_3$, TMS) 7.86 (ddd, 1H, *J* = 0.6, 1.3, 7.4 Hz, H-9), 7.54 (dt, 1H, *J* = 0.35, 8.3 Hz, H-6), 7.45 (ddd, , 1H, *J* = 1.3, 7.2, 8.4 Hz, H-7), 7.32 (ddd, 1H, *J* = 1, 7.3, 7.7 Hz, H-8), 6.95 (d, 1H, *J* = 2.3 Hz, H-1), 6.58 (d, 1H, *J* = 2.3 Hz, H-3), 5.47 (br. s, OH), 4.81 (br. s, OH).

^{13}C-NMR (100 MHz, $CDCl_3$, TMS) 156.6 (C-5a), 152.27 (C-2), 141.32 (C-4), 139.05 (C-4a), 127.41 (C-7), 125.8 (C-9b), 124.53 (C-9a), 122.76 (C-8), 121.02 (C-9), 111.85 (C-6), 102.57 (C-3), 98.26 (C-1).

C.3 Synthesis of 2`-hydroxyaucuparin

C.3.1 Synthesis of 2`-benzyloxy-3,4,5-trimethoxybiphenyl

5-bromo-1,2,3-trimethoxybenzene (3.6 g, 14.65 mmol), K_2PO_3 (4.65 g, 21.9 mmol) and tetrakis (triphenylphosphine) palladium (340 mg, 0.29 mmol) were added to 50 ml dimethylformamide and continuously stirred under a stream of argon gas. 2-(benzyloxy)phenylboronic acid pinacol ester (5 g, 16.12 mmol) was added and the reaction temperature was raised to 100°C and kept at that temperature for 6 hours. After cooling, the crude reaction mixture was extracted with CH_2Cl_2, washed with water and dried over anhydrous Na_2SO_4. It was then purified using silica gel CC and CH_2Cl_2 as eluent to yield 2´-benzyloxy-3,4,5-trimethoxybiphenyl (1.4 g, 4 mmol, 27.3% yield). Experimental data for 2´-benzyloxy-3,4,5-trimethoxybiphenyl: Figures A.45-A.49

MS (70 eV), *m/z* (% rel abundance) 350 (65, $[M]^+$), 259 (22, $[M]^+$-91 (Ph-CH_2)), 228 (100, $[M]^+$-(15 + 107(Ph-CH_2-O))), 213 (25), 201 (11), 185 (12), 170 (6), 158 (10), , 130 (9), 115 (8), 102 (11), 91 (63, $[Ph\text{-}CH_2]^+$); RI (ZB5-MS) 2720. ^{1}H-NMR (600 MHz, $CDCl_3$, TMS) 7.34 (m, 7H, H-2`, 4`, 2``, 3``, 4``, 5``, 6``), 7.06 (m, 2H, H-3`, 5`), 6.82 (s, 2H, H-2, 6), 5.08 (s, 2H, CH_2, benzylic), 3.89 (s, 3H, 4-OMe), 3.79 (s, 6H, 3,5-OMe).

^{13}C-NMR (150 MHz, $CDCl_3$, TMS) 155.5 (C-2`), 152.62 (C-3,5), 136.93 (C-4), 137 (C-1``), 133.88 (C-1), 130.86 (C-1`), 130.73 (C-6`), 128.61 (C-4`), 128.43 (C-3``, 5``), 127.83 (C-4``), 127.31 (C-2``, 6``), 121.32 (C-5`), 113.17 (C-3`), 106.77 (C-2,6), 70.51 (CH_2, benzylic), 60.89 (4-OMe), 55.94 (3,5-OMe).

C.3.2 Preparation of 2´-hydroxyaucuparin

2´-benzyloxy-3,4,5-trihydroxybiphenyl (1 g, 2.85 mmol) was dissolved in dry ether (10 ml). MgI_2 etherate (42.7 mmol) was prepared as described before (synthesis of eriobofuran) (10.8 g, 42.7 mmol I_2); (2 g, 85.5 mmol Mg)]. Both solutions were mixed and evaporated under reduced pressure. The residue was heated in oil path at 80°C for 8 hours under a stream of argon gas. After cooling to

RT, water (50 ml), $Na_2S_2O_3$, and 5%HCl were added. The aqueous phase was extracted with CH_2Cl_2 (3×50 ml). The resulting organic phase was washed with saturated solution of $NaHCO_3$, brine and dried over anhydrous Na_2SO_4. 2´-hydroxyaucuparin (115 mg, 0.5 mmol, 16% yield) was obtained after purification using silica gel CC and CH_2Cl_2/pet. ether, (90:10) as eluent. The spectroscopic properties were identical to published data (Hüttner et al., 2010).

Experimental data for 2´-hydroxyaucuparin: Figures A.50-A.52

MS (70 eV), *m/z* (% rel abundance) 246 (100, $[M]^+$), 231 (11, $[M]^+$-15), 199 (20), 185 (8), 171 (25), 145 (7), 131 (20), 115 (22), 103 (10), 89 (10), 77 (13), 57 (13); RI (ZB5-MS) 2210. MS of di-TMS derivative (70 eV), *m/z* (% rel abundance) 390 (94, $[M]^+$), 375 (15, $[M]^+$-15), 360 (100, $[M]^+$-30), 345 (5), 330 (30), 315 (11), 256 (11), 165 (7), 89 (7), 73 (52), 59 (8); RI (ZB5-MS) 2198.

^{1}H-NMR (600 MHz, $CDCl_3$, TMS) 7.26 (ddd, 1H, *J* = 1.7, 7.4, 8.1 Hz, 4`-H), 7.23 (ddd, 1H, *J* = 0.4, 1.7, 7.5 Hz, 6`-H), 6.99 (ddd, 1H, *J* = 0.4, 1.2, 8.1 Hz, 3`-H), 6.98 (ddd, 1H, *J* = 1.2, 7.4, 7.5 Hz, 5`-H), 6.65 (s, 2H, 2,6-H), 5.6 (s, 1H, OH), 5.35 (s, 1H, OH), 3.92 (s, 6H, OMe).

^{13}C-NMR (150 MHz, $CDCl_3$, TMS) 152.46 (C-2`), 147.65 (C-3,5), 134.52 (C-4), 129.99 (C-6`), 129.04 (C-4`), 128.18 (C-1`), 127.81 (C-1), 120.67 (C-5`), 115.6 (C-3`), 105.67 (C-2,6), 56.39 (OMe)

C.4 Synthesis of Aucuparin and noraucuparin

C.4.1 Synthesis of 3,4,5-trimethxoybiphenyl

A mixture of 3,4,5-trimethxoybenzene (5.14 g, 20.8 mmol), tetrakis (triphenylphosphine palladium (1.5 g) were stirred in toluene (75 ml), under stream of argon gas. A solution of Na_2CO_3 (4M, 15 ml) was added drop wise. Then, phenylboronic acid (2.7 g, 22 mmol, an ethanolic solution) was added drop wise. The reaction was refluxed for 2 h at 80°C. After that, the reaction was cooled to RT and the reaction was stopped by the addition of hydrogen peroxide (6 ml) and left stirring for 60 min. The product mixture was filtered and washed with NaOH (2×30 ml). The organic phase was passed through Na_2SO_4 and evaporated to dryness. The reaction product was purified by silica gel CC and CH_2Cl_2 as eluent. The yield was 60% (3 g, 12.3 mmol). The spectroscopic properties were identical to published data (Hüttner et al., 2010).

C4.2 Synthesis of aucuparin

Demethylation of 3,4,5-trimethoxybiphenyl (400 mg, 1.64 mmol) was carried out using magnesium iodide etherate solution (30 × equivalent), as described before (synthesis of eriobofuran). It was freshly prepared from I_2 (12.48g, 49.17 mmol) and Mg powder (2.4 g, 0.098 mol). The solutions of both reactants in diethyl ether were mixed and evaporated to dryness. The residue was heated on an oil bath at 80°C for 11 h, under a stream of argon gas and protected from light. The residue was dissolved in water and $Na_2S_2O_3$ was added to remove I_2. The solution was acidified and extracted with CH_2Cl_2 (2 x 50 ml). The organic layer was washed with $NaHCO_3$ solution (1 x 100 ml) and with brine solution (1 x 100 ml) and dried over anhydrous Na_2SO_4. The concentrated residue was purified by silica gel CC and CH_2Cl_2 as eluent. The yield was 76.9% (290 mg, 1.26 mmol) and the spectroscopic properties were identical to published data (Hüttner et al., 2010).

C.4.3 Synthesis of noraucuparin

Aucuparin (240 mg, 1.04 mmol) was dissolved in 10 ml CH_2Cl_2. Cold (4 °C) BBr_3 solution (1 ml, 1 M in CH_2Cl_2) was added. Then, a $CaCl_2$ filled drying tube is attached to keep out moisture. The reaction mixture was stirred at room temperature for 3 h. Then additional BBr_3 solution (0.5 ml, 1 M in CH_2Cl_2) was added and the reaction was continued for another 3 hrs. The reaction was stopped by the drop wise addition of water. The reaction product was acidified with aqueous HCl (5 %). The organic layer was separated and the aqueous layer was further extracted with CH_2Cl_2 (2 x 10 ml). The organic layer was evaporated and noraucuparin was isolated by silica gel CC using CH_2Cl_2 as eluent to yield 100 mg (0.46 mmol, 45%). The spectroscopic properties were identical to published data (Hüttner et al., 2010).

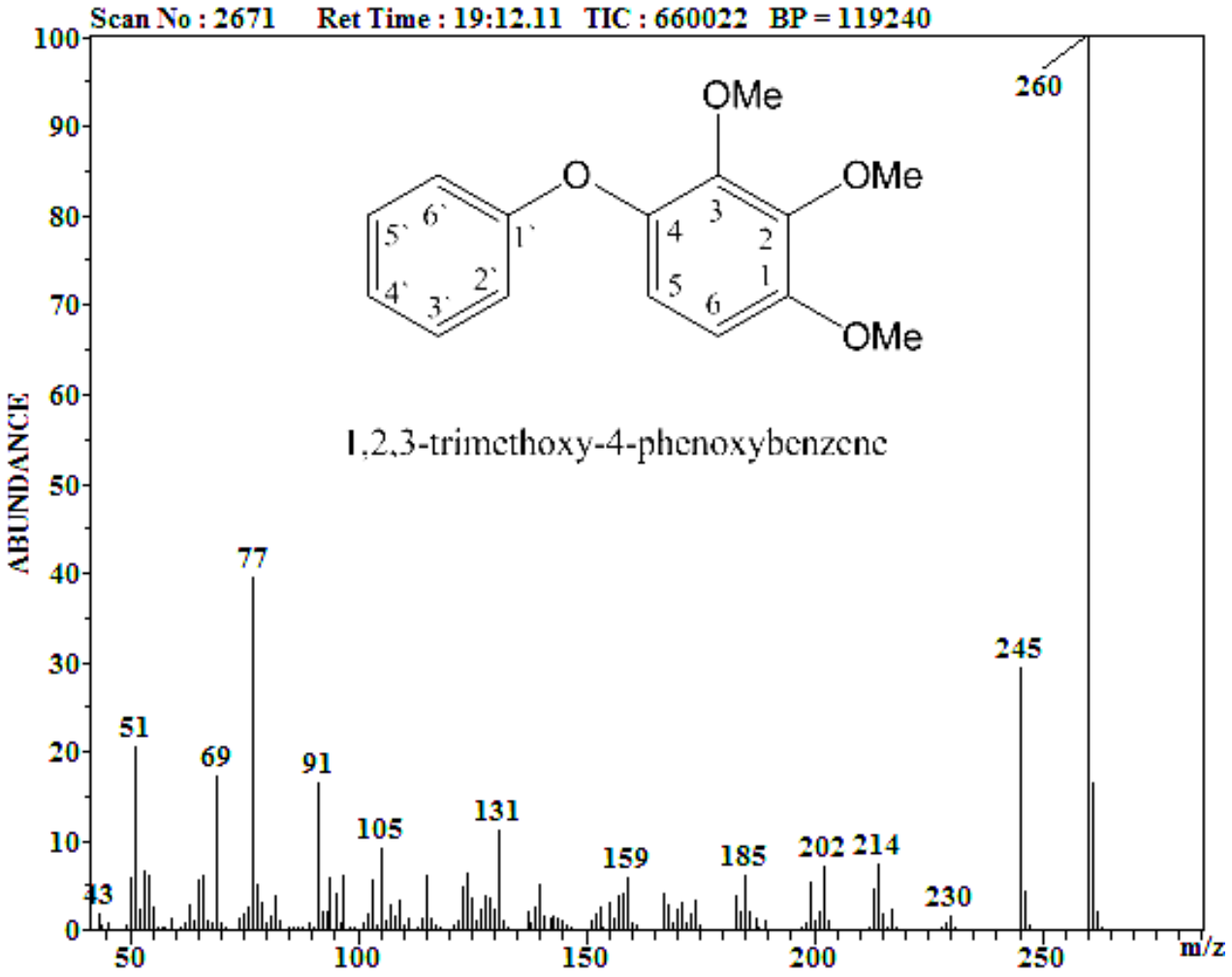

Figure A.1: Mass spectrum of 1,2,3-trimethoxy-4-phenoxybenzene.

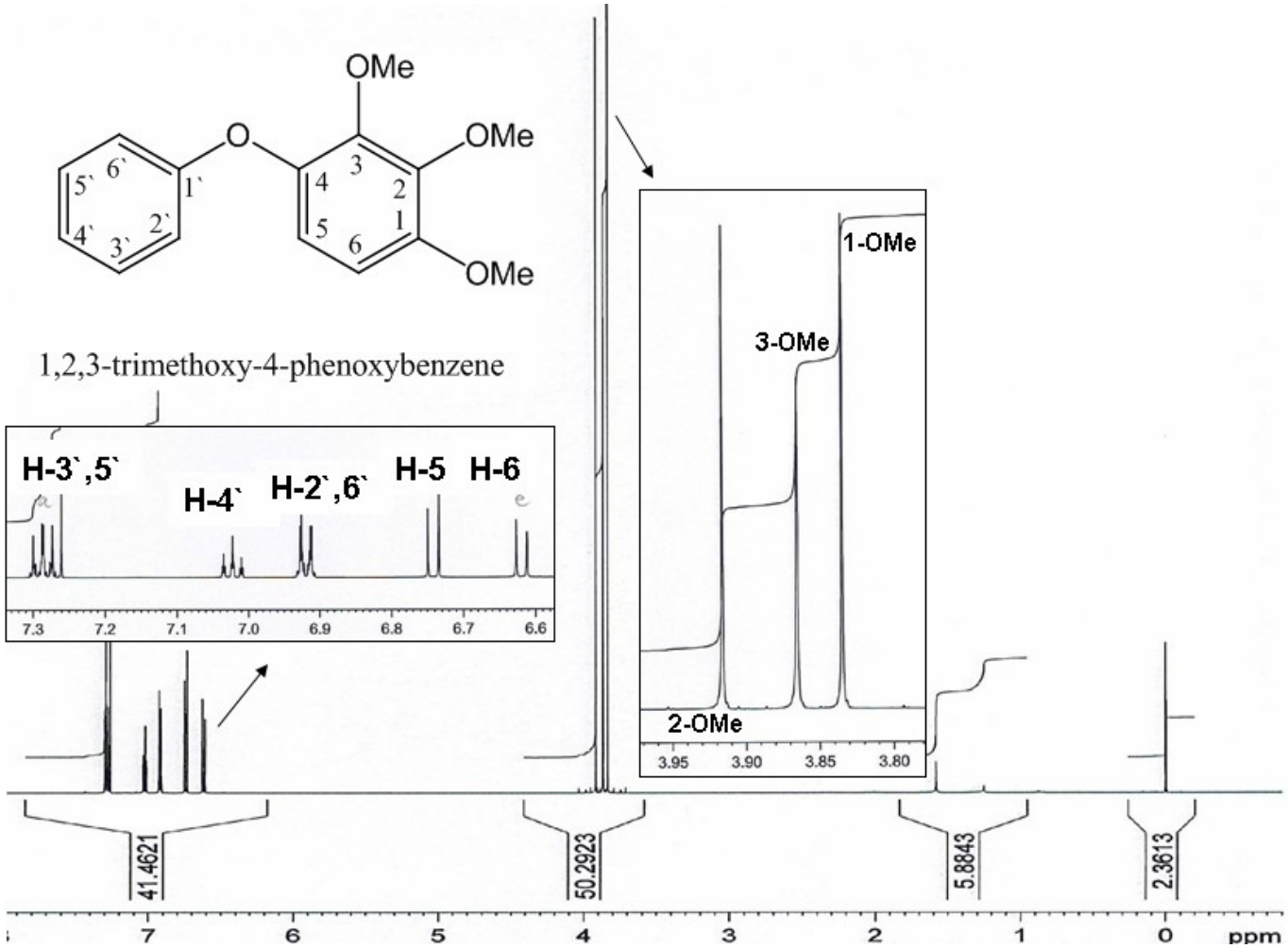

Figure A.2: [1]H-NMR of 1,2,3-trimethoxy-4-phenoxybenzene

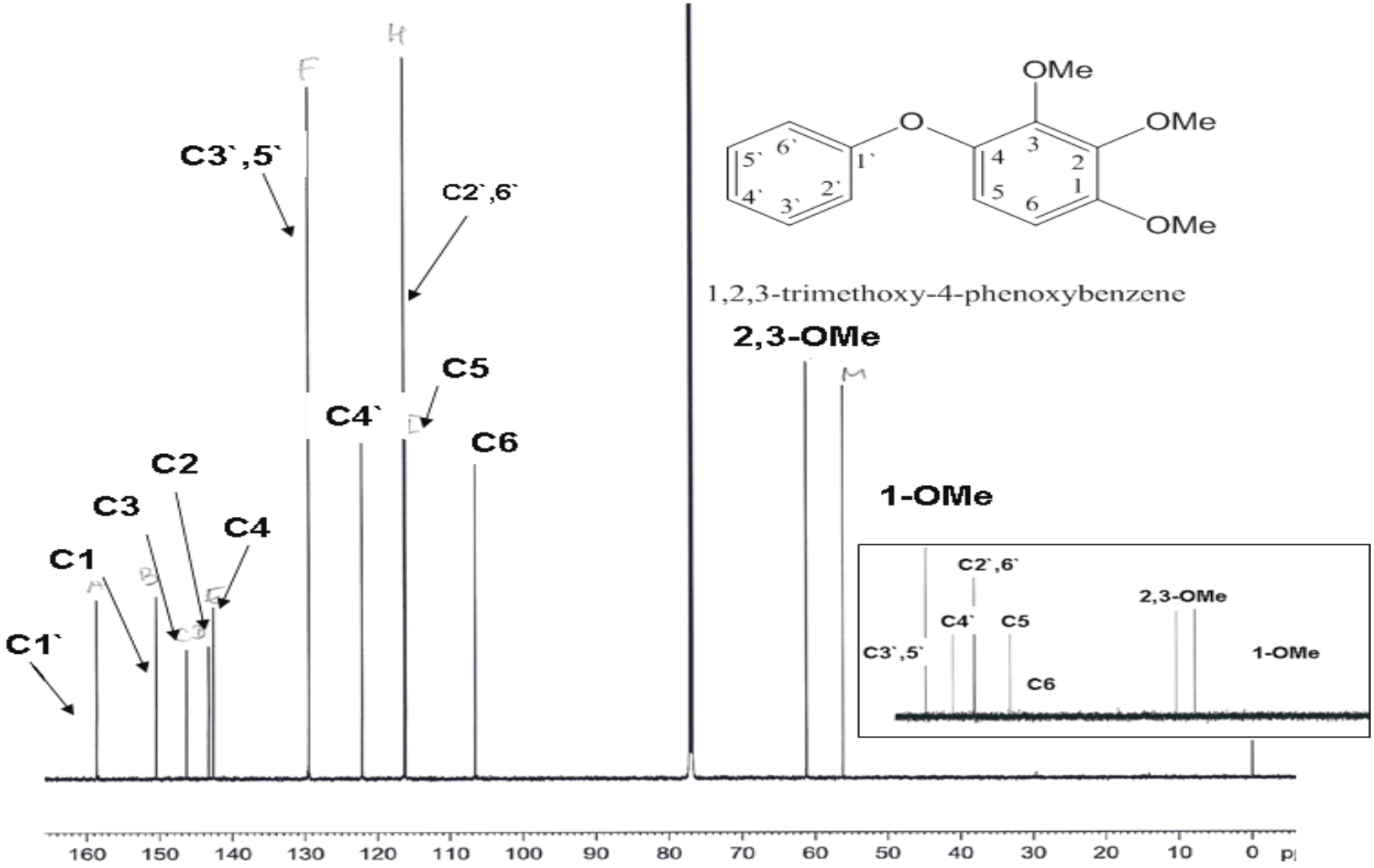

Figure A.3: ^{13}C-NMR and ^{13}C-DEPT 135 of 1,2,3-trimethoxy-4-phenoxybenzene

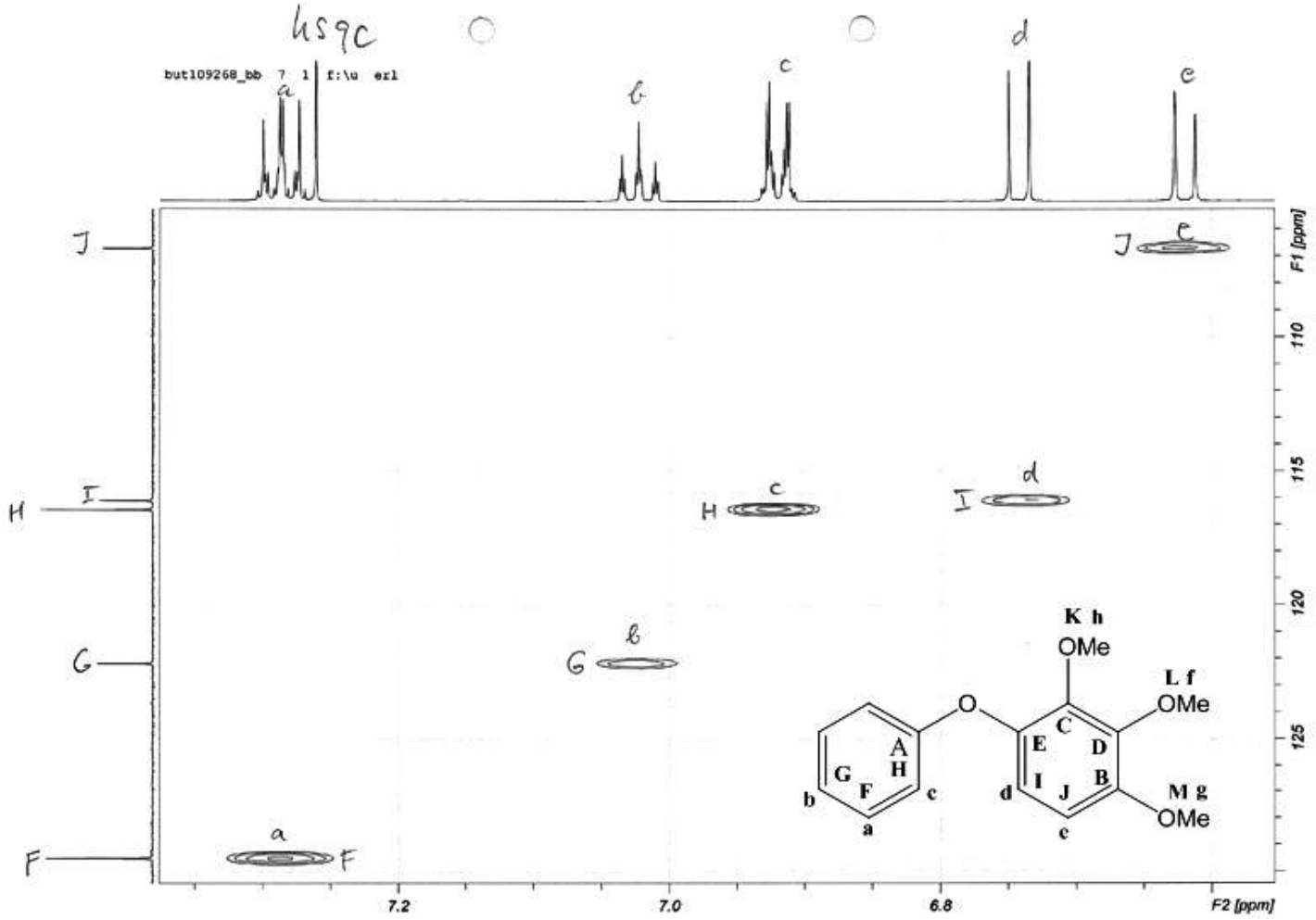

Figure A.4: HSQC spectrum of 1,2,3-trimethoxy-4-phenoxybenzene

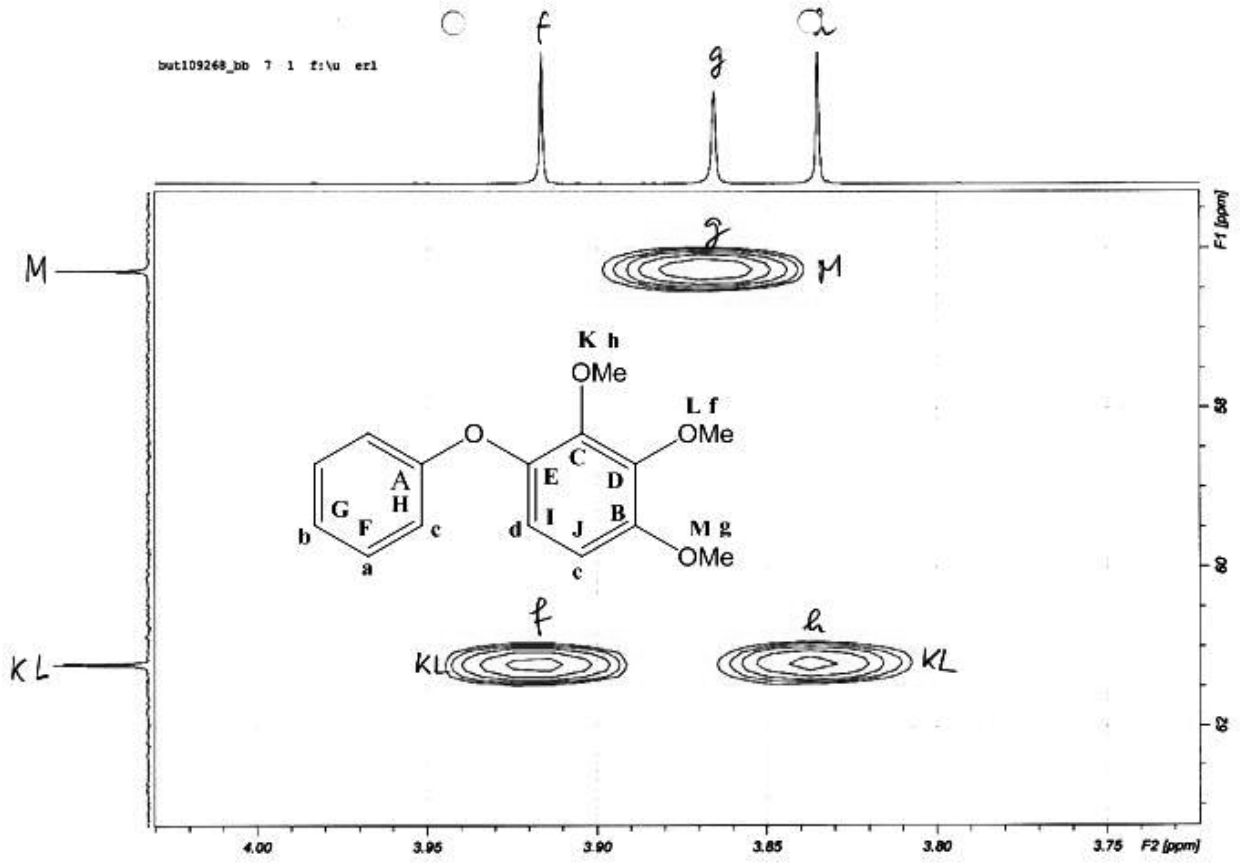

Figure A.5: HSQC spectrum of 1,2,3-trimethoxy-4-phenoxybenzene displaying the assignment of the methoxy groups.

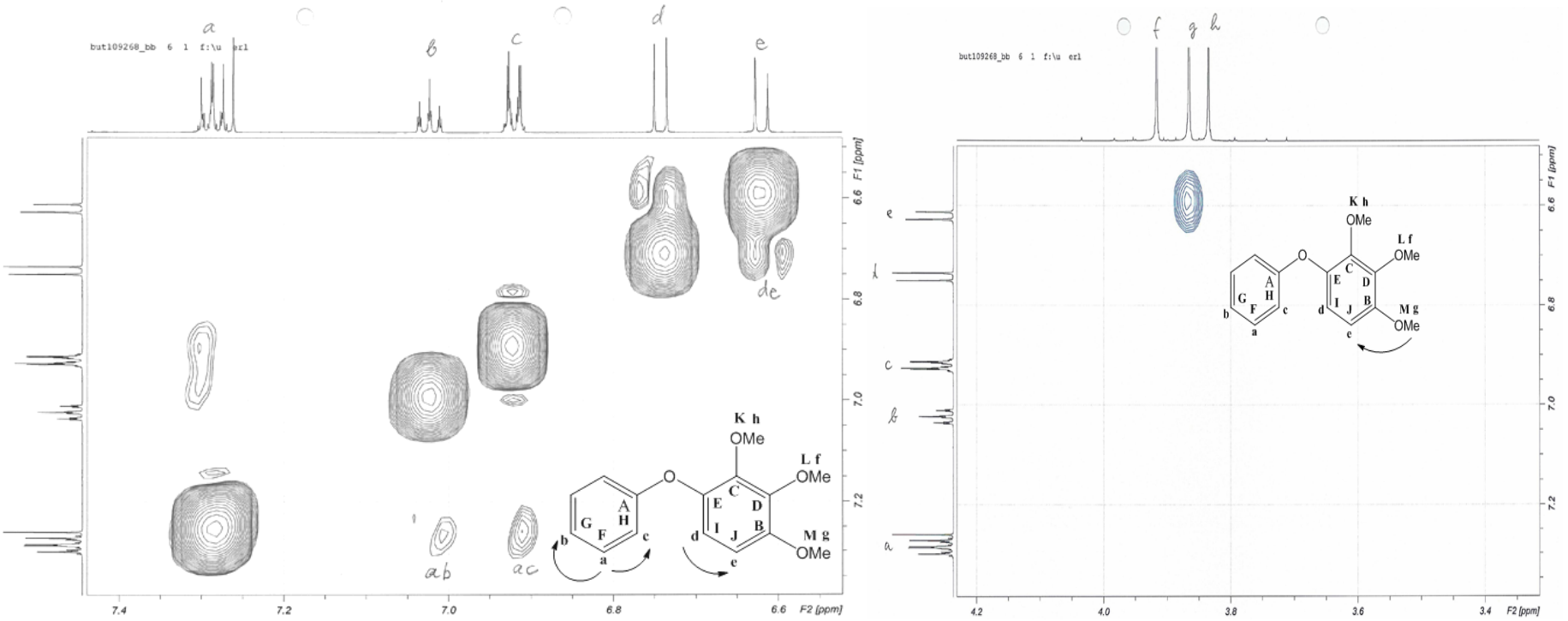

Figure A.6: NOESY spectrum of 1,2,3-trimethoxy-4-phenoxybenzene.

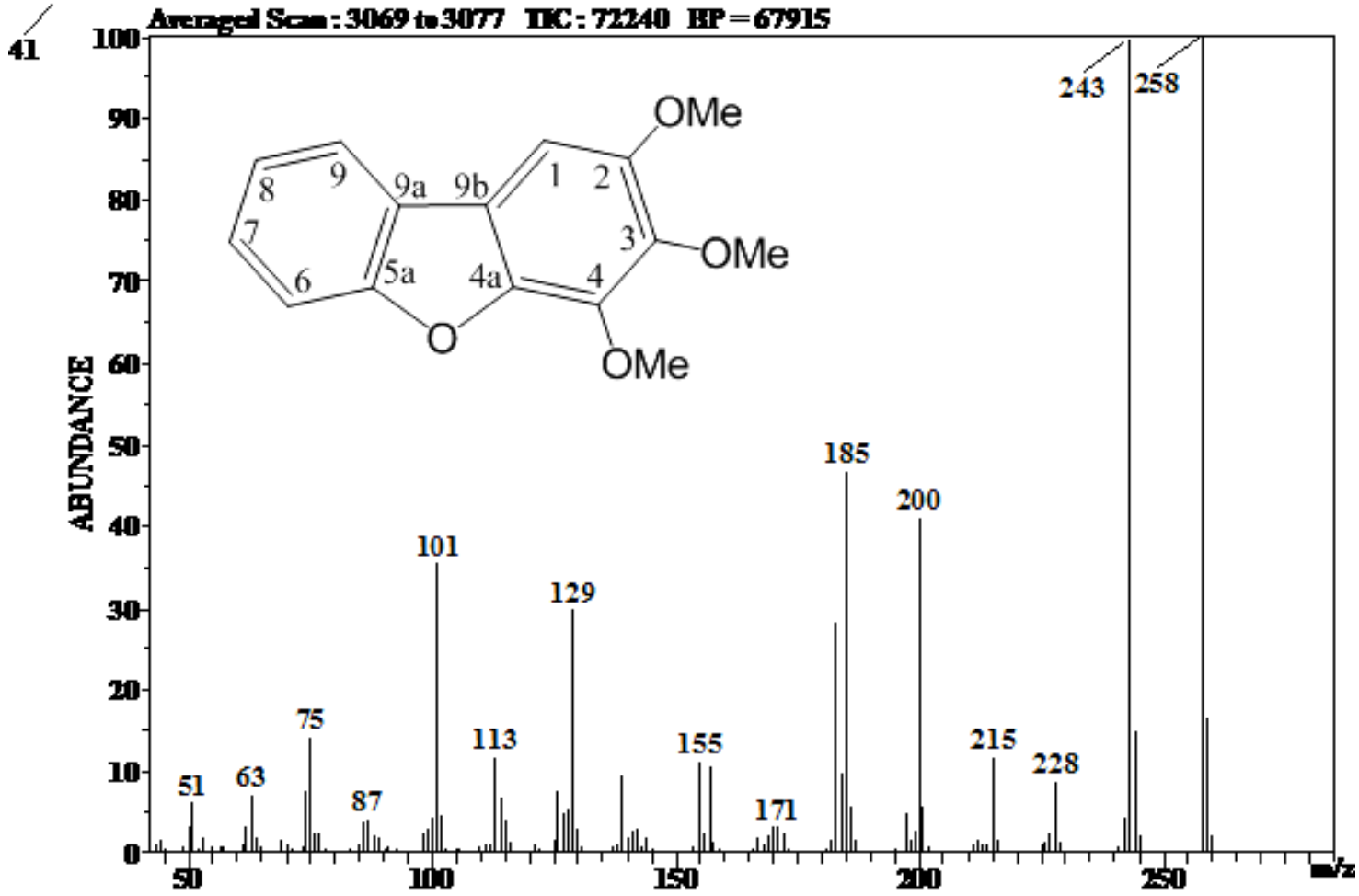

Figure A.7: Mass spectrum of 2,3,4-trimethoxydibenzofuran.

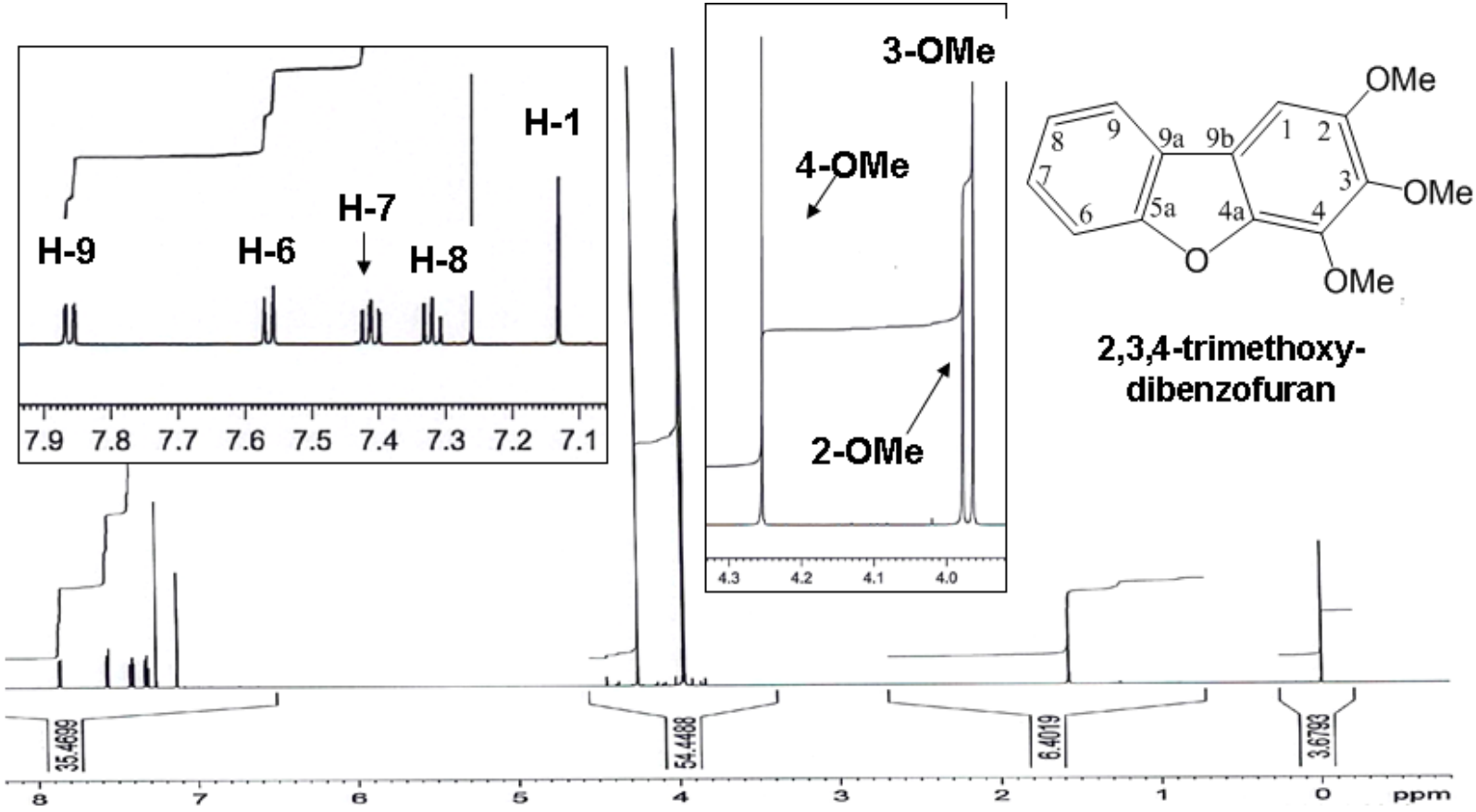

Figure A.8: [1]H-NMR of 2,3,4-trimethoxydibenzofuran.

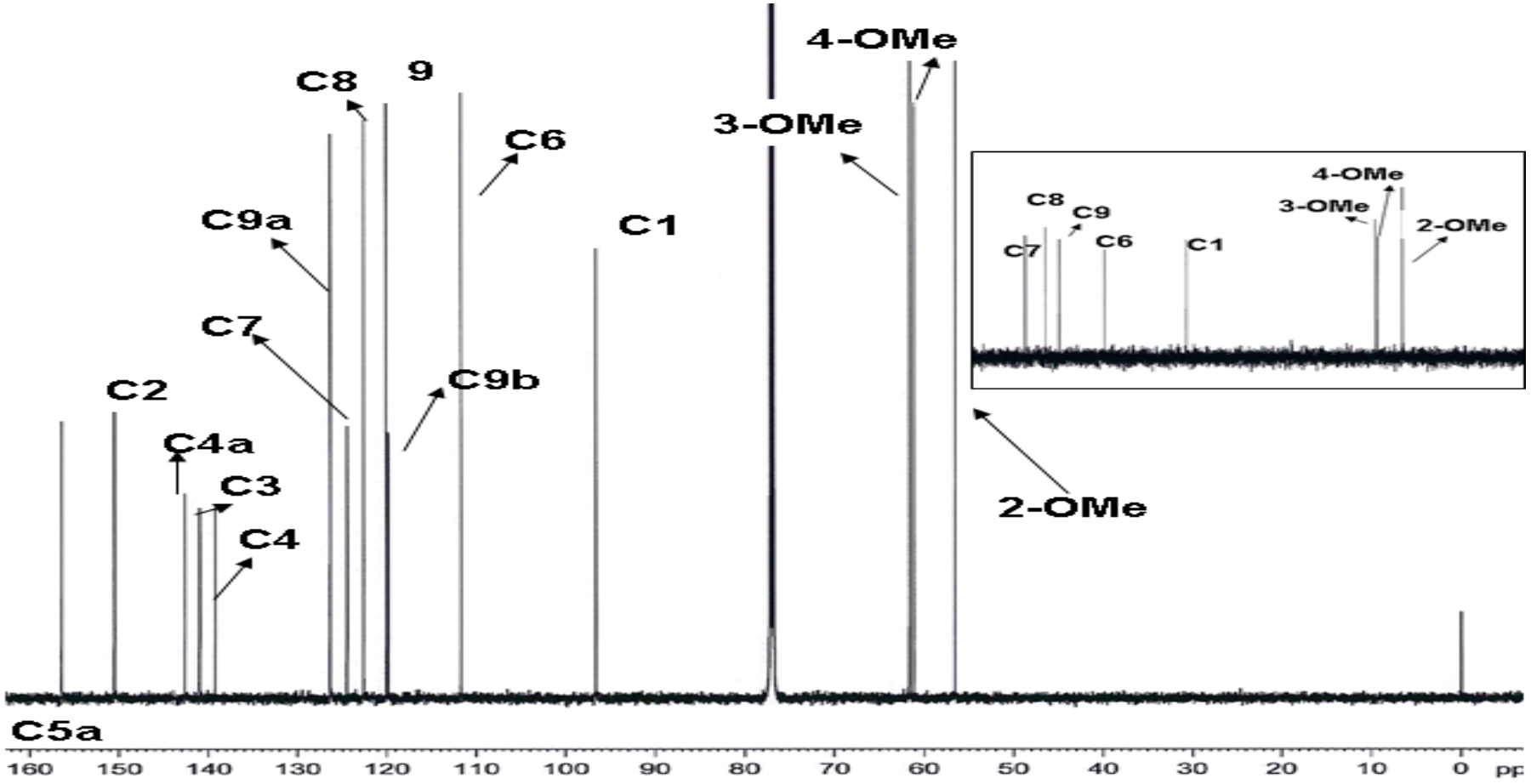

Figure A.9: ^{13}C-NMR and ^{13}C-DEPT 135 of 2,3,4-trimethoxydibenzofuran.

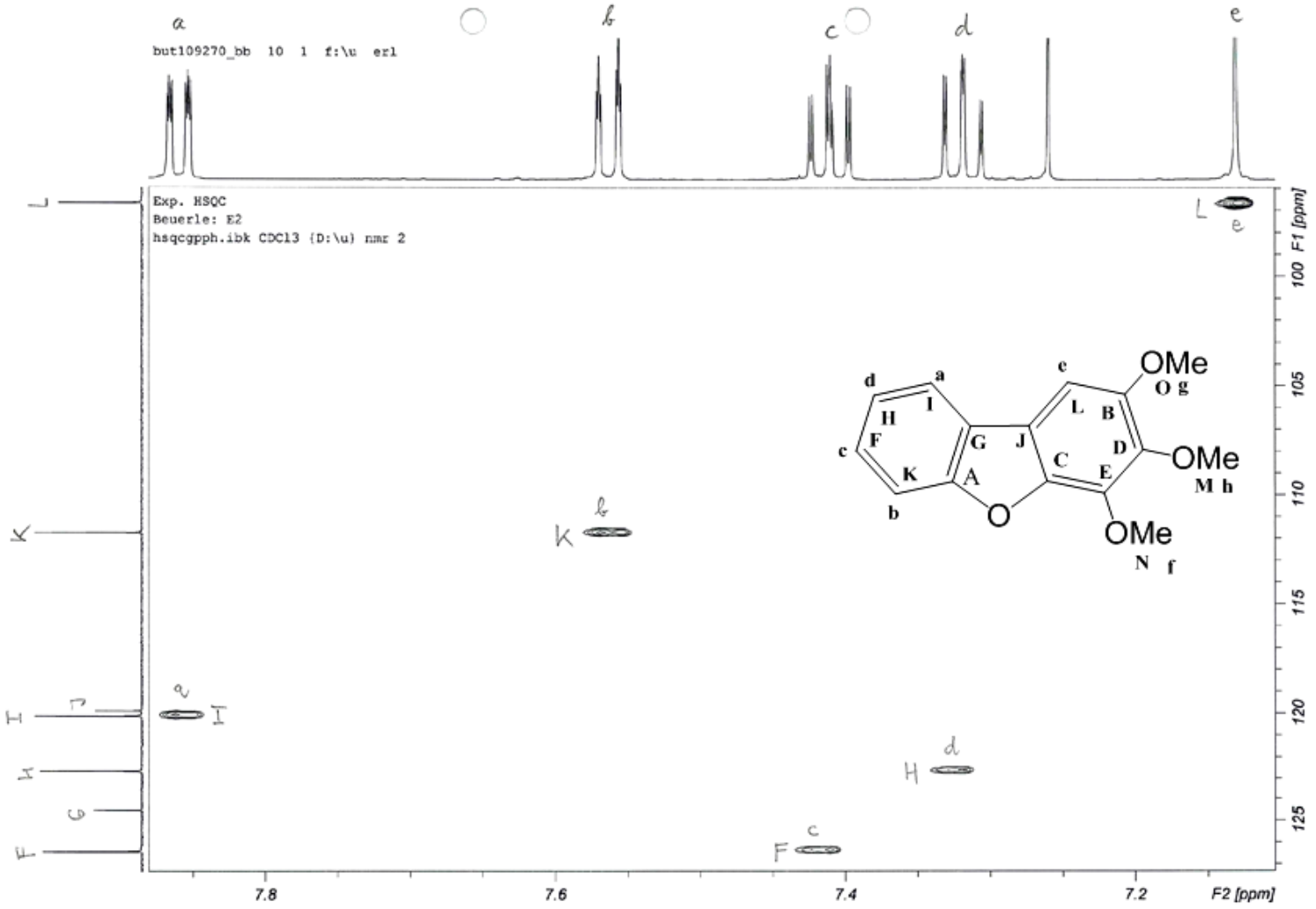

Figure A.10: HSQC spectrum of 2,3,4-trimethoxydibenzofuran.

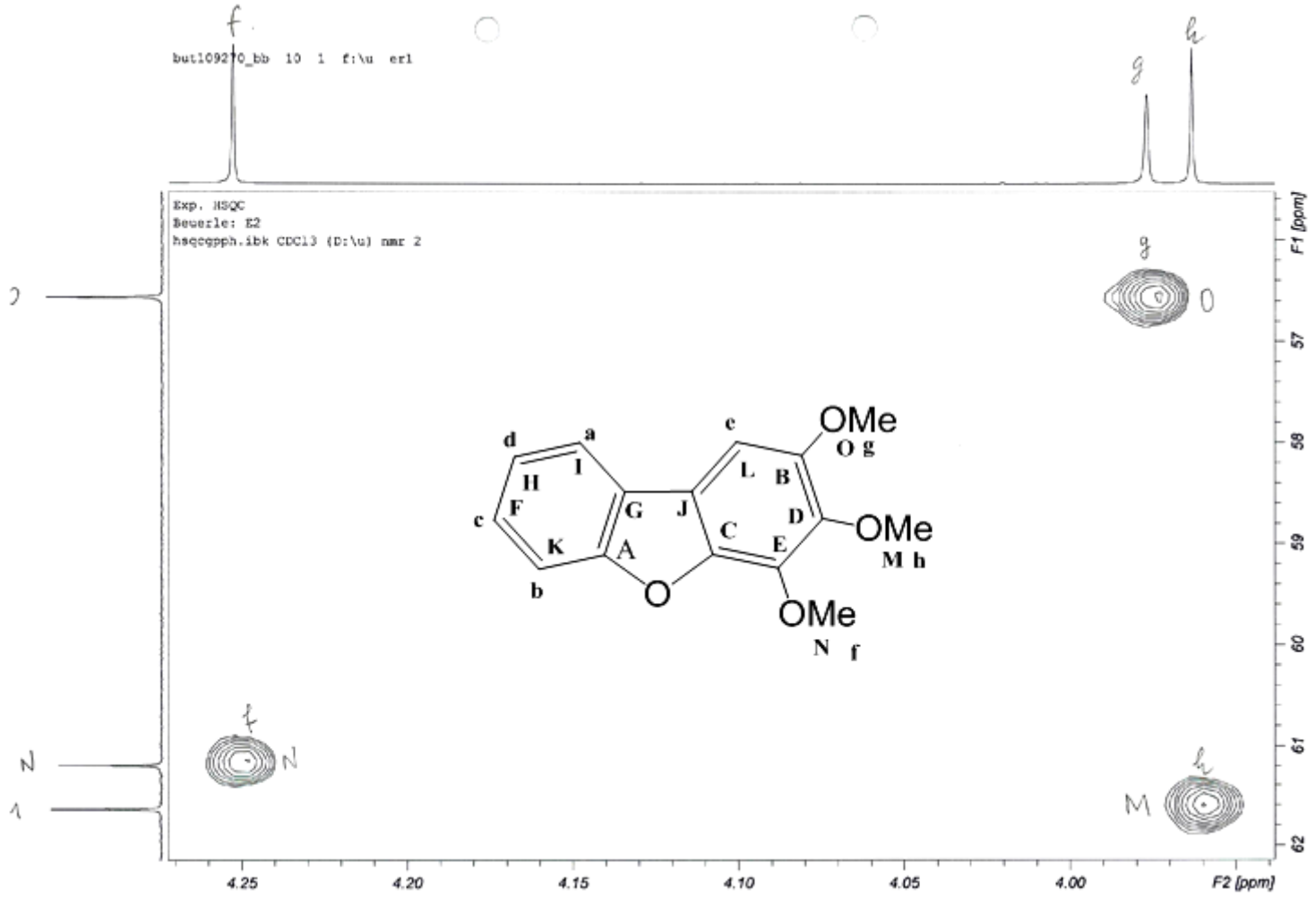

Figure A.11: HSQC spectrum of 2,3,4-trimethoxydibenzofuran displaying the assignment of the methoxy groups.

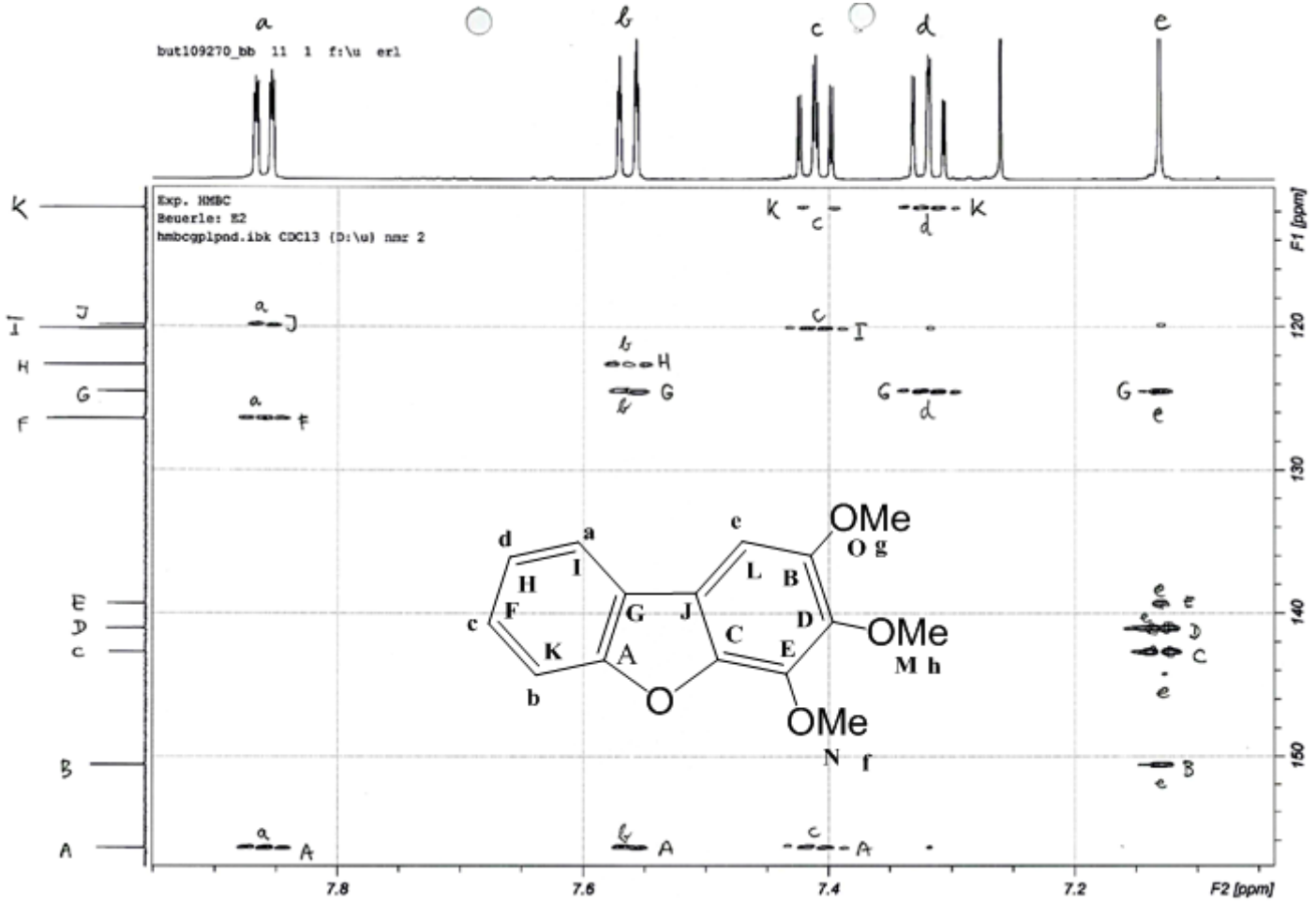

Figure A.12: HMBC spectrum of 2,3,4-trimethoxydibenzofuran.

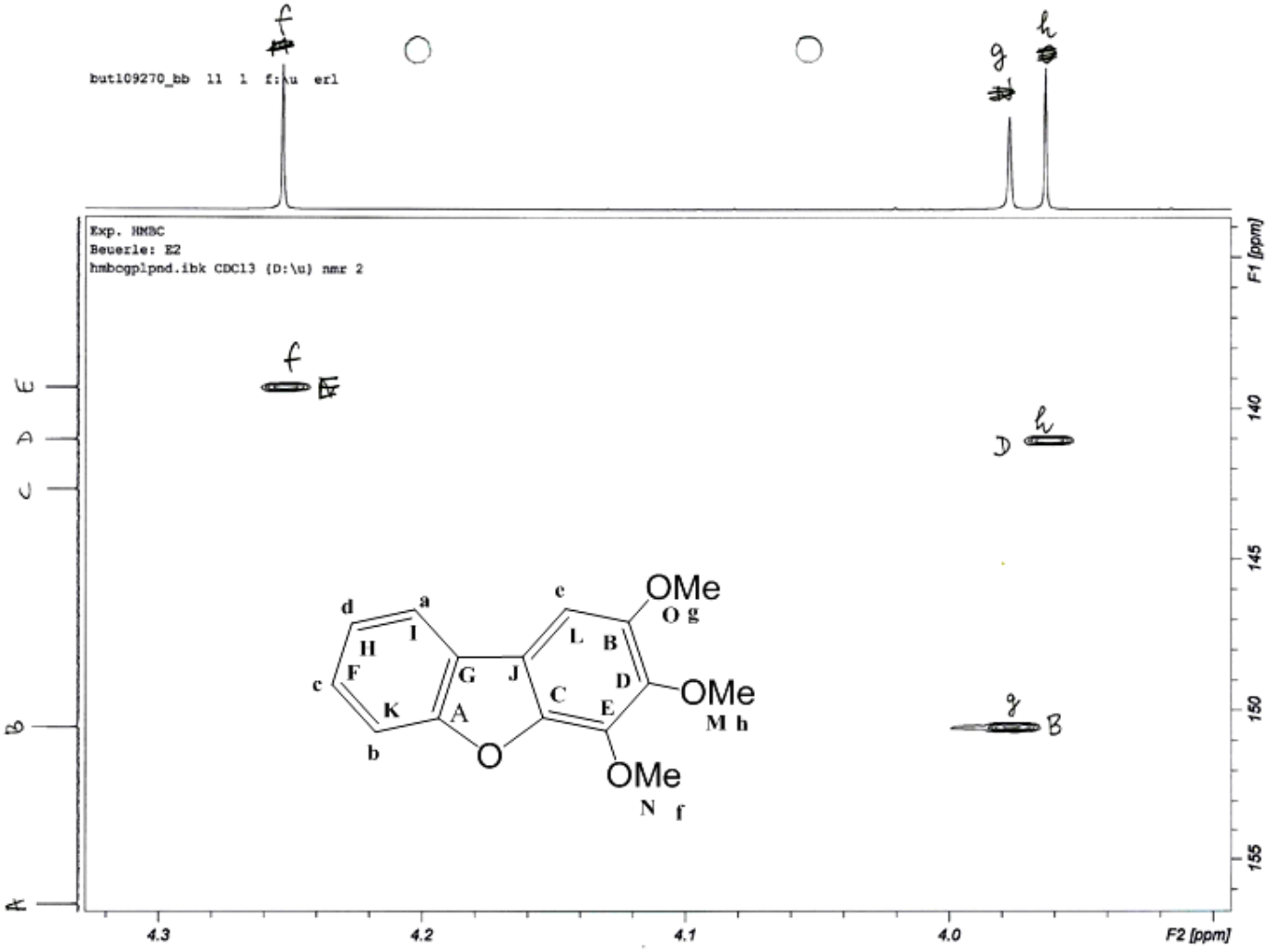

Figure A.13: HMBC spectrum of 2,3,4-trimethoxydibenzofuran showing the coupling of the methoxy protons.

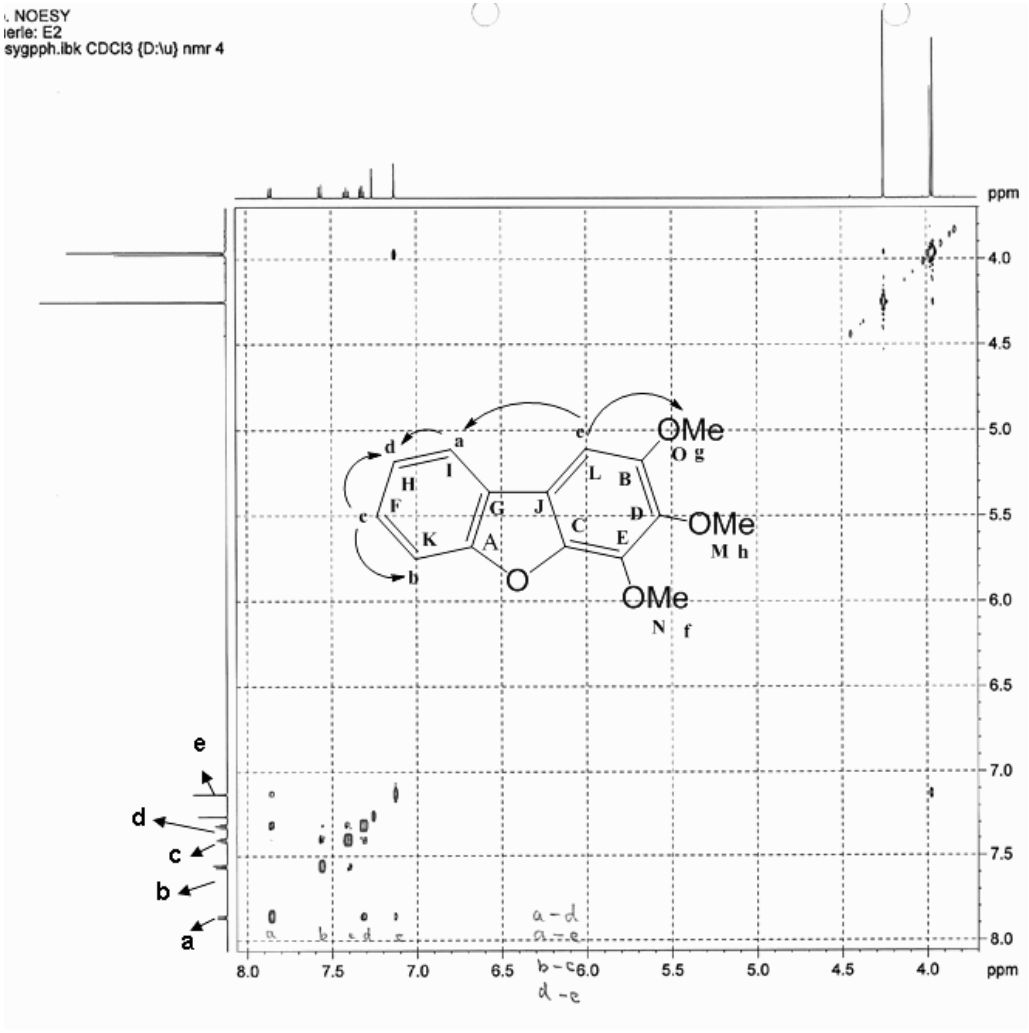

Figure A.14: NOESY spectrum of 2,3,4-trimethoxydibenzofuran.

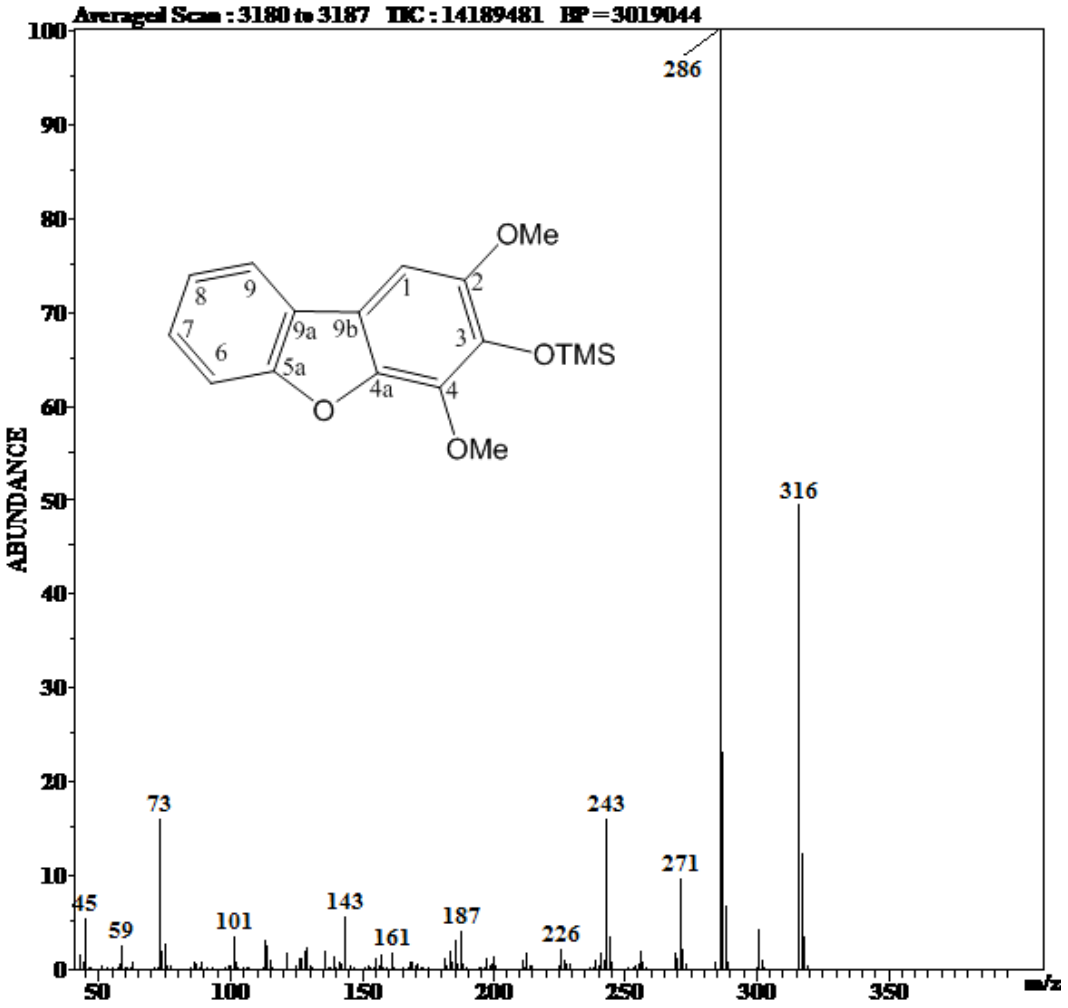

Figure A.15: Mass spectrum of silylated eriobofuran.

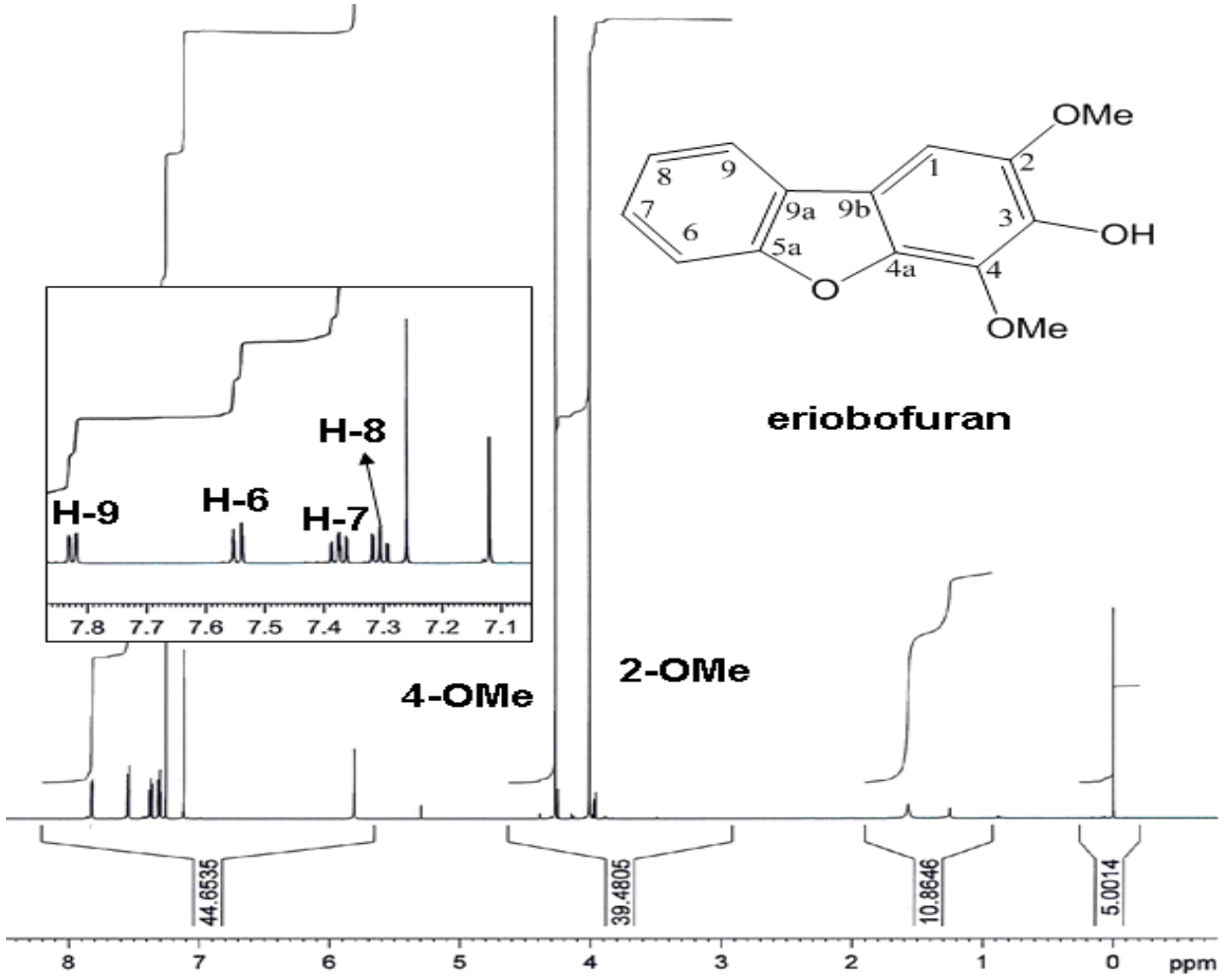

Figure A.16: ^{1}H-NMR of eriobofuran.

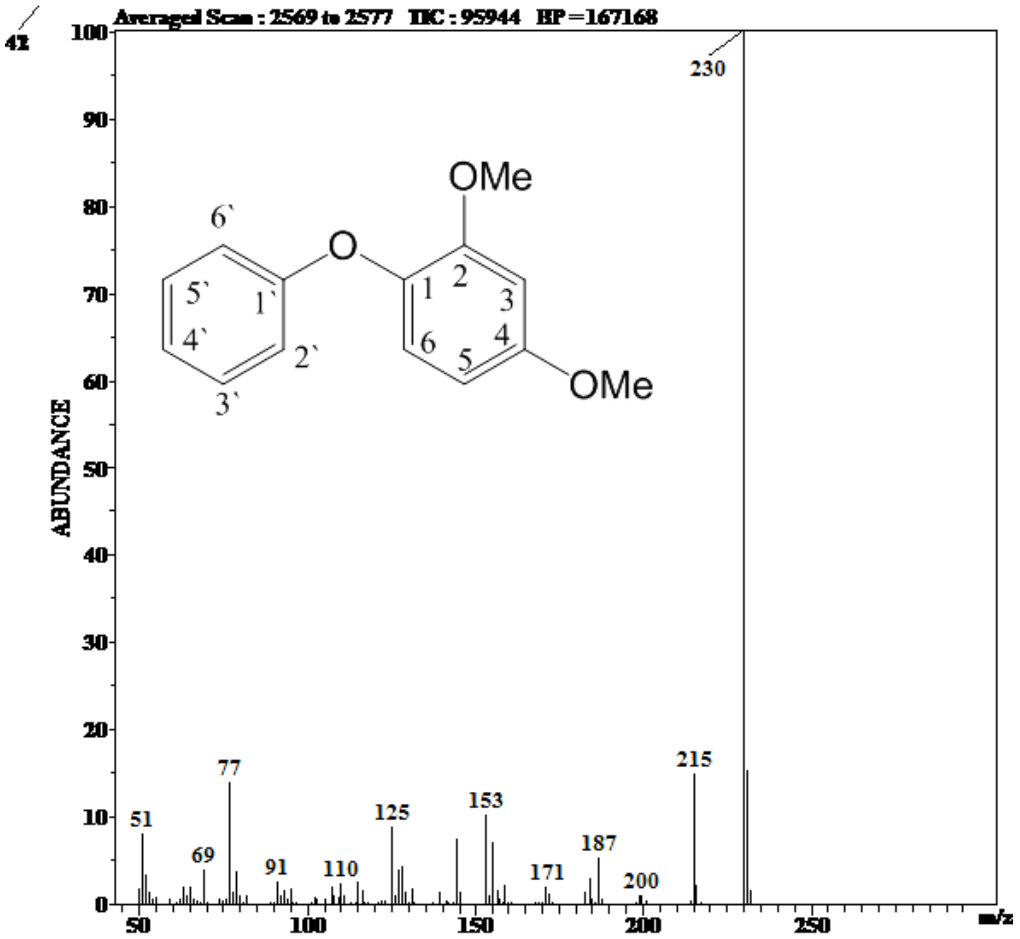

Figure A.17: Mass spectrum of 2,4-dimethoxy-1-phenoxybenzene.

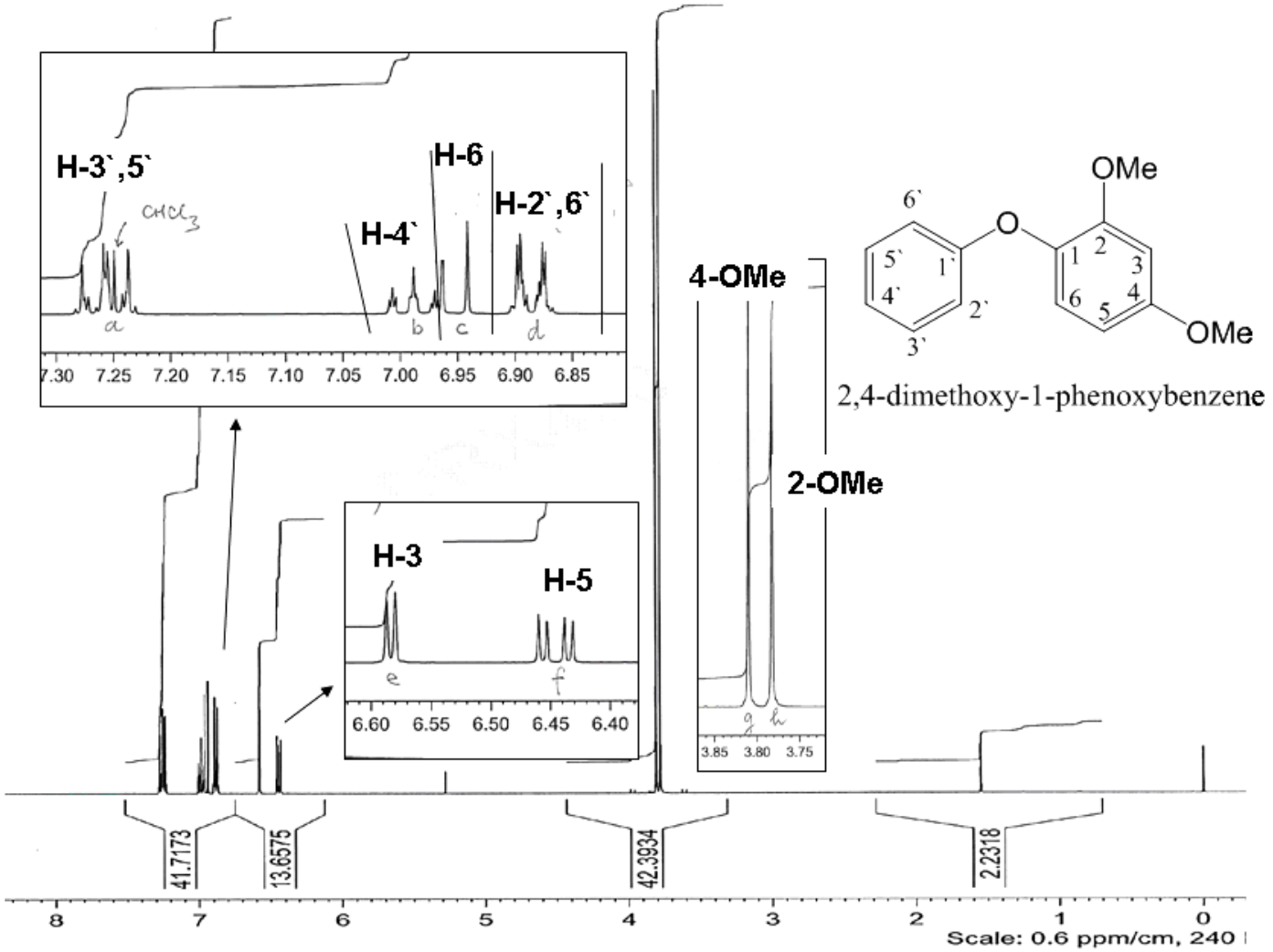

Figure A.18: ^{1}H-NMR of 2,4-dimethoxy-1-phenoxybenzene.

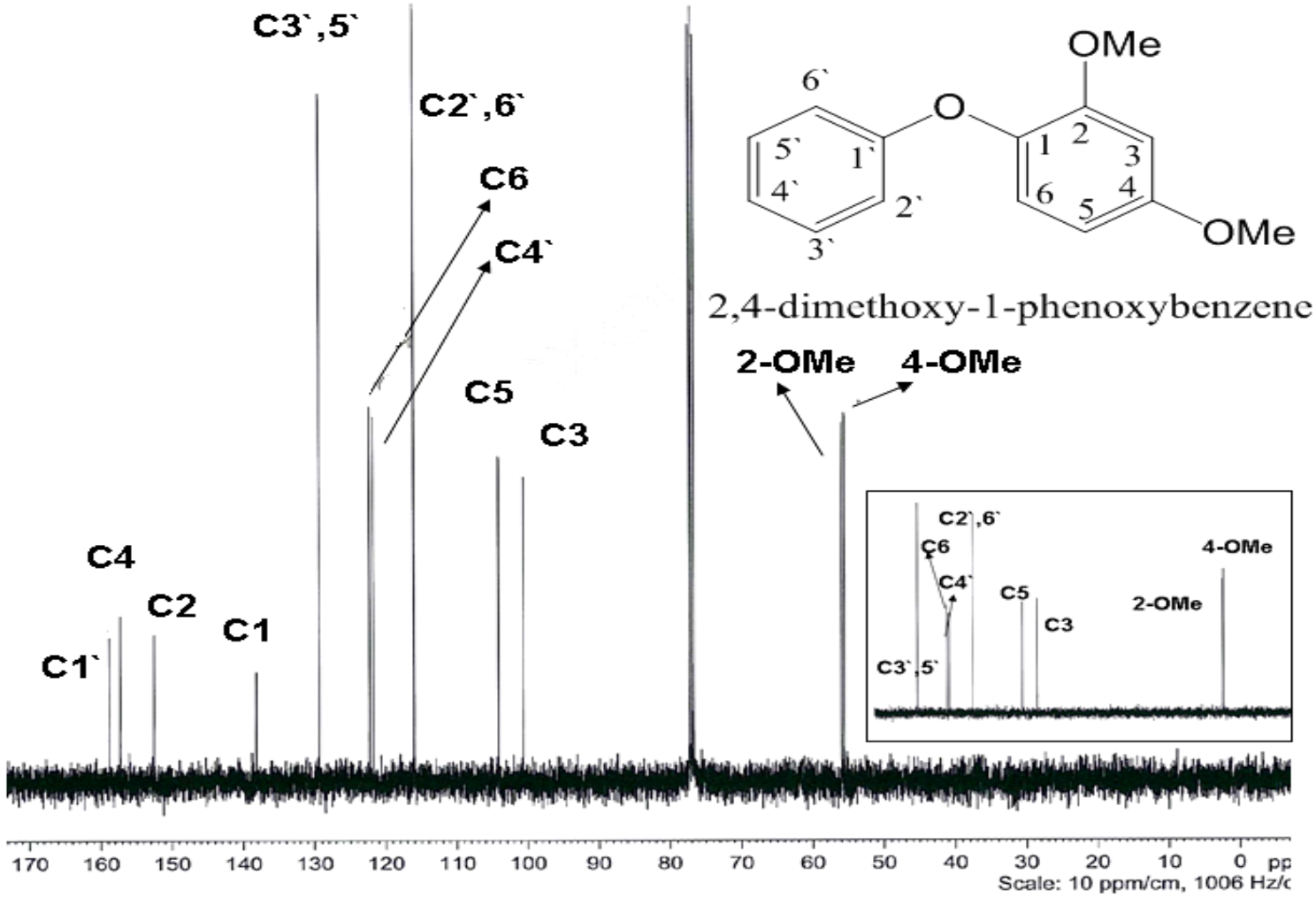

Figure A.19: ^{13}C-NMR and ^{13}C-DEPT 135 of 2,4-dimethoxy-1-phenoxybenzene.

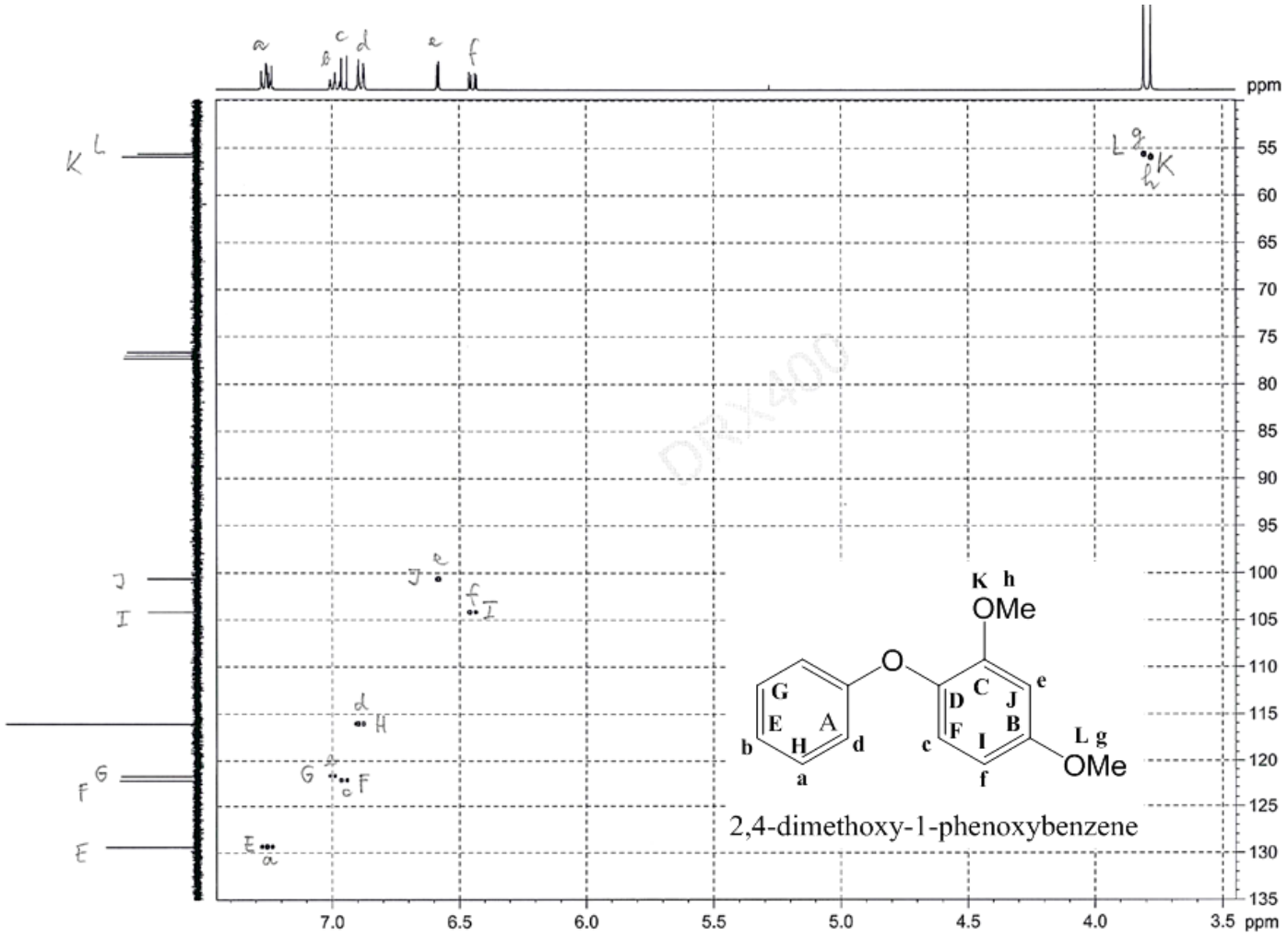

Figure A.20: HSQC spectrum of 2,4-dimethoxy-1-phenoxybenzene.

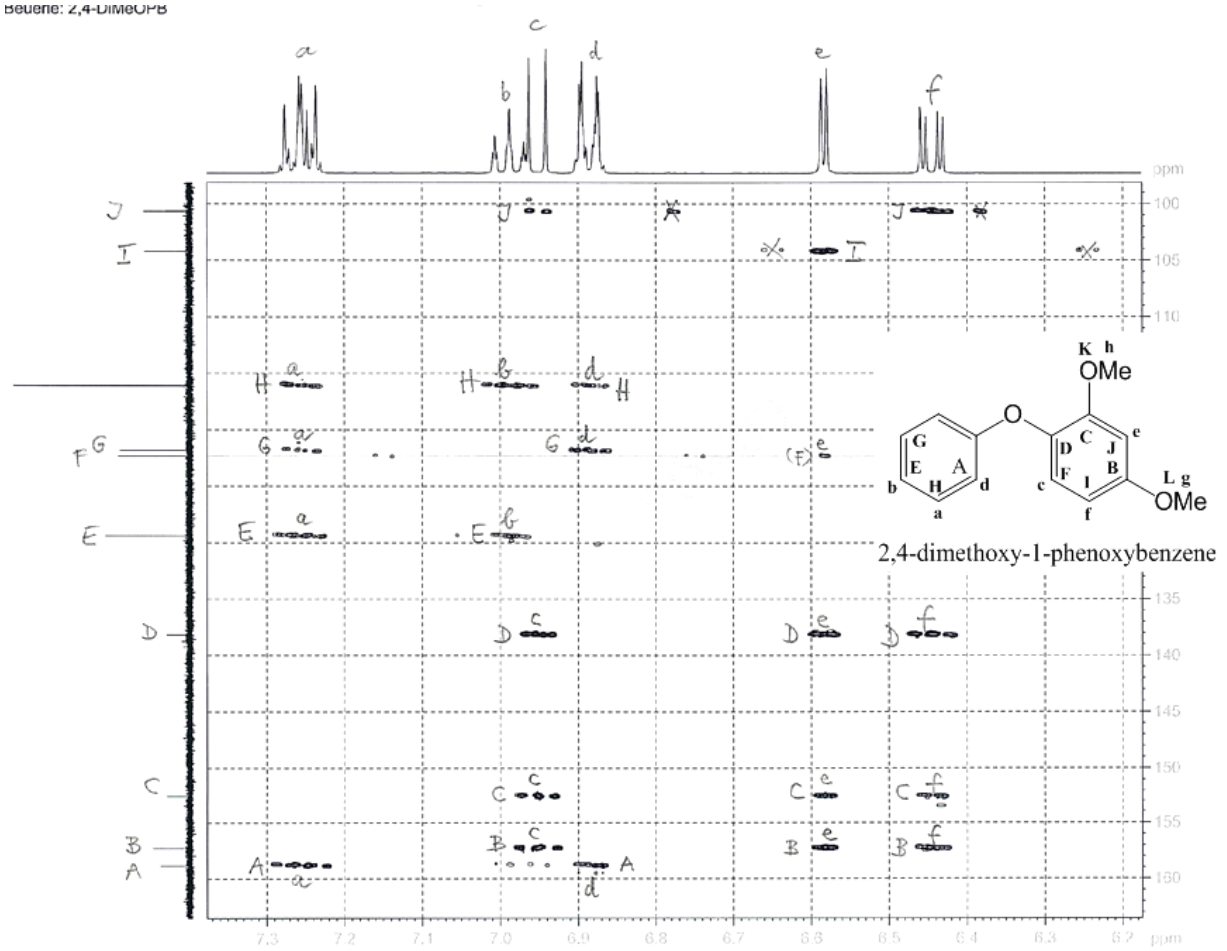

Figure A.21: HMBC spectrum of 2,4-dimethoxy-1-phenoxybenzene.

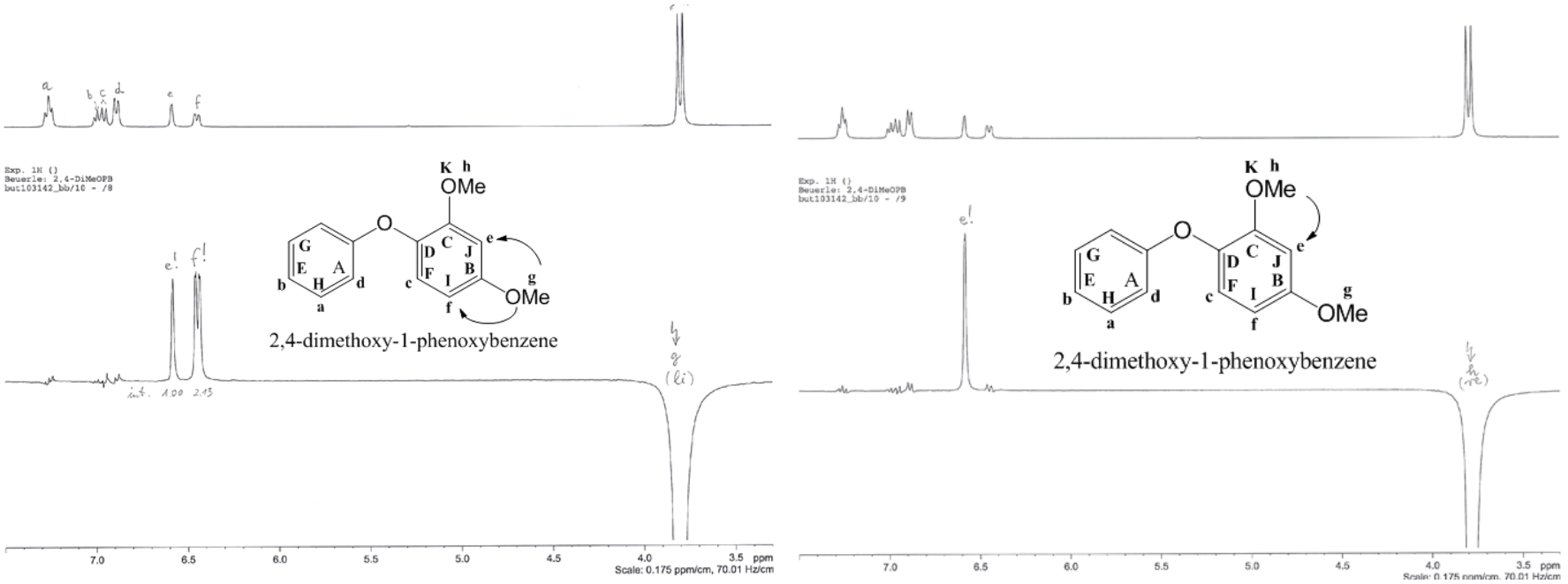

Figure A.22: NOESY spectrum of 2,4-dimethoxy-1-phenoxybenzene.

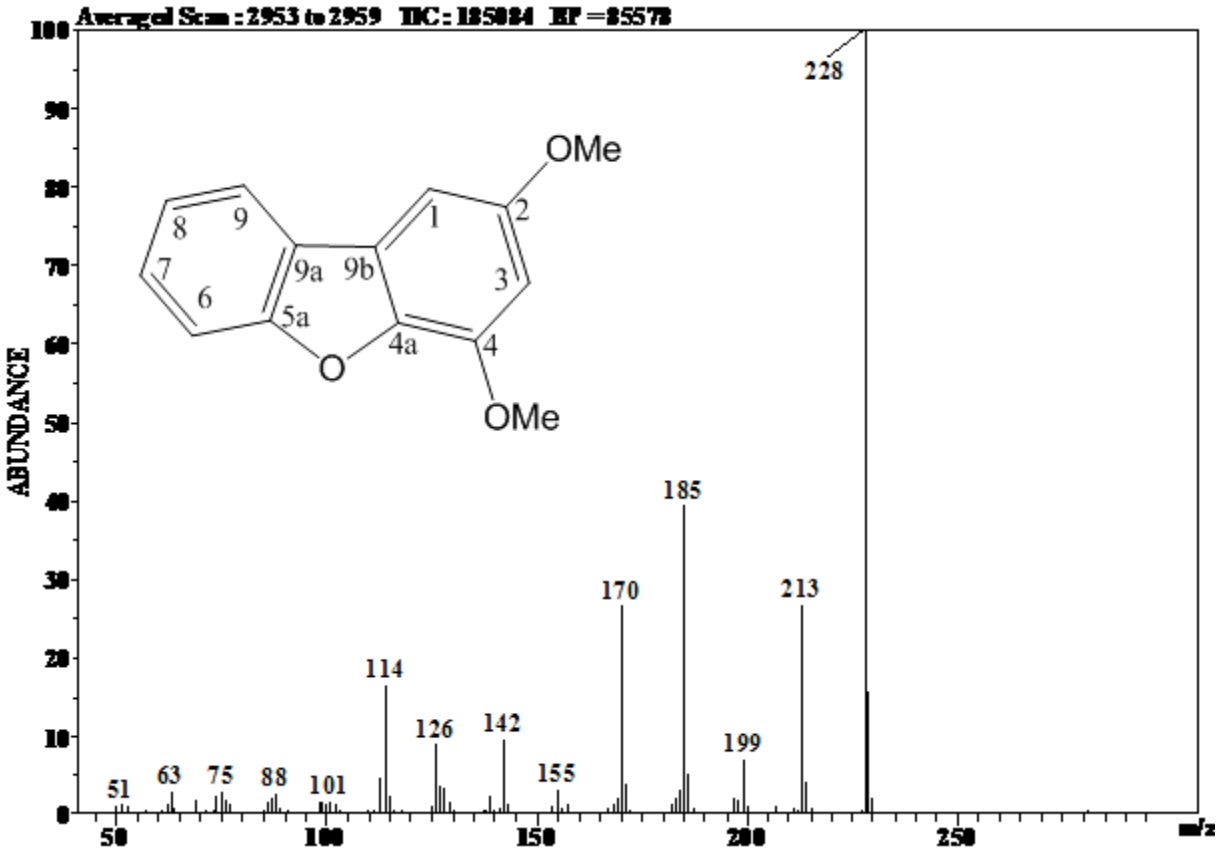

Figure A.23: Mass spectrum of 2,4-dimethoxydibenzofuran.

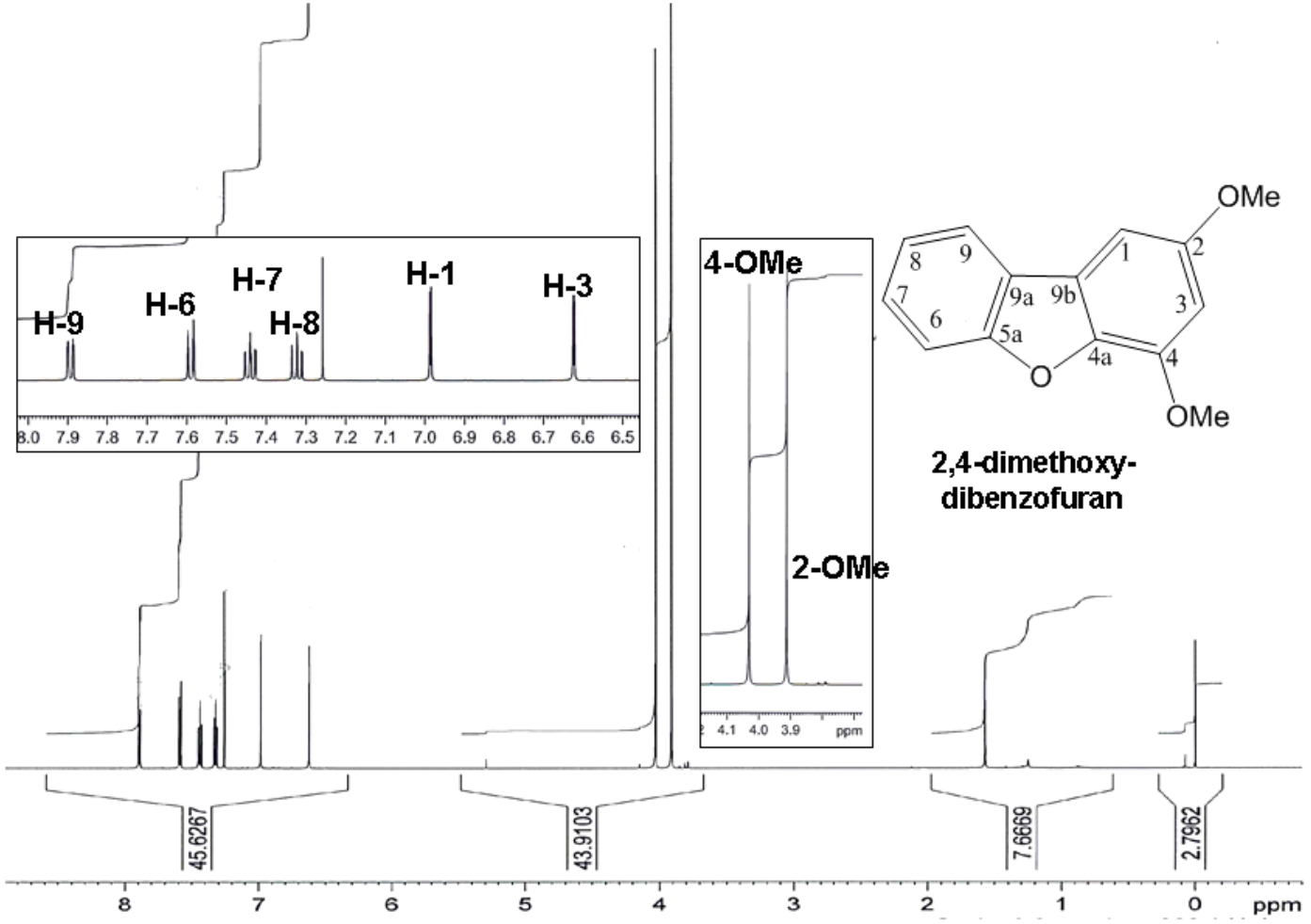

Figure A.24: ^{1}H-NMR of 2,4-dimethoxydibenzofuran.

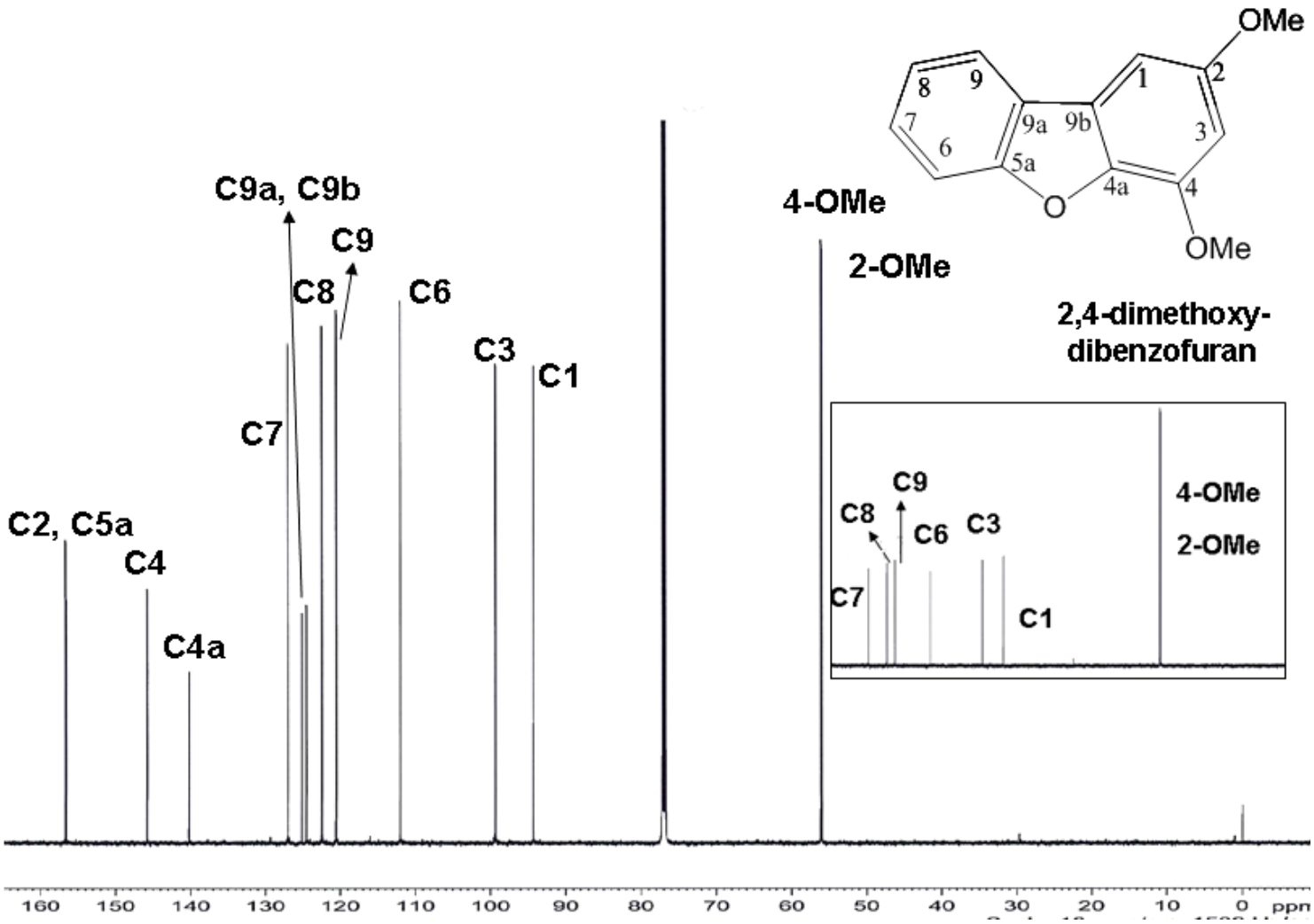

Figure A.25: ^{13}C-NMR and ^{13}C-DEPT 135 of 2,4-dimethoxydibenzofuran.

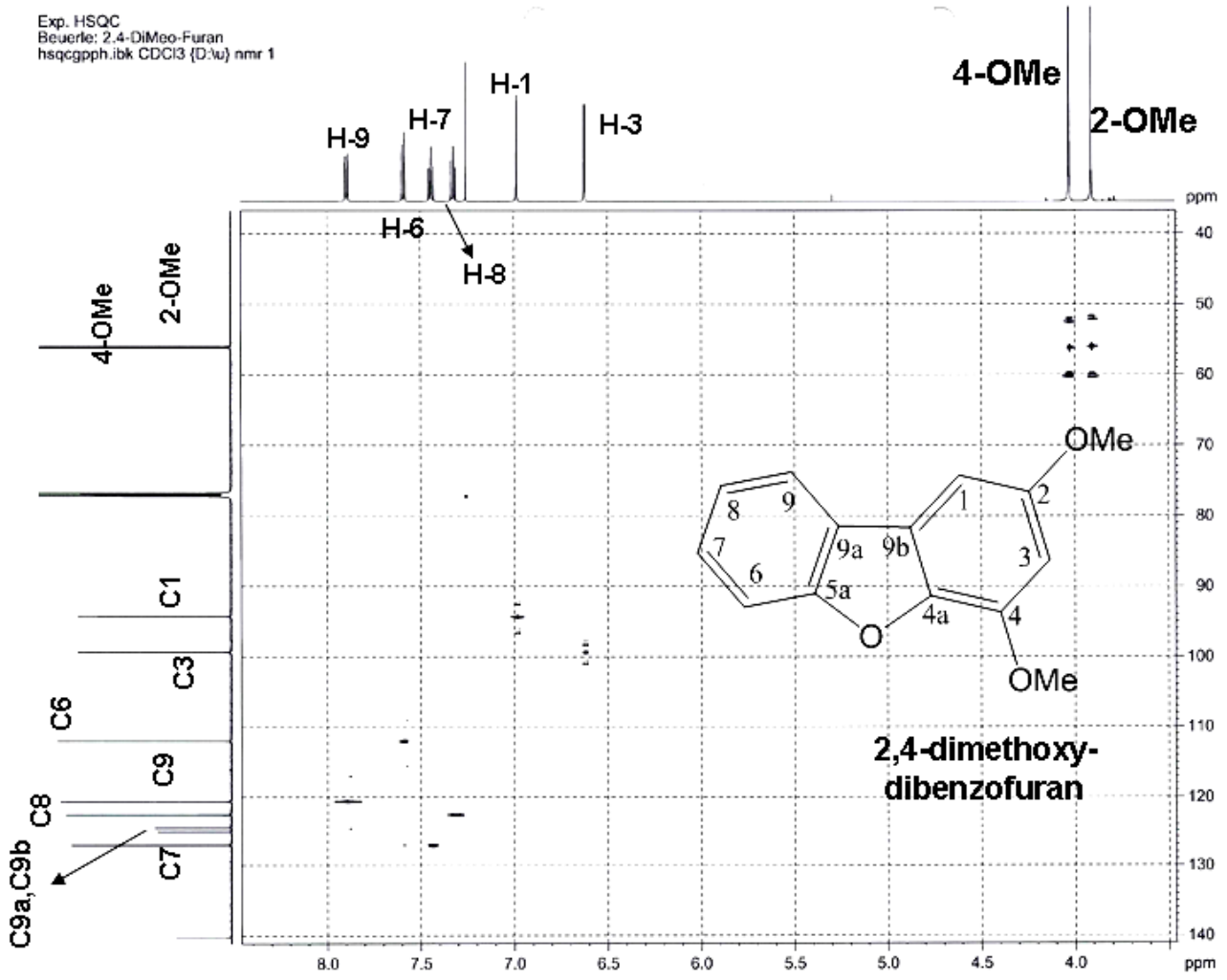

Figure A.26: HSQC spectrum of 2,4-dimethoxydibenzofuran.

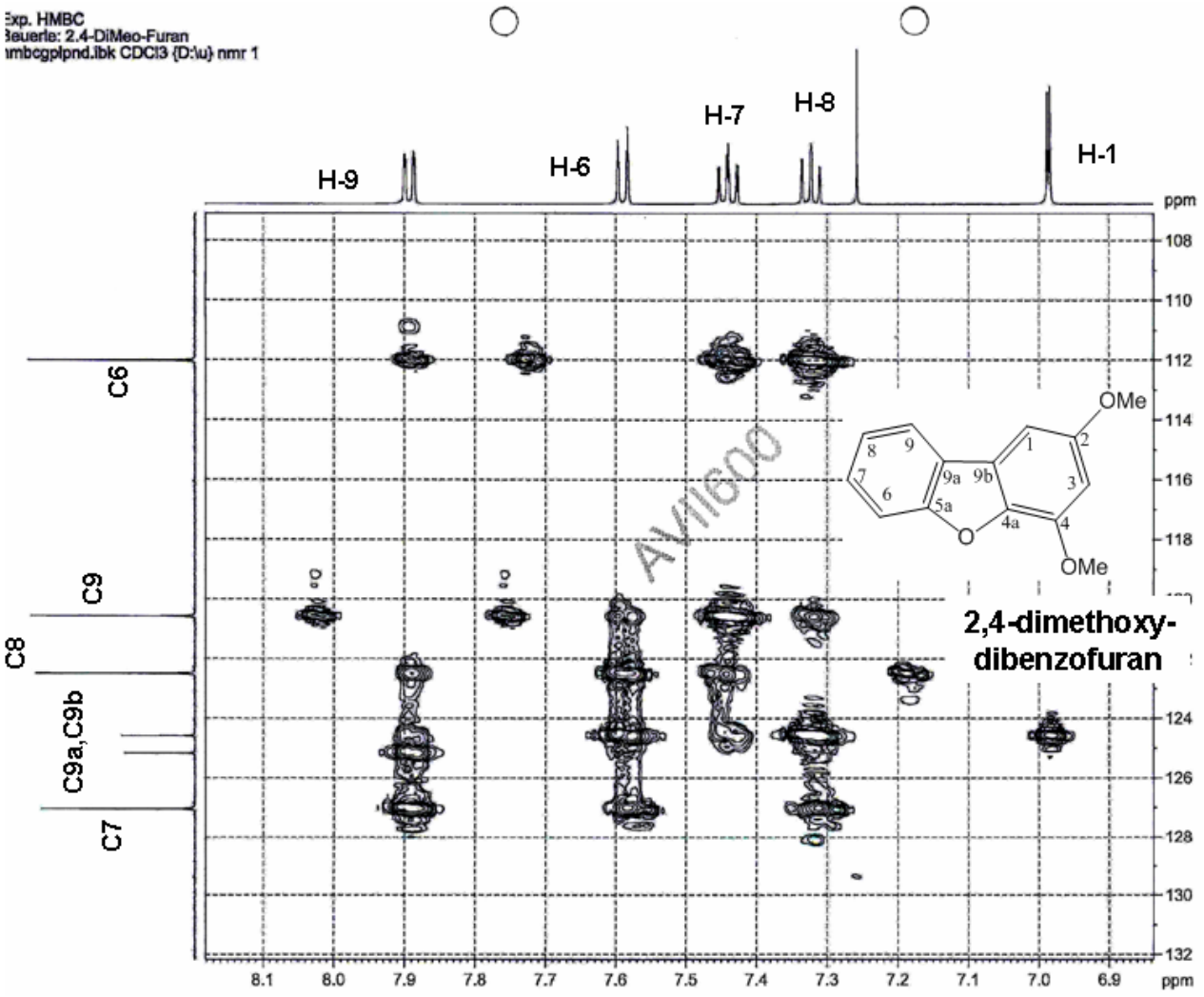

Figure A.27: HMBC spectrum of 2,4-dimethoxydibenzofuran.

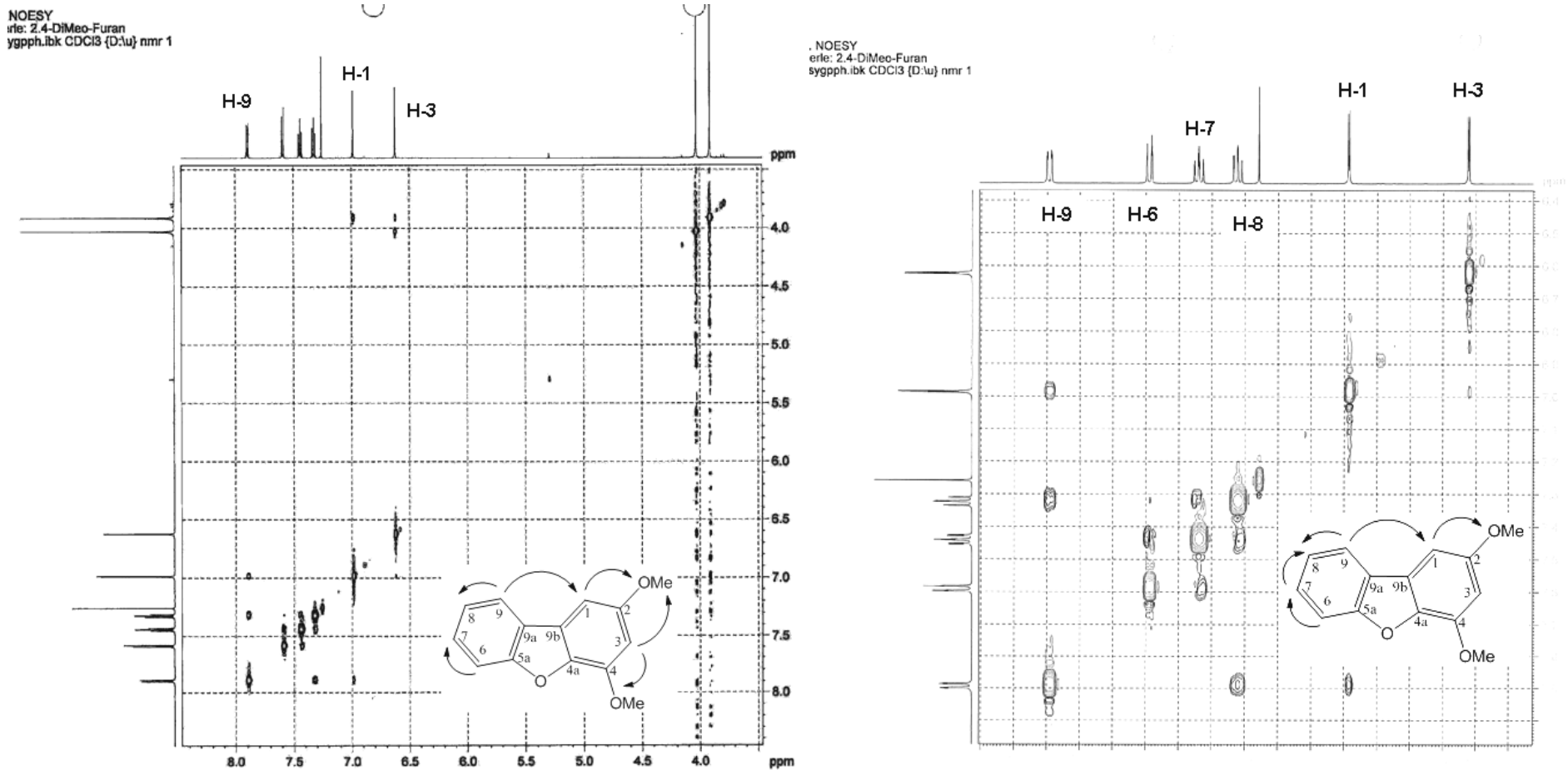

Figure A.28: NOESY spectrum of 2,4-dimethoxydibenzofuran.

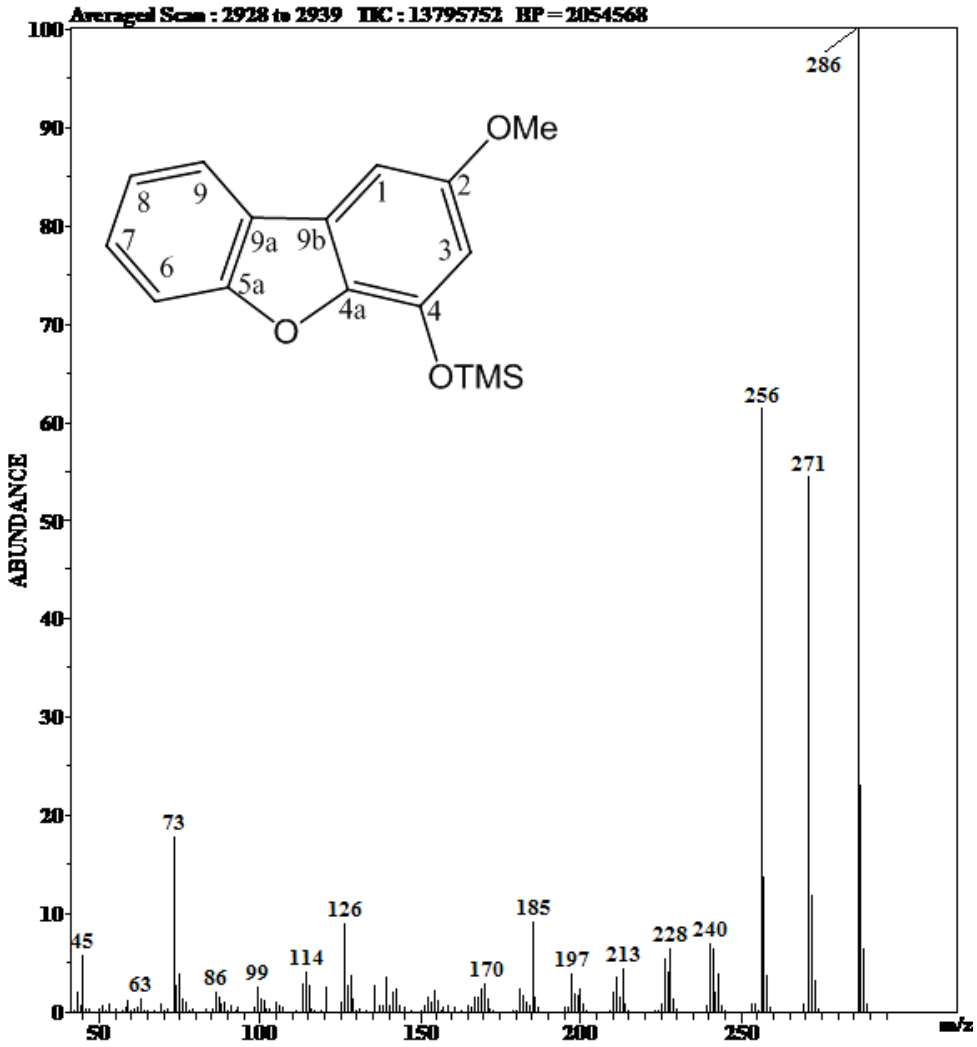

Figure A.29: Mass spectrum of silylated 4-hydroxy-2-methoxydibenzofuran.

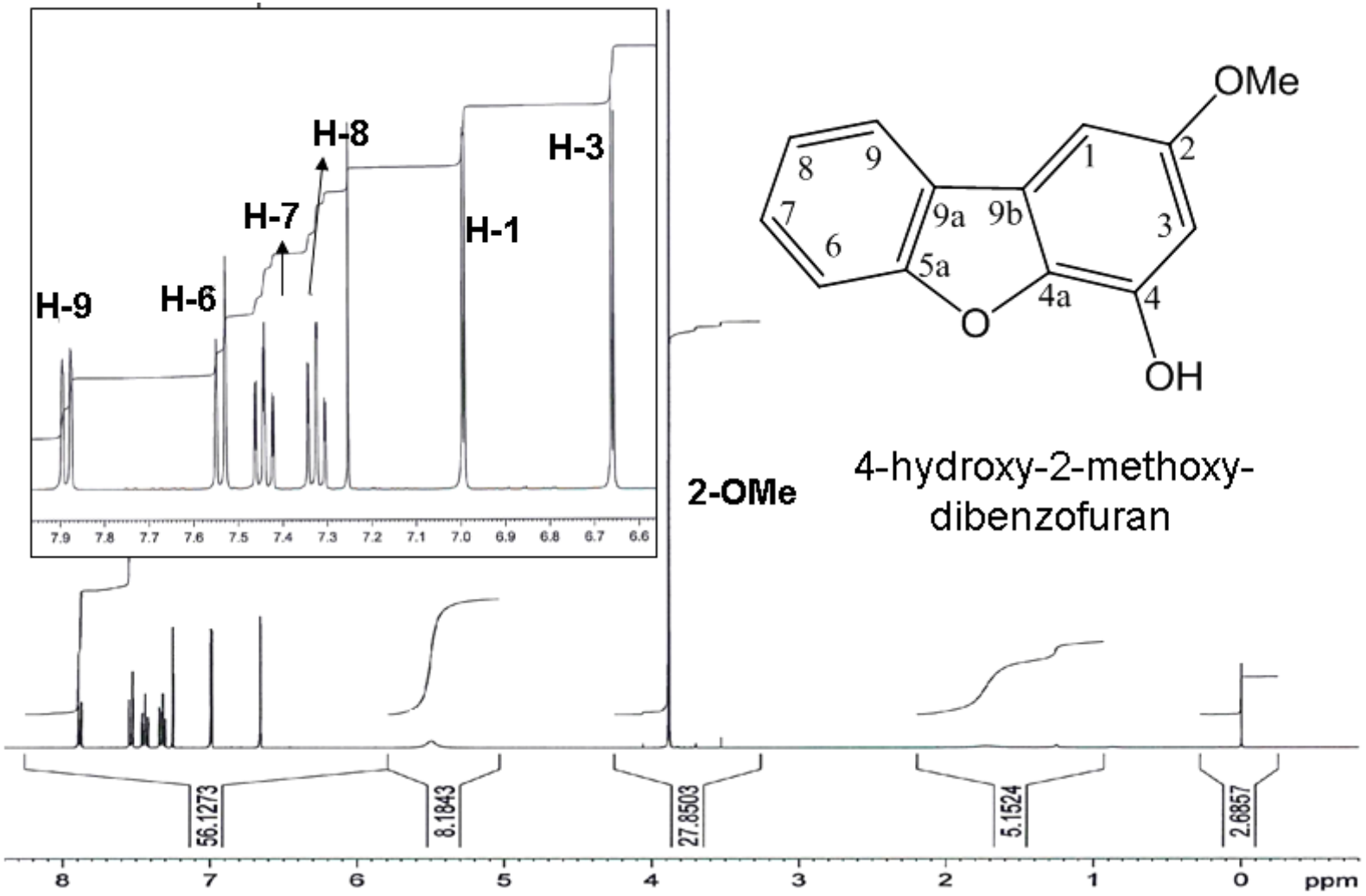

Figure A.30: [1]H-NMR of 4-hydroxy-2-methoxydibenzofuran.

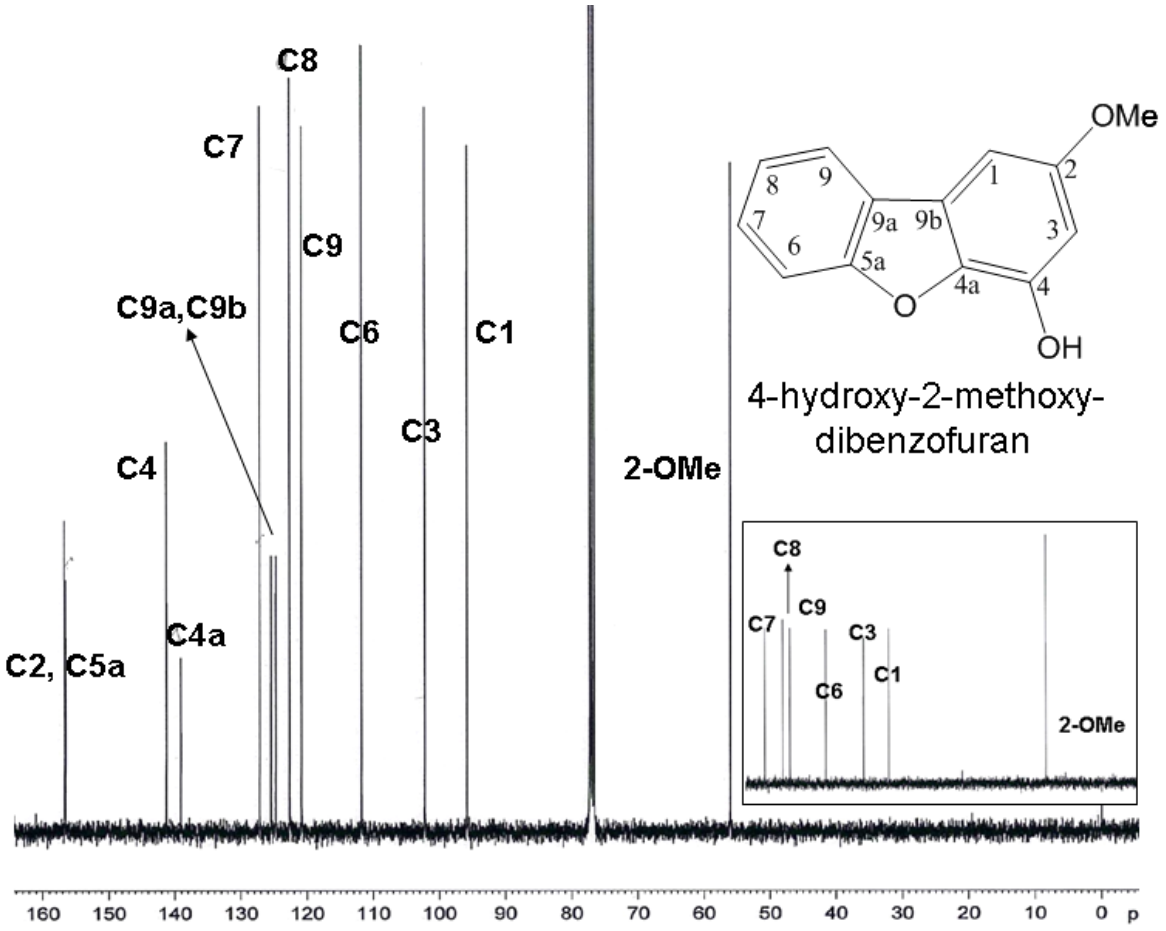

Figure A.31: ^{13}C-NMR and ^{13}C-DEPT 135 of 4-hydroxy-2-methoxydibenzofuran.

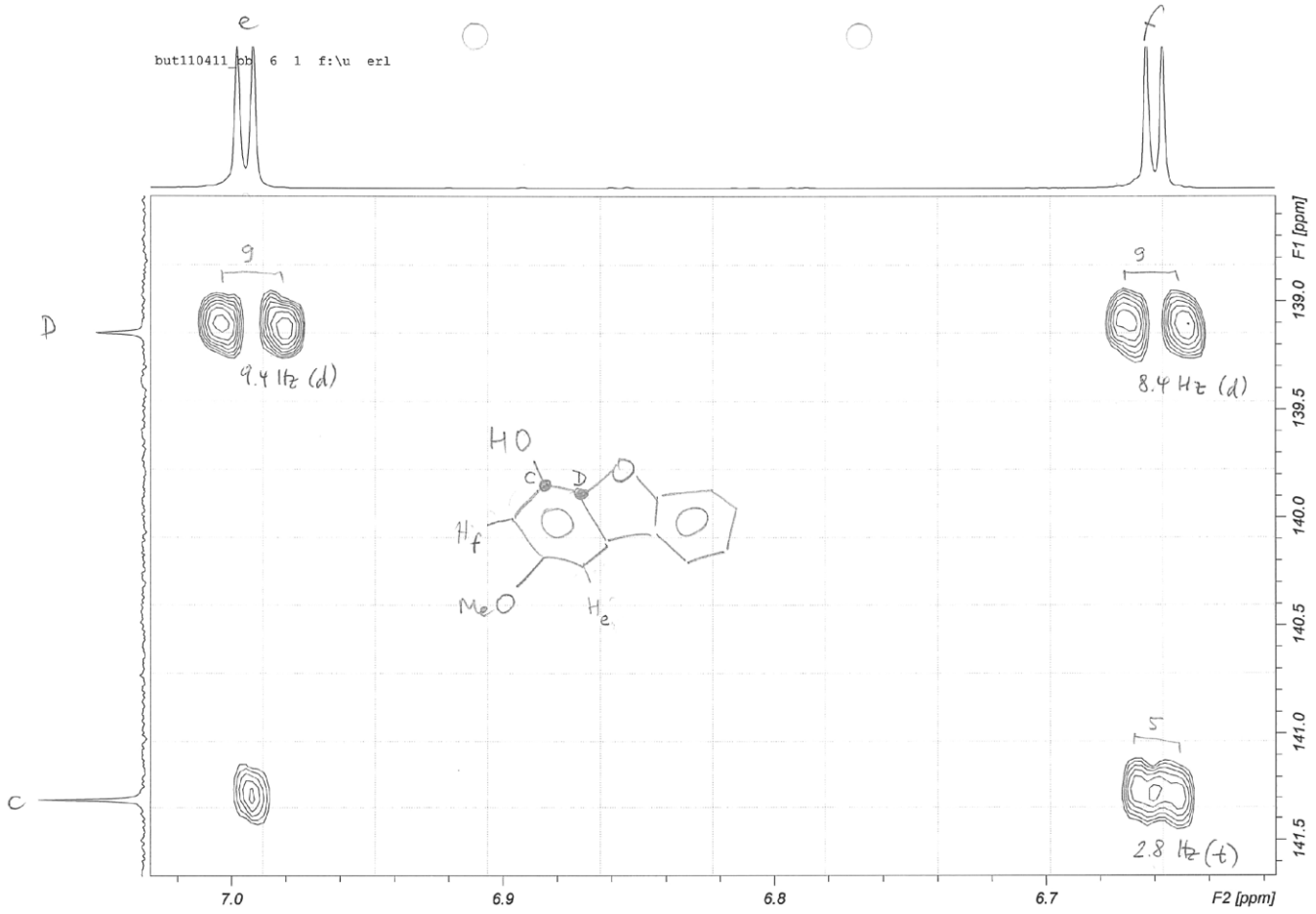

Figure A.32: HMBC spectrum of 4-hydroxy-2-methoxydibenzofuran.

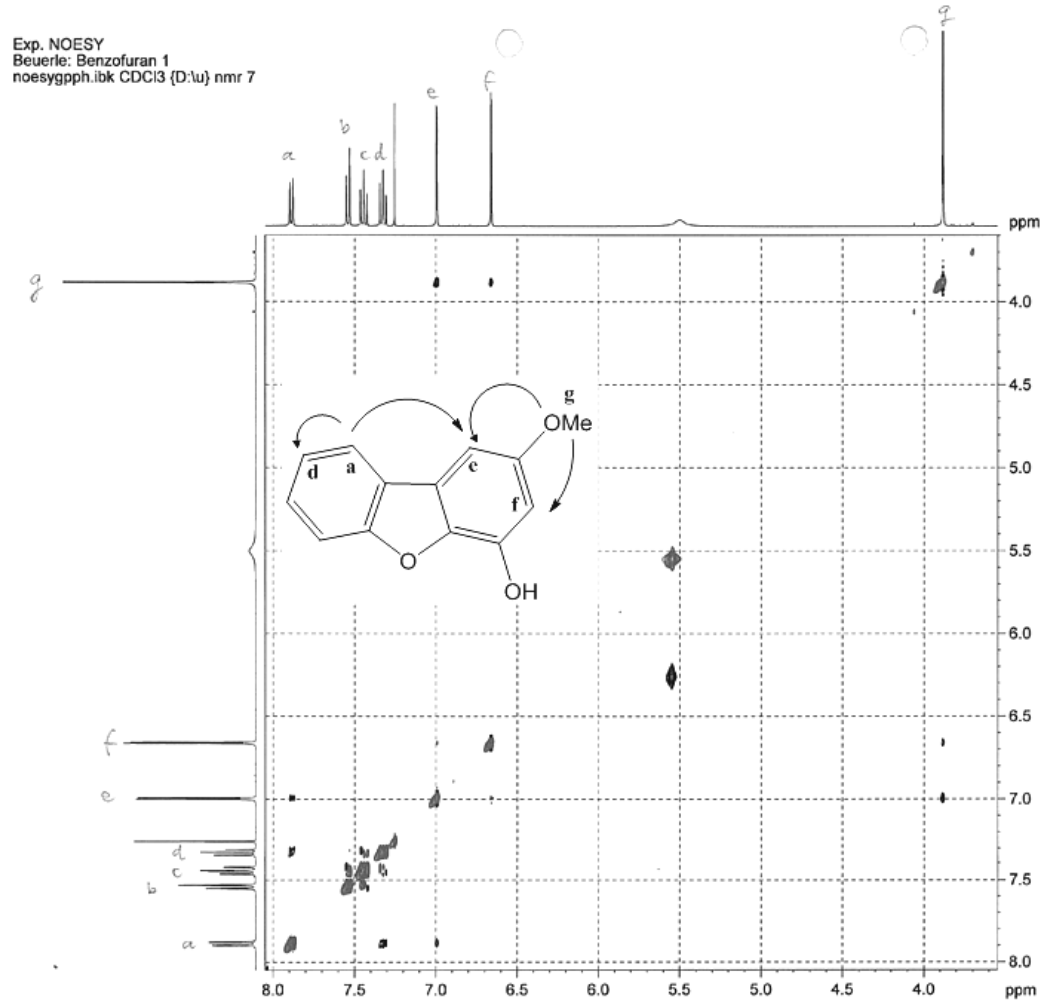

Figure A.33: NOESY spectrum of 4-hydroxy-2-methoxydibenzofuran.

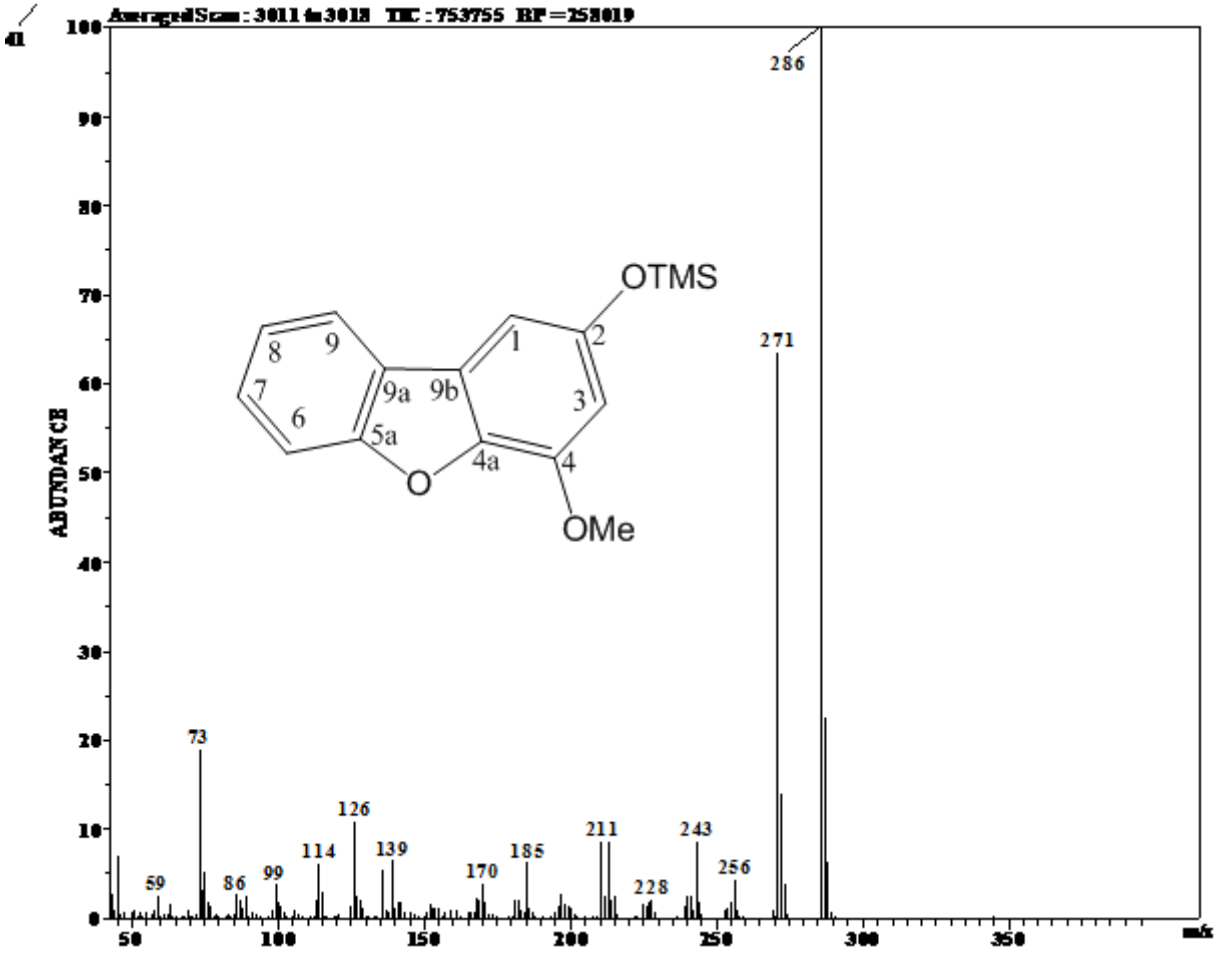

Figure A.34: Mass spectrum of 2-hydroxy-4-methoxydibenzofuran.

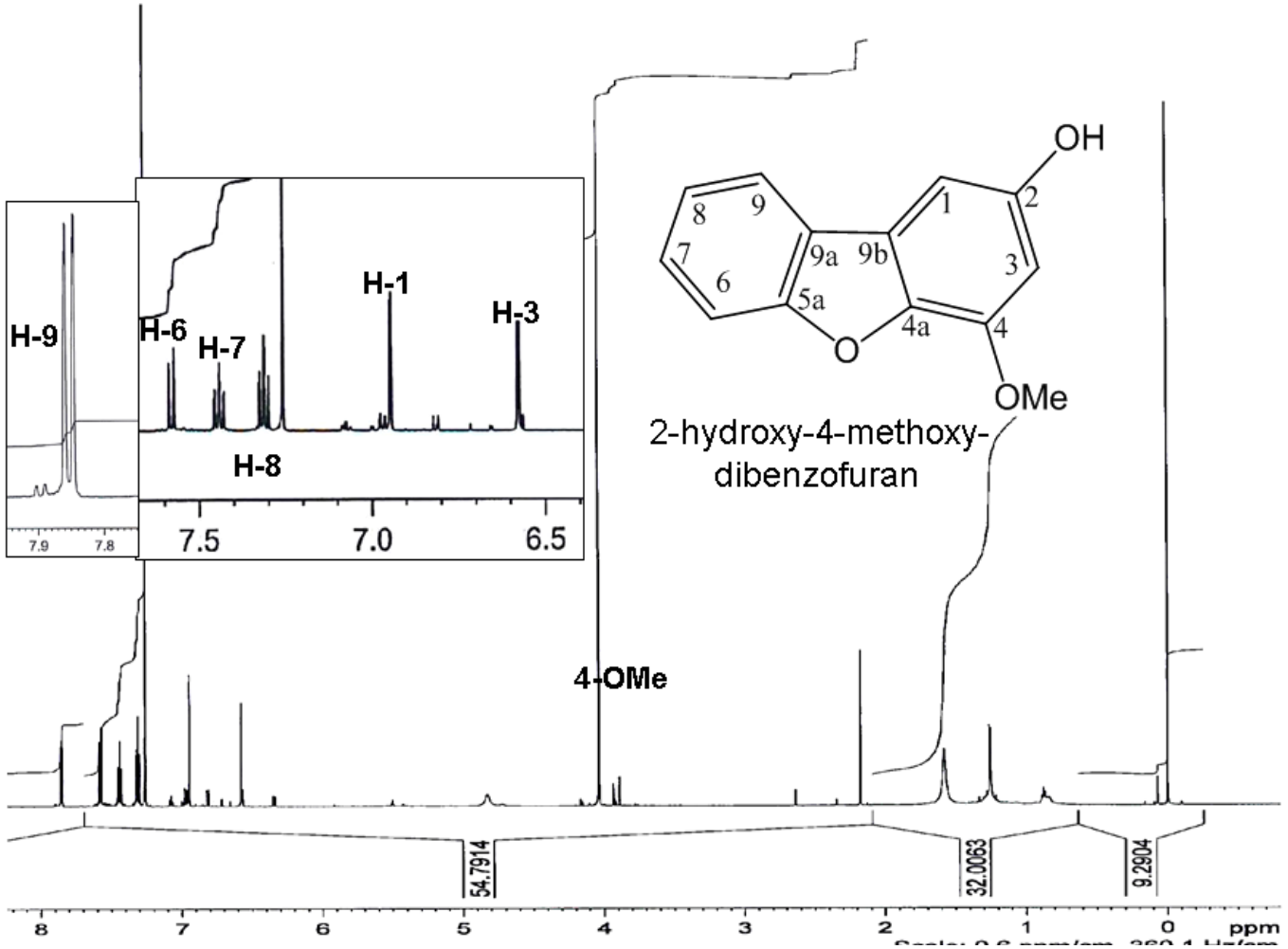

Figure A.35: ^{1}H-NMR of 2-hydroxy-4-methoxydibenzofuran.

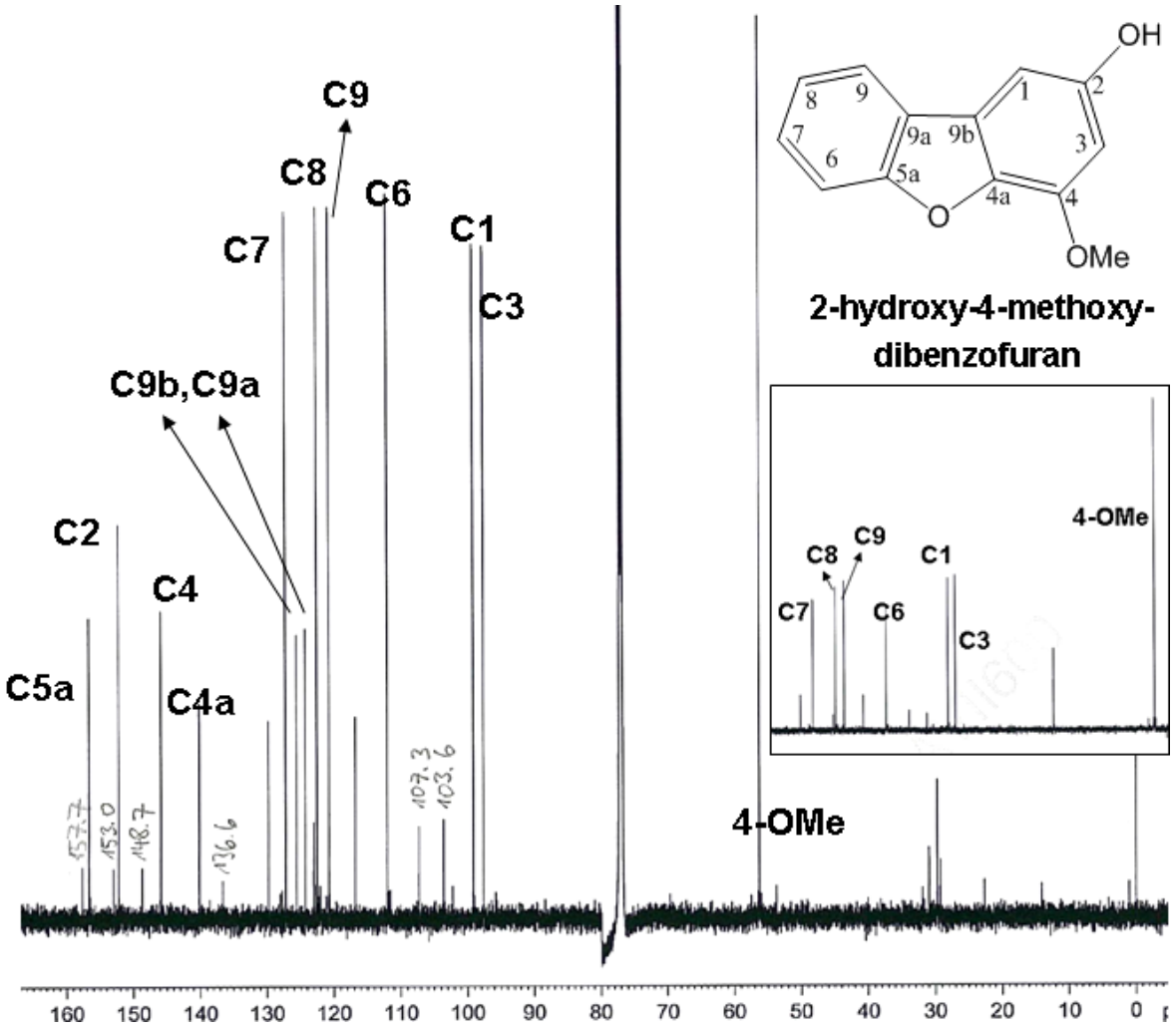

Figure A.36: ^{13}C-NMR and ^{13}C-DEPT 135 of 2-hydroxy-4-methoxydibenzofuran.

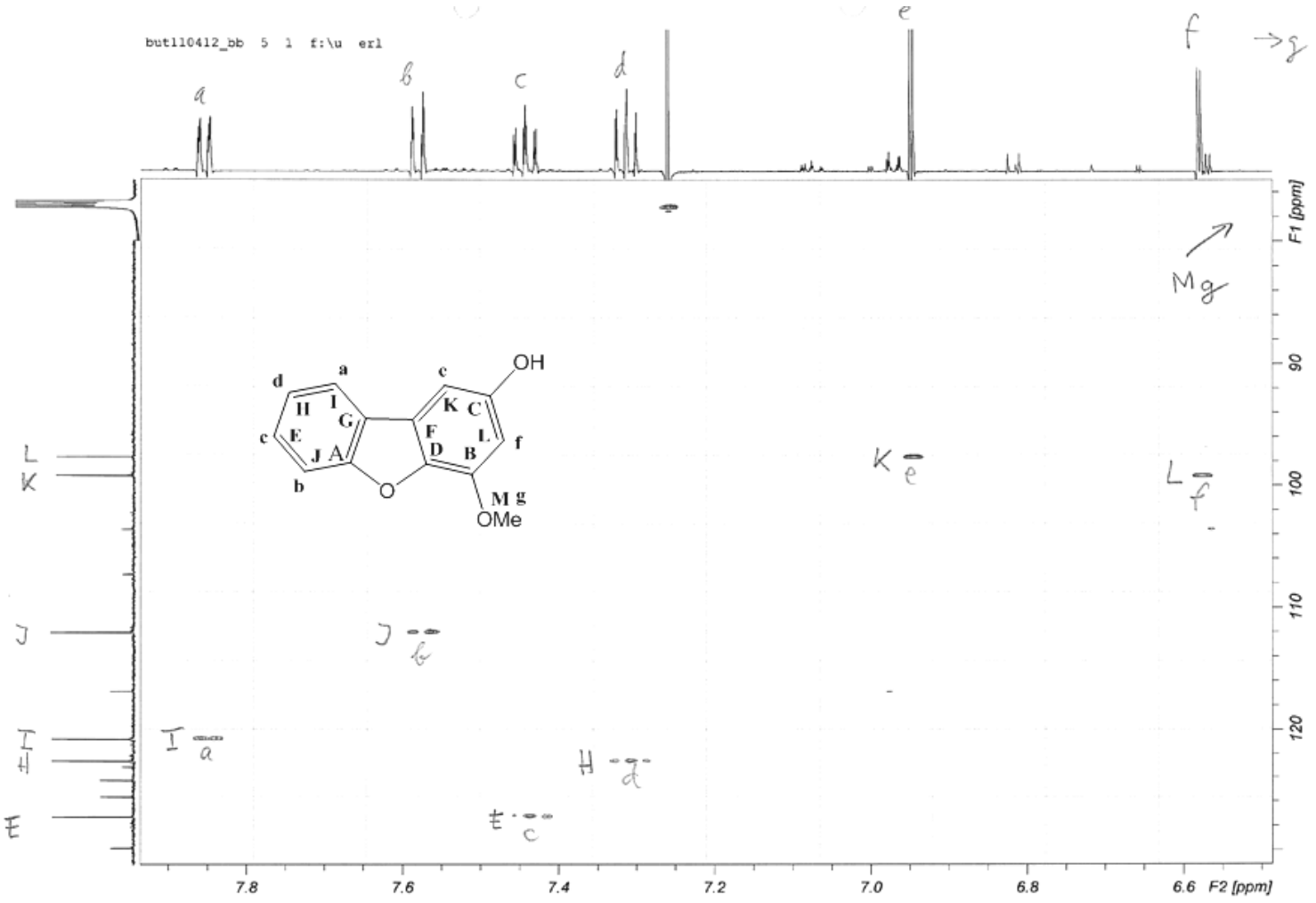

Figure A.37: HSQC spectrum of 2-hydroxy-4-methoxydibenzofuran.

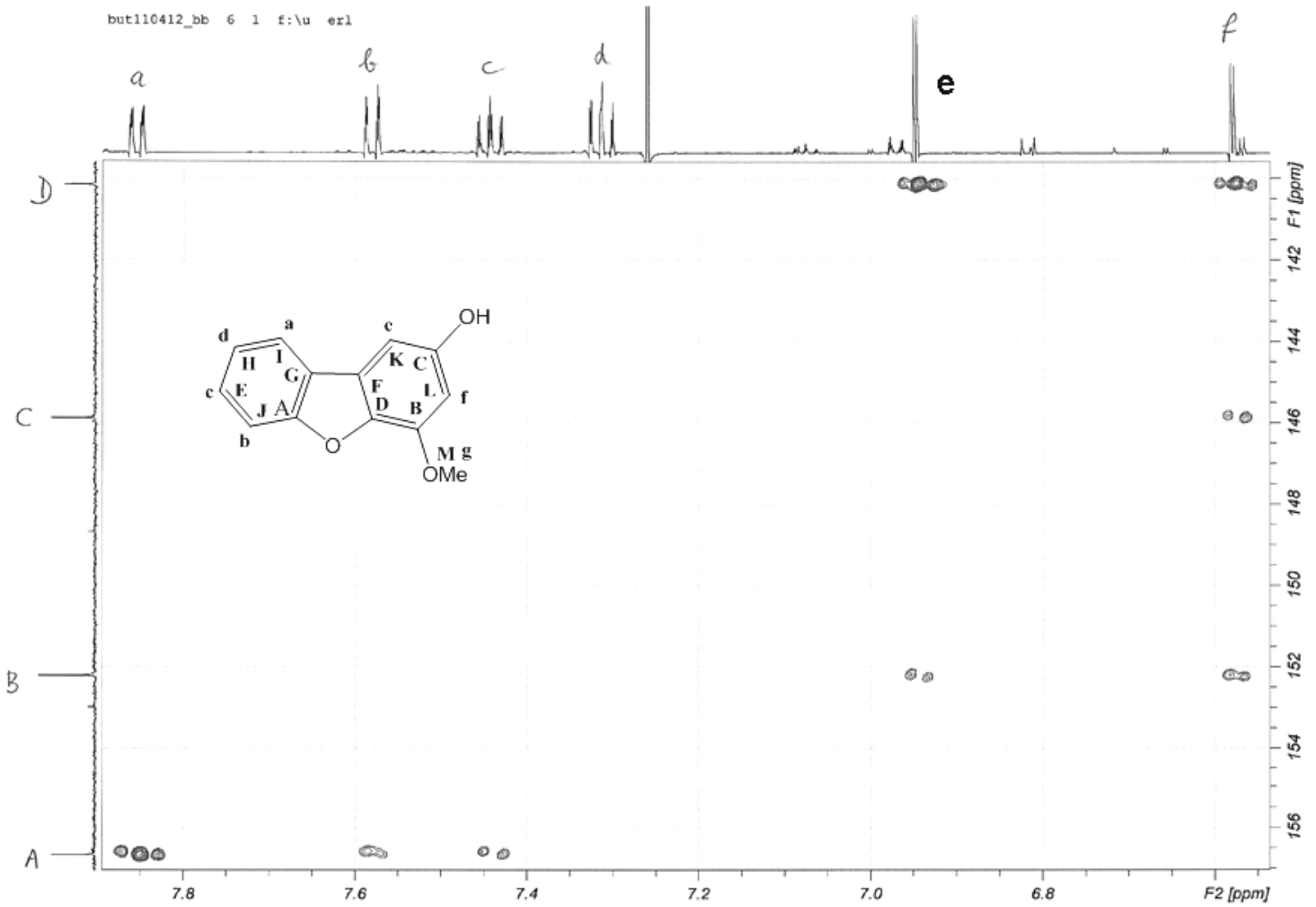

Figure A.38: HMBC spectrum of 2-hydroxy-4-methoxydibenzofuran.

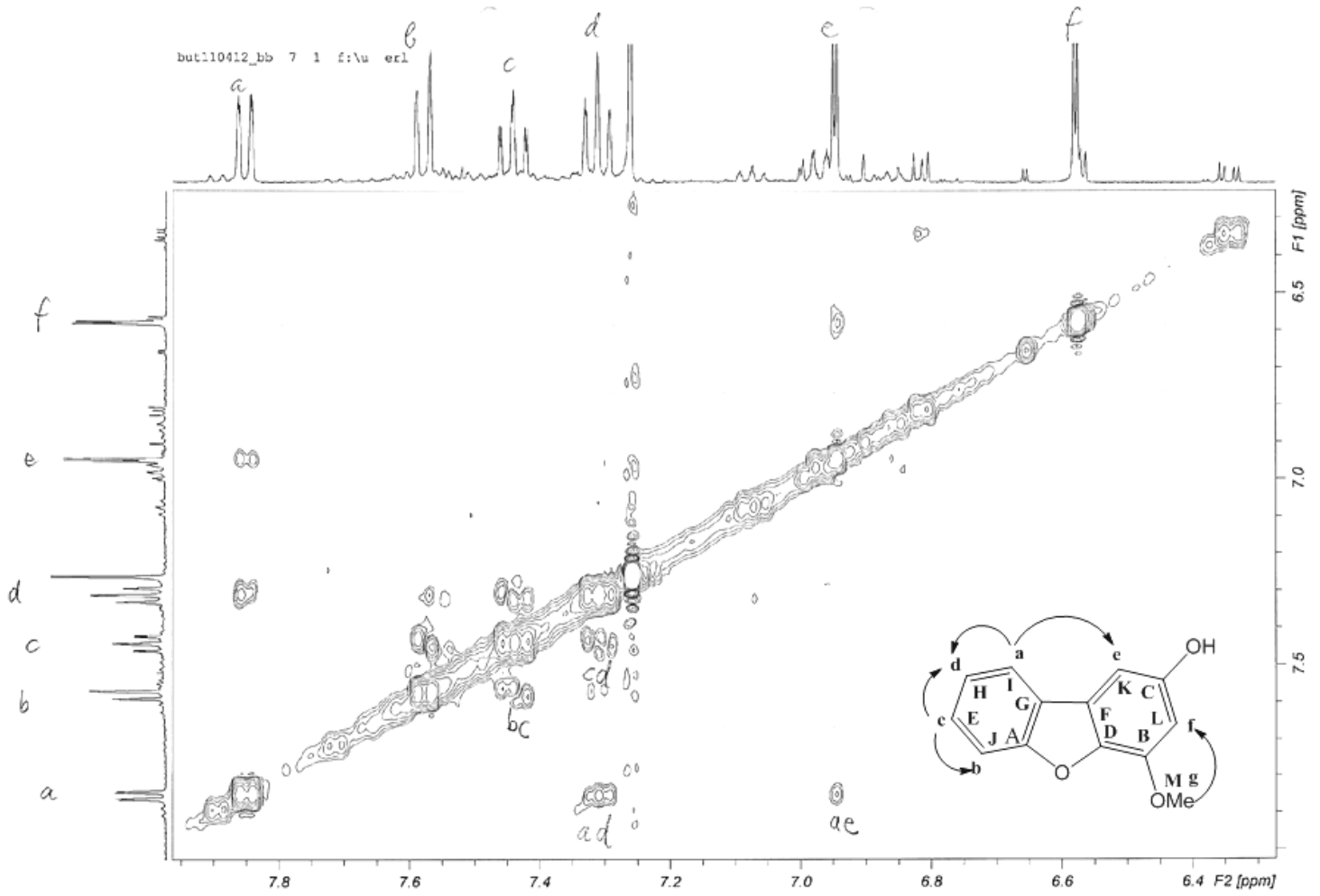

Figure A.39: NOESY spectrum of 2-hydroxy-4-methoxydibenzofuran.

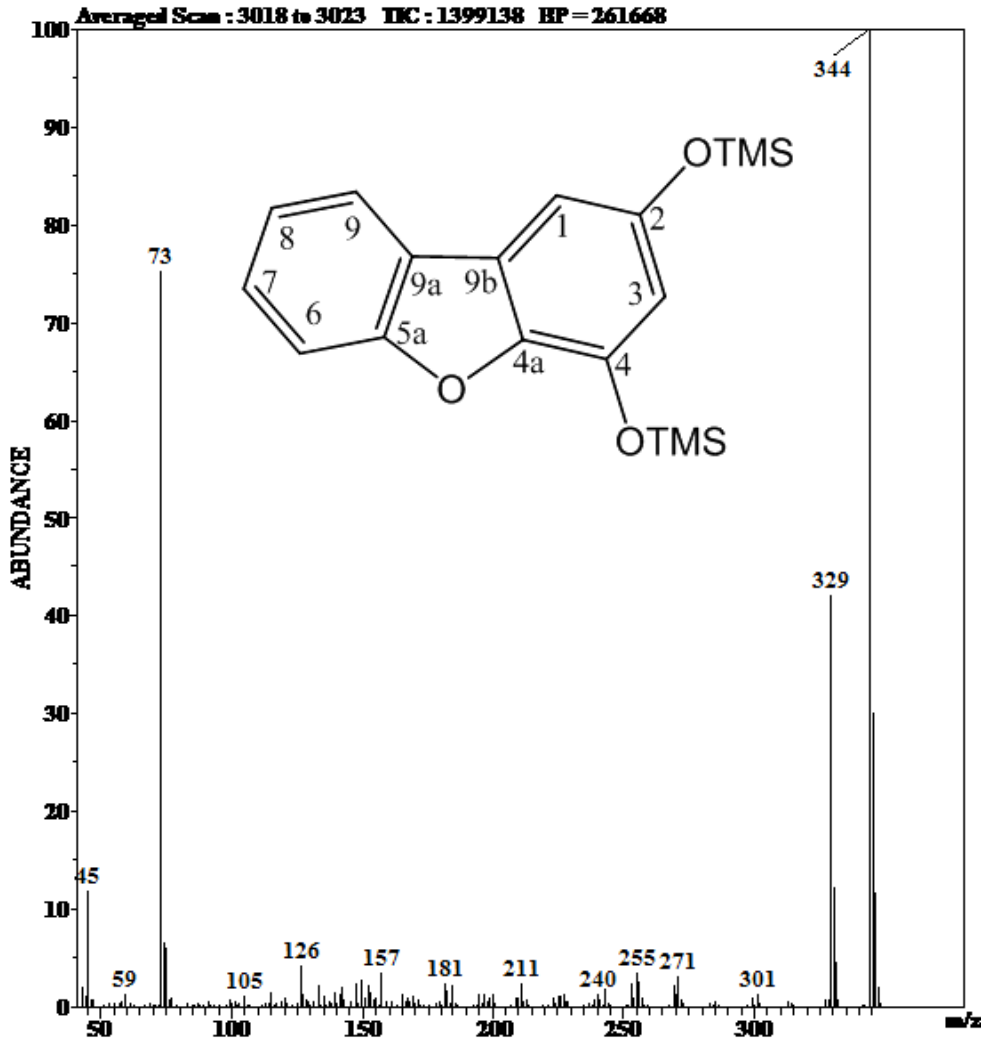

Figure A.40: Mass spectrum of silylated 2,4-dihydroxydibenzofuran.

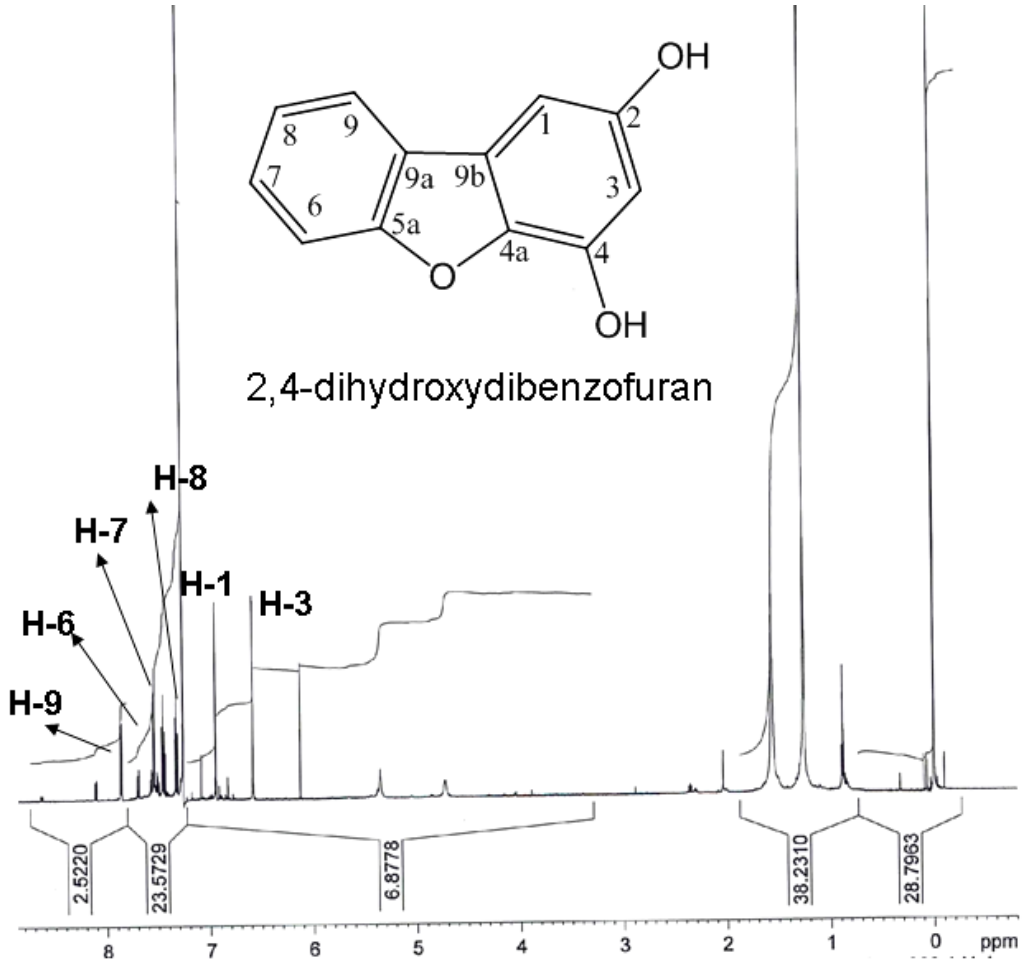

Figure A.41: ^{1}H-NMR of 2,4-dihydroxydibenzofuran.

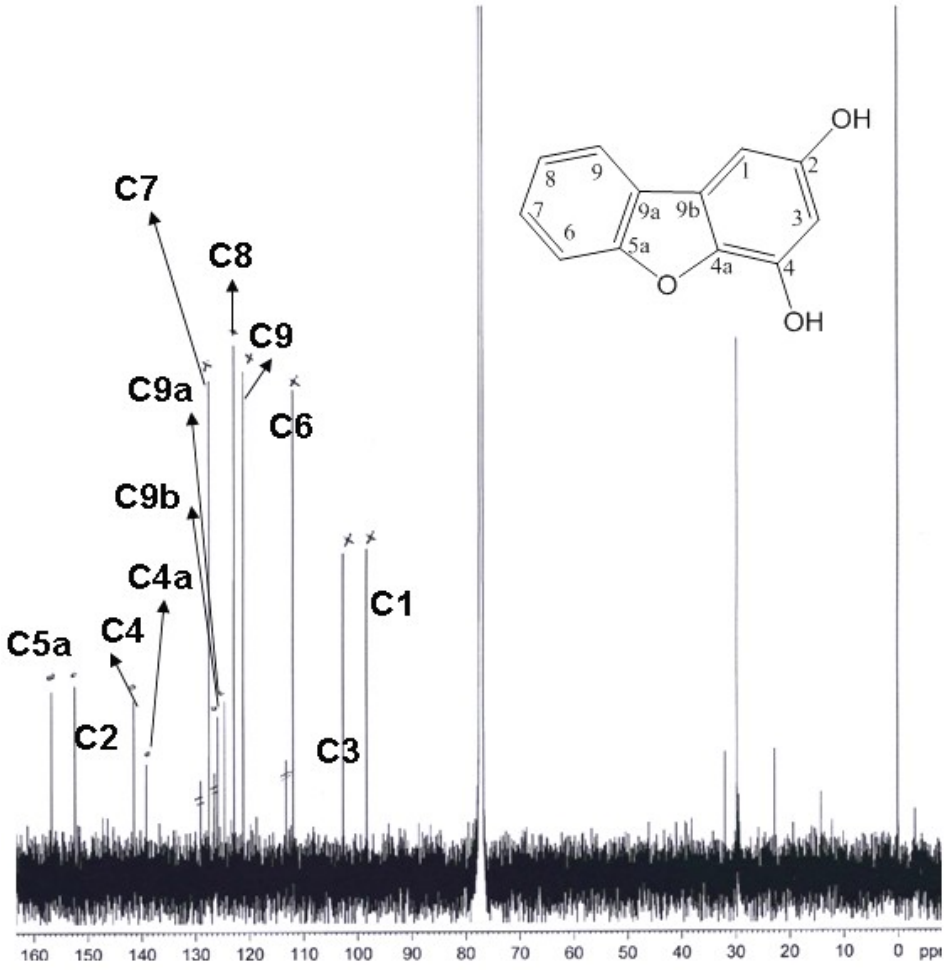

Figure A.42: ^{13}C-NMR of 2,4-dihydroxydibenzofuran.

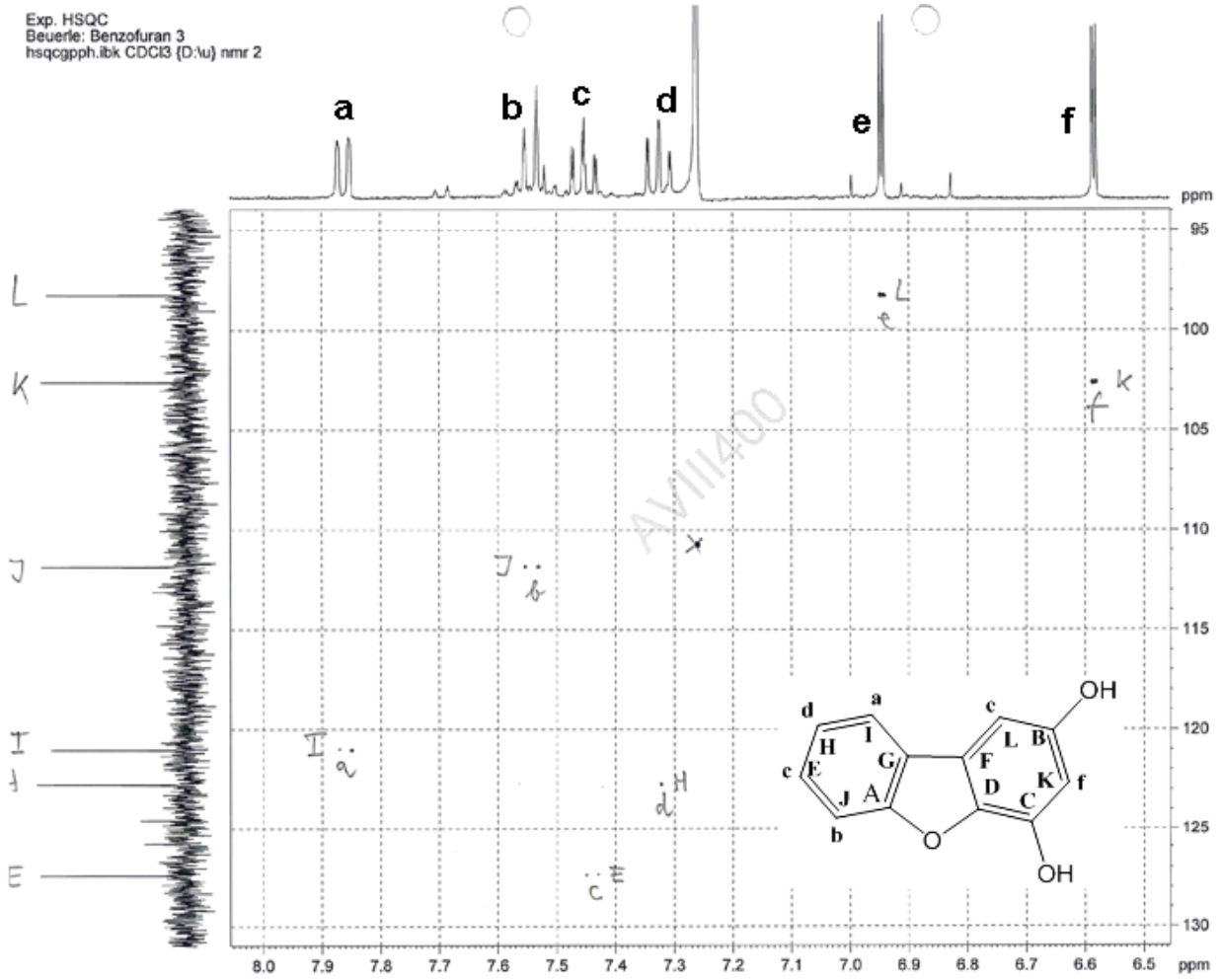

Figure A.43: HSQC spectrum of 2,4-dihydroxydibenzofuran.

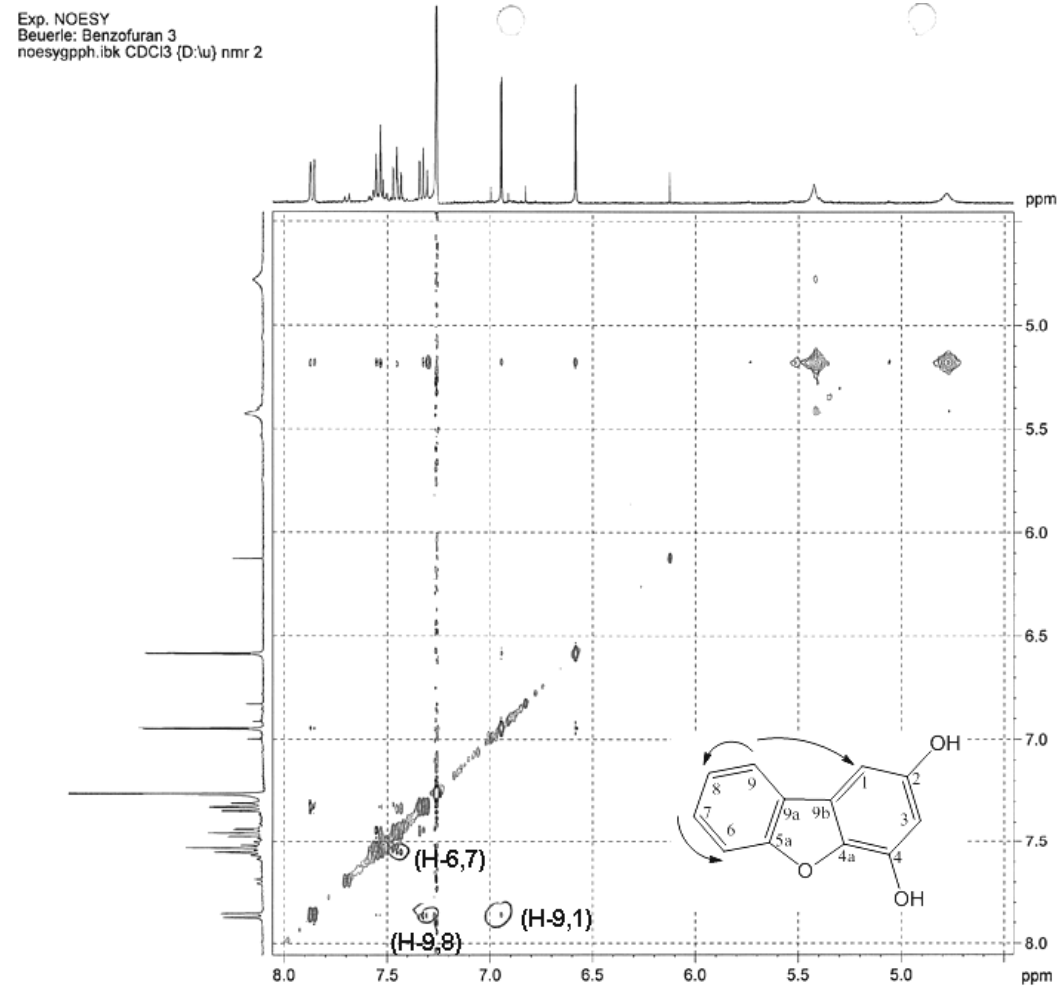

Figure A.44: NOESY spectrum of 2,4-dihydroxydibenzofuran.

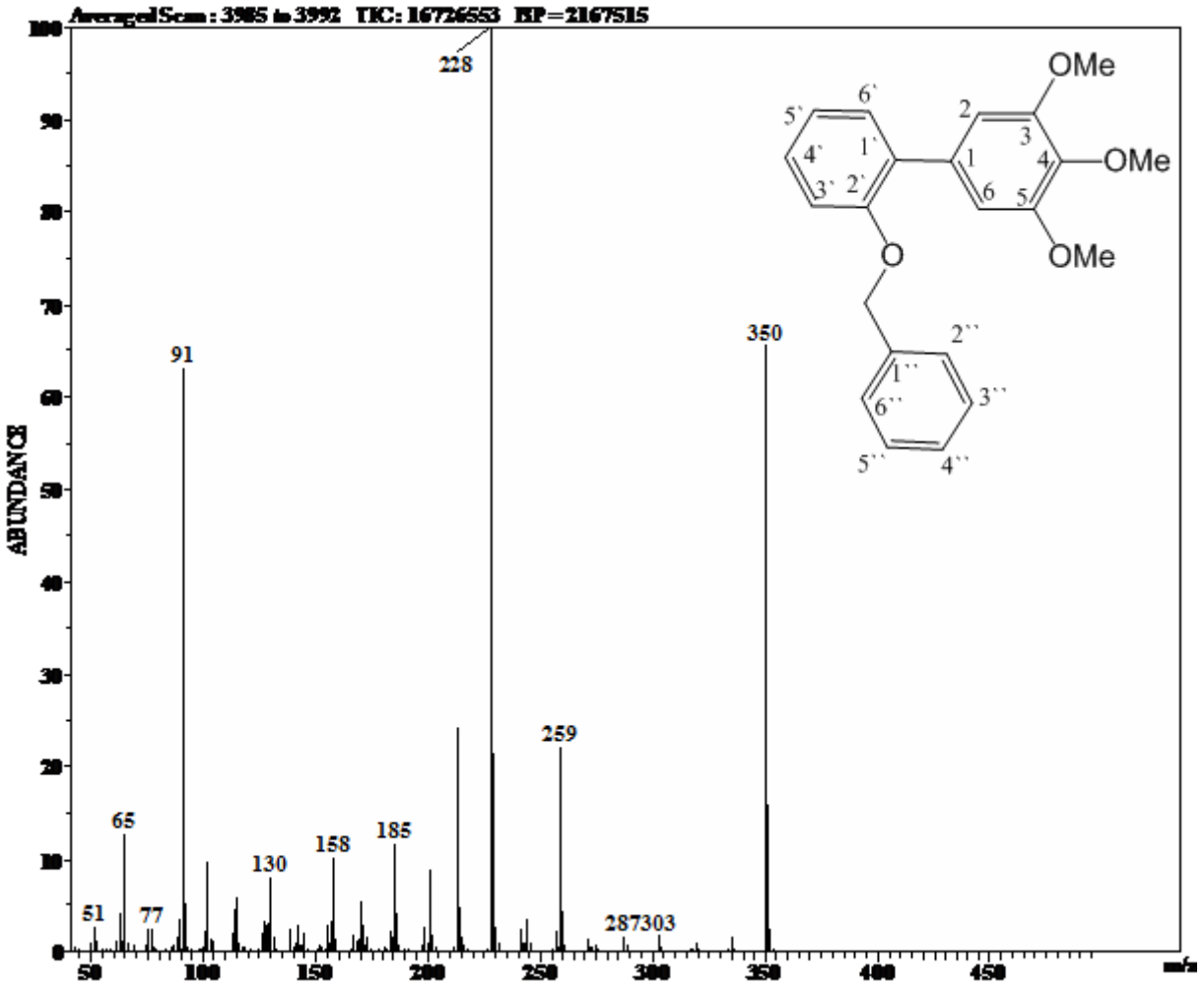

Figure A.45: Mass spectrum of 2`-benzyloxy-3,4,5-trimethoxybiphenyl .

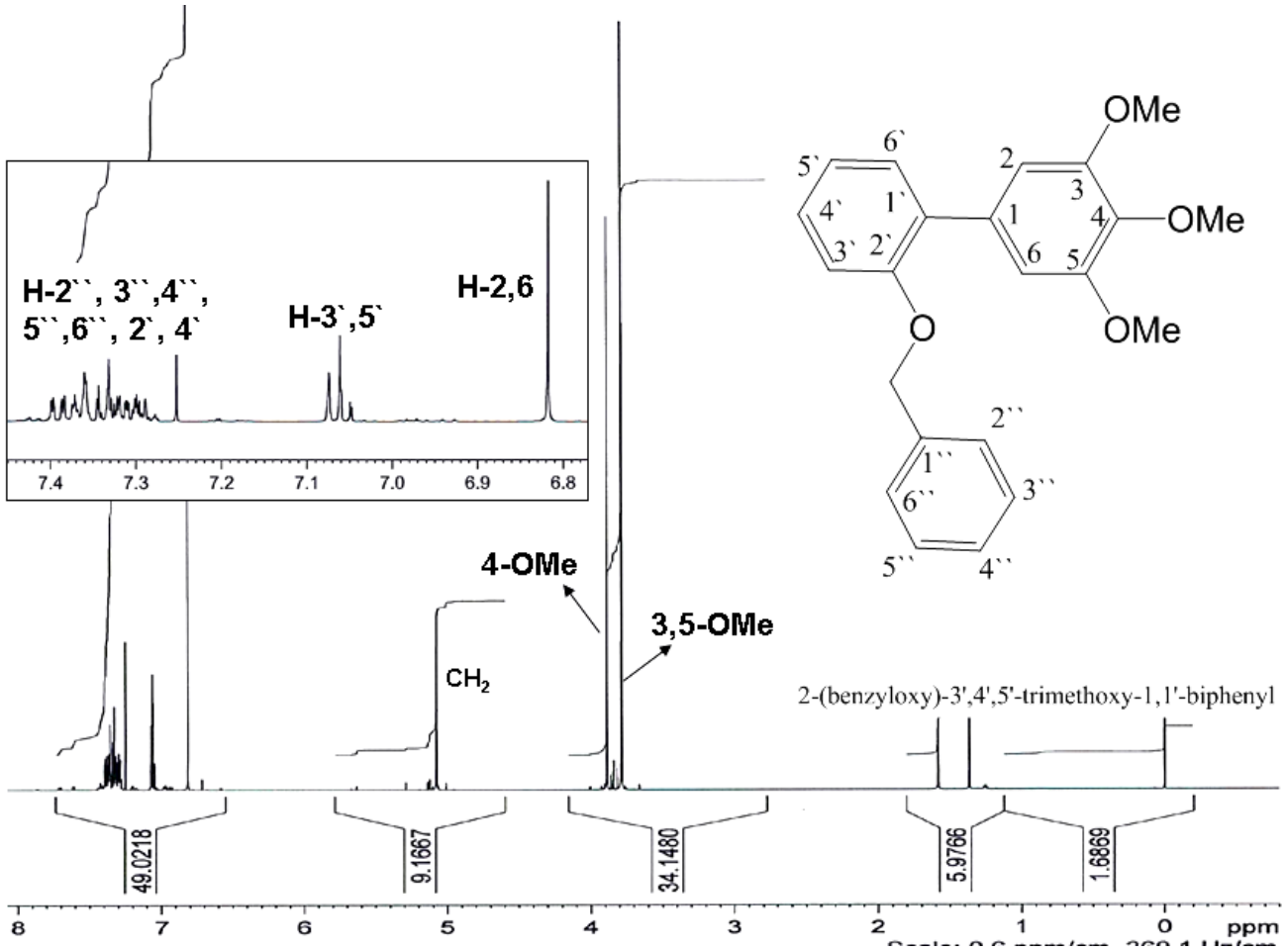

Figure A.46: ^{1}H-NMR of 2`-benzyloxy-3,4,5-trimethoxybiphenyl.

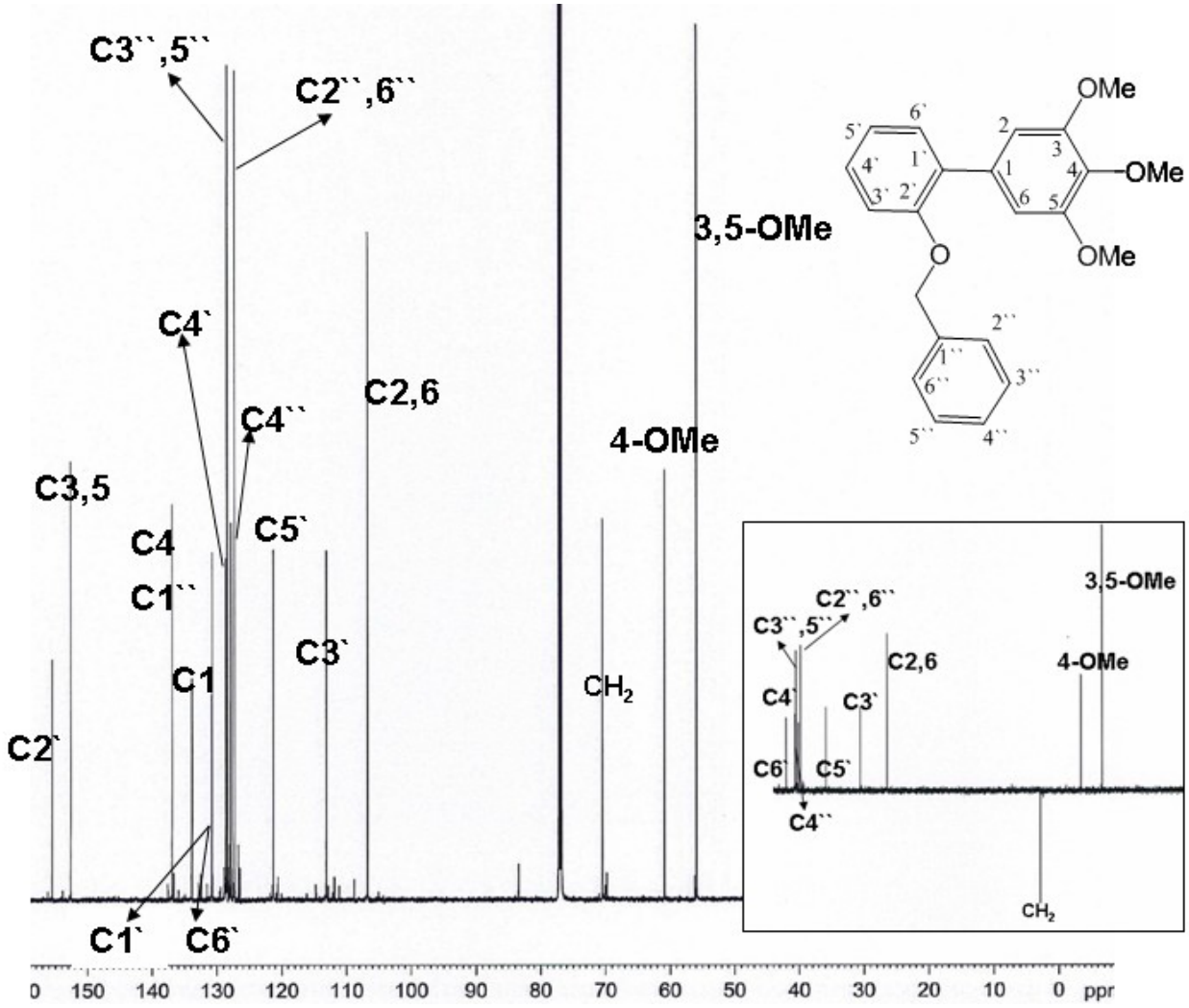

Figure A.47: ^{13}C-NMR and ^{13}C-DEPT 135 of 2`-benzyloxy-3,4,5-trimethoxybiphenyl.

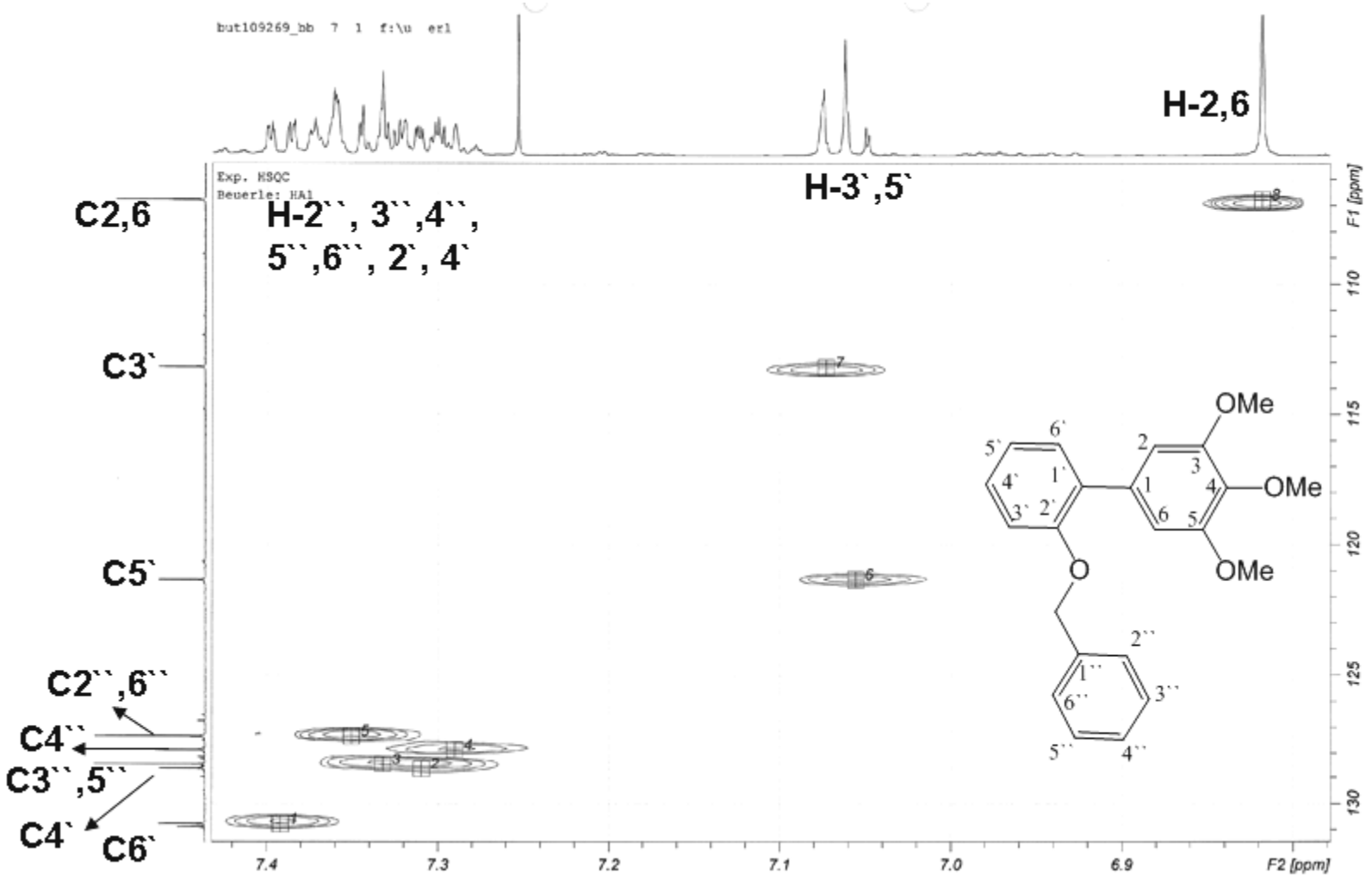

Figure A.48: HSQC spectrum of 2`-benzyloxy-3,4,5-trimethoxybiphenyl.

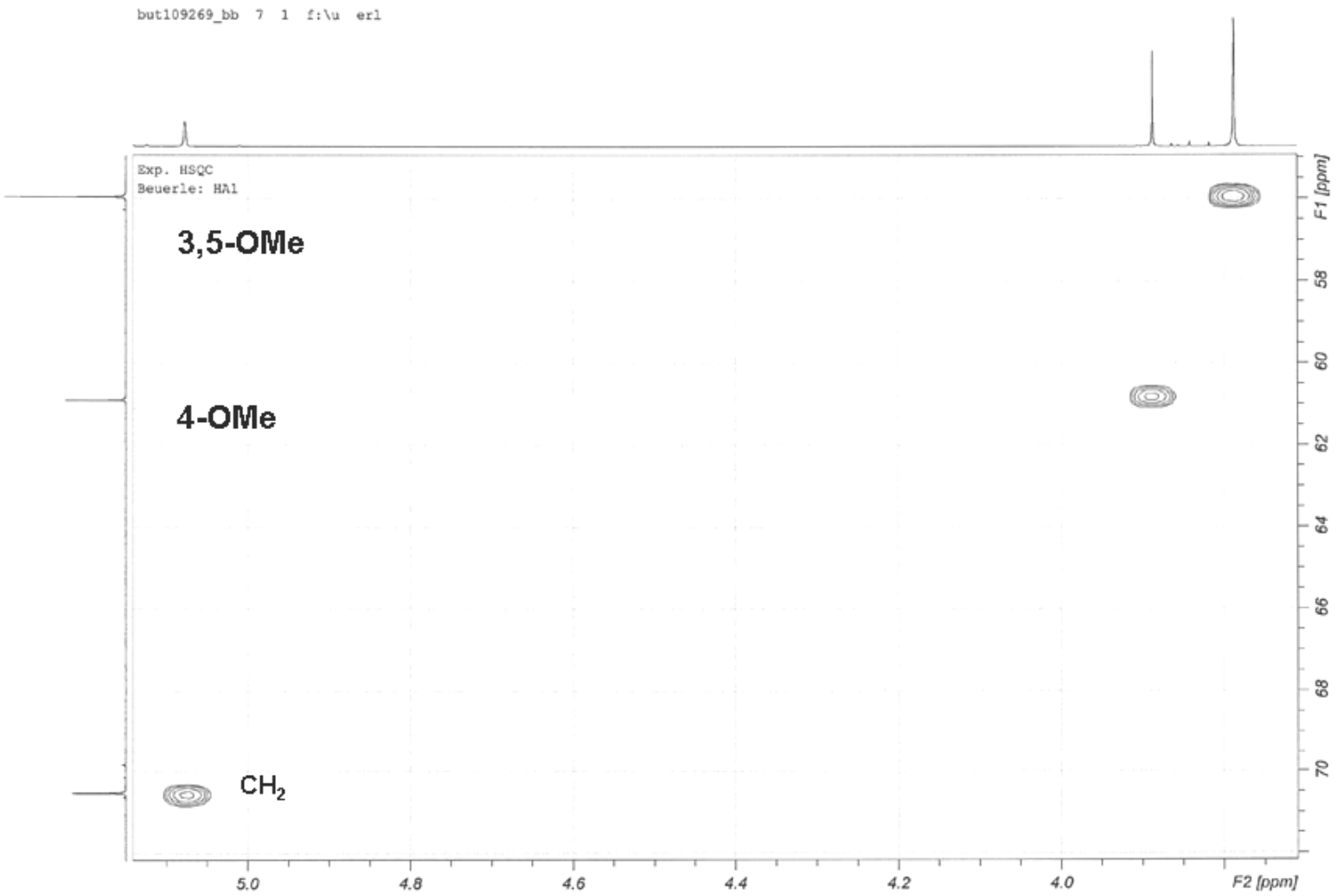

Figure A.49: HSQC spectrum of 2`-benzyloxy-3,4,5-trimethoxybiphenyl displaying the assignment of the methoxy groups.

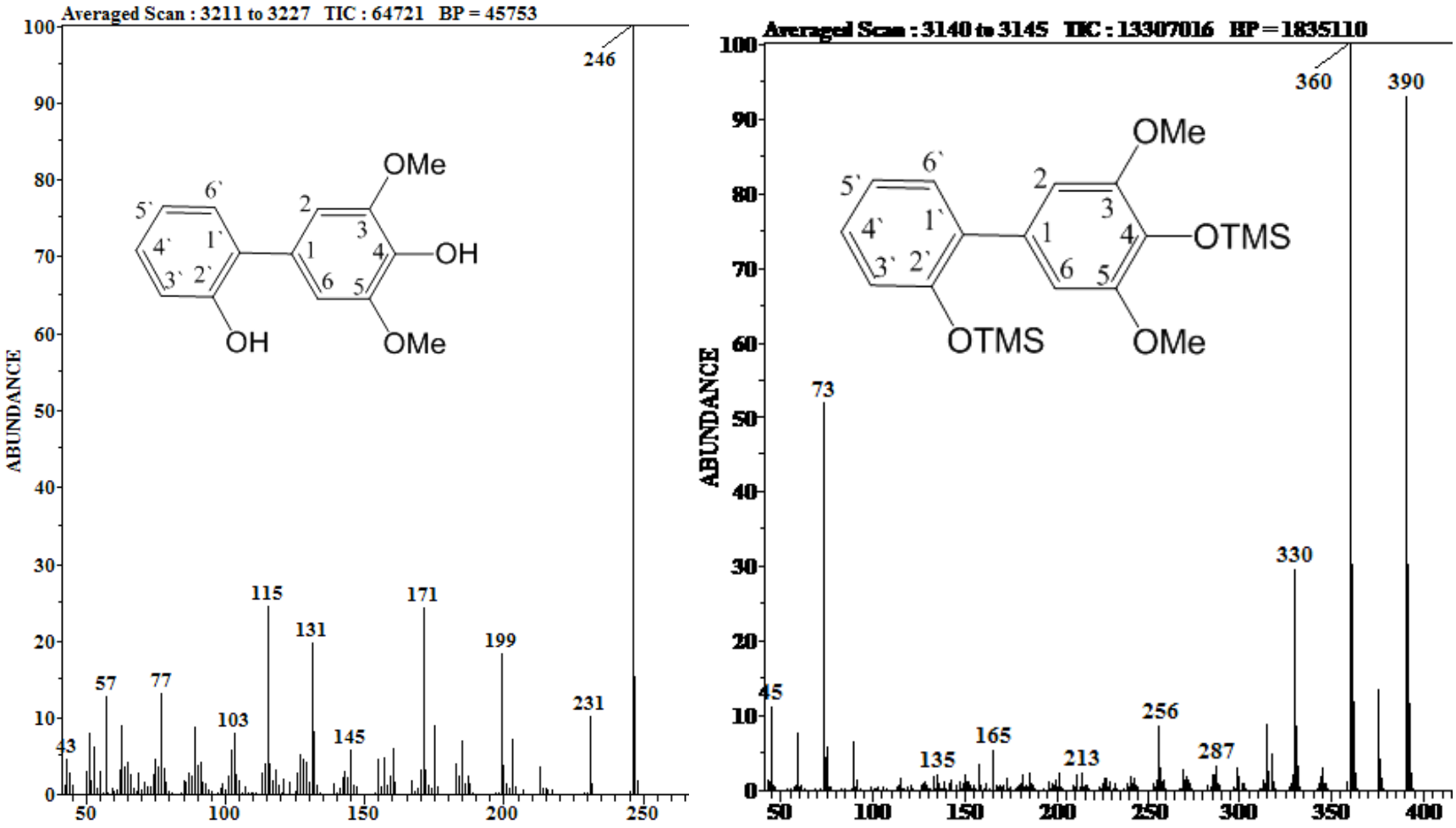

Figure A.50: Mass spectra of 2`-hydroxyaucuparin.

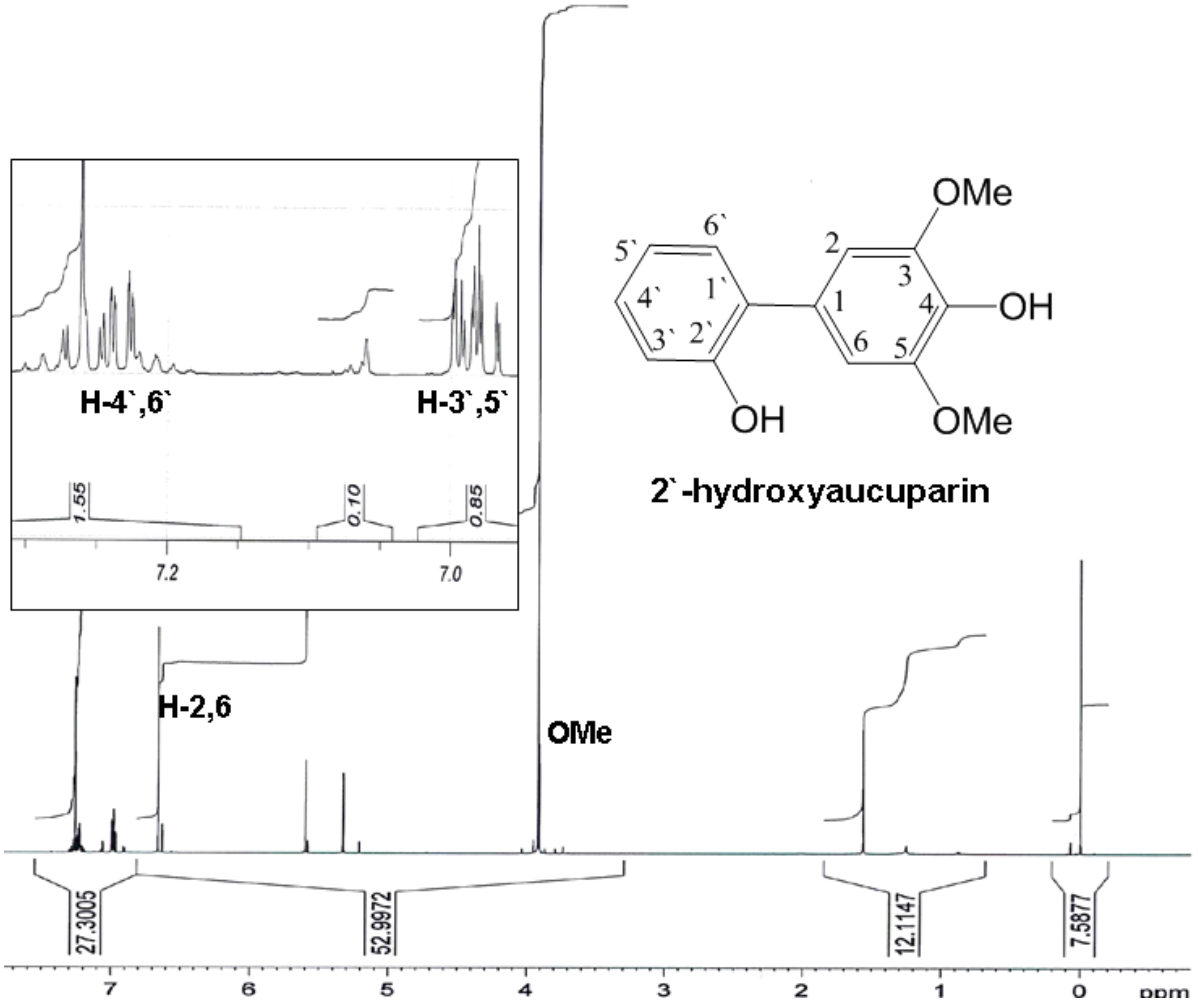

Figure A.51: [1]H-NMR of 2`-hydroxyaucuparin.

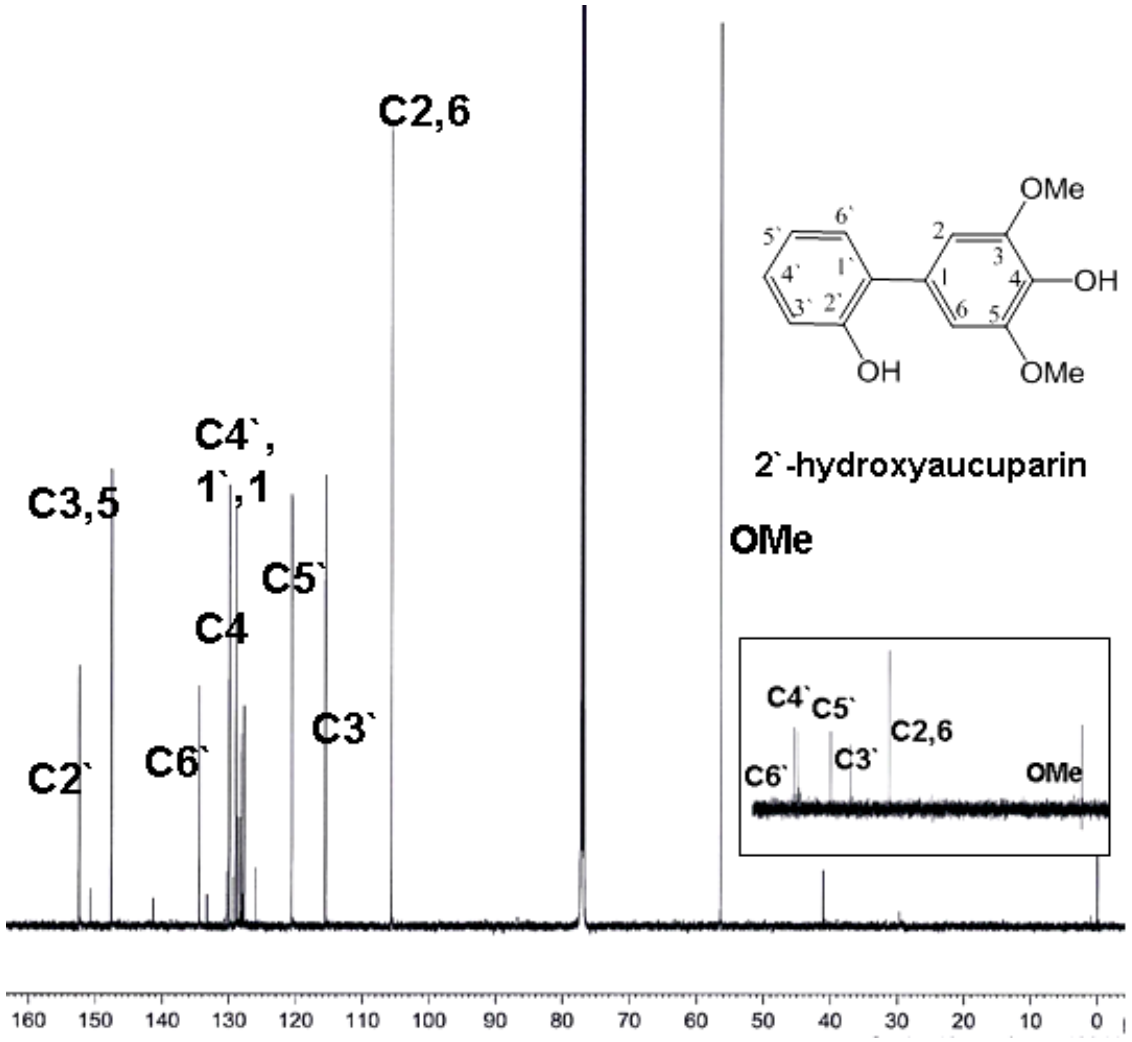

Figure A.52: ^{13}C-NMR and ^{13}C-DEPT 135 of 2`-hydroxyaucuparin.